AUGUST 1987

ENVIRONMENTAL SCIENCE & TECHNOLOGY

ES&T

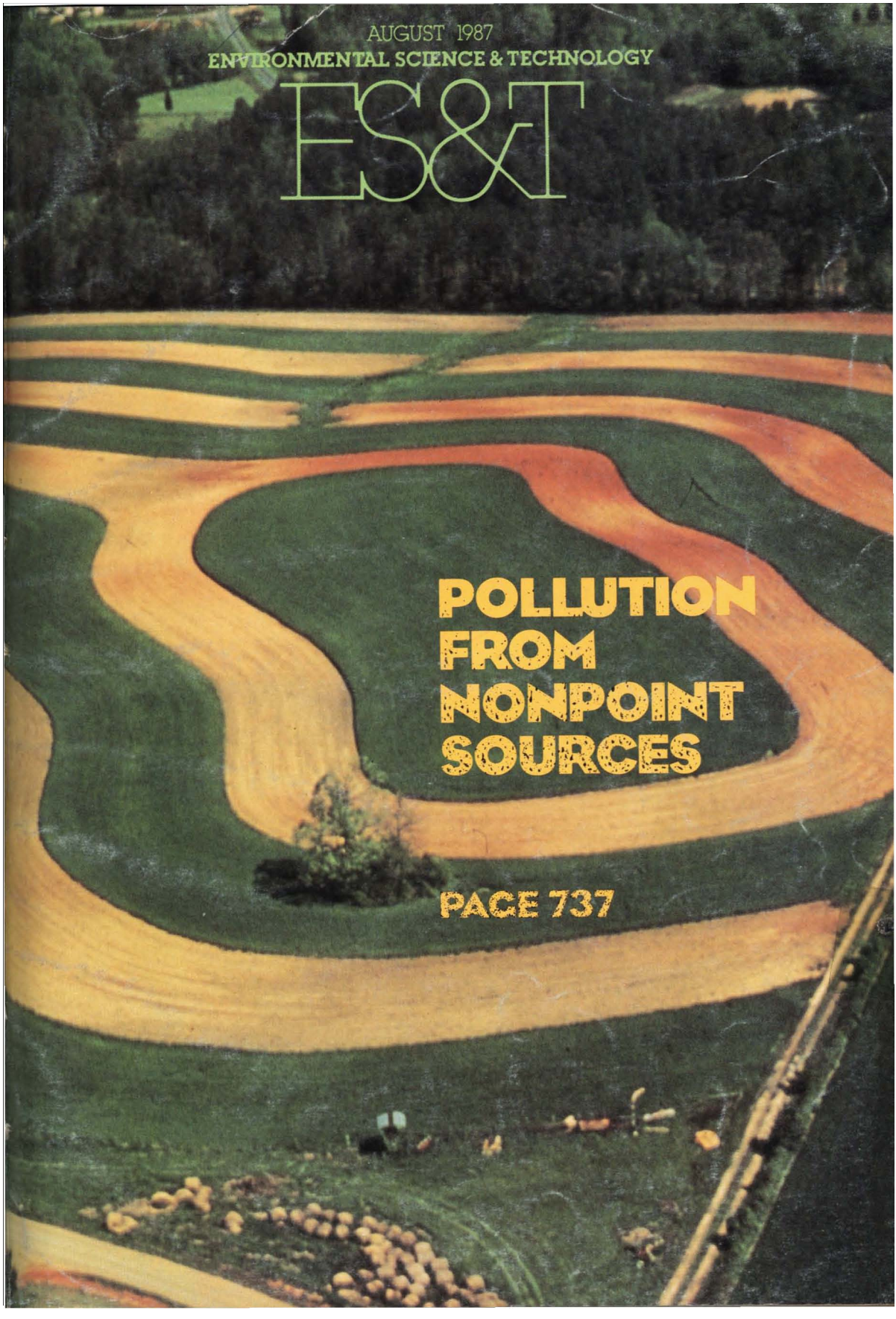

POLLUTION FROM NONPOINT SOURCES

PAGE 737

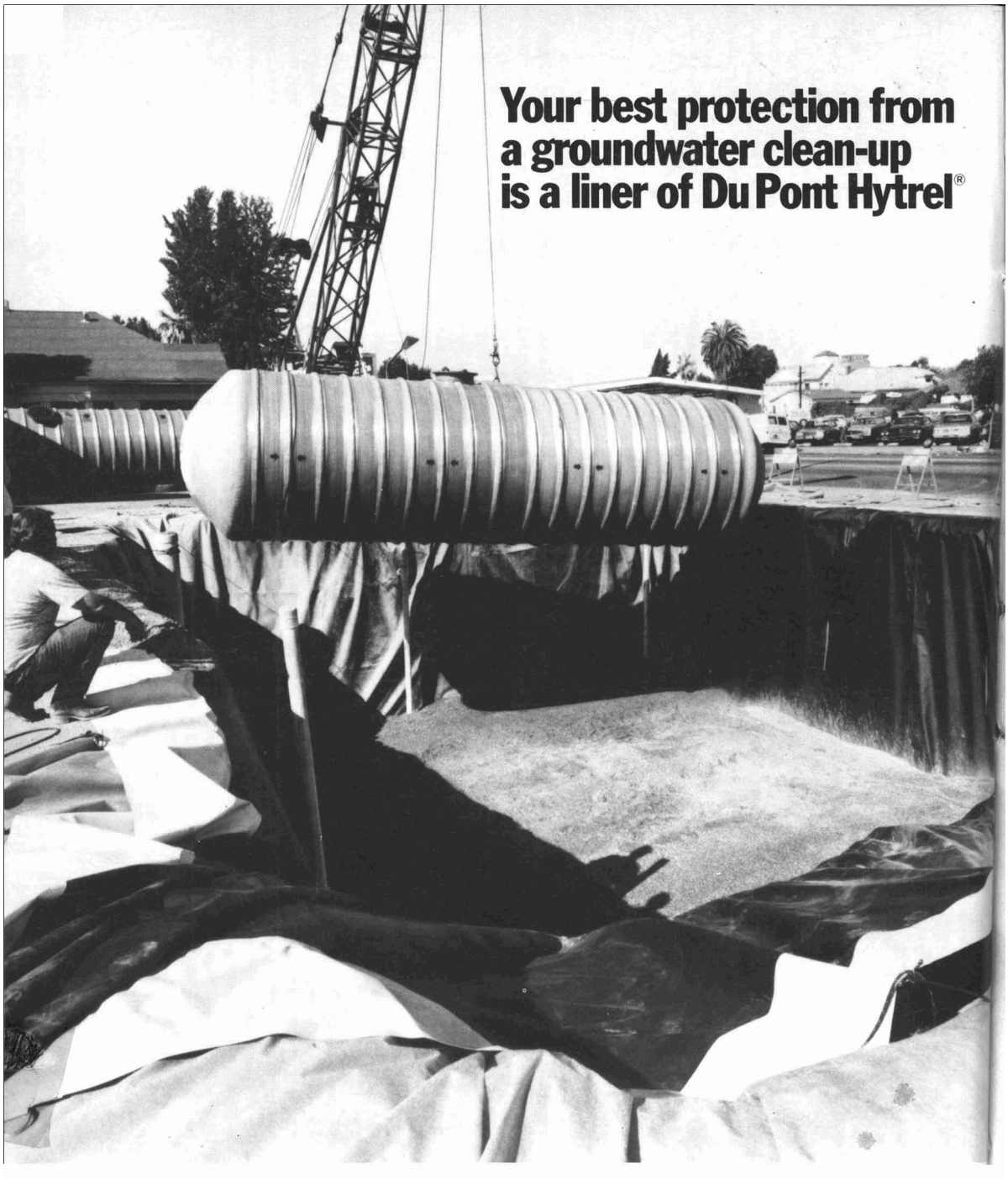

A secondary containment liner of Du Pont HYTREL* polyester elastomer helps keep storage tank and piping leaks from contaminating groundwater. In fact, it can protect you from groundwater clean-ups that have already cost other companies millions of dollars.

A liner of HYTREL offers extremely low permeability. It provides superior resistance to over 200 chemicals, including common petroleum products.

Unlike double-wall tanks, a liner of HYTREL protects against leaks from pipes. And it's easier to transport and install.

A liner of HYTREL is more flexible and more resistant to wear and tear than ordinary liners. And it can withstand the stress of extreme temperatures.

So protect against a groundwater clean-up that could clean you out. Insist on liners of HYTREL, made only by Du Pont. For more information, dial Du Pont first at (800) 527-2601.

*Du Pont makes HYTREL polyester elastomer, not secondary containment liners.

DU PONT

REG. U.S. PAT. & TM. OFF.

Environmental Science & Technology

Please send *research* manuscripts to Manuscript Reviewing, *feature* manuscripts to Managing Editor. For editorial policy, author's guide, and peer review policy, see the January 1987 issue, page 27, or write Monica Creamer, Manuscript Reviewing Office, *ES&T.* A sample copyright transfer form, which may be copied, appears on the inside back cover of the January 1987 issue.

Environmental Science & Technology, ES&T (ISSN 0013-936X), is published monthly by the American Chemical Society at 1155 16th Street, N.W., Washington, D.C. 20036. Second-class postage paid at Washington, D.C., and at additional mailing offices. POSTMASTER: Send address changes to *Environmental Science & Technology,* Membership & Subscription Services, P.O. Box 3337, Columbus, Ohio 43210.

SUBSCRIPTION PRICES 1987: Members, $30 per year; nonmembers (for personal use), $45 per year; institutions, $176 per year. Foreign postage, $8 additional for Canada and Mexico, $16 additional for Europe including air service, and $24 additional for all other countries including air service. Single issues, $15 for current year; $19 for prior years. Back volumes, $219 each. For foreign rates add $2 for single issues and $10 for back volumes. Rates above do not apply to nonmember subscribers in Japan, who must enter subscription orders with Maruzen Company Ltd., 3-10 Nihon bashi 2 chome, Chuo-ku, Tokyo 103, Japan. Tel: (03) 272-7211.

SUBSCRIPTION SERVICE: Orders for new subscriptions, single issues, back volumes, and microform editions should be sent with payment to Office of the Treasurer, Financial Operations, ACS, 1155 16th St., N.W., Washington, D.C. 20036. Phone orders may be placed, using Visa, Master Card, or American Express, by calling the ACS Sales Office toll free (800) ACS-5558 from anywhere in the continental U.S. (In the Washington, D.C., area call 872-4600.) Changes of address, subscription renewals, claims for missing issues, and inquiries concerning records and accounts should be directed to Manager, Membership and Subscription Services, ACS, P.O. Box 3337, Columbus, Ohio 43210. Changes of address should allow six weeks and be accompanied by old and new addresses and a recent mailing label. Claims for missing issues will not be allowed if loss was due to insufficient notice of change of address, if claim is dated more than 90 days after the issue date for North American subscribers or more than one year for foreign subscribers, or if the reason given is "missing from files."

ES&T CONTENTS

Volume 21, Number 8, August 1987

CRITICAL REVIEW

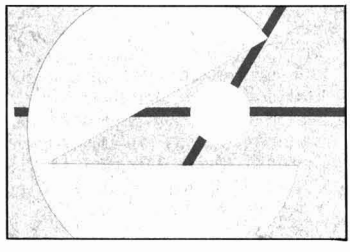

FEATURE

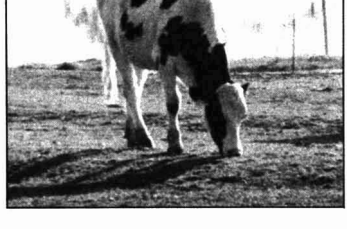

VIEWS

REGULATORY FOCUS

DEPARTMENTS

UPCOMING

Cancer risk series, Part I—the role chemicals play in carcinogenesis

How personal computers facilitate environmental engineering—trends and perspectives

RESEARCH

ESTHAG 21(8)713–824 (1987)

ISSN 0013 936X

Cover: Department of Agricultural Communications, North Carolina State University

Credits: 737, 741, Department of Agricultural Communications, North Carolina State University

754
An abundant chlorinated furanone in the spent chlorination liquor from pulp bleaching. Lars M. Strömberg,* Filipe de Sousa, Pierre Ljungquist, Bruce McKague, and Knut P. Kringstad

A large peak occurring in the gas chromatograms (ECD) when spent liquors are analyzed for chlorinated phenols is identified and characterized.

■ 757
Characterization of mutagenic subfractions of diesel exhaust modified by ceramic particulate traps. Linda D. Dorie,* Susan T. Bagley, David G. Leddy, and John H. Johnson

Protocols are developed to characterize the chemical and biological changes produced in hydrocarbon emissions by the use of ceramic particulate traps.

765
Toxic chemicals, including aromatic and chlorinated hydrocarbons and their derivatives, and liver lesions in white croaker *(Genyonemus lineatus)* from the vicinity of Los Angeles. Donald C. Malins,* Bruce B. McCain, Donald W. Brown, Mark S. Myers, Margaret M. Krahn, and Sin-Lam Chan

A bottom-feeding fish species from the Los Angeles area is contaminated with aromatic and chlorinated hydrocarbons and derivatives and shows evidence of liver lesions (e.g., cancer).

771
Movement and neutralization of alkaline leachate at coal ash disposal sites. Masahiro Sakata

The results of chemical analysis done on core samples of coal ash and soil taken from two coal ash disposal sites in Japan are discussed.

777
Aqueous ozonolysis products of methyl and dimethylnaphthalenes. Michael D. Gaul,* Gregor A. Junk, and Harry J. Svec

The ozonolyses of 1- and 2-methylnaphthalene and 1,2-, 1,3-, 1,4-, and 2,3-dimethylnaphthalene are performed in dilute aqueous solution, and the resulting nonperoxidic products are characterized.

785
Biouptake of chlorinated hydrocarbons from laboratory-spiked and field sediments by oligochaete worms. Barry G. Oliver

Uptake and depuration of 37 chemicals from spiked Lake Ontario sediments by oligochaete worms are studied at 8 °C and 20 °C in laboratory aquaria.

791
Structural characterization of aquatic humic material. 2. Phenolic content and its relationship to chlorination mechanism in an isolated aquatic fulvic acid. Daniel L. Norwood,* Russell F. Christman, and Patrick G. Hatcher

Results from a combination of analytical techniques further implicate phenolic structures in aquatic humic material as precursors for organohalides found in drinking water.

798
Field comparison of polyurethane foam and XAD-2 resin for air sampling for polynuclear aromatic hydrocarbons. Jane C. Chuang,* Steve W. Hannan, and Nancy K. Wilson

The sampling efficiencies of XAD-2 resin and polyurethane foam are studied under summer and winter ambient conditions.

■ 804
Reaction kinetics of hydrogen peroxide with copper and iron in seawater. James W. Moffett and Rod G. Zika*

Cu(I) oxidation and Fe(II) oxidation by H_2O_2 are at least as important a source of OH radicals in the ocean as nitrite photolysis.

810
Quantitation of the losses of gaseous sulfur compounds to enclosure walls. William C. Kuster and Paul D. Goldan*

Different materials are evaluated for use in the measurement of the flux of gaseous sulfur compounds from natural systems, where losses to the enclosure walls can be severe.

815
Mutagenic activity associated with cooling tower waters treated with a biocide containing 5-chloro-2-methyl-4-isothiazolin-3-one. George M. Woodall, Oscar C. Pancorbo,* R. Dean Blevins, and Kenneth E. Ferslew

The Ames *Salmonella*–mammalian test is used to determine the mutagenetic potential of water from a cooling tower treated with an organic biocide.

NOTES

821
Correlation of octanol/water partition coefficients and total molecular surface area for highly hydrophobic aromatic compounds. William J. Doucette* and Anders W. Andren

The relationship between calculated total molecular surface area (TSA) and the octanol/water partition coefficient (K_{ow}) is examined for a set of 32 highly hydrophobic aromatic compounds.

*To whom correspondence should be addressed.

■ This article contains supplementary material in microform. See ordering instructions at end of paper.

ES&T
GUEST EDITORIAL

Sunscreen

In September 1987, 31 nations will meet in Montreal to sign an agreement to freeze, and then to reduce, the rate of production of chlorofluorocarbons (CFCs)—gases that have been linked both to the destruction of stratospheric ozone and to future changes in climate. Such an international environmental agreement would be an historic step toward controlling a major threat to the atmosphere, the global climate, and human health.

Managing threats to the global environment poses tremendous challenges because of the limited success of past international environmental agreements and inequities in the standards of living among nations. The motto, *sic utere tuo ut alienum non laedas* ("use your property so as not to injure your neighbors")—often considered to be a guiding principle of international law—has had little practical influence on states' actions. Even the 1972 United Nations Stockholm Conference Declaration—that each nation has the "responsibility to ensure that activities within their jurisdiction or control do not cause damage to the environment of other states or of areas beyond the limits of national jurisdiction"—is rarely and imperfectly translated into international agreements.

In the case of controlling CFCs, however, the situation is ripe for an agreement. The scientific evidence of the atmospheric effects of CFCs is compelling, economic alternatives and substitutes are available for the most damaging of these gases, and the environmental and societal costs incurred by the destruction of ozone and from climatic changes could be overwhelming.

Yet ideological forces in the U.S. government are trying to prevent the United States from signing the final protocol despite strong support from certain sectors of the government, the scientific community, environmental groups, and even segments of the chemical industry. Last-minute opposition was signaled by Secretary of the Interior Donald Hodel and the president's science advisor, William R. Graham, Jr., who are concerned that such an accord would violate President Reagan's philosophy of minimal government regulation. This opposition has arisen despite previous administration agreement on the strong negotiating position of the United States during the talks.

Hodel's suggestion that wearing hats, sunglasses, and sunscreen could mitigate the effects of increased ultraviolet radiation is too ludicrous to deserve much comment. To their credit, EPA and the Department of State—which are responsible for the environmental negotiations in Geneva and Vienna—appear to be strongly resisting any change in the agreement, which would be a landmark in international cooperation on global environmental problems.

More is at stake here than just the CFC agreement. The reputation of the United States as a reliable negotiating partner—in arms control, environmental management, or other areas—has been seriously tarnished because of a series of agreements initially approved by the United States and then violated or abandoned. If the United States—a major producer of CFCs—were to reverse its previously strong support of the CFC protocol and back out at this point, the possibility of an effective agreement would be greatly reduced and the United States' reputation for reliability would suffer further embarrassment.

In the long term, the world faces a series of environmental threats of a magnitude never before experienced, including the possibility of massive global climatic changes. The origins and consequences of these threats are international, and there is little hope that the worst impacts can be prevented unless international environmental mechanisms are developed for addressing them. An agreement to limit or reduce emissions of CFCs would be a giant step in the right direction.

Peter H. Gleick

***Peter H. Gleick** is a MacArthur Foundation Fellow in International Security and a visiting research scholar at the University of California, Berkeley. He is a member of the Climate and Water panel of the American Association for the Advancement of Science and is active in assessing the diverse environmental impacts of global climatic changes. Previously he was deputy assistant for energy and environment to Edmund G. Brown, Jr., governor of California.*

0013-936X/87/0921-0715$01.50/0

ES&T
LETTERS

Heavy metals removal

Dear Sir: As researchers in the field of heavy metal removal by hydroxide and sulfide precipitation treatments, we wish to respond to the section on hydroxide, sulfide, and carbonate precipitation of heavy metals in "Removing dissolved inorganic contaminants from water" (*ES&T*, November 1986, pp. 1072–80).

We have been active in this field for more than four years and have published in excess of a dozen papers in the area. In the review by Clifford et al. many of the advantages cited for sulfide precipitation are described. However, the authors downplay the sulfide precipitation technology: "An obvious disadvantage of the process is the generation of toxic H_2S gas during precipitation. Furthermore, the excess sulfide ions in the treated water must be removed by aeration or oxidation with chlorine. Although technically effective, sulfide precipitation is a relatively complex and expensive process." Such concerns are indeed true for systems employing overstoichiometric addition of sulfide or for cases operating at very low pH conditions (pH < 4).

One of the primary advantages cited for employment of the insoluble sulfide precipitation technology, which uses either FeS or CaS reagents, is the elimination of the potential of H_2S gas evolution due to the very low solubilities of these sparingly soluble salts. However, eliminating sulfide reagent overdose in soluble sulfide precipitation processes prevents formation of the odor causing H_2S gas.

In currently operated soluble–sulfide systems that do not match demand, the process tanks must be enclosed and vacuum-evacuated to minimize sulfide odor problems. A combination of sulfide and lime processes for removal of heavy metals such as Pb, Zn, Cu, Cd, As, and Hg has been in successful operation since 1978 at the Boliden Metal Corporation in Sweden. The full-scale plant capacity is 200 mr/hr (1.27×10^6 gal/day) from nonferrous metal production processing.

The authors also state that "Heavy metals, such as barium, cadmium, copper, lead, mercury, nickel, silver, and zinc can be removed by hydroxide or sulfide precipitation or by a combination of the two processes." No advantages are cited for this coprecipitation process, which employs both hydroxide and sulfide precipitation. We have investigated the effect of sulfide dosage on multimetal-laden wastewaters. Attention has been focused primarily on the understoichiometric addition of sulfide. The sulfide is added stoichiometrically for the least soluble of the metal sulfides contained in the multimetal system. We have employed dosages as low as 0.5x stoichiometric dosage (for the entire metal system) and have still observed excellent removals ($> 99\%$) of the metals, even in the presence of complexing agents.

Another benefit is the absence of any noticeable H_2S gas evolution in our reaction systems. Another advantage is the excellent removal of the other metals involved through a coprecipitation mechanism. Metal sulfide precipitation systems yield significantly lower residual metal concentrations than can be obtained solely by hydroxide precipitation; with more stringent residual metal concentrations being considered by EPA and various industries, hydroxide treatment alone may not be able to meet these new metals concentration criteria.

The sludge dewatering characteristics and settling properties are much better for the metal sulfide systems than for the corresponding metal hydroxide system due to the formation of a more crystalline precipitate. The systems can also be operated at a much lower pH condition (pH 3–5) than that for semicomparable metal removal by hydroxide precipitation (typically pH 9–11). Many of the industrial plating wastewaters could be treated with this operation without pH adjustment and at much lower chemical costs due to the lower pH condition involved.

We wish to point out that this sulfide and sulfide–hydroxide precipitation technology is gaining popularity as a removal technique for heavy metals from solution. Several ongoing studies of sulfide precipitation of heavy metals are in progress at various universities, consulting firms, research laboratories, and industries, and at least four full-scale applications have been or are being installed at various industries.

Robert W. Peters
Purdue University
West Lafayette, Ind. 47907

Dibakar Bhattacharyya
University of Kentucky
Lexington, Ky. 40506

The authors reply:

We are grateful to *ES&T* for making available to its readers more details on sulfide and combined hydroxide–sulfide precipitation through the publication of these letters. This detail was not possible in our "all-encompassing" article.

We are somewhat surprised by the nature of the Peters and Bhattacharyya letter, because we believe that we have briefly and fairly pointed out the salient advantages and disadvantages of the sulfide precipitation process. Quoting from p. 1074 of our original article:

"Sulfide precipitation using soluble Na_2S or sparingly soluble FeS can remove heavy metals effectively even in the presence of complexing and chelating agents. Because metal sulfides are generally less soluble than the corresponding hydroxides, better removal efficiencies are achieved with sulfide precipitation over a broad pH range. In addition, metal sulfides are less amphoteric and are less likely to resolubilize than are metal hydroxides. Finally, sulfide sludges usually have smaller volumes and are easier to dewater than are hydroxide sludges.

"An obvious disadvantage of the process is the generation of toxic H_2S gas during precipitation. Furthermore,

Continued on p. 745

0013-936X/87/0921-0716$01.50/0

Linking Value to Performance.

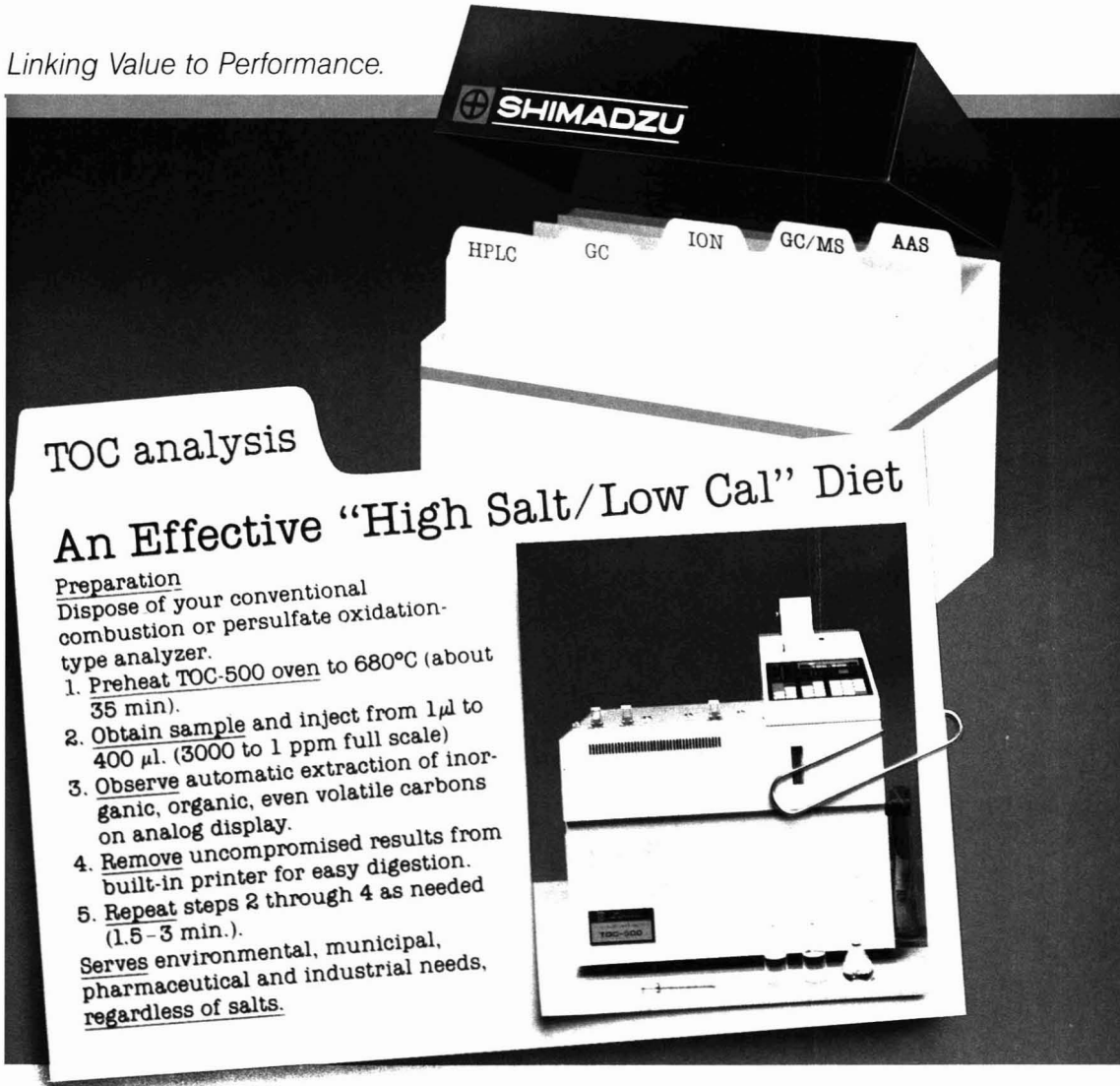

Shimadzu's recipe for troublefree TOC.

Shimadzu's new TOC-500 Total Organic Carbon Analyzer trims maintenance costs by doing away with the molten salts that devitrify combustion tubes at high temperatures and generally foul an analyzer's insides. And it does this with "low-cal" heat—only 680°C, well below saline melting points. This low-cal diet means vastly extended combustion tube, catalyst and furnace life, low downtime (a new combustion tube takes only 5 minutes to install, without furnace-cooling), and high reproducibility.

That's only the beginning. You also get up to five times faster results, often with more sensitivity than wet chemical methods. Because the TOC-500 measures peak area rather than peak height, it gives you uncompromised precision. And Shimadzu's proprietary catalyst system and humidified carrier gas assure a low system blank.

And that's not all: The TOC-500 can take injection gulps from 1 μl to 400 μl and still stay agile. It has a standard IC channel, analyzes sea water as easily as ultrapure, can handle volatile organic carbons, and offers a 36-place autosampler option and fast, versatile microcomputer-controlled data processing.

Use the TOC-500 to monitor industrial effluents, municipal waste water systems, water potability, product purity, sea water organics, or use it for any other similar application—and see why over 300 of these instruments have been in the field for more than three years without having a furnace failure.

Let us show you some of the attractive curves and figures the budget-slimming, "high-salt/low cal" TOC-500 can produce for you. Call or write for further details.

Shimadzu Scientific Instruments, Inc.
7102 Riverwood Drive, Columbia, MD 21046
(301) 381-1227

SHIMADZU

INTERNATIONAL

The United Nations Environment Program (UNEP, Nairobi, Kenya) established the Global 500 honors list during World Environment Day ceremonies on June 5. By 1992 the list will recognize 500 individuals and organizations that have made contributions toward preserving and improving the global environment. Administrators, journalists, scientists, parliamentarians, and urban and rural activists may try to qualify for a listing. Global 500 was announced on the 15th anniversary of the founding of UNEP.

FEDERAL

EPA Administrator Lee Thomas signed an advance notice of rule making regarding the technical assistance grants (TAG) program authorized under Section 117(e) of the Superfund Amendments and Reauthorization Act of 1986 (*Fed. Regist.* **1987,** *52*, 22244). The objective of the TAG program is to assist citizens of communities affected by Superfund site cleanups in interpreting technical information pertaining to the cleanup and in making informed comments. The sites involved are those listed on the National Priority List. The TAG program can provide grants of up to $50,000 to groups that need assistance in preparing technical comments.

Sen. Dave Durenberger (R-Minn.) has introduced what he says is "a comprehensive groundwater bill" whose initial goal is the "non-degradation of groundwater." According to Durenberger, "Non-degradation doesn't mean zero discharge, nor does it mean banning septic tanks and fertilizer applications. But it does mean preventing contamination of our groundwater resources wherever we reasonably can." Durenberger adds that his bill focuses on sources of contamination and calls for EPA to assist states in establishing standards for corrective action at facilities that

Durenberger: Prevent degradation

are potential sources of contamination. He hopes that his bill will be to groundwater what the Clean Water Act is to the protection of surface water.

Certain Reagan administration officials have voiced opposition to a recent 31-nation agreement to freeze levels of production of chlorofluorocarbons (CFCs) and to reduce their production by 20% over the next 10 years. The aim of the agreement is to protect the Earth's stratospheric ozone layer that filters out ultraviolet rays. Interior Secretary Donald Hodel, concerned about the increase in government regulation that would result from the agreement, suggested a controversial alternative of personal protection whereby individuals would wear hats and sunglasses and use sun-screening lotions. White House Science Adviser William Graham, Jr., cited "substantial uncertainties" concerning the causes and rate of ozone loss. State Department and EPA officials who helped to negotiate the CFC agreement fear that their positions may be undercut by the administration.

The National Acid Precipitation Assessment Program (NAPAP) has suspended its efforts to evaluate the economic benefits of acid deposition control, according to a report by the General Accounting Office (GAO). The report says that this work was stopped because of flaws in scientific techniques and inadequate data. GAO analysts also say that NAPAP's estimates of damage to forests use hypothetical scenarios. They add that NAPAP's director of research informed them that the program will carry out no further economic analyses of effects of acid deposition until these effects can be quantified. NAPAP, which has spent about $300 million on acid deposition research since 1982, consists of officials from EPA and the Departments of Agriculture, Commerce, Energy, and the Interior.

Regulations issued on June 3 by EPA tighten ambient air quality standards for fine particles. Under prior regulations, all particulate matter was limited to 260 $\mu g/m^3$ of ambient air. Under the new rules, the 24-hour standard for particles with diameters of 10 μm or less will be 150 $\mu g/m^3$. Moreover, there will be an annual standard of 50 $\mu g/m^3$. Fine particles such as dust, dirt, soot, and smoke are considered a threat to human health because they can reach the deepest portions of the lungs and cause respiratory problems. Regulations aimed at controlling these particles, which may cost industry as much as $1.9 billion, will have the biggest impact on electric utilities and on iron and steel plants. States are given five years to come into compliance.

EPA has proposed to make it easier for mobile hazardous-waste treatment units to obtain permits. Currently, owners of mobile units must follow the same cumbersome and time-consuming procedures as those for stationary facilities, for which it takes about a year to obtain a permit. Under EPA's proposal, the amount of time involved would be reduced to "a few months," and one permit would apply throughout a state. The mobile unit, however, also would require a site-specific permit that incorporates general operating conditions as well as those pertaining to

0013-936X/87/0921-0718$01.50/0

the particular site. Agency spokesmen say that they took this action to encourage alternatives to land disposal of waste and to help reduce risks inherent in the transportation of hazardous wastes.

STATES

Atmospheric scientists will fly through storm clouds over Ohio to collect air and rain samples in an attempt to understand conditions that cause acid rain and to find ways to control it. Alistair Leslie of Battelle (Richland, Wash.) said that most samples will be collected in the vicinity of Columbus "because many of the materials suspected of causing acid rain, such as SO_2, NO_x, and hydrogen peroxide can be found there." The Ohio study will focus on convective systems such as thunderstorms, but samples also will be taken from clouds in cold, warm, and stationary frontal systems and during periods of clear air. Information obtained will be used to update computer models. The work is being carried out for the U.S. Department of Energy.

New Jersey Gov. Thomas Kean has halted all development on the state's remaining 300,000 acres of wetlands through December 1988. He said that the purpose of his executive order is to protect water quality, fish, and wildlife and to provide flood control. Kean's action directs Richard Dewling, New Jersey's commissioner of environmental protection, to deny all permits in wetlands unless a developer applying for a permit demonstrates "a compelling public need or an extraordinary hardship." The order excludes the coastal wetlands, Pinelands, and Hackensack Meadowlands, which are governed by other laws. Commercial developers are considering a court challenge to Kean's order.

The state of Washington has proposed several environmental priorities for fiscal year 1988. One is to maintain existing basic programs. Another is to develop a state plan for complying with EPA's new standards for particles less than 10 μm in diameter and to strengthen controls on toxic air contaminants. State officials also plan to devise a comprehensive approach to groundwater management, including wellhead and sole-source aquifer protection. They also plan to implement a pretreatment program for toxic materials discharged indirectly through privately owned treatment works. Hazardous-

Soil treatment system

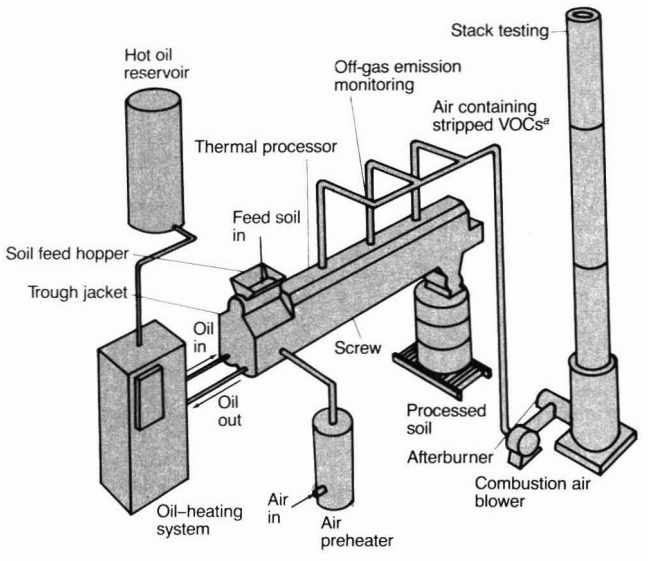

[a]VOCs = volatile organic carbons

Source: *The Weston Way* **1987**, *13*(2), 27–29; Roy F. Weston, Inc.: West Chester, Pa.

waste management, including tighter controls on radioactive waste disposal at Hanford, will be part of the general program, as will implementation of the Safe Drinking Water Act amendments of 1986. The tasks will be apportioned among the Departments of Ecology and Social and Health Services.

Small businesses in Pennsylvania can get help in minimizing their production of hazardous waste from a report, "Hazardous Waste Minimization Manual for Small Quantity Generation," published by the University of Pittsburgh's Center for Hazardous Materials Research. The 250-page report discusses the advantages of waste minimization, regulations affecting small-quantity generators, compliance with the Pennsylvania right-to-know law, conducting waste audits, and waste minimization practices specific to industries or to particular wastes. Eleven industry sectors, including electroplating printing and dry cleaning, are covered.

SCIENCE

Ozone cannot account for the total amount of decline of some American forests, according to scientists at the Electric Power Research Institute (EPRI, Palo Alto, Calif.). Other causes of stress should be examined, including climate, disease, and forest management practices. In examining 11 case studies from four regions of the United States, an EPRI project team found that only the ponderosa pine forests of the San Bernardino Mountains (Calif.) had damage from ozone, and that this forest's population is changing over to ozone-tolerant oaks and shrubs. The EPRI scientists say that ozone may be one factor contributing to forest decline, but that it must be evaluated in conjunction with other factors.

The dispersal and dilution of pollution in the ocean may be much slower and less widespread than originally thought, according to Frederick Browand of the University of Southern California. Pollutants generally sink to depths below 92 m, where turbulence and mixing are infrequent and concentrations of pollutants can remain localized and undiluted for months. Browand notes that upper, turbulent layers and lower, calmer layers of the ocean occasionally are mixed, and he suggests that the nature and frequency of this type of mixing should be studied carefully. If it must be done at all, ocean disposal of wastes might be carried out in a highly selective manner and timed to coincide with periods of mixing, he says.

TECHNOLOGY

Soils contaminated by material from leaking underground storage tanks can be treated by a process called Low Temperature Thermal Treatment, developed by Roy F. Weston, Inc. (West Chester, Pa.). Contaminated soils go through a screw conveyor where organic contaminants are volatilized at temperatures of up to 316 °C. A purge gas, normally air, enhances contaminant removal. The removed organic contaminants can be destroyed by high-temperature incineration in an afterburner or recovered by condensation or adsorption onto granular activated carbon. The system, which can be designed to be mobile, was developed under contract with the U.S. Army Toxic and Hazardous Materials Agency.

Ozone is an effective biocide for cooling tower water, says H. Banks Edwards, P.E. (*Journal of the Cooling Tower Institute* 1987, *8*(2), 10–21). He explains that water and sewage costs are reduced because of the elimination of blowdown (bleed-off of spent tower water). Edwards says that ozone also reduces or eliminates biomass, including the Legionnaires Disease Bacteria, and that it oxidizes numerous organic and inorganic contaminants. Moreover, neither pH control nor other chemicals are needed when ozone is applied at 10,000–15,000 ppm. Edwards adds that additional costs for electric power to generate the ozone and for laboratory analysis of treated tower water are more than offset by reduced costs for water, sewage treatment, chemicals, and maintenance.

Organic air contaminant sources, whether natural, manmade, or both, can be identified by a radiocarbon dating method developed by the National Bureau of Standards (NBS). The sample is converted to a solid carbon pellet about the size of a dime, whose ratio of unstable carbon-14 to stable carbon-12 is determined in a minicounter by accelerator mass spectroscopy. For example, lower levels of carbon-14 that contain carbon monoxide (CO), such as that found in air samples from Clark County, Nev., show that the most likely source of the CO is automotive exhaust from the combustion of fossil fuels. A higher proportion of carbon-14 to carbon-12 would suggest a source such as wood burning or tree emissions. NBS scientists envision this method as a way to pinpoint sources of pollution for regulatory action and to help to exonerate those sources that do not emit organic pollutants to the air.

Nuclear power plant wastes could be stored at the plants for the next 100,000 years at much lower cost than hauling them to central repositories and burying them, says Duane Chapman of Cornell University. Two wastes are involved: used uranium fuel and contaminated material from the plant. But the plants themselves, which could be contaminated, may remain on site after closure, Chapman points out, adding, "If the reactors will be left on site, why move hundreds of thousands of tons of spent fuel around the country?" Chapman notes that plant dismantlement technology is poorly understood and could cost as much as $3 billion per plant. In addition, central repositories are very expensive, and because spent fuel loses 98% of its radioactivity in 100 years, it becomes less dangerous with the passage of time.

BUSINESS

Scientists from General Electric have stated that polychlorinated biphenyls (PCBs) are being broken down in New York's Hudson River by a two-stage natural bacterial process. PCBs containing three or more chlorine atoms are broken down into PCBs containing fewer chlorines, which then can be destroyed by aerobic bacteria (*Science* **1987,** *236,* 709). The scientists estimate that 40–70 tons of PCBs already have been decomposed in this manner (as of 1977, there were believed to be 137 tons of PCBs in the Hudson River near Fort Edward and Hudson Falls, N.Y.). Stephen Safe of Texas A. & M. University concurs with this finding, but Edward Horn of the New York State Department of Health and others have stated that searches for microbes that could efficiently degrade PCBs have been unsuccessful.

Edward Addison, president of the Southern Company (Atlanta, Ga.) has characterized the acid rain bill Congress is considering as "premature, punitive, and costly." He told his company's stockholders' meeting that although coal use by utilities increased by more than 80% between 1973 and 1985, sulfur dioxide emissions decreased by 28% during the same period. "An acid rain law—imposing harsh, new limits on sulfur dioxide emissions—is definitely not needed now and may be not needed

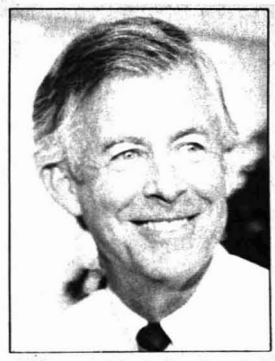

Addison: Acid rain law not needed

ever," he said, adding, "There is no crisis from acid rain." Addison said that his statement was based on "careful scientific study" that "will deflate the pressure for a multibillion-dollar program that our country simply doesn't need."

The scientific community generally supports nuclear energy, according to the Atomic Industrial Forum (AIF, Bethesda, Md.). Citing results of a survey by the Center for Media and Public Affairs, AIF spokesmen say that 71% of the scientists surveyed believe a Chernobyl-type nuclear accident is improbable in the United States. Seventeen percent viewed such an accident as probable and 12% expressed no opinion. In addition, 88% of the respondents forecast that nuclear plants will be important in meeting U.S. electricity demands in the future; the remainder attach importance to nuclear power's future role but are not as sanguine. Moreover, 66% of the scientists queried consider nuclear power as safe, 17% disagree, and 17% did not express an opinion. Respondents included 580 scientists selected from *American Men and Women of Science.*

Pyrochem (Coffeyville, Kan.), a partnership between Westinghouse and National Electric, has received a burn permit from EPA's Region VII office. The permit includes the incineration of polychlorinated biphenyls (PCBs). The Pyrochem process uses a rotary slagging kiln with a refractory surface coated with molten glass. This construction allows higher temperatures and improves heat transfer. The incinerator now may burn PCB-containing capacitors, liquids, soils, and debris. The permit, which was issued in late May after the incinerator had been in limited operation for nine months, expires July 31, 1996.

ONLY CARLO ERBA CAN MAKE IT THIS SIMPLE...

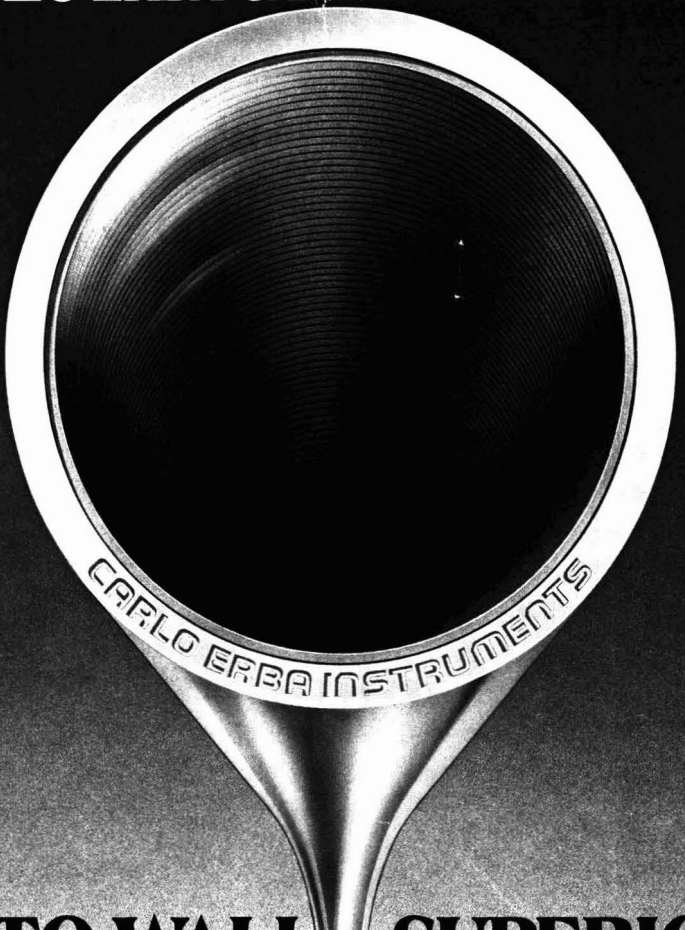

WALL-TO-WALL SUPERIORITY

Capillary GC: 1,000,000 Theoretical Plates Don't Miss Much

The highest resolution known is possible only through the utilization of wall-coated open tubular columns. This unparalleled resolution is achieved by the column's one million theoretical plates. You don't miss much of what you need to detect with capillary Gas Chromatography from Carlo Erba. You are assured of enhanced simplicity and uncompromising performance for a wide range of applications.

Vega: Higher Resolution Every Day

The Vega Series provides higher resolution in virtually all applications routinely performed in today's labs. Extremely compact, yet fully expandable with a wide range of accessories. Easy to use Vega Series combines powerful automation that includes programmable method entry with the capability to store eight methods; maximized sample throughput and unique design that reduces electronics to two boards making service quick and easy.

Mega: Highest Resolution Beyond Routine Needs

For true analytical excellence, the Mega Series provides the highest resolution obtainable. You can depend on unsurpassed temperature stability that results from our ultra stable column oven. The unique cold on-column auto sampler and patented cold on-column injector provide highly reproducible injection volumes with no sample discrimination. Selective detectors are interchangeable in seconds. They can be operated in series to provide more information from each injection. Unmatched for ease of operation, the Mega Series meets any analytical challenge through modular design, automation and a wide selection of options based on need and budget.

Tailor Made: Choose Your Options and Run

You can choose from the broadest range of options to construct the best system for your laboratory. And...you receive it ready to run.

Local Support: Leading Technology Backed by Service You Expect

State of the art technology from Carlo Erba is supported locally across the nation. You can rely on our technical support just as you can rely on our Vega and Mega—the best of capillary GC.

For wall-to-wall superiority, talk to us person-to-person: toll free 1-800-631-1369, in NJ, 201-843-2320.

HAAKE BUCHLER INSTRUMENTS, INC.
244 Saddle River Road
Saddle Brook, NJ 07662-6001

ES&T
CRITICAL REVIEW

Transformations of halogenated aliphatic compounds

Oxidation, reduction, substitution, and dehydrohalogenation reactions occur abiotically or in microbial and mammalian systems

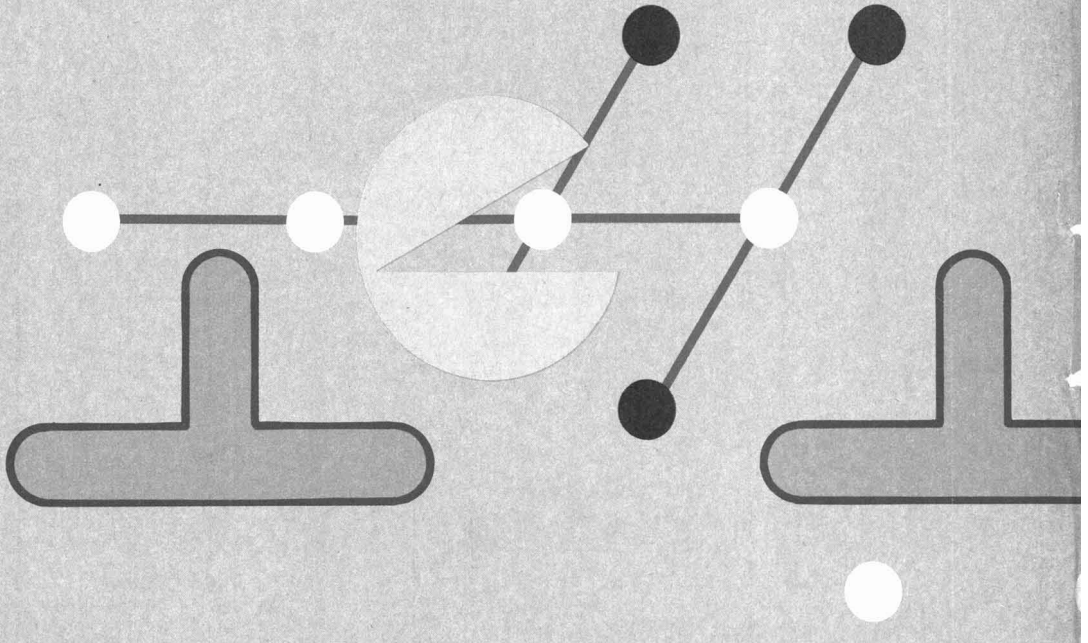

Timothy M. Vogel
Michigan State University
East Lansing, Mich. 48824

Craig S. Criddle
Perry L. McCarty
Stanford University
Stanford, Calif. 94305

Halogenated aliphatic compounds are prevalent groundwater contaminants and are significant components of hazardous wastes and landfill leachates. Most hazardous halogenated aliphatic compounds released from industrial, commercial, and agricultural sources are brominated or chlorinated alkanes and alkenes that contain between one and three carbon atoms. Chlorinated ethanes and ethenes are in common use as cleaning solvents in dry-cleaning operations and semiconductor manufacture. Some brominated compounds, such as 1,2-dibromoethane (EDB) and 1,2-dibromo-3-chloropropane (DBCP), are used as pesticides (*1*, *2*). In addition, brominated and chlorinated methanes are produced as a result of chlorination of water (*3*). The production and use of halogenated aliphatic compounds and their apparent hazard to human health (Table 1) (*4–6*) have prompted investigations concerning their fate in the human body, in subsurface waters, and in treatment facilities. In most of these environments, photolysis is not an important transformation process, but other abiotic transformations can be significant. Often, biologically mediated transformations are the most important.

This article summarizes and systematizes the current understanding of abiotic and biotic chemistry of halogenated aliphatic compounds. Knowledge of abiotic transformations can provide a conceptual framework for understanding biologically mediated transformations. Most abiotic transformations are slow, but they can still be significant within the time scales commonly associated with groundwater movement. In contrast, biotic transformations typically proceed much faster, provided that there are sufficient substrate and nutrients and a microbial population that can mediate such transformations. Recent studies, which describe transformations of halogenated aliphatic compounds in microbial and mammalian systems, are also discussed in this article. These studies reveal broad patterns of transformation in biological systems in general.

All three systems (abiotic, mammalian, and microbial) have similarities in

0013-936X/87/0921-0722$01.50/0

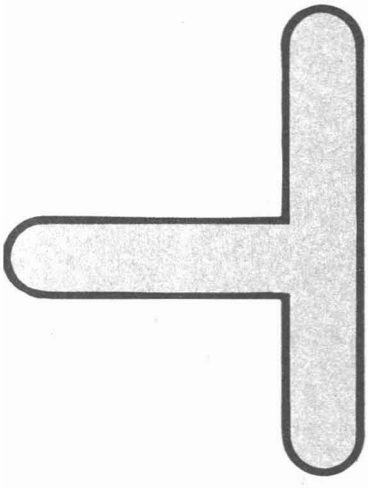

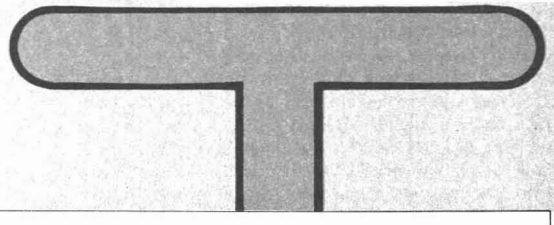

TABLE 1
Production, proposed maximum contaminant levels, and toxicity ratings of common halogenated aliphatic compounds

Compound	Production[a] (million lb/yr)	MCL[b] (μg/L)	Carcinogenicity[c]
Trihalomethanes		100	
Vinyl chloride	7000	1	1
1,1-Dichloroethylene	200	7	3
trans-1,2-Dichloroethylene	<0.001	—	—
Trichloroethylene	200	5	3
Tetrachloroethylene	550	—	3
1,1-Dichloroethane	<0.001	—	—
1,2-Dichloroethane	12,000	5	2
1,1,1-Trichloroethane	600	200	3
1,2-Dibromoethane	332[d]	—	3[d]

[a]Reference 4.
[b]Maximum contaminent level, Reference 5.
[c]Carcinogenicity: 1 = chemical is carcinogenic; 2 = chemical probably is carcinogenic; 3 = chemical cannot be classified.
[d]Reference 6.

reaction mechanisms and transformation products. They also have differences. For each, the transformation of halogenated aliphatic compounds can be divided into two general classes: reactions that require external electron transfer (oxidations and reductions) and those that do not (substitutions and dehydrohalogenations). External electron transfer is defined as the transfer of electrons to and from some agent other than the halogenated compound itself. Processes discussed in this article and terms that frequently appear are defined in the side bar. Examples of transformations are listed in Figure 1. Common abbreviations for the various halogenated aliphatic compounds are listed in Table 2.

Substitution

Halogenated aliphatic compounds undergo substitution and dehydrohalo-

Definitions of terms

Coupling—a reaction in which two alkyl or aryl groups connect together.

Dehydrohalogenation—elimination of HX to form an alkene.

Dihalo-elimination—reductive elimination of two halide substituents to form an alkene.

Electrophile—a reacting specie that accepts an electron pair.

Elimination—a reaction in which two groups, such as hydrogen and chlorine, are lost from adjacent carbon atoms so that a double bond is formed.

Epoxidation—a reaction in which an epoxide is generated.

Hydrogenolysis—a reduction in which a carbon–halogen bond is broken and hydrogen replaces the halogen substituent.

Hydroxylation—addition of a hydroxyl group.

Ionization potential—the difference between the energy of ultraviolet radiation used to bombard a molecule and the energy of the ejected electron.

Monooxygenase—an enzyme that catalyzes reactions in which one atom of O_2 appears in the product and the other in H_2O.

Nucleophile—a reacting specie that brings an electron pair.

Solvolysis—a reaction in which the solvent serves as the nucleophile.

Substitution—a reaction in which one substituent on a molecule is replaced by another.

genation in water in the absence of inorganic or biochemical catalysts. In general, these reactions proceed slowly, with half-lives of days to centuries. However, rates can be accelerated by the activity of biologically derived enzymes such as hydrolases or glutathione *S*-transferases.

Solvolysis of halogenated aliphatic compounds in water (hydrolysis) leads initially to the production of alcohols (*7*) (Figure 1, Ia). If these alcohols are halogenated, then subsequent hydrolysis to acids or diols can occur. Hydroxy substitution generally occurs at the halogenated carbon. In general, these substitution reactions are bimolecular. Nevertheless, pseudo-first-order kinetics are observed in aqueous solutions in which water is the dominant nucleophile. These reactions are potentially faster at higher pH, and the hydroxide ion acts as the nucleophile. However, below pH 11, a pH dependence for substitution reactions is generally not observed (*8, 9*). High ionic strength may increase the likelihood of unimolecular reactions as a result of increased stability of charged intermediates.

A summary of half-lives for several chlorinated and brominated aliphatic compounds in aqueous solution is shown in Table 3 (*8–20*). In general, monochloro- and monobromoalkanes hydrolyze with half-lives of about one month at 25 °C; polychlorinated species hydrolyze less readily. For dichlorinated alkanes, substitution (hydrolysis) is more likely than dehydrohalogenation, which also is possible. The nature of the halogen substituents and the degree of halogenation influence substitution rates (Figure 2). Bromine, a better leaving group than chlorine (*7*), is lost from haloaliphatic compounds more readily than is chlorine. Increased halogenation leads to slower substitution reactions and longer half-lives (*8, 9*). Abiotic substitution reactions might also be enhanced by catalysts such as clays (*20*).

Sulfides also react with halogenated aliphatics via substitution to produce mercaptans (*21*) (Figure 1, Ib). Chemically, the sulfhydryl group (SH-) is more reactive than the hydroxyl group (OH-) or water (*7*), although concentrations in natural waters are usually not high enough for sulfhydryl-related reactions to dominate.

Substitution reactions also can occur in mammalian systems (Table 4) (*22–29*). Glutathione reacts with halogenated aliphatic compounds to produce sulfur-containing compounds. Under proper conditions, these compounds are further transformed into mercapturic acids (*28*). Some chlorinated alkanes are transformed into alcohols in

FIGURE 1
Abiotic and biotic reactions of halogenated aliphatic compounds

Reactions	Examples
I. Substitution	
(a) solvolysis, hydrolysis $RX + H_2O \longrightarrow ROH + HX$	$CH_3CH_2CH_2Br + H_2O \longrightarrow CH_3CH_2CH_2OH + HBr$
(b) conjugation and other nucleophilic reactions $RX + N^- \longrightarrow RN + X^-$	$CH_3CH_2Br + HS^- \longrightarrow CH_3CH_2SH + Br^-$
II. Dehydrohalogenation $-\overset{|}{\underset{X}{C}}-\overset{|}{\underset{H}{C}}- \longrightarrow \diagup C=C \diagdown + HX$	$CCl_3CH_3 \longrightarrow CCl_2CH_2 + HCl$
III. Oxidation	
(a) α-hydroxylation $-\overset{|}{\underset{H}{C}}-X + H_2O \longrightarrow -\overset{|}{\underset{OH}{C}}-X + 2H^+ + 2e^-$	$CH_3CHCl_2 + H_2O \longrightarrow CH_3CCl_2OH + 2H^+ + 2e^-$
(b) halosyl oxidation $-\overset{|}{C}-X + H_2O \longrightarrow -\overset{|}{C}-\overset{+}{X}O^- + 2H^+ + 2e^-$	$CH_3CHCl_2 + H_2O \longrightarrow CH_3CHClC\overset{+}{l}O^- + 2H^+ + 2e^-$
(c) epoxidation $C=C + H_2O \longrightarrow \diagup C-C \diagdown + 2H^+ + 2e^-$	$CHClCCl_2 + H_2O \longrightarrow CHClOCCl_2 + 2H^+ + 2e^-$
(d) biohalogenation (alkenes) $C=C + X^- + H_2O \longrightarrow -\overset{|}{\underset{OH}{C}}-\overset{|}{\underset{X}{C}}- + H^+ + 2e^-$	$CH_2CH_2 + Cl^- + H_2O \longrightarrow CH_2OHCH_2Cl + H^+ + 2e^-$
IV. Reduction	
(a) hydrogenolysis $RX + H^+ + 2e^- \longrightarrow RH + X^-$	$CCl_4 + H^+ + 2e^- \longrightarrow CHCl_3 + Cl^-$
(b) dihalo-elimination $-\overset{|}{\underset{X}{C}}-\overset{|}{\underset{X}{C}}- + 2e^- \longrightarrow C=C + 2X^-$	$CCl_3CCl_3 + 2e^- \longrightarrow CCl_2CCl_2 + 2Cl^-$
(c) coupling $2RX + 2e^- \longrightarrow R-R + 2X^-$	$2CCl_4 + 2e^- \longrightarrow CCl_3CCl_3 + 2Cl^-$

FIGURE 2
Estimated half-lives for some halogenated aliphatic compounds

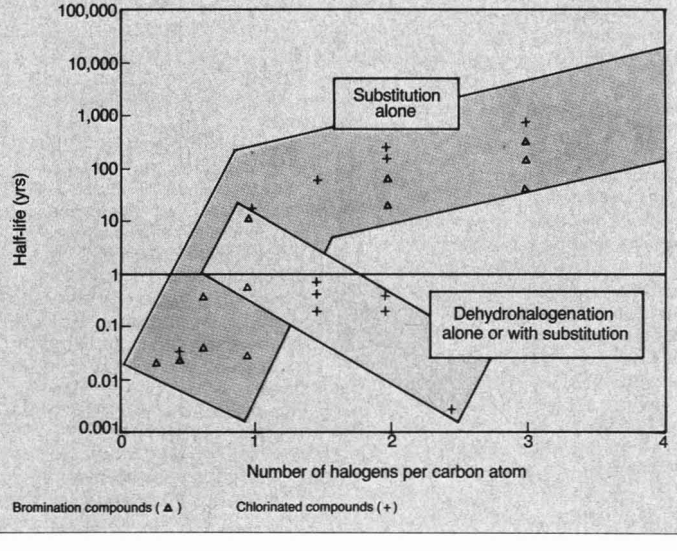

live mice, but the responsible agents are unknown. Such reactions may be simple substitution reactions—the oxidation states of carbon in both reactant and product are the same. Examples are the conversion of tetrachloromethane to carbon dioxide or dichloromethane to carbon monoxide. These reactions might in reality be a sequential combination of reductions and oxidations. For example, tetrachloromethane can be reduced to trichloromethane and subsequently oxidized to carbon dioxide via phosgene (*30*). However, for many of the transformations in mammalian systems, complete mechanistic interpretations are not yet possible because there is insufficient information.

Dehydrohalogenation

Halogenated alkanes in water also can undergo elimination reactions that produce alkenes (Figure 1, IIa). Elimination of HX is termed dehydrohalogenation or, less frequently, dehydrodehalogenation. These reactions consist of removal of a halogen from one carbon atom and concomitant (E2) or subsequent (E1) removal of a hydrogen atom from an adjacent carbon. Although the formal oxidation state of a halogenated aliphatic compound decreases as a result of the loss of a halogen, it increases with loss of hydrogen. Dehydrohalogenation reactions thus do not include external electron transfer, and no net change occurs in the oxidation state of the reacting molecule.

Monohalogenated aliphatics apparently do not undergo dehydrohalogenation in water under normal environmental conditions (see Table 3), and such reactions are unlikely to occur (*7*). Polychlorinated alkanes undergo dehydrohalogenation under extreme basic conditions (*17*), and at pH 7 (*12*). These reactions generally follow bimolecular kinetics, depending on hydroxide ion concentration. Under normal pH conditions (near pH 7), dehydrohalogenation by interaction with weaker bases (e.g., water) might be important. The number and kind of halogen substituents have a strong influence on dehydrohalogenation rates. When more chlorine substituents are attached to the carbon atom that loses a chlorine substituent, faster rates are observed. Brominated compounds tend to undergo dehydrohalogenation with fewer halogen substituents and more rapidly than their chlorinated analogues (Figure 2). Dehydrohalogenation reactions do not appear to occur with vicinal dichloroalkanes (chlorine on adjacent carbon atoms) (*12*), but they do occur, at least partially, with vicinal dibromoalkanes (*9*). This increased rate of dehydrohalogenation from compounds that contain

TABLE 2
Abbreviations used for chemical species

Abbreviation	Chemical name	Alternative chemical name
A	Ethane	
BCM	Bromochloromethane	
BDCM	Bromodichloromethane	
BF	Tribromomethane	Bromoform
BM	Bromomethane	
BTCM	Bromotrichloromethane	
CA	Chloroethane	
CF	Trichloromethane	Chloroform
CM	Chloromethane	Methyl chloride
CT	Tetrachloromethane	Carbon tetrachloride
DBCM	Dibromochloromethane	
DBCP	1,2-Dibromo-3-chloropropane	
DBDCM	Dibromodichloromethane	
DBM	Dibromomethane	
DCA	Dichloroethane	
DCE	Dichloroethene	
E	Ethene	Ethylene
EDB	Dibromoethane	Ethylene dibromide
HCE	Hexachloroethane	
M	Methane	
MC	Dichloromethane	Methylene chloride
PCA	Pentachloroethane	
PCE	Tetrachloroethene	Perchloroethylene
TCBM	Tribromochloromethane	
TCA	1,1,1-Trichloroethane	Methyl chloroform
TCE	Trichloroethene	
TEBM	Tetrabromomethane	Carbon tetrabromide
TECA	Tetrachloroethane	
VC	Chloroethene	Vinyl chloride

TABLE 3
Environmental half-lives and products from abiotic hydrolysis or dehydrohalogenation of halogenated aliphatic compounds at 20 °C

Compound	Half-life years (reference)	Product(s) (reference)
Methanes		
Dichloromethane	1.5 (*10*), 704 (*8*)	
Trichloromethane	1.3 (*10*), 3500 (*8*)	
Tetrachloromethane	7000 (*8*)	
Bromomethane	0.10 (*8*)	
Dibromomethane	183 (*8*)	
Tribromomethane	686 (*8*)	
Bromochloromethane	44 (*8*)	
Bromodichloromethane	137 (*8*)	
Dibromochloromethane	274 (*8*)	
Ethanes		
Chloroethane	0.12 (*11*)[a]	Ethanol (*11*)[a]
1,2-Dichloroethane	50 (*12*)	
1,1,1-Trichloroethane	0.5 (*10*), 1.7 (*12*)	Acetic acid (*12–14*)
	0.8 (*15*)[b], 2.5 (*16*)[c]	1,1-Dichloroethylene (*14–16*)
1,1,2–Trichloroethane	170 (*12*)	1,1-Dichloroethene (*17*)
1,1,1,2-Tetrachloroethane	384 (*12*)	Trichloroethene (*12*)
1,1,2,2-Tetrachloroethane	0.8 (*12*)	Trichloroethene (*12*)
1,1,2,2,2-Pentachloroethane	0.01 (*12*)	Tetrachloroethene (*12*)
Bromoethane	0.08 (*8*)	
1,2-Dibromoethane	2.5 (*9*)	Bromoethene (*9*)
	2.5 (*18*)	Ethylene glycol (*18*)
Ethenes		
Trichloroethene	0.9 (*10*), 2.5 (*15*)[b]	
Tetrachloroethene	0.7 (*10*), 6 (*15*)[b]	
Propanes		
1-Bromopropane	0.07 (*8*)	
1,2-Dibromopropane	0.88 (*9*)	Bromopropene (*9*)
1,3-Dibromopropane	0.13 (*9*)	Bromopropanol (*9*)
1,2-Dibromo-3-chloropropane	35 (*19*)	Bromochloropropene (*19*)

[a]Extrapolated by Z from Reference 11. [b]At 10 °C in sea water. [c]At 20 °C.

bromine substituents is consistent with the findings of Burlinson et al., who noted that bromine is eliminated from DBCP six times faster than is chlorine (*19*).

Few halogenated aliphatic compounds undergo dehydrohalogenation in mammalian systems, but there are some. 1,1,2,2-Tetrachloroethane and 1,1,1,2,2-pentachloroethane undergo dehydrohalogenation to trichloroethene and tetrachloroethene, respectively, in live mice and under reducing conditions in hepatic microsomes (Table 4).

Reaction rates. Most experiments that are used to determine reaction rates in water are performed at elevated temperatures, because reaction rates are too slow at environmental temperatures. Rates measured at higher temperatures may then be extrapolated to lower temperatures, using the Arrhenius equation (*7*):

$$\ln \frac{k_2}{k_1} = \frac{E_a}{R}\left(\frac{T_2 - T_1}{T_1 T_2}\right)$$

in which k is a rate constant, E_a is the activation energy (kJ/mol), R is the universal gas constant (8.314 J/mol-K), and T is the temperature (K). Activation energies for abiotic transformation of halogenated aliphatic compounds in aqueous solutions are about 100 ± 10 kJ/mol (*8, 9*). This translates to a 3.5-fold decrease in reaction rate for each 10 °C decrease in temperature. Many of the half-lives listed in Table 3 were extrapolated in this manner from studies conducted at higher temperatures.

Rates are often determined by use of aqueous solutions that contain high concentrations of organic solvents (e.g., 10% dioxane) (*8*). However, different investigators often report different rates, mechanisms, and products for the same compound (Table 3). In some cases, substitution may prevail at one temperature and dehydrohalogenation at another. These difficulties are at least partially responsible for the differences in reported rates (Table 3). Therefore, caution is required in using extrapolated rates, and more research is needed.

With the caution noted above, re-

FIGURE 3
Products from epoxidation of carbon–carbon double bonds

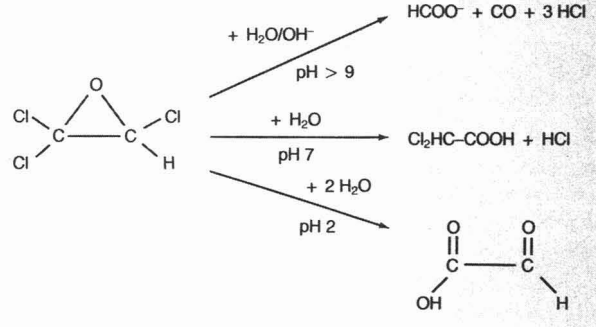

FIGURE 4
Estimated relative half-reaction reduction potentials[a]

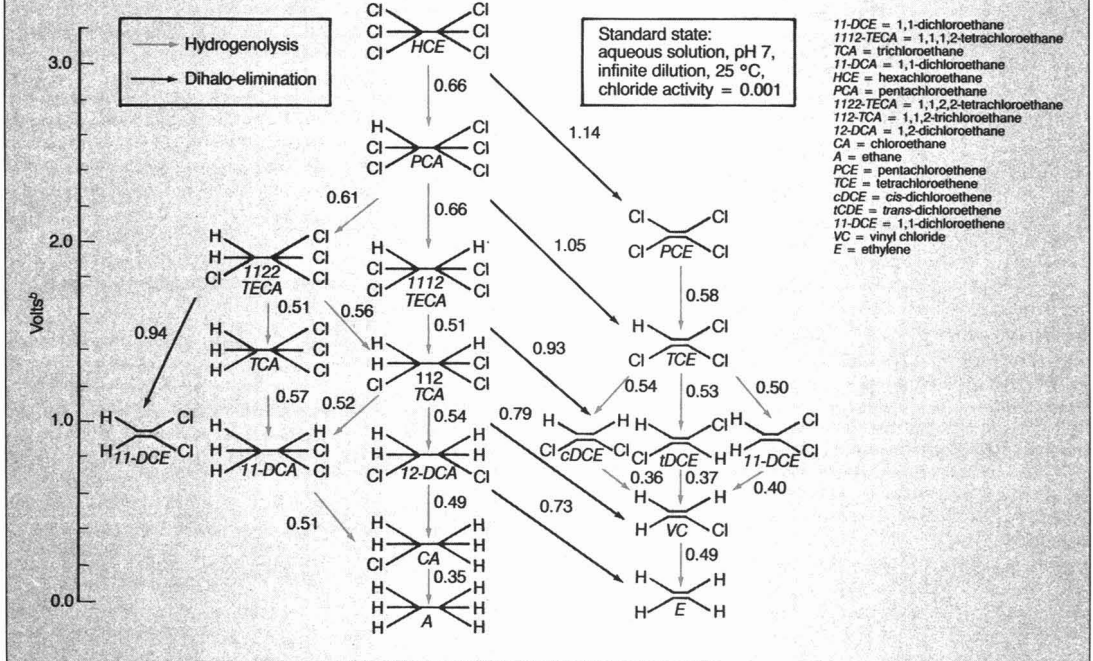

[a]In volts, for dechlorination of chlorinated alkanes and alkenes. Relative potentials are illustrated by the vertical position of the compounds. Box describes the calculations of reduction potentials.
[b]Scale of reduction potential with respect to ethane.

ported reaction rates from Table 3 are plotted as a function of the number of halogen substituents per carbon atom in Figure 2. With the possible exception of tetrachloromethane, compounds that are susceptible to substitution reactions, such as monohaloalkanes or 1,3-dihaloalkanes, and those that are susceptible to dehydrohalogenation, such as polyhaloalkanes, behave similarly in water and mammalian systems. Increased halogenation tends to decrease substitution reaction rates and increase dehydrohalogenation rates. Consequently, most highly halogenated aliphatic compounds, with the exception of C_1 compounds, mainly undergo dehydrohalogenation (Figure 2), although some undergo both reactions (*14*). Rates of dehydrohalogenation and substitution in mammalian systems generally have not been reported and are no doubt quite complex because of the many potential facilitating enzymes present. Hence, comparison of these rates with rates in water cannot be made.

Oxidations and reductions

Unlike substitutions and dehydrohalogenations, oxidations and reductions require external electron acceptors and donors, respectively (Figure 1, III and IV). Generally, organic compounds acting as electron donors undergo oxidation reactions. However, because of the electronegative character of halogen substituents on aliphatic compounds, polyhalogenated aliphatic compounds often behave as electron acceptors or oxidants and are reduced in the process. Thus, halogenated aliphatic compounds may be either oxidized or reduced, depending on their structure and environmental conditions. In most reactions described to date, the electron acceptors and donors used to oxidize and reduce halogenated aliphatic compounds are derived from biological systems.

Oxidations. Biologically mediated oxidation of organic compounds has been studied extensively. Organic compounds generally represent reduced forms of carbon, and, as such, oxidation is energetically favorable. In contrast, halogenated aliphatic compounds are relatively oxidized by the presence of halogen substituents: the more halogen substituents, the more oxidized the compound, and the more susceptible it is to reduction. Thus, with increased halogenation, reduction becomes more likely than does oxidation.

Most oxidations observed in mammalian systems (Table 5) (*23–26, 31–43*) involve monooxygenase that contains cytochrome P450. Cytochrome P450 is a heme-containing protein (with iron–porphyrin active sites) that can mediate both oxidation and reduc-

Calculations for reduction potentials

The procedure for estimating half-reaction reduction potentials contained in Figures 4–6 is as follows. Three steps were involved in the calculations for T = 25 °C (298 K). The first was estimation of the aqueous-phase free energy of formation for the compound, the second was computation of free energy changes for a given half-reaction, and the third was calculation of reduction potentials using the Nernst relationship.

1. Aqueous-phase free energy of formation values were estimated from published gas-phase free energy of formation [ΔG°_f (g)] data (*52*) and published (*71*) and estimated (*68*) values of Henry's constant (H), which related activity in the gas phase to activity in the aqueous phase at equilibrium.

$$\Delta G^\circ_f (aq) = \Delta G^\circ_f (g) + RT\ln H$$

2. Free energy changes for a given half-reaction were computed to be consistent with general principles and with Figure 5 based on the equation

$$\tfrac{1}{2}RX + \tfrac{1}{2}H_+ + e^- \longrightarrow \tfrac{1}{2}RH + \tfrac{1}{2}X^-$$ as follows:

$$\Delta G^\circ (aq) = \Sigma G^\circ_f (aq) \text{ for products } - \Sigma G^\circ_f (aq) \text{ for reactants}$$

ΔG° (aq) = standard free energy change for half-reaction,

and values thus calculated were adjusted to the desired reference state

($[H^+] = 10^{-7}$, $[Cl^-] = 10^{-3}$, $[Br^-] = 10^{-5}$), using:

$$\Delta G^{\circ\prime} = \Delta G^\circ + \tfrac{1}{2}RT\ln([X^-]/[H^+])$$

3. Reduction potentials were obtained from the Nernst relationship:

$$E^{\circ\prime} = \Delta G^{\circ\prime}/nF$$

$$\text{or } pE^{\circ\prime} = nFE^{\circ\prime}/2.3RT$$

$E^{\circ\prime}$ = reduction potential (volts)
R = universal gas constant (8.314 J/K-mol)
n = electron equivalents transferred (*52*)
F = Faraday's constant (96,487 J/volt-equivalent)
T = temperature (K)

TABLE 4
Substitution and dehydrohalogenation reactions of halogenated aliphatics in mammalian systems

Compound	Product(s)	Systems[a]	Reference
Methanes			
Dichloromethane	Carbon monoxide	hm/N	(*22*)
Tetrachloromethane	Carbon dioxide	h/GO	(*23*)
Dibromomethane	Carbon monoxide	hm/NO	(*22*)
Ethanes			
1,1,2-Trichloroethane	Dichloroethanol	M	(*24*)
1,1,2,2-Tetrachloroethane	Trichloroethanol	M	(*25*)
	Trichloroethene	M	(*25*)
1,1,1,2-Tetrachloroethane	Trichloroethanol	M	(*26*)
Pentachloroethane	Tetrachloroethene	M	(*27*)
Ethenes			
Chloroethene	Glutathione-dependent sulfur-containing organic compound	R/G	(*28*)
1,1-Dichloroethene	Glutathione-dependent sulfur-containing organic compound	R/G	(*29*)

[a]Slashes separate conditions for an individual experiment. hm = hepatic (rat liver) microsomes; R = live rats; M = live mice; N = NADH dependence; G = glutathione dependence; O = presence of oxygen.

tion reactions. Cytochrome P450-containing monooxygenase mediates oxidation of halogenated aliphatic compounds by three general mechanisms: by incorporation of oxygen in the carbon–hydrogen bond (α-hydroxylation) (*30, 44*) (Figure 1, IIIa); by oxidation of a halogen substituent (*44, 45*) (Figure 1, IIIb); and by oxidation of a carbon–carbon double bond via epoxidation (*30, 44, 46–48*) (Figure 1, IIIc).

The first mechanism leads to a substitution product, an alcohol. However, mechanistic studies have shown that atomic oxygen, derived from molecular oxygen, is inserted into the carbon–hydrogen bond (*22, 33*). Subsequently, for halogenated alcohols, the hydrogen of the hydroxy group and a halogen substituent leave as the hydrogen ion (H^+) and the halide ion (X^-), resulting in an aldehyde. Halogenated formaldehyde can be chemically transformed into carbon monoxide.

The second mechanism, halogen oxidation, proceeds via an unstable halosyl intermediate ($CH_2X^+{=}O^-$). Presumably, this species hydrolyzes rapidly to produce an alcohol and hypochlorite ion (*49*). Because an alcohol is produced, the overall reaction resembles a substitution reaction. No net oxidation of the organic compound occurs (*30*). Also, because halosoaliphatic compounds have not yet been detected, this mechanism might not actually occur with halogenated aliphatic compounds.

α-Hydroxylation of halogenated aliphatic compounds would result in the formation of acids and alcohols as described above. In contrast, β-elimination of a halosyl intermediate could result in an alkene. Therefore, the observation of alkene formation from halogenated propanes was reported by Tachizawa et al. to be indicative of a halosyl mechanism (*45*). They documented propene formation and noted that brominated alkanes undergo transformation to alkenes more readily than do chlorinated alkanes.

In mammalian systems, dihalogenated aliphatic compounds are susceptible to oxidation by either of the above mechanisms. For example, transformation of dihalomethanes to carbon monoxide under aerobic conditions has been reported (Table 4) (*22*). Overall, this is a substitution reaction, but it involves an oxidation step. Oxidation proceeds sequentially from halogenated alcohol to halogenated aldehyde before final reduction to carbon monoxide. Yllner observed that mice transformed polychlorinated ethanes to chlorinated aliphatic acids (*24–27, 34*).

The following characteristics of the third mechanism, epoxidation or the oxidation of a carbon–carbon double bond, are well documented for mammalian systems. Epoxidation is the first step in alkene oxidation that is pro-

FIGURE 5
Estimated relative half-reaction reduction potentials[a]

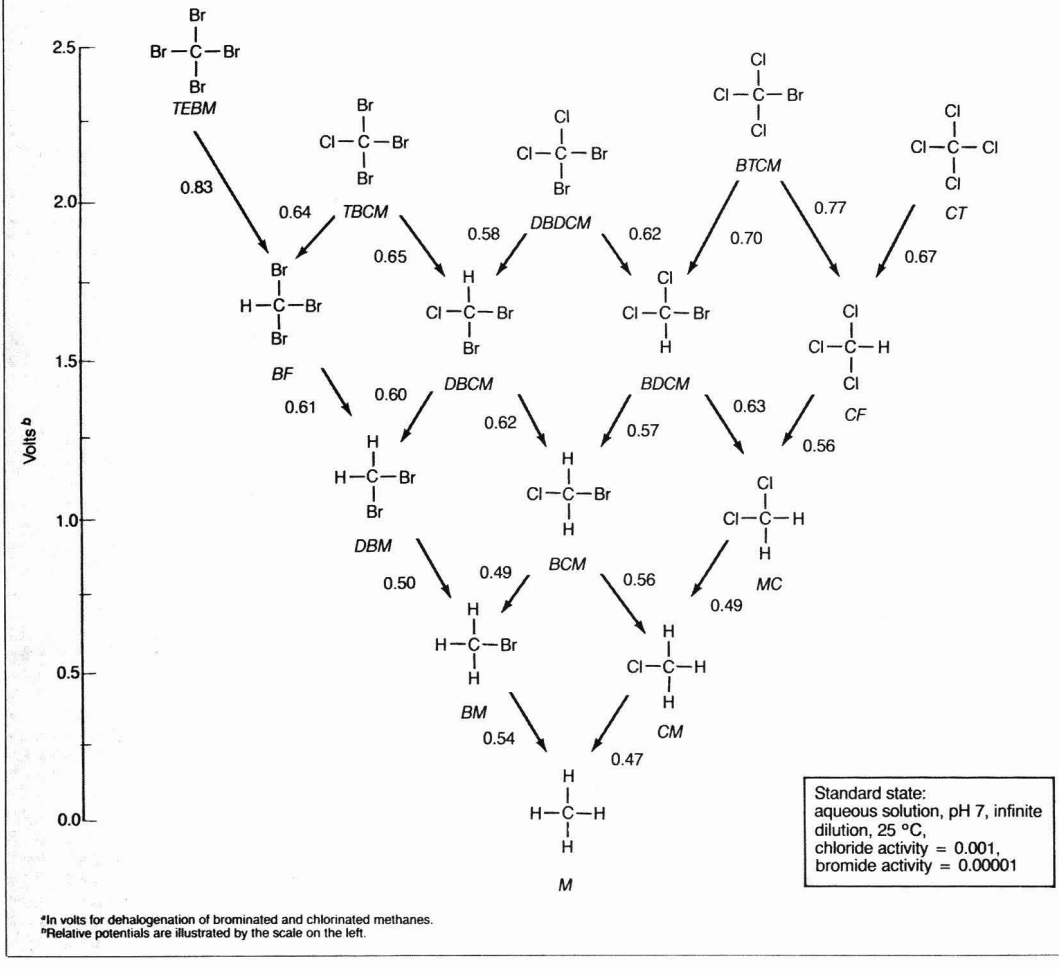

[a]In volts for dehalogenation of brominated and chlorinated methanes.
[b]Relative potentials are illustrated by the scale on the left.

moted by cytochrome P450-containing monooxygenase. The oxygen that is incorporated into halogenated alkenes is derived from molecular oxygen (*22, 33, 48*). The epoxide is normally short-lived and might undergo one of several different reactions. Halogenated aldehydes or acyl chlorides are common intermediates and are often subsequently transformed into acids (oxidation), alcohols (reduction), or hydrolyzed to acids or carbon monoxide (via acyl chlorides) (*30, 44, 48*).

Epoxide chemistry in aqueous solutions partially explains the fate of epoxides in mammals. In aqueous solution, for example, trichloroethene epoxide decomposes to formyl chloride and dichloromethanol. Subsequently, formyl chloride eliminates hydrogen chloride (HCl) to form carbon monoxide, and dichloromethanol hydrolyzes to form formate (*49*). These two products predominate at pH > 9. At lower pH, other products dominate: at pH 7, dichloroacetic acid is produced; and at pH 2, glyoxylic acid is produced.

All the products shown in Figure 3 have been observed in mammalian systems. In addition, transformation of chlorinated ethenes proceeds via chlorine migration to produce chloral (2,2,2-trichloroacetaldehyde) (*50*) (Table 5). The production of compounds such as chloral in mammalian systems, but not in aqueous solutions, may be the result of the interaction between the chlorinated epoxide and the cytochrome P450-based monooxygenase (*47*). It also may be the result of the formation of an intermediate other than the epoxide (incorporation of oxygen into the halogenated alkene) and the concomitant formation of a cationic or radical intermediate (*50*).

Ozonation of halogenated alkenes could serve as a chemical model for the epoxidation of these compounds in mammalian systems. The reaction is largely an electrophilic attack at the double bond by ozone. Ozonation rates of chlorinated ethenes decrease as the number of chlorine substituents increases (*51*). In addition, the inductive effect of additional chlorine substituents is more important in the reduction of reaction rates than the increased steric hindrance of these substituents. Ionization potential (IP) is an adequate predictor of relative ozonation rates (Table 6) (*52*). Mesomeric delocalization of positive charge by chlorine substituents decreases both IP and ozonation rates. Therefore, IP might be a reasonable predictor of relative rates of epoxidations of halogenated alkenes in biological systems.

Another substance that can be involved in the oxidation of halogenated aliphatic compounds by biological systems is glutathione. Glutathione-mediated oxidations generally occur in the soluble or cytosolic fraction of cells (*30*). Oxidation is initiated by nucleophilic attack of glutathione on the electrophilic carbon (generally one bound to a halogen) (*31*). Dihalomethanes are oxidized to formaldehyde and formic acid following conjugation with cytosolic glutathione (Table 5).

One final category of oxidation involving halogenated compounds is the phenomenon of biohalogenation. This process is widespread in nature, occurring in certain species of bacteria, fungi, algae, higher plants, and animals. It is brought about by the activity of haloperoxidases in the presence of hydrogen peroxide (Figure 1, IIId). The chemistry of these transformations is similar to that of hypohalous acids; unsaturated substrates such as ethene may be converted to halohydrins or dihalides by this process (*53*).

Reductions. Certain transition metals and transition metal complexes

TABLE 5
Oxidation of halogenated aliphatic compounds in mammalian systems

Compound	Product(s)	System[a]	Reference
Methanes			
Dichloromethane	Formaldehyde	hm/N/O	(*31*)
	Carbon dioxide	hm/O	(*32*)
Trichloromethane	Carbon dioxide	h/G/O	(*23*)
	Carbon dioxide via phosgene	hm/P/O	(*33*)
Ethanes			
1,2–Dichloroethane	Chloroacetic acid, carbon dioxide	M	(*34*)
1,1,2-Trichloroethane	Dichloroacetic acid, chloroacetic acid, carbon dioxide	M	(*24*)
1,1,2,2-Tetrachloroethane	Trichloroacetic acid	M	(*25*)
	Dichloroacetic acid, carbon dioxide	M	(*25, 35*)
		M	(*25*)
1,1,1,2-Tetrachloroethane	Trichloroacetic acid	M	(*26*)
Pentachloroethane	Trichloroacetic acid	M	(*27*)
1,2-Dibromoethane	Bromoacetaldehyde	R/G	(*36*)
Ethenes			
Chloroethene	Chloroacetic acid	hm/O	(*37*)
	2-Chloroacetaldehyde, glycolaldehyde, 2-chloroethanol	hm/P/N	(*38*)
1,1-Dichloroethene	Chloroacetic acid	hm/O	(*37*)
1,2-Dichloroethene	Dichloroacetic acid	hm/O	(*37*)
Trichloroethene	Dichloroacetic acid	R, M	(*39, 40*)
	Trichloroethanol,	hm/O	(*25, 39, 41*)
	Trichloroacetic acid	hm/P, R	
	Carbon monoxide	hm/P	(*41*)
	Carbon dioxide	hm/P	(*41*)
	Glyoxylic acid	hm/P	(*41*)
Tetrachloroethene	Trichloroacetic acid	hm/O, hm/P/N	(*37, 42*)
Bromoethene	Bromoacetaldehyde	hm/P/N	(*43*)

[a]Commas separate different experimental systems that result in similar products. Slashes separate conditions for an individual experiment. hm = hepatic (rat liver) microsomes; R = live rats; M = live mice. N = NADH dependence; P = cytochrome P450 dependence; G = glutathione dependence; O = presence of oxygen.

TABLE 6
Ionization potentials (IP) and ozonation rates (k) for some halogenated aliphatic compounds

Compound	No. of chlorines	IP[a]	k[b] (L/mol s)
Tetrachloroethene	4	9.32	1.0
Trichloroethene	3	9.45	3.6
1,2-Dichloroethene	2	9.6	591
Chloroethene	1	9.99	1180
Ethene	0	10.51	>20,000

[a]Reference 52.
[b]Reference 51.

reduce halogenated aliphatic compounds (Table 7) (*54–61*). As a result, these metals and metal complexes are themselves oxidized. Because transition metal complexes are frequently located at the active sites of the macromolecules that are used for electron transfer in living organisms, reactions between metal complexes and halogenated aliphatic compounds are useful models that simulate transformations in living organisms. Transition metals may also play a role in the abiotic reduction of certain halogenated aliphatic compounds in groundwater.

Initially, most reductions by transition metal complexes involve the transfer of a single electron and the formation of an alkyl radical. This occurs with a variety of transition metals, including nickel (*61*), iron (*62*), chromium (*63*) and cobalt (*64*), although some two-electron reductions also occur with cobalt (*54, 65*). Formation of an alkyl radical upon removal of a halogen substituent is the first and, in most cases, the rate-limiting step in the two-step reduction of halogenated aliphatic compounds:

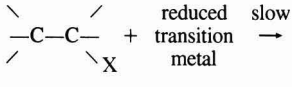

The alkyl radical that results from the above step can undergo several reactions. The simplest of these involves scavenging a hydrogen atom from the immediate surrounding matrix—possibly from the complex itself (*55*):

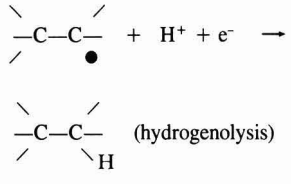

Another involves the loss of a second halogen substituent from a carbon atom adjacent to the radical carbon to form an alkene (*66*). The alkene that results from this last step is more stable and has two fewer halogen substituents, thus decreasing the likelihood of further reduction:

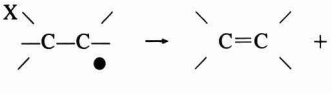

A final possibility is dimerization of the radicals:

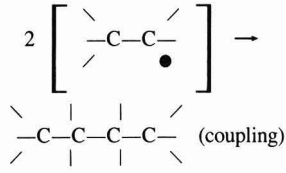

Reduction of polyhalogenated alkanes can result in the production of both alkanes and alkenes, as illustrated in Figure 1.

Formation of the alkyl radical appears to involve either the transfer of an electron to the reduced transition metal, with a standard reduction potential as the driving force, or the transfer of a halogen atom, a process governed by

FIGURE 6
Half-life reduction potentials for reducing and oxidizing agents[ab]

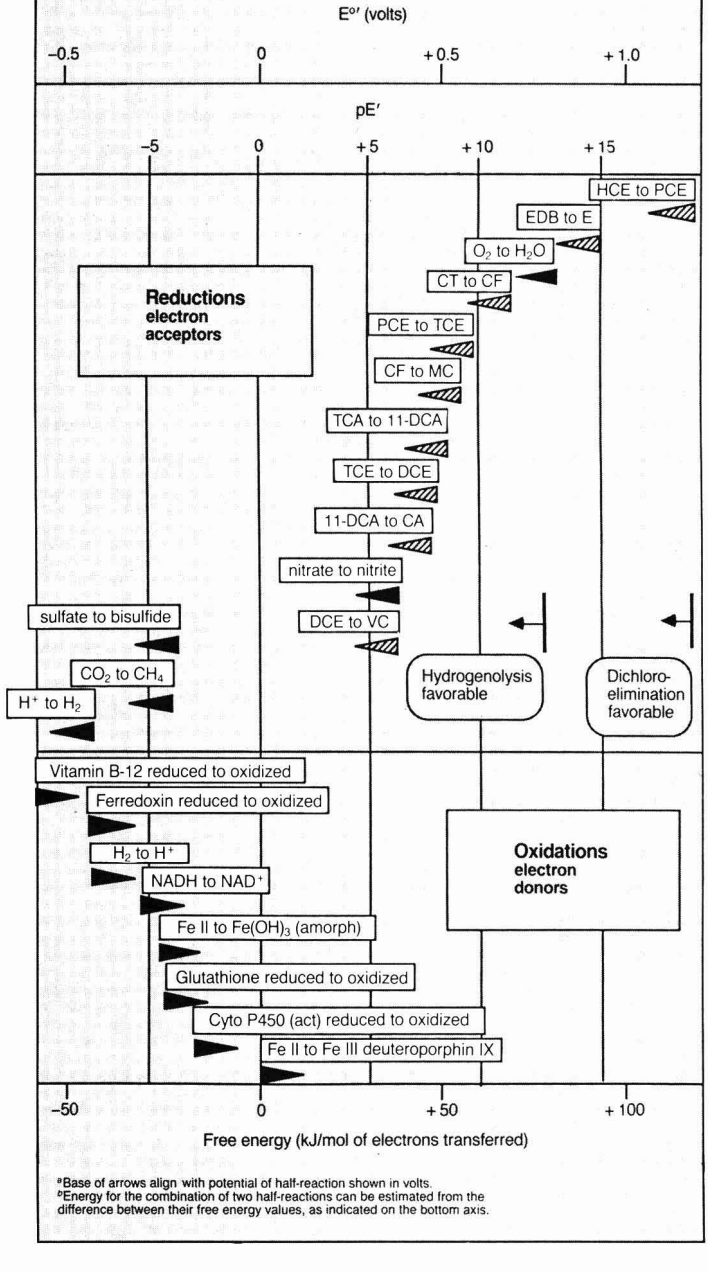

[a]Base of arrows align with potential of half-reaction shown in volts.
[b]Energy for the combination of two half-reactions can be estimated from the difference between their free energy values, as indicated on the bottom axis.

carbon–halogen bond energies. Regardless of the exact mechanism, however, relative rates for reduction of halogenated aliphatic compounds should follow certain patterns (*61*). In general, smaller carbon–halogen bond energies are conducive to faster one-electron (two-step) reductions. An example is the reduction of halogenated aliphatics by iron(II) porphyrins. Because the rate-limiting step in the two-step reduction is probably the formation of the carbon radical (*62*), the heat of formation of the alkyl radicals is one measure of the carbon–halogen bond strength and should be inversely proportional to the rate of reduction.

This is shown in Table 8 for pseudo-first-order reduction rates derived from data from Klecka and Gonsior (*58*). As another measure, Eberson (*67*) suggested that although rates might differ with different reductants (iron porphyrin and the like), for a given reductant, the relative rates of reduction of halogenated aliphatic compounds should correlate with their relative standard reduction potentials (assuming no change in mechanism). Relative standard reduction potentials can be estimated for many halogenated aliphatic compounds using the values as shown in Figures 4 and 5. The calculation method is described in the sidebar on p. 727 (*68–71*).

Highly halogenated aliphatic compounds have higher relative standard potentials than do their less halogenated counterparts, as indicated by the vertical positioning of compounds in Figures 4 and 5. Thus more energy is released upon reduction of the more highly halogenated compounds.

Another type of comparison between reduction potentials is illustrated in Figure 6. Here, biologically relevant reductants, as well as oxidants, are included. Note that hexachloroethane (HCE) is a stronger electron acceptor than is oxygen, and several halogenated compounds, such as tetrachloromethane, tetrachloroethene, and trichloromethane, are stronger acceptors than nitrate. This suggests environmental conditions under which their reduction is likely. Also, as illustrated in the lower portion of Figure 6, several biologically active donors, and even ferrous ion, have lower reduction potentials than do most of the halogenated aliphatic compounds, and they could be involved in halogen removal by reductions. Thermodynamic considerations can help indicate which halogenated aliphatic compounds might be coupled by reduction with the oxidation of individual electron donors typically found in biological systems.

Many of the reductions indicated above occur in mammalian systems (*30, 44*). All three kinds of reduction—hydrogenolysis, in which a hydrogen atom replaces a halogen substituent (Figure 1, IVa); dihalo-elimination, in which two halogens are removed from adjacent carbons (Figure 1, IVb); and coupling (Figure 1, IVc)—have been observed in mammalian systems (Table 9) (*27, 72, 81*). Hexachloroethane, pentachloroethane, and tetrachloromethane are reductively dehalogenated (by hydrogenolyis) to pentachloroethane, tetrachloroethane, and trichloromethane, respectively. Also, hexachloroethane and pentachloroethane are reduced (by dihalo-elimination) to the alkenes, tetrachloroethene and trichloroethene.

Most research in mammalian systems implicates cytochrome P450 as the active reducing agent. Reduction results when halogenated aliphatics outcompete with oxygen (when present) for the electrons supplied by nicotinamide adenine dinucleotide phosphate (NADPH) (*44*). The mechanism involves formation of either a carbon radical or a di-

TABLE 7
Reduction of halogenated aliphatic compounds by transition metal complexes

Compound	Products	Reductant	Reference
Methanes			
Chloromethane	Alkylated co-complex	Co(I) chelates	(*54*)
Dichloromethane	Methane	$Cr(II)SO_4$	(*55*)
	Cl-alkylated B_{12}	B_{12}-Co(III) (methylcobalamine)	(*56*)
Trichloromethane	Methane	$Cr(II)SO_4$	(*55*)
	Dichloromethane	Fe(II)P	(*57*)
	Dichloromethane	Fe(II)P	(*58*)
	Cl-alkylated B_{12}	B_{12}-Co(III)	(*56*)
Tetrachloromethane	Methane	$Cr(II)SO_4$	(*55*)
	Chloroform	Fe(II)P	(*57, 58*)
	Cl-alkylated B_{12}	B_{12}-Co(III)	(*56*)
Bromomethane	Methane	$Cr(II)SO_4$	(*55*)
	Alkylated co-complex	Co(I)-complex	(*54*)
Dibromomethane	Methane, ethene	Fe(II)P	(*57*)
Tribromomethane	Br_2-alkylated B_{12}	B_{12}-Co(III)	(*56*)
Ethanes			
Chloroethane	Alkylated co-complex	Co(I)-complex	(*54*)
1,1-Dichloroethane	Ethane, ethanol	$Cr(II)SO_4$	(*55*)
1,1,1-Trichloroethane	Ethane, ethanol, ethene, chloroethene	$Cr(II)SO_4$	(*55*)
	1,1-Dichloroethane	Fe(II)	(*57*)
	1,1-Dichloroethane	Fe(II)P	(*58*)
Hexachloroethane	Tetrachloroethene	Fe(II)P	(*57, 59*)
	Tetrachloroethene	$Cr(II)SO_4$	(*60*)
Bromoethane	Ethane	Ni(I)	(*60*)
1,1-Dibromoethane	Ethane, ethanol	$Cr(II)SO_4$	(*55*)
1,2-Dibromoethane	Ethene	Fe(II)	(*57*)
	Ethene	Fe(II)P	(*58*)
Propanes			
1-Chloropropane	Alkylated co-complex	Co(I)-complex	(*54*)
1,1-Dichloropropane	Propane, propanol, propene	$Cr(II)SO_4$	(*55*)
1-Bromopropane	Alkylated co-complex	Co(I)-complex	(*54*)
1,2-Dibromo-3-chloropropane	Propene, allyl chloride	$Cr(II)SO_4$	(*60*)

Note: The homolytic cleavage of cobalt–carbon bonds requires 15–30 kcal/mol and can occur at relatively low temperatures.

TABLE 8
Pseudo-first-order reduction rates and heat of formation of carbon radicals for some chlorinated aliphatic compounds

Compound	k (d^{-1})[a]	Heat of radical formation[b] (kJ/mol)
Dichloropropane	<0.001	117.6
Trichloromethane	0.00165	100.8
1,1,1-Trichloroethane	0.058	92.0
Tetrachloromethane	115	78.2

[a]Reference 58.
[b]References 52 and 67.

halocarbene complex with cytochrome P450.

Evidence for a carbon radical follows from two general observations: the observed production of hexachloroethane from carbon tetrachloride (Figure 1, IVc and Table 9), apparently as a result of trichloromethyl radical dimerization, and indications of radical formation in chemical studies that involve iron(II) porphyrin. Formation of a carbon radical depends on the strength of the carbon–halogen bond (and standard reduction potential). This bond is weaker for brominated than for chlorinated compounds. Thus brominated aliphatics should be more susceptible to reduction by cytochrome P450 than are chlorinated compounds. The number of halogen substituents also is an important factor in determining the feasibility of radical formation.

Evidence for the production of a dihalogenated carbene intermediate comes from observations of the reduction of polyhalogenated methanes. A dihalogenated carbene complex would be expected to hydrolyze to carbon monoxide, and carbon monoxide has been produced from trichloromethane and tetrachloromethane (Table 9). However, compounds having less than three halogen substituents apparently do not undergo reduction to carbon monoxide by cytochrome P450 (*73*).

Halogenated aliphatic compounds with few halogen substituents generally are not reduced or are reduced relatively slowly in mammalian systems. For example, 1,2-dichloroethane is not significantly reduced under anaerobic conditions by cytochrome P450 (*82*). However, both 1,2-dichloroethane and 1,2-dibromoethane are transformed to ethene in mammalian systems (Table 9). Livesey and Anders indicated that this reduction requires the presence of reduced glutathione in hepatic microsomes (*80*). They also postulated the following two-step process, involving nucleophilic attack by glutathione (GSH) and a thiol sulfur (RSH):

$$GSH + Cl{-}CH_2{-}CH_2{-}Cl \rightarrow GS{-}CH_2{-}CH_2{-}Cl + HCl$$

$$RSH + GS{-}CH_2{-}CH_2{-}Cl \rightarrow GSSR + HCl + CH_2{=}CH_2$$

Microbially mediated reactions

Some of the dehalogenating agents found in mammalian systems are manifest in microbial populations as well. Many microorganisms contain cytochrome P450 that is similar to mammalian P450 even in regard to halogenated compound transformation (*83*). For example, cytochrome P450 from *Pseudomonas putida* closely resembles microsomal P450 (*84*), and whole cells can use it to mediate the reduction of carbon tetrachloride and bromotrichloromethane to chloroform (*85, 86*). Glutathione also is widely distributed among gram-negative bacteria (87), and it is used by *Hyphomicrobium sp.* in the metabolism of dichloromethane (*89*). In general, however, microorga-

FIGURE 7
Relative rates of reduction and oxidation[a]

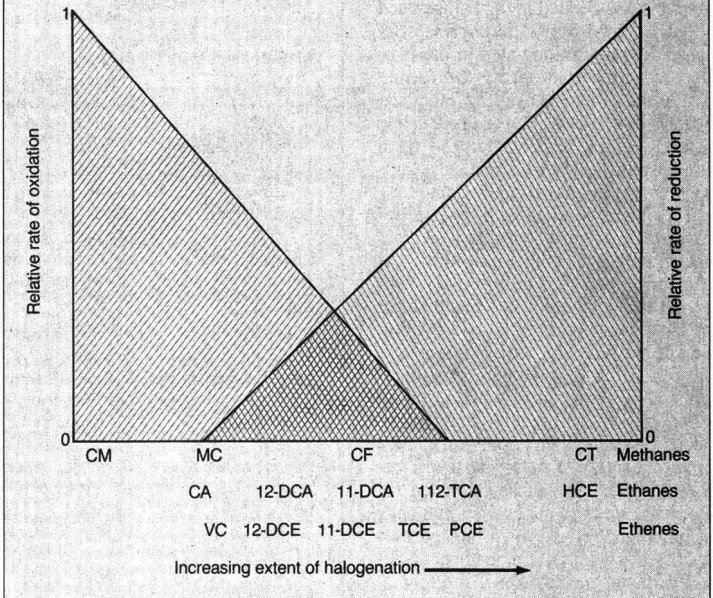

[a]As a function of the extent of halogenation.

FIGURE 8
Pathways for the transformation of TCA under methanogenic conditions[a]

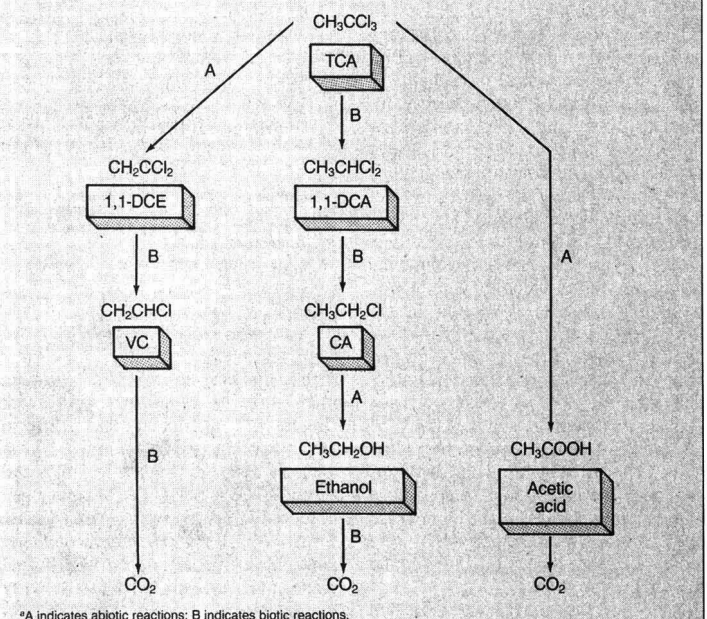

[a]A indicates abiotic reactions; B indicates biotic reactions.
Source: Reference 97.

nisms are capable of more diverse biochemical reactions than are mammalian systems.

Microorganisms obtain energy from a wide variety of electron donors and acceptors under different redox conditions (Table 10). Aerobic metabolism dominates where sufficient oxygen is present. Where oxygen is depleted, however, other electron acceptors, such as nitrate, sulfate, and carbon dioxide, are used. Differences in available electron acceptors and in the resulting redox conditions also appear to affect the potential and pathways for transformation of different halogenated aliphatic compounds. Another factor affecting the potential for transformation is the reactivity of enzymes and coenzymes associated with different microorganisms.

Regardless of the metabolic differences between microorganisms and mammalian systems, the types of reactions mediated by bacteria and mammalian systems are similar. Like mammalian systems, bacteria mediate substitution reactions with monohalogenated or dihalogenated aliphatic compounds (Table 11) (*18, 88–111*). For example, aerobic bacteria isolated from a contaminated soil transform 1,2-dichloroethane to chloroethanol, which is subsequently mineralized to carbon dioxide (*100*). However, the pathways for the observed mineralization of many halogenated organics are unknown. A compound such as tetrachloromethane, which is mineralized to carbon dioxide (Table 11), may undergo reduction to dichloromethane and subsequent oxidation to carbon dioxide, as previously described for mammalian systems. In addition, different organisms may participate in different steps of the overall mineralization of a compound.

Bacteria also oxidize chlorinated alkenes, presumably via epoxidation (Table 11). Because many halogenated aliphatic compounds are eventually mineralized to carbon dioxide, other oxidation pathways may be involved. Some net oxidations, such as the mineralization of dichloromethane to carbon dioxide, could proceed either by oxidation via phosgene ($COCl_2$) or by substitution via alcohols. In general, oxidation pathways are not well known. Ionization potentials, which are used to predict ozonation rates for halogenated alkenes, might also be used to model oxidations in microbial systems. However, the number of halogen substituents may be a more reasonable predictor of oxidations—the more halogen substituents, the less susceptible the compound is to oxidation. This is consistent with Figure 6.

Polychlorinated methanes, ethanes, and ethenes are reduced by microbial consortia or mixed cultures (Table 11). Generally, reduction entails the replacement of halogen substituents by hydrogen (hydrogenolysis) (vertical arrows in Figure 4). However, reduction can also involve the loss of two halogens (dihalo-elimination) (wide arrows in Figure 4), as in the case of hexachloroethane transformation to pentachloroethane and of 1,2-dibromoethane transformation to ethylene (Table 11). These two dihalo-eliminations can occur under aerobic conditions, whereas hydrogenolysis has only been observed under anaerobic conditions. Thus reductions proceed by the same general pathways, regardless of whether transition metals, mammalian systems, or microorganisms provide the reductant.

Methanogens, which grow under some of the most severely reducing conditions (Table 10), do not have the cytochrome systems that are present in aerobic organisms. However, methanogens do have nickel-containing enzymes or cofactors such as F430 (*112*). Reduced nickel complexes can reduce halogenated aliphatic compounds (Table 7). Indeed, several of the microbial reductants have much greater reducing potentials than the mammalian enzymes do (see Table 12) (*54, 67, 84, 113*), and this may lead to a broader reductive dehalogenation ability.

For comparison, Figure 7 illustrates the half-reaction reduction potentials for halogenated aliphatic compounds that function as electron acceptors. Possible electron donors are shown as well. Common electron acceptors, such as oxygen, nitrate, sulfate, and carbon dioxide, also are plotted in Figure 6. Here, the various couples are arranged according to their standard half-reaction reduction potentials at pH 7. Each arrow points in the direction for which the stated transformation is thermodynamically possible. In the direction opposite to the arrow, the reverse reaction is thermodynamically favorable. Thus a direct, graphic reading can be obtained for the free-energy change associated with the coupling of two half-reactions. For example, combining the

TABLE 9
Reductions of halogenated aliphatic compounds in mammalian systems

Compound	Product(s)	System[a]	Reference
Methanes			
Trichloromethane	Carbon monoxide	hm/P/r	(*72, 73*)
	Dichloromethane		(*74*)
Tetrachloromethane	Carbon monoxide	hm/P/N	(*75*)
	Trichloromethane	R, hm/P	(*73, 75–77*)
		r	(*74, 78, 79*)
	Hexachloroethane	R, B	(*77, 78*)
Bromotrichloromethane	Trichloromethane	R	(*77*)
	Hexachloroethane		
	Bromodichloromethane		
	Carbon monoxide	hm/P/r	(*73*)
Tribromoethane	Carbon monoxide	hm/P/r	(*73*)
Tetrabromomethane	Carbon monoxide	hm/P/r	(*73*)
Ethanes			
1,2-Dichloroethane	Ethene	hm/G/O	(*80*)
Pentachloroethane	Trichloroethanol	M	(*27*)
	Trichloroethene	M, hm/r	(*27, 79*)
	1,1,2,2-Tetrachloroethane	hm/r, hm P/N/r	(*79*)
Hexachloroethane	Pentachloroethane, Tetrachloroethane	hm/r, S, hm/P/N	(*79, 81*)
1,2-Dibromoethane	Ethene	hm/G/O	(*80*)

[a]Commas separate different experimental systems that result in similar products. Slashes separate information regarding each experiment. hm = hepatic (rat liver) microsomes; R = live rats; B = live rabbits; M = live mice; S = live sheep; N = NADH dependence; P = cytochrome P450 dependence; G = glutathione dependence; O = presence of oxygen; r = reduced or anaerobic conditions reported.

TABLE 10
Electron acceptors in microbial processes

Environment	Electron acceptor	Process	Order of preference
Aerobic	O_2	Aerobic metabolism	1
	NO_3^-	Denitrification	2
Anaerobic	SO_4^{2-}	Sulfate reduction	3
	CO_2	Methanogenesis	4

reduction of hexachloroethane to pentachloroethane with the oxidation of Fe(II) to $Fe(OH)_3$ yields a favorable free-energy change of about 140 kJ per mole of electrons transferred. The reduction of hexachloroethane to pentachloroethane and 1,2-dibromoethane to ethene have higher reduction potentials than those associated with oxygen reduction to water (Figure 6), and these dihalo-eliminations are energetically favored in aerobic systems. This is consistent with the observed transformations of hexachloroethane and 1,2-dibromoethane under aerobic conditions.

In addition, the low potential for reduction of carbon dioxide to methane, compared with the reduction potential for hydrogenolysis of polyhalogenated aliphatic compounds (Figure 6) is consistent with their reported reductive transformations under methanogenic conditions (Table 11). For example, the sequential reduction of tetrachloroethene to trichloroethene, to dichloroethene, and finally to chloroethene (vinyl chloride) occurs under methanogenic conditions (*106*), as does the sequential reduction of tetrachloroethane to 1,l-dichloroethane, and finally to chloroethane (*16, 96, 102*). These pathways follow the hydrogenolysis sequences illustrated by the narrow arrows in Figure 4 for these compounds.

Microbial and mammalian systems follow the same general trends with regard to the oxidation and reduction of halogenated aliphatic compounds: The more halogenated the aliphatic compound, the faster the relative rate of reduction; the less halogenated the compound, the faster the rate of oxidation. Substitution reactions follow the same general trends. Many useful generalizations can be drawn from oxidation–reduction potentials of halogenated aliphatic compounds. Dehydrohalogenation has not yet been reported for microbial systems.

TABLE 11
Biotransformations of halogenated aliphatic compounds by microorganisms

Compound	Product(s)	System[a]	Reference
Methanes			
Chloromethane	Formaldehyde	E	(*88*)
Dichloromethane	Carbon dioxide	O/M	(*89*)
	Carbon dioxide	O/P	(*90*)
	Carbon dioxide	O/M	(*91*)
	Carbon dioxide	O/P	(*92*)
	Formaldehyde	E	(*93*)
Trichloromethane	Carbon dioxide	A/M/m	(*94*)
	Carbon dioxide	O/S	(*95*)
	Dichloromethane	A/M	(*96*)
Tetrachloromethane	Carbon dioxide	A/M/m	(*94*)
	Chloroform	A/M/n	(*97*)
	Carbon dioxide		
	Chloroform	A/S	(*98*)
Bromomethane	Formaldehyde	E/mo	(*89*)
Ethanes			
1,1-Dichloroethane	Chloroethane	A/M/m	(*95*)
1,2-Dichloroethane	Carbon dioxide	O/P/p	(*96*)
	Chloroethanol	O/P/x	(*97*)
	Carbon dioxide	A/M/m	(*94*)
1,1,1-Trichloroethane	1,1-Dichloroethane	A/S	(*98*)
		A/M/m	(*99*)
		A/M	(*102*)
	Not identified	A/M/m	(*94*)
1,1,2,2-Tetrachloroethane	1,1,2-Trichloroethane	A/M/m	(*94*)
		A/M	(*102*)
Hexachloroethane	Tetrachloroethane	O/M/s	(*103*)
Bromoethane		O/P/x	(*101*)
1,2-Dibromoethane	Ethene	O/S	(*104*)
	Ethene	A/M/m/r	(*18*)
	Carbon dioxide	O/S	(*105*)
Ethenes			
Chloroethene	Carbon dioxide	A/M/m	(*106*)
	Carbon dioxide	O/P/mb	(*109*)
Dichloroethene	Chloroethene	A/M/m	(*99, 106*)
	Chloroethene	A/S, A/M	(*102, 107*)
	Carbon dioxide		
Trichloroethene	Dichloroethene	A/M/m	(*106*)
	Dichloroethene	A/S	(*98, 108*)
	Dichloroethene	A/M	(*102*)
	Carbon dioxide	O/P	(*110*)
	Carbon dioxide	O/S	(*111*)
Tetrachloroethene	Trichloroethene	A/M/m	(*94, 106*)
		A/M	(*102*)
Propanes			
1-Chloropropane	—	O/P/x	(*101*)
1,2-Dichloropropane	—	O/P/x	(*101*)
1,2-Dibromo-3-chloropropane	Propanol	O/S	(*104*)

[a]Comma separates different experimental systems that result in similar products. Slashes separate information regarding each experiment. O = aerobic; A = anaerobic, which often is methanogenic (m), but often is not explicitly stated; M = mixed culture; P = pure culture; S = soil or aquifer used as biological seed; E = enzyme derived from microorganism; m = methanogenic culture; x = *Xanthobacter*; mo = monooxygenase; mb = Mycobacterium; p = *Pseudomonas*.

Environmental applications

Application of these general principles to environmental problems is complex . For example, Figure 8 illustrates the different pathways possible for the transformation of 1,1,1-trichloroethane (*97*), which can undergo two abiotic transformations as well as reductive dehalogenation by anaerobic microorganisms. Abiotically, the half-life for 1,1,1-trichloroethane at 25 °C is about two years (Table 3), and biologically it could be much less. The abiotic processes are dehydrohalogenation (*14, 15, 99*), as well as hydrolysis (*12, 13, 14*). Acetic acid, the product of hydrolysis, is fairly inert chemically, but it can be mineralized rapidly by microorganisms. Dehydrohalogenation occurs at about one-fifth the rate of hydrolysis at 40 °C (*19*). The product of dehydrohalogenation, 1,l-dichloroethene, can be transformed further by reductive dehalogenation to chloroethene (vinyl chloride) under methanogenic conditions (Table 11, Figure 8). Under the biological transformation route, 1,1,1-trichloroethane is reduced to 1,1-dichloroethane and then transformed abiotically by hydrolysis to ethanol (Table 3), which can in turn be rapidly mineralized by microorganisms. The products and complex pathways shown in Figure 7 are consistent with field observations of products consistently found present in groundwaters contaminated with 1,1,1-trichloroethane (*114*). Other halogenated aliphatic compounds are also likely to undergo complex transforma-

tions under natural environmental conditions.

Conclusions

The fate of halogenated aliphatic compounds in the environment is dependent on their particular chemical properties and potential chemical and biological transformations. The most likely transformations to occur under given environmental conditions are controlled mainly by the number and type of halogen substituents. Increased halogenation or substitution of bromine for chlorine substituents increases the electrophilicity and oxidation state of the compound, making it more susceptible to dehydrohalogenation and reduction and less susceptible to substitution and oxidation (Figure 7). Oxidations and reductions are more common reactions in mammalian and microbiological systems, where they are mediated by enzymes or coenzymes. For oxidations, initial products are generally alcohols or epoxides. For reductions, products are generally less halogenated than were their precursors. A variety of transition metal complexes, including iron porphyrins, are potential mediators of these reactions.

TABLE 12
Standard potentials (E^o) of biologically relevant electron donors or reductants

Reductants	E^o (volts)	Reference
Vitamin B_{12}	−0.59 to −0.8	(*54*)
Co(I) tetraphenylporphin	−0.56	(*67*)
Ferrodoxin (reduced)	−0.43	(*11*)
H_2	−0.42	(*84*)
Cr(II)	−0.41	(*67*)
NADH + H^+	−0.32	(*84*)
Cytochrome P450 (unactivated)	−0.30	(*111*)
Glutathione (reduced)	−0.23	(*84*)
Cytochrome P450 (activated)	−0.17	(*111*)
Fe(II) deuteroporphin IX	0.00	(*67*)
Ubiquinone (reduced)	0.10	(*84*)
Cytochrome c (+2)	0.22	(*84*)
Fe(II)	0.77	(*84*)
H_2O	0.82	(*84*)

Acknowledgments

This material is based on work supported in part by the National Science Foundation (Grant ECE 8519243) and in part by the Environmental Protection Agency (Grant EPA CR-81220). It has not been subject to EPA's peer and administrative review and therefore should not be assumed to reflect the views or bear the endorsement of that agency.

This article has been reviewed for suitability as an *ES&T* feature by J. M. Wood, University of Minnesota, Navarre, Minn. 55392; and by B. Rittmann, University of Illinois at Urbana–Champaign, Urbana, Ill. 61801.

References

(1) Isaacson, P. J.; Hankin, L.; Frink, C. R. *Science* **1984,** 225, 672.
(2) Nelson, S. J. et al. *Stud. in Environ. Sci.* **1981,** *17,* 35-40.
(3) Rook, J. J. *J. Water Treatment Exam.* **1974,** *23,* 234-43.
(4) Price, P. S. "VOC Degradation." Memo of U.S. Environmental Protection Agency, Office of Water, Washington, D.C. Aug. 21, 1985.
(5) *Fed. Regist.* **1985,** *40,* Parts 141, 142; 46885-46904.
(6) Special Bulletin EDB, *Dangerous Properties of Industrial Materials Report,* Van Nostrand Reinhold Co.: New York, March 1984; pp. 1-31.
(7) March, J. *Advanced Organic Chemistry,* 3rd ed.; Wiley: New York, 1985.
(8) Mabey, W.; Mill, T. *J. Phys. Chem. Ref. Data* **1978,** *7, 383-415.*
(9)Vogel, T. M.; Reinhard, M. *Environ. Sci. Technol.* **1986,** *20,* 992-97.
(10) Dilling, W. L.; Tefertiller, N. B.; Kallos, G. J. *Environ. Sci. Technol.* **1975,** *9,* 833-38.
(11) Laughton, P. M.; Robertson, R. E. *Can. J. Chem.* **1959,** *37,* 1491-97.
(12) Mabey, W. R.; Barich, V.; Mill, T. Presented at the Annual Meeting of the American Chemical Society, Division of Environmental Chemistry, September 1983.
(13) Britton, E. C.; Reed, W. R. *Chem. Abstr.* **1932,** *26,* 5578.
(14) Haag, W. R.; Mill, T.; Richardson, A. *Extended Abstract,* Annual Meeting of the American Chemical Society, 1986.
(15) Pearson, C. R.; McConnell, G. *Proc. R. Soc. London Ser. B.* **1975,** *189,* 305-32.
(16) Vogel, T. M.; McCarty, P. L. *J. Contaminant Hydrology* **1987,** *1,* 299-308.
(17) Walraevens, R.; Trouillet, P.; Devos, A. *Int. J. Chem. Kinetics* **1974,** *7,* 777-86.
(18) Weintraub, R. A.; Jex, G. W.; Moye, H. A. In *Evaluation of Pesticides in Ground Water;* Garner, W. Y.; Honeycutt, R. C.; Nigg, H.N., Eds.; American Chemical Society: Washington, D.C., 1986, pp. 294-310.
(19) Burlinson, N. E.; Lee, L. A.; Rosenblatt, D. H. *Environ. Sci. Technol.* **1982,** *16,* 627-32.
(20) Voudrias, E. A.; Reinhard, M. In *Geochemical Processes at Mineral Surfaces;* Davis, J. A.; Hayes, K. F., Eds.; American Chemical Society: Washington, D.C., 1986; pp. 462-86.
(21) Schwarzenbach, R. et al. *Environ. Sci. Technol.* **1985,** *19,* 322-27.
(22) Kubic, V. L.; Anders, M. W. *Biochem. Pharmacol.* **1978,** *27,* 2349-55.
(23) Rubinstein, D.; Kanics, L. *Can. J. Biochem.* **1964,** *42,* 1577-85.
(24) Yllner, S. *Acta Pharmacol. Toxicol.* **1971,** *30,* 248-56.
(25) Yllner, S. *Acta Pharmacol. Toxicol.* **1971,** *29,* 499-512.
(26) Yllner, S. *Acta Pharmacol. Toxicol.* **1971,** *29,* 471-80.
(27) Yllner, S. *Acta Pharmacol. Toxicol.* **1971,** *29,* 481-89.
(28) Watanabe, P.G. et al. *Toxicol. Appl. Pharmacol.* **1976,** *37,* 49-59.
(29) McKenna, M. J.; Watanabe, P. G.; Gehring, P. J. *Environ. Health Perspect.* **1977,** *21,* 99-105.
(30) Anders, M. W. In *Metabolic Basis of Detoxification;* Jakoby, W. B.; Bend, J. R. Caldwell, J., Eds.; Academic Press: New York, 1982, pp. 29-49.
(31) Ahmed, A. E.; Anders, M. W. *Biochem. Pharmacol.* **1978,** *27,* 2021-25.
(32) Stevens, J. L.; Ratnayake, J. H.; Anders, M. W. *Toxicol. Appl. Pharmacol.* **1980,** *55,* 484-89.
(33) Pohl, L. R. et al. *Biochem. Biophys. Res. Comm.* **1977,** *79,* 684-91.
(34) Yllner, S. *Acta Pharmacol. Toxicol.* **1971,** *30,* 257-65.
(35) Halpert, J. *Drug Metabolism and Disposition, 1982, 10,* 465-68.
(36) Hill, D. L. et al. *Cancer Res.* **1978,** *38,* 2438-42.
(37) Bonse, G. et al. *Biochem. Pharmacol.* **1975,** *24,* 1829-34.
(38) Guengerich, F. P.; Crawford, W. M.; Watanabe, P. G. *Biochemistry,* **1979,** *18,* 5177-82.
(39) Dekant, W.; Metzler, M.; Henschler, D. *Biochem. Pharmacol.* **1984,** *33,* 2021-27.
(40) Hathaway, D. E. *Cancer Lett.* **1980,** *8,* 263-69.
(41) Miller, R. E.; Guengerich, F. P. *Cancer Res.* **1983,** *43,* 1145-52.
(42) Costa, A. K.; Ivanetich, K. M. *Biochem. Pharmacol.* **1980,** *29,* 2863-69.
(43) Guengerich, F. P. et al. *Cancer Res.* **1981,** *41,* 4391-98.
(44) Macdonald, T. L. *CRC Crit. Rev. Toxicol.* **1983,** *11,* 85-120.
(45) Tachizawa, H.; Neal, R. A.; Macdonald, T. L. *Mol. Pharmacol.* **1982,** *22,* 745-51.
(46) Bonse, G.; Henschler, D. *CRC Crit. Rev. Toxicol.* **1976,** *4,* 395-409.
(47) Henschler, D. *Environ. Health Perspect.* **1977,** *21,* 61-64.
(48) Leibman, K. C.; Ortiz, E. *Environ. Health Perspect.* **1977,** *21,* 91-97.
(49) Henschler, D. et al. *Biochem. Pharmacol.* **1979,** *28,* 543-48.
(50) Miller, R. E.; Guengerich, F. P. *Biochemistry* **1982,** *21,* 1090-97.
(51) Williamson, D. G.; Cvetanovic, R. J. *J. Amer. Chem. Soc.* **1968,** *90,* 4248-52.
(52) *Lange's Handbook of Chemistry,* 12th ed.; Dean, J.A., Ed.; McGraw Hill: New York, 1979, pp. 965-94.
(53) Neidleman, S. L.; Geigert, J. *Biohalogenation: Principles, Basic Roles and Applications.* Ellis Horwood: West Sussex, England, 1986.
(54) Schrauzer, G. N.; Deutsch, E. *J. Amer. Chem. Soc.* **1969,** *91,* 3341-49.
(55) Castro, C. E.; Kray, W. C., Jr. *J. Am. Chem. Soc.* **1963,** *85,* 2768-73.
(56) Wood, J. M.; Kennedy, F. S.; Wolfe, R. S. *Biochemistry* **1968,** *7,* 1707-13.
(57) Wade, R. S.; Castro, C. E. *J. Amer. Chem. Soc.* **1973,** *95,* 231-34.
(58) Klecka, G. M.; Gonsior, S. J. *Chemosphere* **1984,** *13,* 391-402.
(59) Mansuy, D.; Fontecave, M. *Biochem. Biophys. Res. Comm.* **1982,** *104,* 1651-57.
(60) Kray, W. C., Jr.; Castro, C. E. *Org. Biol. Chem.* **1964,** *86,* 4603-08.
(61) Bakac, A.; Espenson, J. H. *J. Amer. Chem. Soc.* **1986,** *108,* 713-19.
(62) Castro, C. E. *Environ. Health Perspect.* **1977,** *21,* 279-83.
(63) Kochi, J. K.; Powers, J. W. *J. Amer. Chem. Soc.* **1970,** *92,* 137-46.
(64) Halpern, J.; Maher, J. P. *J. Amer. Chem. Soc.* **1965,** *87,* 5361-66.
(65) Hill, H.A.O. et al. *J. Chem. Soc. (A).* **1971,** 1859-62.

(66) Wade, R. S.; Havlin, R.; Castro, C. E. *J. Amer. Chem. Soc.* **1969,** *91,* 7530.
(67) Eberson, L. *Acta Chem. Scan. Ser. B* **1982,** *36,* 533-43.
(68) Lyman, W. J.; Reehl, W. F.; Rosenblatt, D. H. *Handbook of Chemical Property Estimation Methods;* McGraw-Hill: New York, 1982.
(69) Smith, B. D.: Srivastava, R. *Thermodynamic Data for Pure Compounds, Physical Sciences Data,* Vol. 25 (Part B); Elsevier Press: New York, 1986; p. 109.
(70) Horvath, A. L. *Halogenated Hydrocarbons: Solubility-Miscibility with Water;* Marcel Dekker: New York, 1982, p. 478.
(71) MacKay, D.; Shin, W. Y. *J. Phys. Chem. Ref. Data* **1981,** *10,* 1175-99.
(72) Stevens, J. L.; Anders, M. W. *Chem. Biol. Interact.* **1981,** *37,* 365-74.
(73) Wolf, C. R. et al. *Mol. Pharmacol.* **1977,** *13,* 698-705.
(74) Butler, T. C. *J. Pharmacol. Exp. Ther.* **1961,** *134,* 311-19.
(75) Ahr, H. J. et al. *Biochem. Pharmacol.* **1980,** *29,* 2855-61.
(76) Kubic, V. L.; Anders, M. W. *Chem. Biol. Interact.* **1981,** *34,* 201-07.
(77) Bini, A. et al. *Pharmacol. Res. Comm.* **1975,** *7,* 143-49.
(78) Fowler, J.S.L. *Br. J. Pharmacol.* **1969,** *37,* 733-37.
(79) Nastainczyk, W.; Ahr, H. J.; Ullrich, V. *Biochem. Pharmacol.* **1982,** *31,* 391-96.
(80) Livesey, J. C.; Anders, M. W. *Drug Metab. Dispos.* **1979,** *7,* 199-203.
(81) Fowler, J.S.L. *Br. J. Pharmacol.* **1969,** *35,* 530-42.
(82) Guengerich, F. P.; Crawford, W. M., Jr., Domoradski, J. Y.; Macdonald, T. L.; Watanabe, P. G. *Tox. Appl. Pharmacol.* **1980,** *55,* 303-17.
(83) Sligar, S. G.; Murray, R.I. In *Cytochrome P-450, Structure, Mechanism and Biochemistry;* Ortiz de Montellano, Ed.; Plenum Press: New York, 1986, pp. 492-503.
(84) Murray, R. I. et al. In *Metalloproteins Part I: Metal Proteins with Redox Roles.* Harrison, P., Ed.; Verlag-Chemie, Weinheim: Deerfield Beach, Fla., 1985, pp. 157-206
(85) Lam, T.; Vilker, V. L. *Biotechnol. and Bioeng.* **1987,** *29,* 151-59.
(86) Castro, C. E.; Wade, R. S.; Belser, N. O. *Biochemistry,* **1985,** *24,* 204-10.
(87) Fahey, R. C. et al. *J. Bacteriol.* **1978,** *133* (3), 1126-29.
(88) Stirling, D. I.; Dalton, H. *FEMS Microbiol. Lett.* **1979,** *5,* 315-18.
(89) Rittmann, B. E.; McCarty, P. L. *Appl. Environ. Microbiol.* **1980,** *39,* 1225-26.
(90) Brunner, W.; Staub, D.; Leisinger, T. *Appl. Environ. Microbiol.* **1980,** *40,* 950-58.
(91) Stucki, G. et al. *Arch. Microbiol.* **1981,** *130,* 366-71.
(92) Lapat-Polasko, L. T.; McCarty, P. L.; Zehnder, A.J.B. *Appl. Environ. Microbiol.* **1984,** *47,* 825-30.
(93) Patel, R. N. et al. *Appl. Environ. Microbiol.* **1982,** *44,* 1130-37.
(94) Bouwer, E. J.; McCarty, P. L. *Appl. Environ. Microbiol.* **1983,** *45,* 1286-94.
(95) Strand, S. E.; Shippert, L. *Appl. Environ. Microbiol.* **1986,** *52,* 203-05.
(96) Gossett, J. M. "Anaerobic Degradation of C1 and C2 Chlorinated Hydrocarbons"; final report ESL-TR-85-88; Air Force Engineering and Services Center, Tyndall Air Force Base, Florida, 1985.
(97) Bouwer, E. J.; McCarty, P. L. *Appl. Environ. Microbiol.* **1983,** *45,* 1295-99.
(98) Parsons, F.; Barrio-Lage, G.; Rice, R. *Environ. Toxicol. Chem.* **1985,** *4,* 739-42.
(99) Vogel, T. M.; McCarty, P. L., submitted for publication in *Environ. Sci. Technol.*
(100) Stucki, G.; Krebser, U.; Leisinger, T. *Experientia* **1983,** *39,* 1271-73.
(101) Janssen, D. B. et al. *Appl. Environ. Microbiol.* **1985,** *49,* 673-77.
(102) Hallen, R. T.; Pyne, J. W., Jr.; Molton, P. M. *Extended Abstract,* Annual Meeting of the American Chemical Society, 1986.
(103) Criddle, C. S. et al. *J. Contaminant Hydrology* **1986,** *1,* 133-42.
(104) Castro, C. E.; Belser, N. O. *Environ. Sci. Technol.* **1968,** *2,* 779-83.
(105) Pignatello, J. J. *Appl. Environ. Microbiol.* **1986,** *51,* 588-92.
(106) Vogel, T. M.; McCarty, P. L. *Appl. Environ. Microbiol.* **1985,** *49,* 1080-83.
(107) Parsons, F.; Wood, P. R.; DeMarco, J. *J. Amer. Water Works Assoc.* **1984,** *76* (5), 56-59.
(108) Kleopfer, R. D. et al. *Environ. Sci. Technol.* **1985,** *19,* 277-80.
(109) Hartmans, S.; de Bont, J.A.M.; Tramper, J.; Luyben, K. Ch. A. M. *Biotechnol. Lett.* **1985,** *7,* 383-88.
(110) Nelson, M.J.K. et al. *Appl. Environ. Microbiol.* **1986,** *52,* 383-84.
(111) Wilson, J. T.; Wilson, B. H. *Appl. Environ. Microbiol.* **1985,** *49,* 242-43.
(112) Schonheit, P.; Thauer, R. K. In *Biotechnological Advances in Processing Municipal Wastes for Fuels and Chemicals.* Antonopoulos, A.A., Ed.; ANL/CNSV-TM-167, Argonne National Laboratory; Argonne, 1985, 41-51.
(113) Stryer, L. *Biochemistry,* 2nd ed.; W. H. Freeman: San Francisco, 1981.
(114) Cline, P. V.; Viste, D.R. *Waste Manage. Res.* **1985,** *3,* 351-60.

Perry L. McCarty *is a professor of environmental engineering and science in the civil engineering department of Stanford University. Since 1962 he has taught at Stanford and conducted research on biological processes for water quality control.*

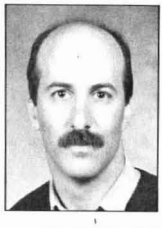

Timothy M. Vogel *(l.) is an assistant professor of civil and environmental engineering at Michigan State University. When this article was written, he was a doctoral candidate at Stanford University. Previously, he was a geochemical oceanographer with the U.S. Geological Survey. His current research focuses on biological and chemical transformations of pollutants in aquatic environments.*

Craig S. Criddle *(r.) is a doctoral candidate in environmental engineering and science at Stanford University. He holds a B.S. and an M.S. in civil and environmental engineering from Utah State University. His research interests are in biological processes for water quality control.*

ES&T FEATURE

Pollution from nonpoint sources

Where we are and where we should go

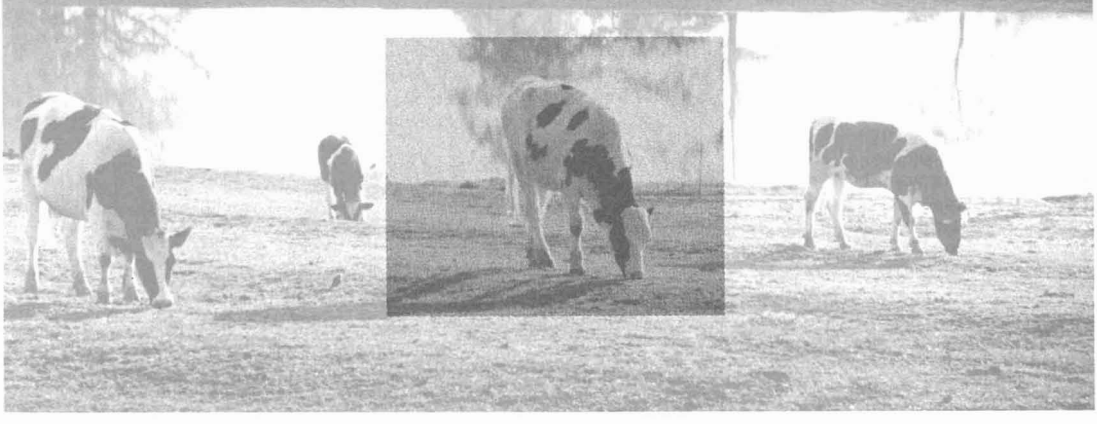

Frank J. Humenik
Michael D. Smolen
Steven A. Dressing
North Carolina State University
Raleigh, N.C. 27695

Recent water quality evaluations and landmark legislation place nonpoint source (NPS) control programs at a pivotal point. Because NPS pollution impacts are site- and source-specific, difficult to identify, and challenging to quantify, assessments of the severity of NPS problems nationwide vary. Some professionals declare nonpoint sources to be the major reason for not reaching water quality goals. Others say, "the majority of the nation's surface waters have minimum to no known significant impacts from NPSs..." (*1*).

The assessments

In the 1982 National Water Quality Inventory, six out of 10 EPA regions reported that NPS pollution is the principal remaining cause of water quality problems in their regions (*2*). Results of that survey showed that despite the variability of NPS problems, agricultural activities—especially tillage practices and animal waste management—constitute the most pervasive problems in every region. The 1984 National Water Quality Inventory noted that NPS is a major problem in 24 states and is the primary cause of use impairments (e.g., degradation of a drinking-water supply) of rivers and streams in three of the western regions (*3*).

The Association of State and Interstate Water Pollution Control Administrators (ASIWPCA) evaluated progress in water quality by comparing state water quality assessments from 1972 and 1982 (*4*, *5*). Table 1 shows improvement in about 13% and degradation in about 3% of the river and stream miles assessed. These statistics were reversed for lakes; deterioration was detected in 13% of the lake acres. There are, however, deficiencies in the ASIWPCA assessment. For example, the river and stream mileage compared between 1972 and 1982 was only about 10–20% of the total river mileage, depending on whether one accepts ASIWPCA's estimate of 1.8 million stream miles or the 3.5 million miles recognized by the U.S. Geologic Survey (USGS), EPA, and the Bureau of the Census. Similarly, the lake and reservoir assessments exclude the area of the Great Lakes and the Great Salt Lake.

Nonpoint source pollution management

Section 319 of the Clean Water Act requires each state to prepare an assessment report and management program for nonpoint source pollution. The Act was reauthorized in February 1987, and these documents are due in August 1988. The assessment report must identify

- waters unlikely to meet water quality standards without additional controls on nonpoint source (NPS) pollution, and
- nonpoint sources causing the problems.

The management program will cover a period of four years and will include

- identification of the measures needed to control NPS pollution identified in the assessment report,
- identification of steps to implement these measures,
- identification of all sources of funding for NPS pollution control,
- certification that state laws have adequate authority to implement the program, and
- a schedule for implementation of the program.

The 1987 Act authorizes $400 million in grants for four years for the states to use in implementing approved management programs.

0013-936X/87/0921-0737$01.50/0

Table 2 provides data from the 1982 ASIWPCA assessment. Almost 30% of river and stream miles and about 13% of lake acres exhibit some degree of use impairment. Waters that were not assessed—about 1 million stream miles according to ASIWPCA and about one-half the lake area—were assumed to have higher quality than those assessed. Interpretation of these assessments requires caution, because the data bases used differ widely. For example, there are large differences among data sources: different state reporting criteria, differences between the 1972 and 1982 data bases, and uncertainties in assessment definitions.

In 1985, at the request of EPA, ASIWPCA assembled a baseline of current NPS information, both quantitative and narrative, from 49 states; Rhode Island was omitted (*1*, *6*). Although a few major water bodies either were not assessed (the Great Salt Lake and Alaskan estuaries) or only partially assessed (the Great Lakes), it is the most extensive NPS data base yet assembled.

Table 3 displays the results of ASIWPCA's assessment of impairment in 400,000 miles of rivers or streams and 15 million acres of lakes and reservoirs. State officials report that about 29% of the river and stream miles and about the same percentage of lakes and reservoirs assessed are moderately to severely impaired. They also report that about 12% of the rivers and streams and 24% of the lakes and reservoirs are threatened by nonpoint source pollution.

Agricultural activities were found to be the main contributors of NPS pollution in both lakes and rivers. After agriculture, urban runoff, resource extraction, and hydromodification are the most widespread causes of NPS pollution. The predominant river NPS pollutant is sediment, and the predominant lake and estuary NPS pollutants are algal nutrients.

Perhaps the most disturbing aspect of the survey is ASWIPCA's conclusion: "States report that the majority of the nation's surface waters have minimal to no known significant impacts from nonpoint sources." This statement is contradicted by their data that show that water resources whose designated uses are "impaired or threatened" make up 41% of the total river mileage assessed, 53% of the total lake surface assessed, and 28% of total estuary surface assessed.

Recent legislation

The Clean Water Act (CWA) Reauthorization, passed by Congress in February 1987 over President Reagan's veto, for the first time specifically addresses NPS pollution. It directs states to submit to EPA a list of waters not meeting CWA goals because of NPS pollution and to submit an NPS management program for those waters. States are required to identify land use sectors that cause major NPS problems, describe their processes for identifying Best Management Practices (BMPs) to control NPS pollution, and formulate implementation schedules. For those states not submitting their own NPS programs, EPA is directed to identify water bodies that do not meet standards and to identify categories of NPS pollution.

The legislation retains national leadership for EPA but requires extensive state support and reliance on existing state and local program authorities and capabilities. This is consistent with EPA's current NPS policy (*7*). Funds are provided to enhance state program capabilities and to secure the essential expertise, but grant funds cannot be used for cost sharing with individuals except in demonstration projects.

The Food and Security Act of 1985 (P.L. 99-198, also known as the Farm Bill) includes a conservation title calling for the elimination of a substantial amount of agricultural pollution from NPS. This title includes two key provisions. The first establishes a Conservation Reserve Program (CRP); the second sets up a Conservation Compliance (CC) program. The CRP will take 40–45 million acres of the most erodible cropland out of agricultural production during a 10-year period by developing rental agreements with landowners.

The CC program seeks to establish an approved conservation plan for all farms that raise row crops on highly erodible land. Highly erodible land is designated by susceptibility to erosion by either wind or water. Under the CC provision, any farmer who cultivates highly erodible land after 1990 without an approved conservation plan will be ineligible to participate in any federal agricultural programs, including commodity price supports, loans, and disaster assistance. The Farm Bill also has a Conservation Easement provision that allows the Farm Home Administration to cancel existing farm debt in exchange for the permanent idling of cropland.

Whether or not water quality benefits accrue from the Act will depend on the extent to which the conservation reserve idles those lands that cause water quality problems and the extent to which the conservation plans, mandated by CC, are oriented to water quality-related problems. In short, a high level of participation in CRP is needed.

Participation in CRP is based on a "free market" concept; during designated sign-up periods farmers and land-

Reauthorization of the Clean Water Act

After nearly two years of deliberation, the Reauthorization Bill passed unanimously at the close of the 99th Congress in October 1986, only to be pocket-vetoed by President Reagan. Identical legislation was introduced in the 100th Congress and approved by 406–8 by the House on January 8th and by 93–6 a few days later in the Senate.

On Jan. 30, 1987, the new Clean Water Act Reauthorization was vetoed by President Reagan because of its impact on the federal deficit. But in his letter to the House, the President indicated strong, fundamental opposition to the NPS provision of the bill. He stated that the legislation

". . .threatens to become the ultimate whip hand for federal regulators," that with it the EPA ". . .will be able to intrude into decisions such as how and where the farmers must plow their fields, what fertilizers they must use, and what kind of cover crops they must plant," making EPA ". . .a major force in local zoning decisions."

The President offered an alternative bill in the Senate with $12 billion for construction grants that would give states complete discretion over participation in the NPS pollution program and use of the federal funds.

The House voted 401–26 to override on Feb. 3, 1987. The Senate followed suit by voting 86–14 the next day, after voting down the President's alternative.

The new Act authorizes $18 billion for construction grants and $2 billion for related projects during an eight-year period. The authorizations for NPS programs, including groundwater protection, total roughly one-half billion dollars. The Act provides a reserve of the greater of $100,000 or 1% of each state's annual construction grant allocation, beginning this fiscal year, to prepare and implement the state's NPS management program. The governor of each state may set aside as much as 20% of construction grant funds for NPS control. In addition, money from a revolving loan fund established by the Act can be used to help phase out federal construction grants.

TABLE 1
Comparison of the water quality of U.S. rivers, streams, lakes, and reservoirs[a]

Description	No. of river and stream miles compared[b]		No. of lake and reservoir acres compared[b]	
Improved	47,000	(13.3%)	390,000	(3.2%)
Degraded	11,000	(3.1%)	1,650,000	(13.6%)
Unchanged	296,000	(83.6%)	10,130,000	(83.2%)
Totals[c]	354,000		12,170,000	

[a]Comparison covers the years 1972–1982.
[b]Data are taken from the 1984 ASIWPCA report (*5*).
[c]Totals differ from those presented in ASIWPCA's summary; miles and acres reported as unknown were omitted.

TABLE 2
Assessment of water quality in U.S. rivers, streams, lakes, and reservoirs[a]

Description	No. of river and stream miles assessed[b]		No. of lake and reservoir acres assessed[b]	
Not supporting designated uses	35,000	(5.1%)	400,000	(2.5%)
Partially supporting uses	167,000	(24.2%)	1,700,000	(10.7%)
Fully supporting uses	488,000	(70.7%)	13,800,000	(86.8%)
Totals[c]	690,000		15,900,000	

[a]Assessment covers 1982
[b]Data are taken from the 1984 ASIWPCA report (*5*).
[c]Totals differ from those presented in ASIWPCA's summary; miles and acres reported as unknown were omitted.

TABLE 3
Assessment of NPS impairment in U.S. rivers, streams, lakes, and reservoirs[a]

Description	No. of river and stream miles assessed[b]		No. of lake and reservoir acres assessed[b]	
Impaired, cause uncertain	9,000	(2.2%)	90,000	(0.6%)
Severely impaired	31,000	(7.6%)	880,000	(5.7%)
Moderately impaired	87,000	(21.5%)	3,500,000	(22.8%)
Supported designated uses	278,000	(68.6%)	10,900,000	(70.9%)
(threatened by NPS)	48,000	(11.8%)	3,700,000	(24.1%)
Totals[b]	405,000		15,370,000	

[a]Data are taken from the appendix to ASIWPCA's 1985 survey (*6*).
[b]Numbers differ from those in ASIWPCA's summary report (*1*) because they were computed directly from the report's appendix of state submissions (*6*).

owners enter bids stating the annual rental payment they would accept to idle their highly erodible cropland. If a bid is accepted, the farmer receives the rental payment plus financial and technical assistance to begin conservation practices and establish grassland or woodland. The use of CRP land for grazing or hay production is not allowed, but there are particularly favorable incentives to establish profitable wildlife areas or stands of marketable trees. As part of the participation agreement, the farmer gives up a portion of his established production base, thereby reducing the amount of money he can receive from acreage diversion or price support programs.

In each of four successive sign-up periods, the stakes have risen. The average bid accepted has increased; in the February 1987 sign-up, the U.S. Department of Agriculture (USDA) offered an additional one-time payment of $2 per bushel for corn land placed in the reserve. In the four sign-up periods, 19.5 million acres—less than half of the goal—has been placed in the reserve. Many farmers are still taking a wait-and-see attitude and gambling that the compliance provisions, which are not scheduled to take effect until 1991, will be reduced in the next farm bill or that the incentives will reach a level they cannot resist.

Early experience

The Clean Water Act of 1972 authorized EPA to demonstrate pollution control technologies in the Great Lakes Basin. The program under which this demonstration was conducted addressed a wide variety of pollution control technologies, such as soil conservation, conservation tillage, and animal waste management, through grants to municipalities and soil and water conservation districts (*8*).

Black Creek (Allen County, Ind.), one of the first watershed-based projects sponsored by the Great Lakes Program, spent more than $800,000 as a cost-sharing incentive for conservation treatment on a 10,000-acre watershed but could not show water quality improvements. The experience demonstrated clearly that the traditional "first-come first-served" distribution of cost-sharing incentives is not effective for water quality improvement because there are too many conservation needs that have little effect on water quality. Consequently, the project's managers developed concepts for targeting critical areas and coordinating treatment among landowners. The legacy of this project includes a hydrologic-water quality simulation model, ANSWERS, which can be used to identify critical areas and to evaluate the effect of treating different areas in a watershed (*9*).

The Black Creek project also provided lessons in sociological and institutional aspects of NPS control. It demonstrated the importance of identifying opinion leaders in the community and showed the efficacy of personal contact with landowners in promoting voluntary participation in conservation practices in critical areas. Moreover, it demonstrated that a local entity, the Soil and Water Conservation District, could administer a nonpoint source abatement program.

In early 1977, USDA and EPA issued a Memorandum of Understanding to conduct the Model Implementation Program (MIP). This program was a large-scale cooperative effort to implement soil conservation and water quality-related agricultural land management practices in watershed projects in Indiana, Nebraska, New York, Oklahoma, South Carolina, South Dakota, and Washington. MIP projects, administered on a watershed basis, used existing program authorities of soil and water conservation districts, USDA-Agricultural Stabilization and Conservation Service (ASCS), USDA-Soil

Conservation Service (SCS), and the Cooperative Extension Services. State environmental agencies monitored water quality to evaluate project results.

The Yakima MIP in Washington state reduced sediment yield from irrigation tracts, and the Cannonsville Reservoir MIP in New York reduced animal waste pollution from barnyards (*10*). Other MIP projects reduced cropland and pasture land erosion, or attempted to prevent groundwater contamination or stream bed erosion. None of the MIP projects, however, demonstrated clear-cut improvements in their designated impaired water resource areas, because monitoring periods were too short (two to three years) and pollution control efforts were generally scattered too widely to produce measureable improvements.

A number of lessons, however, were learned from the MIPs (*11*). For example, the program should be administered on the basis of watershed boundaries rather than political boundaries. The program needs preproject planning and identification of those critical areas in which the largest water quality benefits can be achieved by land treatment. The program also should be directed by an agency with a water quality orientation that can coordinate the efforts of cooperating agencies.

Recent experience

The Rural Clean Water Program (RCWP) began in 1980 in a cooperative model based on the MIP. The program funded 21 watershed projects whose objectives were to improve water quality, to help agricultural landowners and operators employ pollution control practices, and to develop and test programs, policies, and procedures for control of agricultural nonpoint source pollution (*12*).

The RCWP gained considerably from the Great Lakes Program and MIP experiences. The time frames are longer (10–15 years); critical area targeting is required; water quality objectives are clearly specified; and projects monitor water quality. Each project is administered locally and overseen by state and national RCWP coordinating committees.

The RCWP has a much stronger water quality emphasis than any preceding conservation or demonstration program, including the Great Lakes Program and MIP. Approved BMPs include water management systems, animal waste management systems, and fertilizer and pesticide management, all of which are practices and systems designed to improve water quality and are not necessarily oriented to soil conservation or farm productivity.

Seven years into the program, most projects have exceeded their goals of contracting to treat agricultural NPSs in 75% of their critical areas. Projects that have achieved a high level of farmer participation have been successful because they offer cost sharing for practices farmers want, such as animal waste storage structure installation, conservation tillage, and irrigation system improvements. Cost-sharing incentives, however, were unsuccessful in several projects when economic problems were too great in the farm community or when farmers were not enthusiastic about government programs.

The Cooperative Extension Service has stimulated participation in several projects by providing services such as pest-scouting to reduce pesticide use, manure-sampling to promote proper use of manure, and soil-sampling to match fertilizer and manure nutrient use with crop requirements. Indications are that such services may be the most effective and economical approaches to agricultural NPS control.

Negative inducements have been effective for obtaining participation in several projects. Projects in Florida and Oregon have invoked existing local or state regulations to induce farmers to comply with water quality objectives. In Oregon, for example, dairy farmers are penalized by their milk cooperative if they do not use approved animal waste management practices. The combination of negative inducements with offers of cost sharing and technical assistance appears to be a powerful incentive for farmer participation (*10*).

The Rural Clean Water Program is supplemented by a data analysis project known as the National Water Quality Evaluation Project (NWQEP). The project was initiated in 1981 by a Memorandum of Understanding between USDA and EPA and a Cooperative Agreement between USDA-Extension Service and the North Carolina Agricultural Extension Service at North Carolina State University. Through the efforts of the individual RCWP projects and the NWQEP, water quality improvements have been documented in the Snake Creek RCWP in Utah, the Tillamook Bay RCWP in Oregon, and the Rock Creek RCWP in Idaho (*10*, *13*). NWQEP's analysis of NPS projects indicates that a time frame longer than five years generally is necessary to document water quality improvements in an NPS project, but more rapid improvement has been observed in arid regions. The NWQEP efforts are directed toward evaluation and interpretation of water quality results such as these, and it helps extend RCWP findings and experience to potential users of such information.

Urban runoff

The Nationwide Urban Runoff Program (NURP) was developed by EPA in 1978 as a five-year program to obtain data on control of urban runoff quality and its impact on receiving waters. Data from 28 individual projects around the country were contributed. A series of reports on the findings of the program has been published (*14–16*).

The NURP studies confirmed that pollution problems such as coliform bacteria, nutrients, or heavy metals result from urban runoff. The most significant effects of urban stormwater runoff on aquatic life, however, are caused by hydrological changes related to urbanization and construction activities. Analysis of the NURP results indicates that the impact of urban runoff is highly site-specific and depends largely on the fraction of the drainage basin urbanized and the characteristics of the receiving water body.

The NURP studies did not identify easy solutions. However, wet detention basins and infiltration of stormwater through recharge basins were shown to be effective for reducing the volume of surface runoff and pollutant concentrations. Other practices, such as installing stream buffers and grass swales and establishing wetland areas also have been identified as potential urban NPS control practices. Street sweeping was shown to be generally ineffective.

Lessons learned

Water quality improvement, as shown in the ASIWPCA surveys (1972–1982 Progress Report and 1985 NPS Report), has not been overwhelming, although a great deal of money has been spent on point source pollution control. The lack of further deterioration of water quality during a period of industrial growth and population expansion, however, may attest to the success of the point source control programs. NPS pollution is often the limiting factor in improving or maintaining water quality, thus point source control without corresponding NPS pollution control generally will be insufficient. Agricultural pollution is clearly identified as the principal NPS concern nationwide.

The Great Lakes Program, NURP, MIP, RCWP, and other projects have provided considerable experience within the EPA, SCS, ASCS, Extension Service, and soil and water conservation districts. However, they also show that coordination of these distinctly different mission-oriented agencies in a water quality program requires concerted effort. It is especially important that all cooperating agencies participate in project planning, have clearly de-

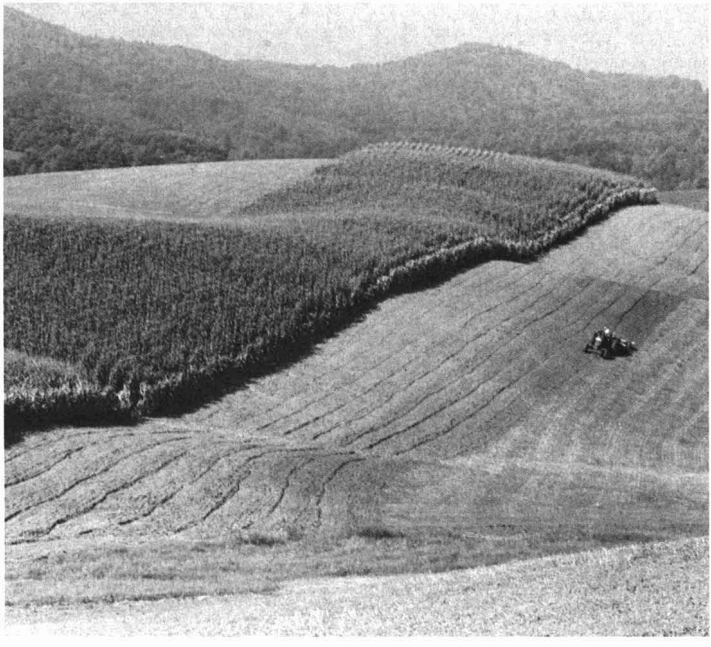

fined arrangements for cost reimbursement, and share goals.

Agricultural BMPs should be selected and approved by teams that include land treatment and water quality professionals. Substantial effort should be devoted to public education, and incentives should be tailored to the needs of individual participants. Program administrators should be particularly sensitive to economic problems and to cultural barriers. Although voluntary programs are preferred, effective and fair enforcement of regulations or penalties can enhance participation and improve results.

Future needs and opportunities

The opportunity is at hand for progress toward national clean water goals by addressing nonpoint sources of pollution. All the elements are present: experience, programming authority, and the authorization to spend as much as one-half billion dollars to address NPS problems in every state. To utilize these elements effectively, however, we need leadership, commitment, and determination. States and localities need access to the best professional experience for developing their programs and targeting their efforts, access to state-of-the-art information on the control of NPS pollution and administration of water quality projects, and guidance to establish formal reporting that maintains program accountability. We need information centers to analyze program results, assemble and repackage the information, and disseminate the information to the states.

The lack of consistent, reliable results from national water quality surveys indicates a clear need to improve our monitoring and assessment capability. We have no permanent monitoring network in place, and we still cannot quantify adequately the improvement or degradation of our nation's water quality. We need national coordination to establish and maintain a consistent monitoring program. EPA must assure that states have a clear set of monitoring objectives, access to the most up-to-date technology, and appropriate standardization to answer basic questions on spatial and temporal trends in water quality.

Many research reports with information concerning the effectiveness of BMPs have been published, but most reflect diverse, isolated conditions. A coherent body of experimentation evaluating the range of BMP effectiveness or the expected performance of systems of BMPs is lacking.

Coordinating the efforts of universities and governmental research agencies, and making information available to the public, would be helpful. An accepted analytic framework or model to evaluate the impact of NPS control programs and to assess progress toward water quality objectives also is needed. NPS models should be developed to meet the needs of project managers and environmental planners.

We need to develop and verify procedures to estimate nonpoint source loading, and we need models to predict the impact of NPS controls. In particular, we need pollutant transport and water quality models that consider the seasonality and inherent variability of NPS pollution. Such models would be particularly useful for addressing the issue of waste load allocation and point–nonpoint tradeoffs. Although analyses of this type are being used for phosphorus control in the Great Lakes, the models involved are not very sophisticated. Advances in this area will improve our ability to compare effectively the costs and benefits of NPS control and point source control and to optimize water quality strategies.

The need for information on the impact of NPS on water quality and effectiveness of NPS control programs and BMP performance will increase dramatically as states plan NPS control programs as mandated by the CWA. EPA is expected to provide this information to the states, but EPA has only limited information at hand. Assembling and distributing such information will be a major undertaking.

Improved technology is needed to manage salinity, protect groundwater from toxic contaminants, manage and dispose of pesticides properly, and control acid mine drainage. Technological advances are needed even in well-known areas such as fertilizer and manure management to meet the needs for agricultural yield and to use nutrients in a manner that would promote more effective pollution control.

Sociological, economic, and legal issues, too, need further research. For example, we need further understanding of the interplay of incentives (cost sharing and technical assistance) and constraints (regulations and penalties) in NPS pollution control programs. We need insight to handle problems of unequal dispersal of project funds (as in targeting one of two neighboring farms), and we need tools and techniques to change public attitudes toward environmental quality (to recognize personal responsibility for waste disposal).

The Farm Bill, with its conservation reserve program and conservation compliance requirement, may be the most effective tool yet for controlling agricultural NPS. States have the opportunity to coordinate their NPS efforts with the Farm Bill programs and steer the conservation reserve to water quality critical areas, thereby removing from production those areas most damaging to land and water resources. Unfortunately, there is continual pressure to weaken this legislation and remove the teeth from its compliance section. Implementation of the conservation provisions competes with ongoing USDA programs because the agencies charged with administering it are under-funded. Moreover, the Farm Bill

comes up for renewal in 1989, one year before the compliance provision takes effect. A concerted effort is needed to support the water quality objectives of the Act and to assure that the conservation compliance provisions are implemented.

Finally, a long-term, coordinated commitment is needed. The MIP projects were too short. Even the 10-year life of RCWP projects is short. Nonpoint source control requires the same level of commitment as point source control even though the methods are very different. A well-developed grass roots approach, in which NPS control is factored into all relevant national, state, and community activities, will go a long way toward achieving effective NPS control.

We have a major opportunity to reduce the impact of NPS pollution. The new version of the CWA and the Farm Bill offer both the means and the motivation to address the NPS pollution problem directly. The CWA directs EPA and the states to assess the problem and implement a program for its control. The Farm Bill offers cost sharing incentives and the threat of future penalties to induce soil conservation on a large portion of the land. Coordination of these programs, along with control of urban NPS and point source pollution, can achieve significant improvements in water quality.

Acknowledgment

This article represents the views of the authors and not the official position of EPA or any other state or federal agency. The authors wish to acknowledge contribution of information on urban NPS pollution control from William Kreutzberger of the North Carolina Division of Environmental Management.

This article has been reviewed for suitability as an *ES&T* feature by Donald R. Nielsen, University of California, Davis, Calif. 95616, and by J. Heaney, University of Florida, Gainesville, Fla. 32601.

References

(1) "America's Clean Water. The States' Nonpoint Source Assessment 1985"; ASIWPCA: Washington, D.C., 1985.
(2) "Nonpoint Source Pollution in the U.S.: Report to Congress"; Office of Water, Criteria and Standards Division; EPA: Washington, D.C., 1984.
(3) "National Water Quality Inventory: 1984 Report to Congress"; EPA 440/4-85-029; EPA: Washington, D.C., 1985.
(4) "America's Clean Water: The States' Evaluation of Progress 1978–1982"; ASIWPCA: Washington, D.C., 1984.
(5) "America's Clean Water. The States' Evaluation of Progress 1978–1982. Appendix"; ASIWPCA: Washington, D.C., 1984.
(6) "America's Clean Water. The States' Nonpoint Source Assessment 1985. Appendix"; ASIWPCA: Washington, D.C., 1985.
(7) "Final Report on the Federal/State/Local Nonpoint Source Task Force and Recommended National Nonpoint Source Policy"; NTIS PB86-187929; EPA: Washington, D.C., 1985.
(8) Newell, A.D. et al. "Overview and Evaluation of Section 108a Great Lakes Demonstration Program"; EPA 905/9-86-001; EPA: Washington, D.C., 1986.
(9) Beasley, D.B.; Huggins, L.F.; Monke, E.J. *Trans. Am. Soc. Agric. Eng.* 1980, *23*, 938–44.
(10) "Status of Agricultural NPS Projects 1985," Report of the National Water Quality Education Project; Biological and Agricultural Engineering Dept., North Carolina State University: Raleigh, N.C., 1985.
(11) "An Evaluation of the Management and Water Quality Aspects of the Model Implementation Program"; Report of the National Water Quality Evaluation Project and Harbridge House; Biological and Agricultural Engineering Dept., North Carolina State University: Raleigh, N.C., 1983.
(12) *Fed. Regist.* **1979**, *44*, 76202–76209.
(13) "Rural Clean Water Program: Status Report on the CM&E Projects 1985," Report of the National Water Quality Evaluation Project; Biological and Agricultural Engineering Dept., North Carolina State University: Raleigh, N.C., 1985.
(14) "Results of the Nationwide Urban Runoff Program, Volume II — Data Appendix"; NTIS PB84-185578; EPA: Washington, D.C., 1982.
(15) "Results of the Nationwide Urban Runoff Program, Volume III — Data Appendix"; NTIS PB84-185578; EPA: Washington, D.C., 1983.
(16) "Results of the Nationwide Urban Runoff Program, Volume I — Final Report"; NTIS PB84-185552; EPA: Washington, D.C., 1983.

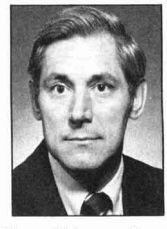

Frank J. Humenik *is a professor of biological and agricultural engineering. He provides leadership for research and extension programs in agricultural waste management, water quality, and water supply.*

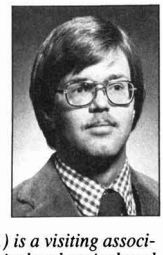

Michael D. Smolen *(l.) is a visiting associate professor of biological and agricultural engineering. He is a group leader for water quality projects sponsored by EPA, USDA, and the state of North Carolina.*

Steven A. Dressing *(r.) is an extension specialist in biological and agricultural engineering. He is assembling a national NPS data base at the EPA NPS Branch.*

ES&T VIEWS

Structure–activity relationships

Criteria for predicting the carcinogenic activity of chemical compounds

By Joseph C. Arcos

It is a sobering fact that the rate of growth of the number of new organic compounds synthesized throughout the world is around 400,000 per year. Of these 400,000 new chemicals, an estimated more than 1000 are introduced yearly into economic use and thus into the environment worldwide. However, because of cost and time limitations and limitations in the number of existing testing facilities, only a small number of these new chemicals can be adequately assayed for carcinogenicity. Hence a significant number of untested or inadequately tested chemical compounds can find their way into consumer items or industrial uses. Moreover, a considerable number of chemicals now in use in industrialized countries were introduced before the present relatively stringent criteria for carcinogen testing and risk assessment were established. Russell Train, former administrator of the EPA, has stated that "less than 2% of the more than 65,000 chemicals in commerce have been adequately tested for their effects on human health and the environment."

These circumstances have sparked a growing interest in formalized schemes and procedures to detect chemicals that may be suspected of carcinogenic activity. The total perspective of known chemical carcinogens (*1–5*) allows a distillation of the general principles for the prediction of potential carcinogenic activity (CA) of untested chemicals.

The three categories of criteria for suspecting chemical compounds of CA are structural criteria, functional criteria, and the "guilt by association" criterion.

Structural criteria represent conclusions drawn from structure–activity relationship (SAR) analysis. SAR analysis uses essentially two approaches, which are based on

- formal structural analogies with established types of chemical carcinogens, and
- considerations of molecular size, shape, and symmetry; of electron distribution; of reactive functional group(s), if any, and of steric factors around these groups; and of the possibility of undergoing metabolism to reactive intermediates—*independently* of any possible analogy with known chemical carcinogens.

Functional criteria represent the sum of the pharmacological and toxicological capabilities that—irrespective of structural type—have shown some degree of correlation with CA (e.g., mutagenicity, induction of DNA repair, immune suppression). Functional criteria complement structural criteria because structural considerations alone cannot forecast entirely new structural types of carcinogens.

The *"guilt-by-association" criterion* points to the potential CA of a compound that—although found inactive under some "standard" conditions of animal bioassay (or genotoxicity testing)—belongs to a chemical class in which several other compounds were found to be potent and multitarget carcinogens (e.g., the 5-nitrofuran-type urinary antibacterials). Such compounds should be re-evaluated to determine whether retesting by bioassay under more stringent conditions is warranted.

Structural criteria

The first approach of SAR analysis compares compounds of unknown activity to structural types known to be carcinogenic. Structural analogy, as used presently, is a relative and subjective concept dependent to some extent on the "eyes of the beholder." There is a beginning of development to place the

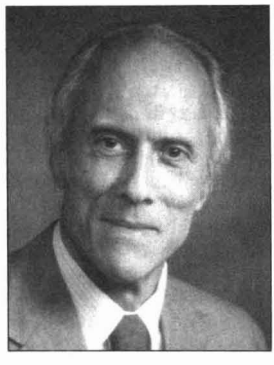

At the spring meeting of the American Chemical Society in Denver, Joseph C. Arcos received the ACS Award for Creative Advances in Environmental Science and Technology. In his award address on the prediction of carcinogenic activity of new organic compounds, he reviewed the general principles of structure–activity relationship analysis for assessing potential carcinogenicity. During the past 20 years he has carried out a broad, analytic survey of the entire literature of chemical carcinogens and has written a six-volume series of monographs entitled "Chemical Induction of Cancer—Structural Bases and Biological Mechanism," (Academic Press, New York/Orlando), which was the basis of this award.

Arcos is a senior science advisor in EPA's Office of Toxic Substances. He also is a clinical professor at Tulane University Medical Center in New Orleans. He received his training in cancer research at the University of Wisconsin during the 1950s. He then joined the University of Florida and in 1960 became affiliated with Tulane University. In 1986, Arcos was named a fellow of the American College of Toxicology for his outstanding contributions to the field of toxicology.

concept on a rigorous, scientific basis using various approaches of molecular topology (such as graph theory) as well as approaches of information theory. Another route using the concept of structural analogy is to identify molecular descriptor structure fragments that are associated with carcinogenic or mutagenic activity (or lack thereof) and then to analyze a new molecule for potential activity against the set of descriptors. A computer-automated structure evaluation (CASE) method, which uses this route, has been developed by Rosenkranz et al. (*6*).

The principal types of known chemical carcinogens that form the backdrop for the evaluation of new compounds by structural analogy are

- aromatic amines,
- azo compounds,
- polynuclear hydrocarbons and heteroaromatics,
- alkylating agents,
- halogenated and polyhalogenated aliphatic and aromatic hydrocarbons and derivatives thereof,
- acylating agents,
- miscellaneous epigenetic carcinogens,
- carcinogenic elements: certain metals and metalloids (e.g., Cd, Cr, Ni, As), and
- foreign-body carcinogens.

The aromatic amines, azo compounds, and polynuclear hydrocarbons and heteroaromatics are arylating agents. After metabolic activation to reactive electrophiles, they become covalently linked to cellular nucleophiles: nucleic acids, and proteins. The activation of most aromatic amines and azo dyes involves a three-step mechanism (beginning with *N*-hydroxylation) yielding two tautomeric forms of the final reactive intermediate, one of which is a carbonium ion. Polynuclear hydrocarbons and heteroaromatics are activated by epoxidation. The transitional forms of these epoxides during nucleophilic attack are carbonium ions; however, for certain polynuclears and ring-methyl polycyclic hydrocarbons there is evidence for one-electron oxidation at carbon leading directly to carbonium ion forms, as a competing or alternate activation pathway. These mechanisms of activation provide a predictive rationale for the increase or decrease of carcinogenic potency of aromatic carcinogens with change of the molecular size, shape, and π-electron distribution and with the introduction or removal of substituents.

The alkylating agents are by far the largest and structurally most heterogeneous group among all carcinogens. These compounds display a virtually unlimited structural variety, and their only common characteristic is that they are or can be metabolically transformed into electrophilic reactive intermediates that can alkylate DNA and other cellular nucleophiles. Some major classes of carcinogenic alkylating agents are nitrogen mustards; haloethers; epoxides; aziridines, lactones and sultones; *N*-nitroso compounds; hydrazo, aliphatic azo, and azoxy compounds and aryldialkyltriazenes; and carbamates. Most of the naturally occurring carcinogens, the mycotoxins and plant carcinogens, are alkylating agents. Some of the halogenated and polyhalogenated hydrocarbons mentioned in the above list also are alkylating agents, whereas some compounds in that class are epigenetically acting carcinogens. The extraordinary structural variety among carcinogenic alkylating and cross-linking agents, as well as the fact that arylation by aromatic amines and polynuclear compounds also leads to carcinogenesis, points to the important concept that the chemical nature of the xenobiotic molecular moiety that becomes attached to key informational macromolecules is probably immaterial as long as these attachments effectively interfere with the normal functioning of synthetic templates. This is consistent with the finding that some acylating agents are also carcinogenic. Benzoyl chloride and dimethylcarbamyl chloride are potent carcinogens in rodents, and there is epidemiologic evidence for increased cancer incidence among benzoyl chloride manufacturing workers.

The significant linking of xenobiotic molecular moieties—arylating, alkylating, and acylating agents—to DNA is probably not a random process. There is increasing evidence that those DNA substitutions and subsequent mutations that actually lead to carcinogenesis are selective and involve specific areas of the genome. Several carcinogens have been shown to activate oncogenes (DNA segments coding for various proteins that play critical roles in cell regulation).

The second approach of SAR analysis includes a thorough consideration of the probable modality of interaction of the compound in question with the tissue target cells. These modalities also constitute the basis of a classification of carcinogens as genotoxic carcinogens, epigenetic carcinogens, or foreign-body carcinogens.

Genotoxic carcinogens are compounds that produce DNA damage through covalent binding (involving, in some cases, strand scission). These are compounds that act as electrophilic reactants either directly or after metabolic activation.

Epigenetic carcinogens are compounds that do not directly damage DNA but act by a variety of not clearly defined extrachromosomal mechanisms such as inhibition of intercellular communication, creation of endocrine imbalance, chronic tissue injury, immune modulation (principally suppression), or induction of peroxisome proliferation.

Foreign-body carcinogens are materials that, by virtue of their critical size and shape as well as surface reactivity, induce carcinogenesis probably by disrupting intercellular homeostasis or by mechanically interfering with conformational changes in chromatin or DNA. There are three classes of foreign-body carcinogens: self-penetrant fibers (epitomized by asbestos); nonfibrous, crystalline, hard silicates; and sheets and platelets implanted in tissues. On the basis of their possible mechanisms of action, carcinogenic water-soluble high polymers have some aspects of both epigenetic and foreign-body carcinogens.

Genotoxic carcinogens acting as electrophilic reactants can be further classified as direct-acting carcinogens, not requiring activation; carcinogens that require simple acid or alkali-catalyzed hydrolysis for activation; and carcinogens that require metabolic activation. Direct-acting carcinogens are often locally active, whereas those that require activation tend to be carcinogenic toward the tissues or organs where activation occurs. Compounds yielding reactive intermediates that are stabilized by resonance often have higher carcinogenic potential, because such reactive intermediates have a better chance of remaining reactive during transport from the cellular site of activation to reach target nucleophiles. In general, a compound should be suspected to be carcinogenic if its metabolic split products are known or suspected to be carcinogenic.

Irrespective of its chemical structure, the carcinogenic potential of a compound is dependent on its physical and chemical properties, which determine its "bioavailability" (i.e., its ability to reach target tissues and enter into cells). The most salient properties are molecular weight, molecular size and shape, physical state, solubility and water/octanol partition coefficient, and chemical reactivity.

Functional criteria

Structural criteria cannot predict entirely new structural types of carcinogens. A major historical example for this is the class of the nitrosamines. When the carcinogenicity of dimethylnitrosamine was discovered in the mid-1950s, there was already a very substantial body of information available on the carcinogenicity and structure-activity relationships of various polynu-

Emerging Developments in Environmental Science

ES&T

ENVIRONMENTAL SCIENCE & TECHNOLOGY

Enter your own monthly subscription to ES&T and be among the first to get the most authoritative technical and scientific information on environmental issues.

☐ **YES! I want my own one-year subscription to ENVIRONMENTAL SCIENCE & TECHNOLOGY at the rate checked below:**

1987 Published monthly	U.S.	Canada & Mexico	Europe	All Other Countries
ACS Members	☐ $ 30	☐ $38	☐ $46	☐ $54
Nonmembers—Personal	☐ $ 45	☐ $53	☐ $61	☐ $69
Nonmembers—Institutional	☐ $176	☐ $184	☐ $192	☐ $200

☐ Payment Enclosed (Payable to American Chemical Society)
☐ Bill Me ☐ Bill Company
Charge my ☐ VISA/MasterCard ☐ Access
☐ Diners Club/Carte Blanche ☐ Barclaycard

Card No. _____

Expires _____ Interbank No. _____
(M/C and Access)

Signature _____

Name _____

Title _____ Employer _____

Address ☐ Home
☐ Business _____

City, State, Zip _____

Employer's Business: ☐ Manufacturing ☐ Academic ☐ Government
☐ Other _____

Member rates are for personal use only.
Subscriptions outside the U.S., Canada, and Mexico are delivered via air service. Foreign payment must be made in U.S. currency by international money order, UNESCO coupons, U.S. bank draft, or order through your subscription agency. For nonmember rates in Japan, contact Maruzen Co., Ltd. Please allow 45 days for your first copy to be mailed. Redeem until December 31, 1987.

680 **MAIL THIS POSTAGE-PAID CARD TODAY!** 3847A

(800) 424-6747 (U.S. only)

NO POSTAGE
NECESSARY
IF MAILED
IN THE
UNITED STATES

BUSINESS REPLY MAIL

FIRST CLASS PERMIT NO. 10094 WASHINGTON, D.C.

POSTAGE WILL BE PAID BY ADDRESSEE

American Chemical Society
Marketing Communications Department
1155 Sixteenth Street, N.W.
Washington, D.C. 20036-9976

CALL
TOLL
FREE

(800) 424-6747 (U.S. only)

NO POSTAGE
NECESSARY
IF MAILED
IN THE
UNITED STATES

BUSINESS REPLY MAIL

FIRST CLASS PERMIT NO. 10094 WASHINGTON, D.C.

POSTAGE WILL BE PAID BY ADDRESSEE

American Chemical Society
Marketing Communications Department
1155 Sixteenth Street, N.W.
Washington, D.C. 20036-9976

clear compounds, aromatic amines, azo dyes, and aliphatic alkylating agents. Yet all this information did not suggest the carcinogenicity of the nitrosamines. Recent unexplainable examples are the carcinogenicity of 11-aminoundecanoic acid, of the strong chelating agent ethylenediamine tetra(methylene phosphonic acid), and the evidence that such simple compounds as the odd-carbon straight-chain acids—propionic, valeric, and heptanoic acid—appear to be weak carcinogens in some animal bioassay systems. There is no known rationale for predicting the carcinogenicity of these five compounds within the present conceptual framework of the SAR of carcinogens.

The reliability of prediction could be considerably enhanced, however, by complementing the framework of structural criteria with another conceptual framework of evaluation for potential carcinogenicity. Functional criteria represent the pharmacological or toxicological capabilities that, irrespective of chemical structure, have been correlated with CA or construed as possible component factors in the induction of malignancy.

The following capabilities represent functional criteria for suspecting compounds of CA. Compounds are suspect if they induce or are *in vitro* cell transformation, mutations or chromosomal aberrations, an euploidy, unscheduled DNA synthesis, sister chromatid exchange, spindle poisons, covalent binding to DNA or RNA, structural analogues of DNA bases, inhibitors of intercellular communication and cell membrane function, ribosome degranulation from the endoplasmic reticulum, stimulators of tissue hyperplasia and induction of microsomal mixed-function oxidases, peroxisome proliferation, generation of reactive oxygen species by macrophage stimulation, teratogenic compounds, inhibitors of mitochondrial respiration and uncouplers of oxidative phosphorylation, antineoplastic agents, immune-suppressive agents, chronic hormonal imbalance and overstimulation, inhibitors of spermatogenesis, hepatonecrotic, very strong surface-active agents or hydrogen bond reactors, or strong chelating agents.

Construction of an expert system

The formalism summarized under "structural criteria" allows an identification of the molecular features that correlate with CA. Structural and functional criteria can be stated as formal rules for constructing an expert system program. Expert system software is useful when knowledge lends itself to systematic classification and neat packaging. Thus an expert system is a springboard for establishing the prediction of CA as a consistent area of expertise that can be updated as new data become available.

References

(1) Arcos, J. C.; Argus, M. F. *Chemical Induction of Cancer. Vol. IIA. Polynuclear Hydrocarbons and Heteroaromatics;* Academic: New York, 1974.
(2) Arcos, J. C.; Argus, M. F. *Chemical Induction of Cancer. Vol. IIB. Aromatic Amines and Azo Compounds;* Academic: New York, 1974.
(3) Arcos, J. C.; Woo, Y. T.; Argus, M. F. *Chemical Induction of Cancer. Vol. IIIA. Aliphatic Carcinogens;* Academic: New York, 1982.
(4) Woo, Y. T.; Lai, D. Y.; Arcos, J.C.; Argus, M.F. *Chemical Induction of Cancer. Vol. IIIB. Aliphatic and Polyhalogenated Carcinogens.* Academic: Orlando, Fla., 1985.
(5) Woo, Y. T.; Lai, D. Y.; Arcos, J. C.; Argus, M.F. *Chemical Induction of Cancer. Vol. IIIC. Natural, Metal, Fiber, and Polymer Carcinogens.* Academic: Orlando, Fla. In press.
(6) Rosenkranz, H. S.; Mitchell, C. S.; Klopman, G. *Mutation Res.* **1985**, *150*, 1.

Continued from Letters, p. 716

the excess sulfide ions in the treated water must be removed by aeration or oxidation with chlorine. Although technically effective, sulfide precipitation is a relatively complex and expensive process (*12–13*)."

As one can see, we have no major disagreement with Peters and Bhattacharyya except in our relative levels of enthusiasm for sulfide precipitation. Perhaps we should have added the word "potential" ahead of generation of toxic H_2S gas, because such generation can be avoided by complex design and careful operation.

Much attention has been given to the advantages. Let us reiterate the major disadvantages, first regarding soluble sulfide precipitation (SSP) as quoted directly from "Control and Treatment Technology for the Metal Finishing Industry—Sulfide Precipitation" (EPA 625/880-003, 1980). "In practice, considering typical response lags of instruments and incremental reagent addition, control of the level of dissolved sulfide and pH would require fine tuning and rigorous maintenance to prevent an H_2S odor problem in the work area. In currently operating treatment systems, the H_2S odor problem is eliminated by enclosing and vacuum evacuating the process vessels." This is true in spite of the use of pH and ion-specific electrodes to control the addition of soluble sulfide. In regard to insoluble sulfide precipitation (ISP), from this same comprehensive report we quote: "It [careful pH control] is more important to eliminate the danger of the FeS slurry coming in contact with acidic wastewater; FeS is soluble in acidic solutions, and mixing it with low-pH wastewater would result in the emission of toxic H_2S fumes in the work area." and further, "If the pH of the waste stream drops below 7, valves automatically reroute the feed back to the second-stage neutralizer."

Two significant disadvantages have not yet been mentioned. One is associated with the potential generation of H_2S from SSP and ISP sludges when they are subjected to the required acidic leaching tests. This toxic off-gas would place such sludges into the hazardous category. Another disadvantage of the ISP process using FeS is the added precipitation of a stoichiometric amount of $Fe(OH)_2$ from the hydrolysis of the released Fe_2+. Furthermore, if sulfide and hydroxide are used together in the same precipitation step, all the metals will be precipitated as sulfides, thereby increasing the sulfide demand which is already 2 to 4 times stoichiometric in the case of ISP. In summary, sulfide precipitation can often produce lower effluent metals concentrations than hydroxide precipitation, but sulfide precipitation is potentially more hazardous and generally more complex and costly.

Finally, let us take this opportunity to correct an error in our paper regarding the solubility of barium sulfide that was pointed out to us by John L. Gray, president of Chemical Products Corp., Cartersville, Ga., reportedly "the only remaining basic barium chemical manufacturer in the United States." We stated that "heavy metals such as barium, cadmium, copper, lead, mercury, nickel, silver, and zinc can be removed by hydroxide or sulfide precipitation or by a combination of the two processes." Barium sulfide and hydroxide, Gray points out, are readily soluble in water and cannot be removed by such precipitation processes. We agree. The inclusion of barium into this group was an oversight on our part. Note that barium is not included with these same heavy metals in Table 1, where hydroxide and sulfide contaminant removal efficiency are summarized.

Dennis Clifford
University of Houston
Houston, Tex. 77004

Sludge disposal studies

Richard M. Dowd

EPA is presently developing new criteria for sewage sludge treatment and disposal. The resulting regulations are expected to affect industrial discharges to publicly owned treatment works (POTWs), largely through requiring increased wastewater pretreatment before discharge to municipal sewer systems. EPA's Science Advisory Board (SAB) has reviewed three EPA reports addressing sludge disposal and reuse and has submitted recommendations to EPA Administrator Lee M. Thomas.

The first report, prepared by EPA's Office of Water Regulations and Standards (OWRS), covers four sludge-disposal options: landfilling, land application and distribution, incineration, and ocean disposal. It addresses methodologies for evaluating the scientific validity of each option, the identification and consistency of needed data, and modeling requirements. The document represents the beginning of a framework for evaluating sludge management risks and developing national criteria, an approach endorsed by the SAB.

Among other issues, the SAB review focused on the use of "reasonable worst-case" estimates; it pointed out that the report reflects many conservative, subjective assumptions in positing its reasonable worst cases. Because it could not determine whether the worst-case scenarios developed were too conservative (i.e., unrealistic), the SAB recommended that detailed sensitivity analyses be conducted to determine their reasonableness, the uncertainties associated with typical results, and the probability distribution of exposures and risks based on specific assumptions and scenarios.

The SAB also found that the OWRS risk assessment methodologies for the four sludge disposal options were not consistent, and good comparability among the alternatives was therefore lacking. Other specific comments included

- the need for clear distinctions between risk assessment and related concepts and methodologies such as hazard assessment, dose-response models, vulnerability analysis, risk–benefit analysis, and exposure assessment;
- SAB support for good mathematical modeling and appropriate use of quantitative evaluation for technical, economic, institutional, political, and social dimensions; and
- the importance of including effects on species other than humans.

The SAB recommends that the term "most-exposed individual" be replaced by "most-exposed unit" to signal EPA's concern with effects besides human health risks.

Alternatives to ocean disposal

The second EPA report, prepared by the Office of Policy Planning and Evaluation (OPPE), provides a methodology for evaluating landfill and land application alternatives to ocean disposal of POTW sludge. The SAB's major findings include the following:

- regarding OPPE's proposal that EPA analyses of dumping sites be done on a regional basis, the entire United States coastline could not be represented by six coastal sites with respect to variations in soil, climate, and hydrologic and POTW disposal conditions;
- the report should consider codisposal of POTW sludges in landfills, along with other municipal and industrial wastes;
- because conditions at individual sites may differ significantly from model predictions, the SAB recommends sensitivity analyses to evaluate the precision of the parameters in the models; and
- the documentation provided is inadequate to support the use of the Pesticide Root Zone Model proposed to describe transport of chemicals in the soil, and there is no discussion of validation for using the Analytic Transport 1-2-3 Dimension Model or the Exposure Analysis Modeling System model for transport in surface water. Also, use of the Universal Soil Loss Equation model, developed to predict soil movement within a field, is suggested to predict sediment yield to a stream, but other models should be considered for this purpose.

Ocean dumping regulations

The third report reviewed by the SAB was the Office of Marine and Estuarine Protection (OMEP) technical document supporting revisions to the agency's ocean dumping regulations for sewage sludges and dredged materials. The two main issues are technical justification for the separate regulatory treatment of the disposal of sewage sludges and dredge materials, and consideration of both the need for ocean disposal and the availability and impacts of land-based alternatives. The SAB found that the report's conclusions were not adequately supported by the data and that separate testing of dredged material is not always justified. It therefore recommended that a protocol be developed to identify, for each site, any differences between dredged materials and sewage sludge in order to make appropriate decisions on disposal options.

Although publication of the regulations is tentatively set for the fall, the time needed to perform the additional work recommended by the SAB may require some extension of schedules.

Richard M. Dowd, Ph.D., is president of R. M. Dowd & Company, scientific and environmental policy consultants in Washington, D.C.

CLASSIFIED SECTION

ENVIRONMENTAL ENGINEERING FACULTY POSITION CLARKSON UNIVERSITY

The Department of Civil and Environmental Engineering, Clarkson University is accepting applications for a tenure-track position in **Environmental Engineering** at the assistant or associate professor level. Ph.D. required. Responsibilities include undergraduate and graduate teaching and contribution to an active graduate research program. Research interests should be in biological or chemical processes in water and wastewater treatment systems or in natural waters. Send resume to Dr. Norbert L. Ackermann, Dept. of Civil and Environ. Engr., Clarkson University, Potsdam, NY 13676. Equal Opportunity Employer.

CHEMIST (MASS SPECTROSCOPIST)—Minimum one year experience analyzing environmental samples by gas chromatography/mass spectroscopy. Knowledge of EPA's Contract Lab Program and dioxin analysis preferred. Perform data validation and laboratory oversite for Quality Assurance Management Section of Environmental Protection Agency, Region 9. Submit resume to EPA, 215 Fremont Street, San Francisco, CA 94105, (Attn: P-6).

SENIOR STACK TESTER

Applicants must be experienced in all EPA Methods and continuous monitoring. Lab and GC experience helpful. Send resume to: Pape & Steiner Environmental Services, 5801 Norris Road, Bakersfield, California 93308.

EOE/MF

FEDERAL ENVIRONMENTAL EXECUTIVE

Supervisory General Engineer, GM-15, to serve as Deputy/Technical Director of U.S. Army Toxic and Hazardous Materials Agency, Aberdeen Proving Ground (APG), Maryland 21010-5401. Provides centralized program direction for hazardous waste cleanup activities at all active Army and National Guard sites throughout the U.S. Interfaces with Environmental Protection Agency and other federal and environmental regulatory agencies and higher levels of Army management, Department of Defense, and the Congress. Salary range $53,830-$69,976. Position requires Bachelor's Degree (or higher) in engineering and three years' professional experience. Resumes may be sent to Mrs. Lora Mioduski, Civilian Personnel Office, Recruitment and Placement Division, Aberdeen Proving Ground, MD 21005-5001. For additional information, call (301) 278-5247/4254. APG is an Equal Employment Opportunity employer.

ENVIRONMENTAL ENGINEERING POSITIONS

Three positions in Environmental Engineering are available in the Civil Engineering Department of the University of Wisconsin-Milwaukee. The work involves modeling and experimental studies related to the history of pollution as revealed in lake sediments. The positions and requirements are as follows: Postdoctoral research associate with strong background in computer modeling. Two research assistantships for M.S. or Ph.D. students with interest and skills in application of radiotracers to sedimentation processes or chemical analysis for metals and polycyclic aromatic hydrocarbons (PAH's). Send application with three references to: Dr. Erik R. Christensen, Department of Civil Engineering, University of Wisconsin-Milwaukee, Milwaukee, WI 53201.

Environmental Consulting – Several Positions

Interesting work involving hazardous waste/materials for a nationwide clientele. B.S. or M.S. with excellent grades in Environmental Chemistry or Engineering, strong technical skills and 0-5 years' experience. Projects are in the areas of environmental data management (PC-based) and chemical transport, fate and exposure modeling and data analysis.

Resumes to:

Gradient Corporation

44 Brattle Street
Cambridge, MA 02138

STAFF SCIENTIST

Project leader for environmental fate studies. Design and perform experiments in microbial metabolism and chemical degradation of pesticides in soil and water. Identify metabolites and degradates using chemical and spectroscopic techniques. Isolate and purify metabolites using TLC and HPLC. Evaluate data by statistical methods. Prepare protocols, monthly reports and manuscripts for publication. Provide work direction for 3 laboratory chemists. Ph.D. in microbiology and minimum 1 year training in analytical organic research and 2 years of environmental fate studies and 2 years post-doctoral research in microbiology. $16.25/hr, 40 hr/wk. Resume to Job Service, 206 N. Broom, Box 7163, Madison, WI 53707. Contact George Kammerer (608) 266-3140.

OFFICE OF THE PROGRAM MANAGER FOR CHEMICAL MUNITIONS
ABERDEEN PROVING GROUND, MARYLAND

The Office of the Program Manager for Chemical Munitions (OPMCM) has been charged by Public Law 99-145 to dispose of United States unitary lethal chemical stockpile of chemical munitions and agents.

- OPMCM is seeking professional engineers in the fields of Chemical, Mechanical, Industrial, Environmental, and General Engineering to help with the implementation of PL 99-145.
- Emphasis on process design, construction and operation of complex processes dealing with lethal materials and the issues of safety, environmental, and plant integration addressing these issues.
- Minimum requirements include:
  3 years of professional experience
  Full 4 year professional engineering degree (graduate courses or degree desirable)
- Excellent salaries (53K–69K)
  Liberal insurance, retirement, leave program
- Direct inquiries and resumes to:

Civilian Personnel Office
Attention: Ms. Lora Mioduski
Aberdeen Proving Ground, Maryland 21005-5001
(301) 278-5247/3437

ABERDEEN PROVING GROUND IS AN EQUAL OPPORTUNITY EMPLOYER

CLASSIFIED ADVERTISING RATES

Rate based on number of insertions used within 12 months from date of first insertion and not on the number of inches used. Space in classified advertising cannot be combined for frequency with ROP advertising. Classified advertising accepted in inch multiples only.

Unit	1-T	3-T	6-T	12-T	24-T
1 inch	$100	$95	$90	$85	$80

(Check Classified Advertising Department for rates if advertisement is larger than 10″.)

SHIPPING INSTRUCTIONS: Send all material to

Environmental Science & Technology

Classified Advertising Department

500 Post Road East

Westport, CT 06881

(203) 226-7131

professional consulting services directory

INDEX TO THE ADVERTISERS IN THIS ISSUE

Advertising Management for the
American Chemical Society Publications

CENTCOM, LTD.

President
Thomas N. J. Koerwer

Executive Vice President **James A. Byrne**
Senior Vice President **Benjamin W. Jones**
Clay S. Holden, *Vice President*
Robert L. Voepel, *Vice President*
Joseph P. Stenza, *Production Director*

500 Post Road East
P.O. Box 231
Westport, Connecticut 06880
(Area Code 203) 226-7131
Telex No. 643310

ADVERTISING SALES MANAGER
James A. Byrne, *VP*

ADVERTISING PRODUCTION MANAGER
Jay S. Francis

SALES REPRESENTATIVES

Philadelphia, Pa. . . . Patricia O'Donnell, CENTCOM, LTD., GSB Building, Suite 725, 1 Belmont Ave., Bala Cynwyd, Pa 19004 (Area Code 215) 667-9666

New York, N.Y. . . . Dean A. Baldwin, CENTCOM, LTD., 60 E. 42nd Street, New York 10165 (Area Code 212) 972-9660

Westport, Ct. . . . Edward M. Black, CENTCOM, LTD., 500 Post Road East, P.O. Box 231, Westport, Ct 06880 (Area Code 203) 226-7131

Cleveland, OH. . . .Bruce Poorman, John Guyot, CENTCOM, LTD., 325 Front St., Berea, OH 44017 (Area Code 312) 234-1333

Chicago, Ill. . . . Michael J. Pak, CENTCOM, LTD., 540 Frontage Rd., Northfield, Ill 60093 (Area Code 312) 441-6383

Houston, Tx. . . . Michael J. Pak, CENTCOM, LTD., (Area Code 312) 441-6383

San Francisco, Ca. . . . Paul M. Butts, CENTCOM, LTD., Suite 1070, 2672 Bayshore Frontage Road, Mountainview, CA 94043. (Area Code 415) 969-4604

Los Angeles, Ca. . . . Clay S. Holden, CENTCOM, LTD., 3142 Pacific Coast Highway, Suite 200, Torrance, CA 90505 (Area Code 213) 325-1903

Boston, Ma. . . . Edward M. Black, CENTCOM, LTD., (Area Code 203) 226-7131

Atlanta, Ga. . . . Edward M. Black, CENTCOM, LTD., (Area Code 203) 226-7131

Denver, Co. . . . Paul M. Butts, CENTCOM, LTD., (Area Code 415) 969-4604

ES&T
RESEARCH

A Method for the Collection, Handling, and Analysis of Trace Metals in Precipitation†

J. M. Tramontano,* J. R. Scudlark, and T. M. Church

College of Marine Studies, University of Delaware, Newark, Delaware 19716

■ A method is described for the automated collection, proper handling, and accurate analysis of trace metals in precipitation. The method has been successfully used in both rural coastal (Lewes, DE) and semiremote (Bermuda) marine environments but should be generally applicable. The collection device is a commercially modified automatic collector with polyethylene bag liners in the collecting buckets. Strict protocols for acid washing, deployment, and blanking are necessary to ensure accurate contamination-free samples. The freshly collected event samples are postacidified below pH 1.6 with ultraclean HCl to ensure desorption and preservation of the sample. Trace metal concentrations are quantitatively analyzed by heated graphite atomization in an atomic absorption spectrophotometer. A comparison of the results obtained by this method with earlier published trace metal results suggests that serious sampling and analytical artifacts may be present in most earlier data bases.

Introduction

Atmospheric transport and deposition are important processes in the global cycling of trace metals. The atmospheric flux of trace metals is a major component in both marine (*1–4*) and terrestrial (*5–9*) environments. In fact, some reports indicate that the concentrations of Pb, Hg, Cu, Zn, and Cd in precipitation from the eastern U.S. exceed the levels toxic to aquatic organisms (*10*) and are linked to deterioration in forest productivity (*11*). Trace metals are also important catalysts of SO_2 oxidation in atmospheric aerosols (*12*). In order to determine the pathways and environmental impact of trace metals in precipitation, precise and accurate measurements of trace metal concentration are essential.

As was first demonstrated by Patterson and Settle (*13*), extreme care must be taken to avoid contamination when collecting and analyzing for trace metals in aqueous environmental samples. Another problem is that trace metal samples require preservation because of adsorption onto the walls of collection devices and storage bottles. Other difficulties include accurately analyzing submicrogram concentrations and the exclusion of dry deposition. Thus, as we will demonstrate, the accurate measurement of trace metal concentrations in wet deposition requires a protocol even more rigorous than the methods used in the collection of precipitation for pH and major ions.

The routine monitoring of trace metals in continental precipitation has been undertaken by a number of investigators (see ref 10). However, only a few of these studies address the problems of contamination or preservation. In fact, though trace metal contamination during the collection of precipitation samples has been shown to be a problem (*14, 15*), little has been published on collection techniques and analytical procedures needed to limit sample contamination (*16*), particularly in routine (automated) monitoring of continental precipitation.

In the collection of precipitation samples for trace metals from remote regions, investigators (*1, 5, 17, 18*) have utilized extreme precautions to limit sample contamination. These include all-plastic, manually deployed funnel and bottle-style collectors, extensive acid washing of equipment and sample bottles, the use of ultraclean water and acids, and restricting sample manipulation and analysis to clean rooms. However, to date, no automated sampling protocols have been defined for such sampling.

When our laboratory began routine monitoring of trace metals at Lewes, DE, and High Point, Bermuda, as part of the MAP3S and WATOX programs, we required a simple, automated noncontaminating procedure applicable to both continental and semiremote regions. The manual procedures described for sampling in remote regions are too labor intensive and impractical for long-term continuous monitoring efforts. In addition, we did not know if the rigorous precautions used in very remote regions were necessary or practical for our application. Thus, we proceeded to develop and test a technique for the automated collection, handling, and analysis of trace metals in precipitation.

Procedures

Sampling Location. In general, the collector siting criteria applicable to any precipitation chemistry study (*19*) should be utilized. The site should also be several hundred feet from any metal supports, wires, or poles and remote to any regular vehicular traffic. Additional considerations are site security, accessibility, electric power availability, and potential for land use changes. For our study, sampling was carried out at two collection sites: the middle Atlantic coast (Lewes, DE) and at the midwestern Atlantic island of Bermuda (see ref 20 for a detailed description of the two sites). The collections were made as part of the Western Atlantic Ocean Experiment (WATOX) sponsored

†This is a contribution to the Western Atlantic Ocean Experiment (WATOX) and the Bermuda Biological Station (Contribution No. 1072).

0013-936X/87/0921-0749$01.50/0

Table I. Cleaning Procedure for Plasticware Utilized for the Collection, Storage, and Analysis of Trace Metals in Precipitation

1	wash with soapy deionized water (Fisher Versa-Clean or similar liquid)
2	rinse 3 times with deionized water
3	shake off excess water
4	soak inside with Spex-grade acetone for 10 min
5	shake off excess acetone
6	swirl inside with concentrated reagent ACS HCl
7	rinse 3 times with distilled water
8	swirl inside with concentrated reagent ACS HNO_3
9	rinse 3 times with distilled water
10	place in warm 6 N reagent ACS HNO_3 or HCl bath for 2–3 days
11	transfer to 2 N HNO_3 or HCl bath and soak for 2–3 days
12	rinse outside of container with deionized water
13	rinse inside of container 3 times with double-distilled water
14	rinse inside of container with Q-H_2O
15	dry in a filtered air clean bench or hood
16	place and seal in a polyethylene zipper bag

by the Air Resources Laboratory of NOAA.

Cleaning Procedures. Materials made of polyethylene (CPE) and polypropylene are exclusively used for sampling, storage, and laboratory manipulation. The cleaning procedure is outlined in Table I. Rinse water is either distilled/deionized (DDW) water or water-purified by a Millipore Milli-RO/Milli-Q (Millipore Corp., Bedford, MA) system (MQ-H_2O). For laboratory analyses, distilled/deionized water is further cleaned by subboiling in an all-quartz still (henceforth referred to as Q-H_2O). Likewise, reagent-grade hydrochloric and nitric acids are cleaned in an identical manner (Q-HCl and Q-HNO_3).

Collection Materials. Event samples for trace metal analysis are collected with a modified AeroChem Metrics (ACM) automatic collector (Model 301, AeroChem Metrics, Inc., Bushnell, FL), factory equipped with all-plastic components in the closing lid, displacement of the sensor grid, and Teflon coating on the lid support arms. The modified ACM collector is well suited to the collection of wet deposition, as it is automated, dependable, widely used in precipitation studies, relatively inexpensive, and commercially available. Its automated function is essential for unattended sampling in remote locations or for long-term monitoring.

In this study, commercially available 4-mil (0.004-in.) 10 × 8 × 24 in. round-bottomed polyethylene bags (Associated Bag Co., Milwaukee, WI), rigorously acid washed, are used to line the ACM bucket. As an independent comparison with the automated collector, a manually deployed (MD) sampler is used for a minimum subset of the events. Our MD sampler is a polyethylene funnel, screw fitted onto a 2-L polyethylene bottle of the same design employed by the Global Precipitation Chemistry Project (*5*).

Deployment. An acid-cleaned bag liner is installed into the ACM bucket within a clean bench. To minimize contamination, personnel should wear clean lab coats and polyethylene disposable gloves for this and all other procedures. The top of the bag is folded over the lip of the ACM bucket, and the air under the bag is evacuated by applying a vacuum pump via a small hole near the bottom of the bucket. Once in place, the bag liner is rinsed twice with 250–500 mL of MQ-H_2O, and the bucket is inverted, shaken dry, and doubly sealed in large plastic bags for transport to the collection site. At the site, the bucket with the bag liner is removed from the transport bags, rinsed 3 times with Q-H_2O, swirled, inverted, shaken dry, and installed into the ACM. In the event of an extended dry period (4–5 days), after periods of fog, dew, or high wind causing spurious lid openings or in instances where the amount of precipitation collected is insufficient for analysis, a new bucket and liner should be installed.

The MD collector is acid-cleaned, rinsed in the laboratory, and doubly sealed in large plastic bags for transport to the collection site. At the site, the MD collector is deployed on a plastic pole a few meters above the ground and about 6 m from the ACM collector. The MD collector should be uncovered immediately prior to the precipitation event and recovered as soon as the event has ended. The samples are retrieved, inspected, and noted for the presence of any local debris (insects, bird droppings, plant detritus, etc.). The sample containers are doubly sealed with a clean plastic lid and clean plastic bag and transported upright to a laboratory clean bench or clean room.

Sample Storage. Upon returning from the field, the samples are removed from the transport bags, weighed to determine volume, and acidified to below pH 1.6 (0.4% v/v Q-HCl) directly in the sample containers by the addition of quartz-distilled acid spikes. The samples are then securely covered with a plastic bag and placed in a clean bench. After about a 24-h desorption period, the samples are homogenized by swirling the containers, and 20–30 mL is used to repeatedly rinse the precleaned storage bottles. After the rinsing, the remaining volume is transferred to a storage bottle that is then securely capped, placed in a plastic bag, and sealed for storage.

Operational Blanks. The amount of contamination from the material and methods used in the collection and analysis of trace metal precipitation samples is monitored routinely by operational blanks. These blank experiments are conducted on a bimonthly basis or when (1) a change in field operator occurs, (2) a new batch of spike acid, liner bags, or storage bottles is used, or (3) any changes occur at the sample site, such as any equipment changes or unusual activity in the surroundings (e.g., construction, excavation, traffic). The "field blanks" consist of 500 mL of MQ-water added to a lined ACM bucket and the manual collector after they have been installed in the field as previously described. This procedure is simultaneously performed with identically prepared samplers that remain in the laboratory and are referred to as "lab blanks". In each case, a 50-mL portion of the MQ-water is saved, acidified, and labeled as the "process blank". Field blanks are conducted with the collectors in the closed position (either by unplugging the power to the ACM or covering the MD with a plastic bag). Approximately 24 h later, the blank solutions are retrieved, appropriately labeled, and processed in the same manner as precipitation samples.

Analysis. The concentrations of Cd, Cu, Fe, Mn, Ni, Pb, V, and Zn in precipitation are determined directly by graphite furnace atomic absorption spectroscopy (GFAA). An Instrumentation Laboratory Model 951 atomic absorption spectrophotometer is used together with a Model 555 graphite furnace and Model 254 Fastac auto sampler. Primary standards consist of Spex high-purity metals (Spex Industries, Inc., Edison, NJ) dissolved in 2% Q-HCl. Calibration was made against secondary metal standards diluted into an acid solution of 0.4% v/v Q-HCl to duplicate the sample matrix. The settings for the IL-555 furnace used for the determination of trace metal concentrations are given in Table II.

To determine the accuracy of these methods, several quasi-independent techniques are employed with subaliquots from samples representing the range of sample matrices. They include (1) direct analysis by GFAA with standard calibration curves, (2) direct analysis by GFAA

Table II. Instrumental Parameters for Instrumentation Laboratory Model 951 Atomic Absorption Spectrophotometer Equipped with Model 254 Fastac Autosampler and 555 Atomizer for the Determination of Trace Metals in Wet Deposition

metals	254 deposition, s	°C/s char. 1	°C/s char. 2	°C/s atomize 1	°C/s atomize 2	comments
Fe, Zn	5,[a] 10[b]	600/25	650/5	2400/0	2400/10	
Cu, Mn	5,[a] 20[b]	950/25	1000/5	2250/0	2250/10	
Pb, Cd	10,[a] 25[b]	400/20	450/5	1700/0	2250/5	platform
Ni	40,[a] 80[b]	700/20	700/5	2350/0	2350/5	
V	60,[a] 100[b]	500/15	750/15	2500/0	2500/10	

[a] Lewes samples. [b] Bermuda samples.

with standard addition, and (3) preconcentration by APDC/DDDC/freon extraction into 0.1 N Q-HNO_3 prior to GFAA (*21*).

In addition a 1:10 dilution of NBS certified standard reference material 1643b ("Trace Elements in Water") is analyzed along with the samples.

Results and Discussion

Analysis. (A) Interferences. The major ions in wet deposition samples can interfere with trace metal analysis (*15*). Comparison of the results obtained from selected precipitation samples, in which a portion was directly analyzed with a standard curve calibration and the remainder analyzed after separation by extraction from the major ion matrix, indicates that with the proper pyrolysis program and background corrections (reported in Table II) the major ion matrix is not a problem in the direct analysis of Cd, Cu, Fe, Mn, Ni, V, and Zn. However, the Pb signal is significantly suppressed and must be analyzed with a graphite cuvette and platform. This platform delays atomization and eliminates matrix suppression of Pb and the need for standard additions or extraction.

(B) Precision and Accuracy. The overall analytical precision of trace metal determinations in precipitation is estimated from the average of the standard deviations calculated from a representative number of samples analyzed. Usually, replicate determination of two to three separate aliquots of each sample is involved, depending upon volume. Thus, this estimates both the reproducibility of the GFAA technique and the associated problems of maintaining homogeneity of subsamples. For all of the metals, the average overall precision is about ±10% of the average metal concentration reported for the two locations (*20*).

The accuracy of the analysis is maintained by frequent calibration against dilute high-purity metal standards and NBS metal standards. The calibration of the GFAA technique was checked by several quasi-independent techniques including standard curve calibration, standard additions, and separation/preconcentration of the metals prior to analysis. Results obtained by the various techniques were within 10% for all the metals investigated.

Blanks. Field, laboratory, and process blanks are tested throughout the sampling period. The process blank is a measure of the metal contribution derived from the storage bottles, reagents, and analytical procedures. The average concentrations of the process blanks, in micrograms per liter, are small: Cd < 0.005, Cu < 0.02, Fe < 0.01, Mn < 0.005, Ni < 0.01, Pb < 0.01, V < 0.001, and Zn < 0.01. The process blank for these metals represents only a few percent of the average trace metal concentrations in precipitation (*20*). The laboratory blanks estimate contamination from the collector materials and the laboratory operations, including sample acidification and partitioning. The field blanks estimate contamination from all of the above in addition to any contamination from the field operations such as transport, deployment and recovery, and input of fugitive dust.

The field blanks at both sampling locations average about 6% (with a range of 2–10%) of the mean metal content of precipitation at the coastal and open western Atlantic (*20*). The blank concentrations are somewhat higher in Lewes than in Bermuda, probably due to the comparatively high ambient aerosol trace metal burden in the continental environment. The laboratory blanks are very low, generally (<2–5%), indicating that the material used and laboratory handling are not a significant source of contamination.

The field blanks were used only as an estimate of contamination levels. Blanks values were not used to correct trace metal concentration in collected samples.

Sample Preservation. The necessity to preserve trace metal samples is well established. In this study, preservation is achieved by adding acid to the freshly collected rainwater in the lined ACM buckets soon after the event. A period of 24 h to assure quantitative leaching and recovery of any adsorbed metals is required.

Two experiments were conducted to determine if postacidification quantitatively recovers the original trace metal concentration in the sample. In the first experiment, two lined ACM buckets were simultaneously deployed side-by-side at the beginning of seven different precipitation events (two were conducted at Bermuda and five at Lewes). In each case, one of each sample pair was preacidified by adding 5 mL of a 50% Q-HCl solution before the event and the second postacidified to 0.2% v/v Q-HCl after the end of the event. A desorption period of 6–24 h was allowed prior to transferring to storage bottles. During the experiment, problems were encountered with the preacidified samples, such as the inability to gauge precipitation amounts a priori and the evaporation of the acid spike prior to the event. As a result, postevent pH adjustment had to be made to the samples.

A comparison of concentrations obtained from the pre- and postacidified ACM collectors showed that they were within 20% agreement with an average difference of 7.5%. The good agreement between the acidification procedures would indicate that postacidification is quantitative in reversing any adsorption that may occur during sampling. The exception is Cd, where the mean concentration is 32% greater in the preacidified ACM samples. We attribute this to contamination due to the exposure of the sampling equipment to the concentrated acid prespike, which has also been reported in other studies (*15*).

In the second experiment, 1:10 and 1:20 dilutions of NBS trace metal standard SRM 1643b were made in 1 L of Q-H_2O. The dilutions were then added to deployed sample buckets, allowed to stand unacidified for 24 h, and then processed as samples. Analysis of the concentration of these spike solutions was within 5% of the calculated concentration for Cd, Cu, Fe, Mn, Ni, and Zn, again indicating that postacidification quantitatively reverses any

adsorption that may occur during sampling. The exception is Pb (85% recovery), suggesting some small irreversible loss of Pb to the collector liner.

Particulate Trace Metals in Wet Deposition. In order to determine the total wet flux from precipitation samples, it is necessary to analyze all phases of the trace metals present including entrained particulates. Some particulate material from local and remote sources is incorporated in wet deposition samples by way of condensation nuclei, washout, or inadvertent capture of dry fallout. However, other studies have shown that the amount of particulate Zn, Cd, Pb, and Cu in precipitation is insignificant (*22, 23*). In our study, we have found that the average total mass of particulate (0.4 μm) material in some randomly selected acidified samples is only about 0.8 mg/L. Furthermore, any trace metals in precipitation samples collected by our protocol should be dissolved from particulates by acidification of the samples. Estimates of particulate trace metals in samples collected by our protocol made from filtration and centrifugation studies indicate that insignificant (<10%) amounts of particulate forms (>0.4 μm) of Cd, Cu, Fe, Mn, Ni, Pb, and Zn are present in most events. However, in small (<0.7 cm) precipitation events occurring after extended dry periods there is some (15–20% by weight) particulate Fe and Mn in these select precipitation samples. However, measurable particulate Fe and Mn was present in only three of the seven small precipitation events tested and would represent a very small portion of the total data set. Both Fe and Mn have large crustal sources, which may explain the presence of these refractory particulate forms that may, in fact, represent resuspended soil particles and not wet deposited particulates.

A second experiment was conducted to further test if total metal concentrations are determined and to estimate sample storage stability. Nine samples were repeatedly analyzed for Fe after storage intervals ranging from a few days to 1 year. Results of this experiment revealed that Fe concentration did not significantly change (≤5%) over the time period tested. Since long-term storage under acid conditions would most likely change the dissolved-particulate distribution, these results indicate that the total concentration is determined and the samples are well-preserved and accurately analyzed in total. Thus, we are confident that the concentrations of trace metals in precipitation measured by our method are representative of total wet deposition (dissolved plus particulate).

Sampling Accuracy. The accuracy of our automated sampling protocol was checked by comparing the trace metal concentration to those determined from samples collected manually (MD collector). The MD collector was selected because of its simple and convenient all-plastic construction and because of its widespread use in remote regions by other investigators (*1, 5, 18*). Also, in this study, the MD collector was less susceptible to ground-based contamination because of its higher elevation (3 vs. 1.5 m for the ACM). Comparisons of results from the two collectors were made on more than 40 occasions at both sampling sites over the course of study. Approximately one-third of these comparisons were rejected because the manual collector was not opened at the onset of the precipitation event or one or both of the collectors were visibly compromised with local debris. A comparison of the results from the two collection methods showed that for all the metals the data are highly correlated ($r^2 > 0.88$) with slopes close to 1, indicating excellent agreement between the two sampling techniques. Furthermore, calculations of the average-weighted concentration from the ACM and MD collectors were in good agreement (Table III). Thus, the results from our automatic ACM collector compare well with those of MD collector, and trace metals in precipitation can be accurately collected by an automated network system with our protocol.

Table III. Comparison of the Volume-Weighted Mean Concentration (μg/L) from 25 Events Measured by Simultaneously Deployed Automatic (ACM) and Manual (MD) Samplers at Lewes, DE, and High Point, Bermuda

collector	concentration, μg/L					
	Cd	Cu	Fe	Mn	Pb	Zn
Lewes, DE						
ACM	0.172	1.18	16.4	1.40	3.17	5.39
MD	0.133	0.81	18.2	1.62	2.80	4.69
High Point, Bermuda						
ACM	0.041	0.223	6.21	1.10	0.48	1.30
MD	0.043	0.261	7.56	1.08	0.50	1.62

Table IV. Comparative Concentrations of Trace Metals in Precipitation

metal	literature range,[a] μg/L	no. of references	median,[a] μg/L	Lewes av,[b] μg/L
Cd	0.08–46	23	0.5	0.18
Cu	0.4–150	19	5.4	0.68
Pb	0.59–64	32	12	3.02
Mn	0.2–84	28	5.7	1.4
Ni	0.6–48	15	2.4	0.79
V	0.13–23	6	9	0.7
Zn	<1–311	32	36	6.4

[a] From Galloway et al. (*10*); values reported for rural locations (Tables IV and V). [b] From Church et al. (*20*).

Table V. Comparison of the Mean Concentration (μg/L) from 26 Events Measured from an Automatic Sampler Prepared for Major Ion Collection (ACM-MI) and a Simultaneously Deployed Automatic Collector Prepared for Trace Metal Collection (ACM-TM)

collector	concentration, μg/L					
	Cd	Cu	Fe	Mn	Pb	Zn
ACM-MI	0.320	1.20	10.24	1.79	1.46	15.66
ACM-TM	0.116	0.78	11.59	1.63	3.14	4.57

Results. Table IV presents the trace metal concentrations in precipitation collected at Lewes, DE (*20*), that utilize the protocol we have described. Also included are some trace metal results from similar rural locations as compiled in ref 10. As is apparent in Table IV, the trace metal concentrations reviewed by Galloway et al. (*10*) vary over 3–4 orders of magnitude and have a median concentraiton considerably higher than the average at Lewes. We contend that much of the variability reported in earlier studies resulted from improper collections. Many of these studies analyzed aliquots for trace metal from samples collected by major ion protocols.

To test the necessity of our procedures vs. using aliquots from major ion collectors, 26 side-by-side comparisons were made between a standard ACM collector prepared for major ion collection (*24*) and our modified trace metal collector prepared according to our protocol. Samples from the major ion collector could not be acidified until they were partitioned in storage bottles. Comparison of the mean concentration calculated from each collector for the 26 events (Table V) shows that the metals fall into three groups: Zn and Cd were severely contaminated (>100%) in the major ion sampler; Pb underwent consistent adsorption; Cu, Fe, and Mn were in close agreement. How-

ever, regression analysis of the Cu, Fe, and Mn data was poorly correlated (r^2 = 0.2–0.6), suggesting random contamination and adsorption in the major ion sampler that results in a fortuitous agreement of the means. Attempts at acidification of the standard plastic ACM buckets used for major ion collection produced order of magnitude contamination of Cd, Cu, Mn, Pb, and Zn in controlled laboratory experiments. Therefore, any attempts at acidifying the white plastic ACM bucket prepared for major ion collection would result in serious contamination.

Conclusions

This paper presents a method for accurately collecting and analyzing trace metals in precipitation as developed for semiremote coastal and open oceanic areas of the western Atlantic but generally applicable. The procedure has been used successfully at Lewes, DE, and on Bermuda over a 3-year period as part of the WATOX program. Wet deposition events are sampled by a modified automatic collector, with a polyethylene bag liner in the collector bucket. The accuracy of the collections is randomly checked by simultaneously deploying a manually operated funnel–bottle collector. All collector vessels must be rigorously acid cleaned prior to use. Postacidification by the addition of 0.4% (v/v) ultrapure hydrochloric acid to the sample after the event and 24-h leaching period is necessary to asure quantitative recovery and preserve the sample. A filtered air environment (clean hood or bench) is recommended for preventing contamination during plastiware cleaning, sample acidification, and transfer to storage bottles. Sample analysis is performed by direct atomic absorption spectrophotometry with heated graphite atomization. Sample homogeneity must be maintained during all sample partitioning steps and analysis. Field, laboratory, and process blanks must be run to determine the presence and source of contamination. We contend that earlier investigations that attempted to utilize major ion protocols for trace metal collection suffer from contamination and adsorption artifacts. These artifacts may have resulted in the wide range of trace metal concentrations reported for geographically similar locations (*10*) and the discrepancy between these values and the concentration that we report (Table IV).

Acknowledgments

We thank Timothy D. Jickells for his assistance with the Bermuda phase of the study and for his critique of the manuscript. We also thank James N. Galloway of the University of Virginia for his review and comments.

Registry No. Cd, 7440-43-9; Cu, 7440-50-8; Fe, 7439-89-6; Mn, 7439-96-5; Pb, 7439-92-1; Zn, 7440-66-6; H_2O, 7732-18-5.

Literature Cited

(1) Jickells, T.; Knap, A. H.; Church, T. M. *J. Geophys. Res.* **1984**, *89*, 1423–1428.
(2) Buat-Menard, P.; Ezat, U.; Gaudichet, A. *Precipitation Scavenging, Dry Deposition, and Resuspension*; Elsevier: New York, 1983.
(3) Jickells, T.; Knap, A.; Deuser, W. *Deep-Sea Res., Part A*: **1985**, *31*, 1169.
(4) Bertine, K. K.; Goldberg, E. D. *Science (Washington, D.C.)* **1971**, *173*, 233–235.
(5) Galloway, J. N.; Likens, G. E.; Keene, W.; Miller, J. M. *J. Geophys. Res.* **1982**, *87*, 8771–8786.
(6) Goodman, G. T.; Roberts, T. M. *Nature (London)* **1971**, *231*, 287–292.
(7) Klein, D. H. *Environ. Sci. Technol.* **1972**, *6*, 560–562.
(8) Livett, E. A.; Lee, T. A.; Tallis, J. H. *J. Ecol.* **1979**, *67*, 865–891.
(9) Norton, S. A.; Hanson, D. W.; Campana, R. J. *Effects of Air Pollutants on Mediterranean and Temperate Forest Ecosystems*; Miller, Ed.; U.S. Department of Agriculture: Washington, DC, 1980.
(10) Galloway, J. N.; Thornton, J. D.; Norton, S. A.; Volchok, H. L.; McLean, R. A. N. *Atmos. Environ.* **1982**, *16*, 1677–1700.
(11) Johnson, A. H.; Siccama, T. J. *Environ. Sci. Technol.* **1983**, *17*, 294A–305A.
(12) Graedel, T. E.; Weschler, C. J. *Rev. Geophys. Space Phys.* **1981**, *19*, 505–539.
(13) Patterson, C.; Settle, D. *NBS Spec. Publ. (U.S.)* **1976**, *No. 422*, 321–351.
(14) Slanina, J.; Mols, J.; Baurd, J.; Sloot, H.; Raaphorst, J.; Asman, W. *Int. J. Environ. Chem.* **1979**, *7*, 161–176.
(15) Haraldsson, C.; Magnusson, B. *Proceedings, International Conference on Heavy Metals in the Environment*; CEP Consultants Ltd: Edinburgh, U.K., 1983; pp 82–86.
(16) Ross, H. B. *Atmos. Environ.* **1986**, *20*, 401–405.
(17) Settle, D. M.; Patterson, C. C. *J. Geophys. Res.* **1982**, *87*, 8857–8869.
(18) Arimoto, R.; Duce, R. A.; Ray, B. J.; Unni, C. K. *J. Geophys. Res.* **1985**, *90*, 2391–2408.
(19) *WMO [Publ.]* **1974**, *No. 299*.
(20) Church, T. M.; Tramontano, J. M.; Scudlark, J. R.; Jickells, T. D.; Tokos, J. J., Jr.; Knap, A. H. *Atmos. Environ.* **1984**, *18(12)*, 2657–2664.
(21) Danielsson, L. G.; Magnusson, B.; Westerlund, S. *Anal. Chim. Acta* **1978**, *98*, 47–57.
(22) Nurnberg, H. W.; Valenta, P.; Nguyen, V. D.; Godde, M.; Urano de Carvalho, E. *Fresenius' Z. Anal. Chem.* **1984**, *317*, 314–323.
(23) Lindberg, S. E.; Turner, R. R. *Proceedings, International Conference on Heavy Metals in the Environment*; CEP Consultants Ltd: Edinburgh, U.K., 1983; pp 107–114.
(24) Galloway, J. N.; Hall, C.; Likens, G. E. *Tellus* **1977**, *30*, 71–82.

Received for review November 20, 1986. Revised manuscript received February 6, 1987. Accepted March 18, 1987. This study was supported by a grant from NOAA Air Resources Laboratory.

Environ. Sci. Technol. 1987, 21, 754–756

An Abundant Chlorinated Furanone in the Spent Chlorination Liquor from Pulp Bleaching

Lars M. Strömberg,* Filipe de Sousa, Pierre Ljungquist, Bruce McKague, and Knut P. Kringstad

STFI (Swedish Pulp and Paper Research Institute), P.O. Box 5604, S-114 86 Stockholm, Sweden

■ A large peak always occurring in gas chromatograms (with electron capture detection) [GC (ECD)] when spent pulp chlorination liquors are analyzed for chlorinated phenols was identified as being caused by the presence of 3,4-dichloro-5-(dichloromethyl)-5-hydroxy-2-furanone. The compound exhibits weak mutagenic activity, has a slightly elevated bioaccumulation propensity, but is chemically rather unstable.

Introduction

In recent years, available information on the chemical compositon of spent liquors from the bleaching of chemical pulp has increased (*1*). It has been well established that such liquors may exert acute toxic and genotoxic effects due to the presence of various chlorinated and nonchlorinated compounds of low relative molecular mass (*1*, *2*).

One group of compounds present is comprised of phenols, catechols, and guaiacols chlorinated to various degrees. This group is of particular interest because the compounds contribute to the toxicity of spent bleaching liquors and show a tendency to bioaccumulate (*3*, *4*).

The standard procedure for the qualitative and quantitative determination of chlorinated phenolic compounds includes acetylation of the spent liquor and gas chromatographic (ECD) analysis of the products obtained (*5*). A large peak representing an unknown compound often appears in these chromatograms. The peak is also easily detectable when chlorination products from naturally occurring aquatic humic acid are analyzed (*6*, *7*). Since the peak could not be attributed to any known chlorinated phenols, catechols, or guaiacols, we decided to isolate and characterize the responsible compound.

Experimental Section

Spent Chlorination Liquor. A spent chlorination liquor was prepared from softwood kraft pulp as described previously (*8*). Quantitative determinations of chlorinated phenolic compounds were carried out according to a procedure outlined previously (*5*).

Workup Procedure. A total of 1700 mL of the spent chlorination liquor (natural pH of 1.8) was extracted with 400 mL of diethyl ether [May and Baker Ltd. (pro analysis)] in a liquid–liquid extractor for 24 h. The extract containing a mixture of neutral, acidic, and phenolic compounds was then concentrated to a volume of about 25 mL.

The extract obtained was subsequently treated with 2 × 10 mL of a 0.5 M $NaHCO_3$ solution, and the aqueous phase was acetylated essentially as previously described (*5*, *7*). A small quantity of ascorbic acid was added to prevent oxidation.

Gas Chromatography. The various hexane extracts obtained from the acetylations were injected (1–3 μL) into a Hewlett-Packard 5890 gas chromatograph equipped with an electron capture detector (ECD, 63 Ni). The column was an OV-1701 fused silica capillary column (30 m × 0.32 mm i.d.) manufactured by J & W Scientific Inc. (Cordova, CA). The column temperature was held constant at 190 °C. The quantification procedure was carried out with the internal standard method (response factors related to 2,6-dibromophenol as internal standard). Retention times and quantification data were measured with a Trivector Scientific-Trilab 2000 chromatography data system.

Gas Chromatography/Multistage Mass Spectrometry (GC/MS-MS). The GC/MS and GC/MS-MS investigations were conducted with a Finnigan TSQ-46C mass spectrometer system.

The samples were introduced into the ion source (temperature 120 °C) via the gas chromatograph or a moving-belt LC interface. The conditions for the GC were as follows: oven temperature, 170 °C; injector temperature, 250 °C; GC interface temperature and transfer line temperature, 300 °C. The column used was a DB-1 fused silica capillary column (30 m × 0.252 mm i.d.) manufactured by J & W Scientific Inc. (Cordova, CA). Two ionization techniques were used, positive electron impact (EI, electron energy 70 eV) and positive chemical ionization with methane as a reactant gas (CI, electron energy 150 eV, ion source pressure 1.0 mTorr).

Collision activation experiments (daughter ions) were carried out with the first quadrupole transmitting the ions of interest alternately. In the collision chamber (second quadrupole) these ions were collision-activated with argon at a pressure of 1.5 mTorr and a nominal collision energy of 10 eV. Collision-induced fragments were separated by scanning the third quadrupole from mass m/z 40 to mass m/z 400 in 240 ms in EI and from mass m/z 100 to mass m/z 400 in 240 ms in CI.

Spectroscopic Methods and Equipment. The ^1H NMR and ^{13}C NMR spectra were run on a Bruker WP 200 (200 MHz) and a Varian CFT-20 spectrometer, respectively. The UV and IR spectra were run on a Cary Model 118C UV spectrophotometer and a Perkin-Elmer Model 983 infrared spectrophotometer, respectively.

Synthesis. Two ways of preparing the furanone compounds were used.

In the first, leading to the acetyl derivate 3,4-dichloro-5-(dichloromethyl)-5-acetyl-2-furanone (Figure 1A), chlorine water (4.0 L, containing 15 g of Cl_2) was added to a stirred solution of tetrachloro-*o*-benzoquinone (5.0 g, in 500 mL of acidified water, pH 2) in an amber bottle. The mixture was stirred at room temperature for 4 h and then extracted 3 times with ether (400 mL). After concentration, the extract (50 mL) was shaken twice with 2 × 50 mL of 0.5 M $NaHCO_3$ solution. The resulting aqueous phase was acetylated and extracted with hexane to obtain a crude product mixture. The pure compound was obtained by fractionation on SiO_2 (40 g), eluting with hexane–ether–ethanol (10:5:1). The compound was crystallized twice from acetone: white crystals; mp 90–91 °C; IR (KBr pellet) ν_{max} 2990, 1815, 1780, 1635, 1370, 1185, 1080, 990, 950 cm^{-1}; UV (methanol) λ_{max} 238 nm (9700); ^1H NMR ($CDCl_3$) δ 2.19 (3 H, s, CH_3CO), 6.04 (1 H, s, $-CHCl_2$); ^{13}C NMR ($CDCl_3$) δ 20.98 (C8), 70.82 (C6), 102.79 (C5), 126.24 (C3), 146.72 (C4), 161.75 (C2), 167.85 (C7). Spectra recorded with reduction of decoupling effect "off resonance" showed a doublet (C6) and a quartet (C8). The GC retention time of the acetate relative to the internal standard was 1.13.

0013-936X/87/0921-0754$01.50/0

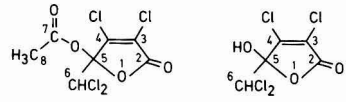

A B

Figure 1. Structural formula for the chlorinated furanones 3,4-dichloro-5-(dichloromethyl)-5-acetyl-2-furanone (A) and 3,4-dichloro-5-(dichloromethyl)-5-hydroxy-2-furanone (B).

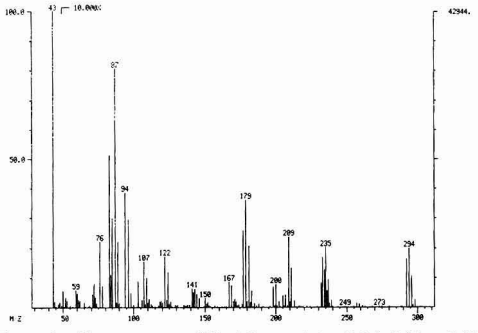

Figure 2. Mass spectrum (EI) of the acetate of 3,4-dichloro-5-(dichloromethyl)-5-hydroxy-2-furanone. The CI mass spectrum of the compound showed the molecular ion was m/z 292. Data for some daughter ion spectra of the molecular ion and fragment ions are presented under Experimental Section.

The mass spectrum (EI) of the acetylated compound is presented in Figure 2.

GC/MS-MS collision activation experiments (daughter ions) gave the following results: daughters (EI) of m/z 292 gave m/z 232 and 209, of m/z 233 gave m/z 205, and 177, of m/z 209 gave m/z 181, of m/z 198 gave m/z 170, 142, and 107, and of m/z 167 gave m/z 139, 111, 103, and 95; daughters (CI) of m/z 295 gave m/z 235, 207, and 179.

The second synthetic path yielded the underivatized compound 3,4-dichloro-5-(dichloromethyl)-5-hydroxy-2-furanone (Figure 1B). A solution of 2,2,4,5-tetrachlorocyclopentene-1,3-dione (ICN Biomedical, 1.0 g) in ether (50 mL) was shaken with 0.1 M K_2CO_3 (200 mL) for a few minutes. The aqueous layer was cooled, acidified with 10% HCl, and extracted with ether. The extract was dried with anhydrous magnesium sulfate and evaporated to give the crude product as a semicrystalline solid. The reaction was also performed by stirring the dione in water overnight, extracting with ether, and evaporating the solvent. The crude product was fractionated on SiO_2 (40 g), eluting with hexane–ether 1:1 and ether. After evaporation of the solvent, trituration with hexane gave the product as tan crystals: mp 66–68 °C [lit. (*9*) mp 70–71 °C]; IR (KBr pellet) ν_{max} 3360, 2990, 1763, 1630, 1378, 1240, 1175, 1015, 920 cm^{-1}; UV (methanol) λ_{max} 233 nm (8700); ^1H NMR ($CDCl_3$) δ 5.99 (s, $-CHCl_2$); ^{13}C NMR ($CDCl_3$) δ 70.71 (C6), 103.54 (C5), 125.01 (C3), 148.19 (C4), 163.12 (C2).

Spectra recorded with reduction of decoupling effect off resonance showed a doublet (C6). The mass spectrum (EI) of the compound is presented in Figure 3.

GC/MS-MS collision activation experiments (daughter ions) gave the following results: daughters (EI) of m/z 250 gave m/z 167 and of m/z 167 gave m/z 139, 111, 103, and 95; daughters (CI) of m/z 251 gave m/z 233, 205, and 177 and of m/z 233 gave m/z 205, 177, and 141.

Acetylation as previously described gave the acetate (Figure 1A).

Mutagenicity Tests. Ether solutions (20 μL/plate) of the underivatized synthesized compound were tested for

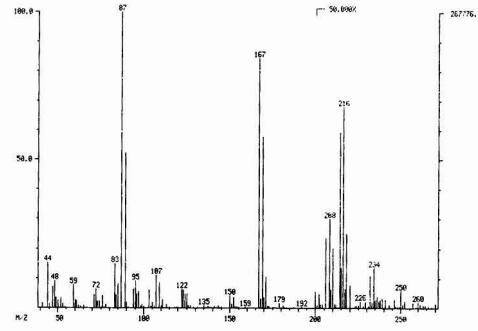

Figure 3. Mass spectrum (EI) of 3,4-dichloro-5-(dichloromethyl)-5-hydroxy-2-furanone. The CI mass spectrum of the compound showed the molecular ion was m/z 250. Data for some daughter ion spectra of the molecular ion and fragment ions are presented under Experimental Section.

mutagenicity with the Ames test (*10*). *Salmonella typhimurium* TA 100 and TA 98 were used without metabolic activation. All reported test values are mean values of six plates. As a positive control for the two strains, quercetin dihydrate (Fluka AG) was used.

Determination of Bioaccumulation Potential. The determination of the bioaccumulation potential was carried out by the 1-octanol/water distribution coefficient (K_{ow}) method (*11*, *12*) and by the method based on reverse-phase thin-layer chromatography (RP-HPTLC), giving R_M^0 values (*13–15*).

Results and Discussion

Figure 2 shows the mass spectrum of the compound responsible for the unknown peak as obtained in the GC (ECD) and GC/MS analysis of the hexane extract of the acetylated ether extract from spent chlorination liquor. From this spectrum and a spectrum obtained in separate experiments with high-resolution GC/MS (VG-7070 EQ, run at VG Analytical, Organic Mass Spectrometry Division, Manchester, U.K.), the following conclusions were drawn: chemical composition $C_7H_4O_4Cl_4$; acetylated; presence of a dichloromethyl group; and basic structure very likely a furanone. For further characterization, large quantities of the compound were produced by chlorinating tetrachloro-*o*-benzoquinone and acetylating the reaction mixture as described under Experimental Section. Tetrachloro-*o*-benzoquinone was selected as starting material because recent investigations suggested furanone derivatives as possible intermediates in the degradation of this particular lignin model compound type by chlorine (*16*). In this way the compound could be characterized by ^1H NMR, ^{13}C NMR, UV, and IR spectroscopy. The results obtained are given under Experimental Section. Altogether the data suggest the compound to be the acetate of 3,4-dichloro-5-(dichloromethyl)-5-hydroxy-2-furanone as shown in Figure 1A.

The availability of the pure acetylated compound made possible the quantitative determination of the furanone in spent chlorination liquors from the bleaching of softwood kraft pulps and oxygen-prebleached softwood kraft pulps. The results showed the content to vary between 5 and 10 g per ton of pulp depending upon the level of the κ number of the pulp inspected. These quantities are of the same order of magnitude as those of chlorinated phenols, catechols, and guaiacols in spent bleach liquors.

Information on possible genetic effects of the compound is of importance because a trichlorinated furanone derivative previously found in such liquors (<0.5 g per ton of

pulp) exhibits strong mutagenic effects as determined by the Ames test (*17*, *18*). The unacetylated 3,4-dichloro-5-(dichloromelthyl)-5-hydroxy-2-furanone could be obtained in high yield by hydrolyzing 2,2,4,5-tetrachlorocyclopentene-1,3-dione as described under Experimental Section. In some parallel investigations we thus found that the 1,3-dione very likely is an important intermediate in pulp chlorination (*19*). The identity of the isolated furanone was confirmed by ^1H NMR, ^{13}C NMR, UV, and IR spectroscopy as can be seen from data given under Experimental Section and from the mass spectrium shown in Figure 3.

The unacetylated furanone was tested by the Ames test with *S. typhimurium* TA 100 as the test organism. The compound exhibits mutagenic activity corresponding to about 40 revertants per nanomole. This is considerably lower than the activity reported for the previously described trichlorinated furanone derivative (*19*). No response was obtained with the strain TA 98 up to a dose of 1 μg/plate.

Measurement of the bioaccumulation potential showed the compound had an octanol/water distribution coefficient, log K_{ow}, of about 2.40 at a water pH of 2. When the RP-HPTLC technique was used for the estimation of log K_{ow}, a R_M^0 value of 2.26 was obtained. These results indicate a slightly elevated bioaccumulation propensity.

Tests of the stability indicated that the major part (95%) of the compound in spent chlorination liquor disappeared after 24 h of storage at pH 8 and ambient temperature. At lower pH levels the compound was considerably more stable.

Conclusions

The tetrachlorinated furanone is a major compound that frequently can be observed when analyzing spent chlorination liquors for the content of chlorinated phenolic compounds. The furanone exhibits mutagenic activity and a slightly elevated bioaccumulation propensity. It may not, however, be a significant water pollutant as it is readily degraded under ambient conditions.

Registry No. B, 108082-06-0.

Literature Cited

(1) Kringstad, K. P.; Lindström, K. *Environ. Sci. Technol.* **1984**, *18*, 236.
(2) Kringstad, K. P.; Stockman, L. G.; Strömberg, L. M. *J. Wood Chem. Technol.* **1984**, *4(3)*, 389.
(3) Landner, L.; Lindström, K.; Karlsson, M.; Nordin, J.; Sörensson, L. *Bull. Environ. Contam. Toxicol.* **1977**, *18*, 663.
(4) Renberg, L.; Svanberg, O.; Bengtsson, B.-E.; Sundström, G. *Chemosphere* **1980**, *9(3)*, 143.
(5) Voss, R. M.; Wearing, J. T.; Wong, A. In *Advances in the Identification and Analysis of Organic Pollutants in Water*; Keith, L. M., Ed.; Ann Arbor Science: Ann Arbor, MI, 1981; Vol. 2, p 1059.
(6) Kringstad, K. P.; Ljungquist, P. O.; de Sousa, F.; Strömberg, L. M. *Environ. Sci. Technol.* **1983**, *17*, 553.
(7) Kringstad, K. P.; de Sousa, F.; Strömberg, L. M. *Environ. Sci. Technol.* **1985**, *19*, 427.
(8) Kringstad, K. P.; Ljungquist, P. O.; de Sousa, F.; Strömberg, L. M. *Environ. Sci. Technol.* **1981**, *15*, 562.
(9) Roedig, A.; Märkl, G. *Justus Liebigs Ann. Chem.* **1960**, *636*, 1.
(10) Maron, D. M.; Ames, B. N. *Mutat. Res.* **1983**, *113*, 173.
(11) Xie, T.-M.; Hulthe, B.; Folestad, S. *Chemosphere* **1984**, *13*, 445.
(12) OECD *OECD Guidelines for Testing of Chemicals*; Organisation for Economic Co-operation and Development: Paris, France, 1981.
(13) Renberg, L. O.; Sundström, G. S.; Rosén-Olofsson, A.-C. *Toxicol. Environ. Chem.* **1985**, *10*, 333.
(14) Butte, W.; Fokken, C.; Klussman, R.; Schuller, D. *J. Chromatogr.* **1981**, *214*, 59.
(15) Kringstad, K.; de Sousa, F.; Strömberg, L. *Environ. Sci. Technol.* **1984**, *18*, 200.
(16) Österberg, F. Ph.D. Dissertation, The Royal Institute of Technology, Stockholm, Sweden, 1984.
(17) Holmbom, B.; Voss, R. H.; Mortimer, R. D.; Wong, A. *Environ. Sci. Technol.* **1984**, *18*, 333.
(18) Padmapriya, A. A.; Just, G.; Lewis, N. G. *Can. J. Chem.* **1985**, *63*, 828.
(19) McKague, A. B.; de Sousa, F.; Strömberg, L. M.; Kringstad, K. P. *Holzforschung* **1987**, *41(3)*.

Received for review September 2, 1986. Revised manuscript received February 6, 1987. Accepted March 26, 1987.

Environ. Sci. Technol. 1987, 21, 757–765

Characterization of Mutagenic Subfractions of Diesel Exhaust Modified by Ceramic Particulate Traps

Linda D. Dorie,* Susan T. Bagley, David G. Leddy, and John H. Johnson

Departments of Mechanical Engineering—Engineering Mechanics, Biological Sciences, and Chemistry and Chemical Engineering, Michigan Technological University, Houghton, Michigan 49931

■ Protocols were developed for collection and characterization of heavy-duty diesel exhaust hydrocarbons. Dichloromethane extracts of particulate and gaseous-phase samples were partitioned between hexane and methanol, and the highly mutagenic (Ames TA98) methanolic fractions were further separated with reverse-phase HPLC. Twenty-eight polycyclic aromatic hydrocarbons (PAH), including 4 nitro- and 13 oxy-PAH derivatives, were tentatively identified in the active (moderately polar) HPLC fractions with GC/MS. In terms of raw exhaust emissions (milligrams per cubic meter), the use of the ceramic traps caused reduced levels of particulate and associated organic compounds. Total mutagenic activity also decreased with the traps, but to a lesser extent than the decrease in particulate. Many of the identified PAH were common to both the particulate and gaseous-phase samples collected under the same conditions. Calculated hydrocarbon balances showed that more hydrocarbons passed through the samplers when the ceramic traps were used.

Introduction

The expanded use of diesel engines has caused an increased awareness of the potential health effects related to the emissions of nitrogen oxides, respirable particulates, and hydrocarbons (especially polycyclic aromatic hydrocarbons or PAH) that are associated with both the particulate and gaseous phases of diesel exhaust. Federal particulate emission standards (*1*), which become effective in 1991, require that particulate levels be reduced to 0.25 g per brake horsepower-hour for heavy-duty diesels. These levels will probably not be achievable without the use of aftertreatment control devices such as particulate traps.

One type of trap being extensively studied is the porous ceramic wall-flow monolith. Significant effort has been expended toward the development (*2*), characterization (*3–13*), and modeling (*14–18*) of this type of trap, which is illustrated in Figure 1. The trap consists of an array of square ceramic channels that are alternately plugged at either their inlet or their outlet ends. The exhaust enters an open channel and must pass through the porous side walls into a neighboring, open-ended channel to exit. Solids are retained while gases pass through the trap; combustible solids are slowly oxidized. This type of aftertreatment device increases both the surface area of the exhaust system and the residence time of the exhausted combustion products within the system. Therefore, in addition to the desired oxidation of particulate, some undesirable reactions (e.g., nitration of PAH) may be promoted that alter the mutagenic activity of the exhaust.

Our previous studies (*4*, *11*, *12*) have shown that emissions of particulates, solids, sulfates, and the soluble organic fraction (SOF) associated with the particulate decreased when the traps were used with a heavy-duty diesel engine operated under steady-state conditions (EPA modes 4 and 5) for load and speed. The mutagenicity of the SOF (measured in revertants per microgram of SOF) was primarily direct acting in nature and was found to increase with the use of the traps (*4*, *11*) although the activity in terms of raw exhaust emissions (measured in revertants per cubic meter) decreased when the traps were used due to decreased emissions of SOF.

It was the aim of this study to develop protocols to further characterize the chemical and biological changes produced in heavy-duty diesel exhaust hydrocarbon emissions by the use of ceramic particulate traps. Particulate-associated hydrocarbons (as collected on Teflon-coated glass-fiber filters) and a portion of the gaseous-phase hydrocarbons termed the vapor-phase organic component (VOC, as collected on XAD-2 resin) were characterized. PAH components of the most mutagenic subfractions (determined by using the *Salmonella*/microsome mutagenicity bioassay or the Ames assay) of Soxhlet-extracted particulate and VOC samples were identified with gas chromatography (GC) and GC/mass spectrometry (GC/MS).

Experimental Methods

Engineering and Sampling Methods. The test engine was a 1979 Caterpillar Model 3208 naturally aspirated, direct-injection, 10.4-L displacement, V-8 diesel operated on No. 2 diesel fuel under EPA steady-state modes 4 and 5, which specify the peak torque speed (1680 rpm) and load (50 and 75% of full load, respectively). Two Corning EX:47 uncatalyzed ceramic traps (Corning Glass Works, Corning, NY) were used (one per cylinder bank).

Particulate and gaseous-phase samples were collected in a stainless steel dilution tunnel in which the volume flow rate (15.2 m^3/min) and dilution ratio (15:1) were held constant. The tunnel parameters and methods employed for the measurement of gaseous emissions were previously reported (*4*).

Particulate samples were collected from the dilution tunnel with the ultrahigh-volume sampling system illustrated in Figure 2. Teflon-coated nonwoven glass-fiber filters, 508 × 508 mm (T60A20, Pallflex Corp., Putnam, CT), were used with nominal sampling times of 20 min each, thus providing ample masses (50–250 mg after solvent extraction) for chemical and biological characterizations.

Accurate mass determinations of collected particulate were made with a tandem collection system (see Figure 2) employing smaller filters (47-mm diameter) of a similar material (Teflon-coated woven glass fiber; Pallflex TX40HI20-WW). Levels of total particulate matter (TPM, determined gravimetrically), SOF (determined gravimetrically after Soxhlet extraction of the filter), the sulfate fraction (SO_4^{2-}, determined by ion chromatography), and solids (SOL, determined by difference where SOL = TPM − SOF − SO_4^{2-}) were obtained from the exposed 47-mm filters.

For the purpose of this study, the "gaseous-phase" component of the diluted exhaust was considered to be that portion of the exhaust passing through the particulate filters (*19–21*). The vapor-phase organic component (VOC) was that portion of the gaseous phase collected with a stainless steel sampler containing 40 g of XAD-2 resin (a styrene/divinylbenzene copolymer), held in place with a stainless steel screen and two layers (upper and lower)

0013-936X/87/0921-0757$01.50/0

Table I. Relative Retention Times and Fraction Assignments for Selected PAH and Derivatives[a]

compound	HPLC relative retention time[b]	HPLC fraction assignment	GC relative retention time[c]	compound	HPLC relative retention time[b]	HPLC fraction assignment	GC relative retention time[c]
2,7-dihydroxynaphthalene	0.14	1	0.59	fluorene	0.79	3, 4	0.40
2-amino-9-hydroxyfluorene	0.22	1	0.77	9-nitrophenanthrene	0.80	3, 4	0.81
1,4-naphthoquinone	0.32	2	0.28	9-nitroanthracene	0.81	3, 4	0.74
2-amino-9-fluorenone	0.41	2	0.78	9,10-dinitroanthracene	0.82	3, 4	0.87
1,5-dinitronaphthalene	0.50	2	0.63	3,3′-dimethylbiphenyl	0.83	3, 4	0.41
1-naphthaldehyde	0.50	2	0.35	dibenzothiophene	0.85	4	0.52
2,4,7-trinitro-9-fluorenone	0.54	2, 3	1.11	phenanthrene	0.85	4	0.54
1-nitronaphthalene	0.56	3	0.41	anthracene	0.88	4	0.54
2-nitrobiphenyl	0.56	3	0.49	fluoranthene	0.96	4	0.71
2-nitronaphthalene	0.59	3	0.41	3-nitrofluoranthene	0.97	4	0.98
anthrone	0.60	3	0.63	1-nitropyrene	1.00	4	1.00
9-fluorenone	0.60	3	0.51	pyrene	1.01	4	0.74
naphthalene	0.61	3	0.14	6-nitrochrysene	1.06	4, 5	1.13
anthracenedione	0.63	3	0.64	benzo[*a*]anthracene	1.11	5	0.92
2,7-dinitrofluorene	0.67	3	1.04	chrysene	1.11	5	0.93
acenaphthene	0.69	3	0.34	6-nitrobenzo[*a*]pyrene	1.24	5	1.26
acenaphthylene	0.69	3	0.31	benzo[*b*]fluoranthene	1.24	5	1.07
1,6-dinitropyrene	0.73	3	1.19	benzo[*k*]fluoranthene	1.24	5	1.08
1-aminopyrene	0.74	3	1.00	benzo[*a*]pyrene	1.30	5, 6	1.11
dibenzofuran	0.74	3	0.34	dibenz[*a,h*]anthracene	1.34	6	1.25
2-nitrofluorene	0.76	3, 4	0.74	benzo[*ghi*]perylene	1.44	6	1.27
9-anthraldehyde	0.77	3, 4	0.75	indeno[1,2,3-*cd*]pyrene	1.46	6	1.24

[a] See text for chromatographic conditions. [b] Retention time relative to 1-nitropyrene, which elutes at approximately 38.1 min. [c] Retention time relative to 1-nitropyrene, which elutes at approximaely 32.8 min.

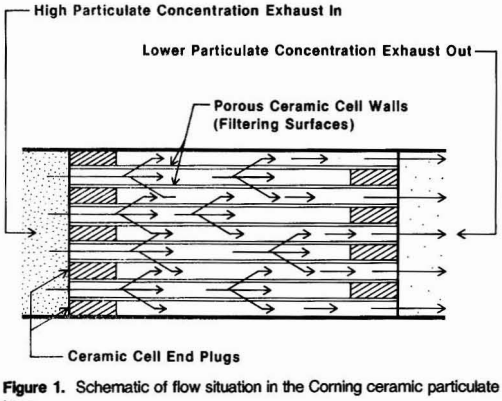

Figure 1. Schematic of flow situation in the Corning ceramic particulate trap.

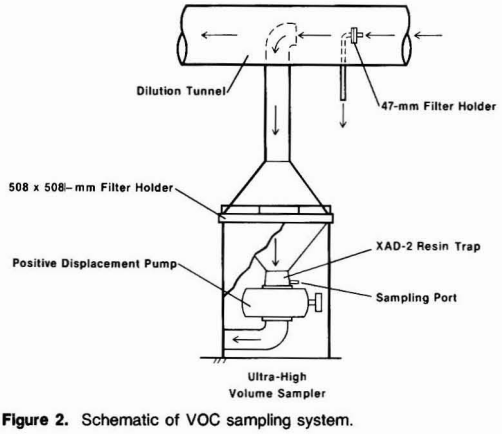

Figure 2. Schematic of VOC sampling system.

of open-cell polyurethane foam (6 mm thick). The XAD-2 resin was not expected to collect all of the gaseous-phase organics, but it has been shown to efficiently collect hydrocarbons containing seven or more carbons as well as the more volatile two- to four-ring PAH (*20–23*). In addition, XAD-2 resin has been shown to be more efficient at collecting these types of hydrocarbons from dilute diesel exhaust than cold-water trapping of the raw exhaust (*23*).

The VOC sampler was located immediately after the 508 × 508 mm filter cassette (see Figure 2). One XAD-2 resin sample and one 47-mm filter were exposed coincidentally with each 508 × 508 mm filter. Exposed filters and resin samples were stored in the dark at −7 °C until they were extracted.

Chemical Methods. As indicated in Figure 3, SOF and VOC from modes 4 and 5 for chemical and biological characterization were obtained from the exposed 508 × 508 mm filters and XAD-2 resin, respectively, by Soxhlet extraction with 400 mL of dichloromethane (Burdick and Jackson Laboratories, Inc., Muskegon, MI) for 24 h. The solvent volume was reduced to 5 mL under reduced pressure by a rotary evaporator with a 35 °C water bath. The extracts were taken to near dryness with a stream of nitrogen. Mode 4 extracts were then partitioned between hexane and methanol to separate the relatively nonpolar (hexane fraction) from the more polar (methanolic fraction) components (Figure 3).

The mode 4 methanolic fractions of the SOF and VOC were further separated with reverse-phase HPLC on a Hewlett-Packard 1084B liquid chromatograph and a Magnum-9 (Whatman Lab Sales, Inc., Hillsboro, OR) 25 cm × 9.4 mm i.d. semipreparative C_{18} column with an average particle size of 10 μm. The initial mobile phase was 45% CH_3CN in water; this concentration was held constant for 5 min after injection, followed by a linear gradient to 100% CH_3CN over 45 min and isocratic elution for 10 min. Then, a second gradient to 95% 2-propanol over 15 min was used and followed by isocratic elution of the final concentration for 15 min. Seven fractions were collected: the first six for a duration of 10 min each followed by one 30-min fraction. The flow rate was 3.0

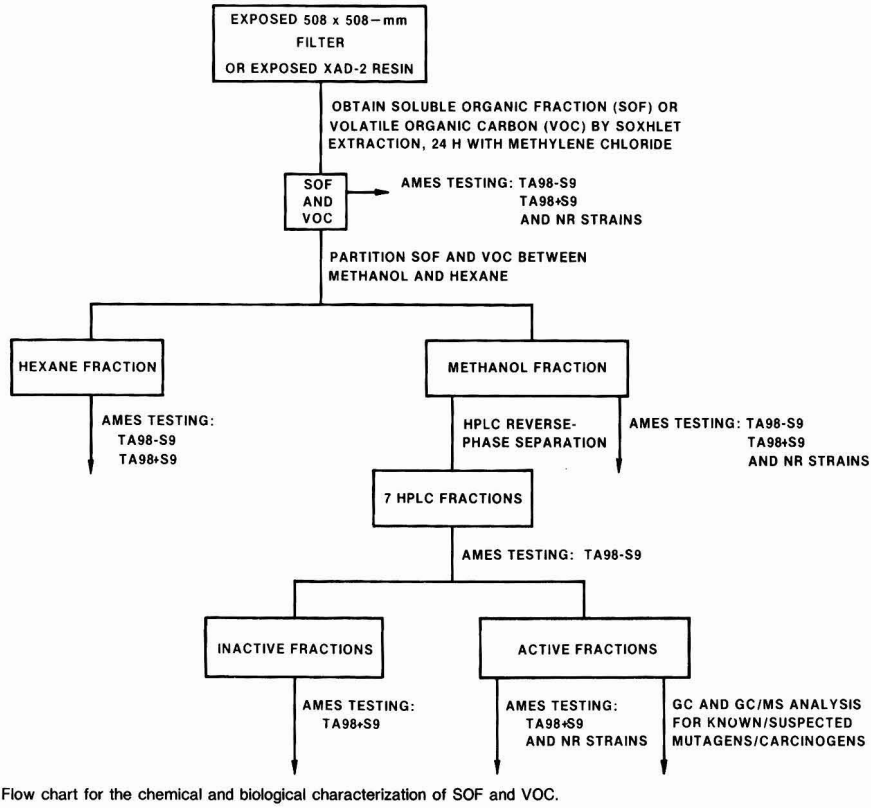

Figure 3. Flow chart for the chemical and biological characterization of SOF and VOC.

mL/min; UV absorbance was monitored at 254 nm. The relative retention times that were determined for PAH reference compounds appear in Table I.

The collected HPLC fractions that showed the most direct-acting mutagenic activity in the Ames assay with strain TA98 were further analyzed by capillary GC and GC/MS (see Figure 3). A 30 m × 0.31 mm i.d. Durabond DB-5 fused silica column with a film thickness of 0.25 μm (J&W Scientific, Inc., Rancho Cordova, CA) was used with He carrier gas (65 ± 5 cm/s at 100 °C) on a Hewlett-Packard 5880A GC with a split/splitless injector and flame-ionization and nitrogen–phosphorus detectors. The column temperature was initially 100 °C for 3.0 min, followed by a linear thermal gradient to 300 °C at 5 deg/min and an isothermal period of 15 min at 300 °C. Injector and detector temperatures were 225 and 350 °C, respectively. Relative retention times for PAH reference compounds are given in Table I.

A Hewlett-Packard 5985 quadrupole mass spectrometer (interfaced to an HP 5840A GC) was tuned in the electron impact (EI) mode with an ionization energy of 70 eV, emission current of 300 μA, ion source temperature of 250 °C, and ionization chamber pressure of approximately 5 × 10^{-6} Torr. The repeller, drawout, ion focus, and entrance lens voltages were optimized in an iterative process that used the m/e 69, 219, and 502 ions of perfluorotributylamine. The GC parameters were identical with those used for the HP 5880.

Biological Methods for Determining Mutagenicity. The integrated chemical and biological analysis scheme is presented in Figure 3. The Ames assay was used with tester strain TA98 (from Dr. Bruce Ames, University of California at Berkeley) and nitroreductase-deficient strains TA98NR and TA98-1,8-DNP_6 (TA98DNP) (from Dr. Herbert Rosenkranz, Case Western Reserve University) with 100 × 15 mm Petri dishes and the methods of Maron and Ames (*24*). A standard 4% S9 mixture was prepared from Aroclor 1254 induced rat liver S9 enzyme (Litton Bionetics, Inc., Charleston, SC) and used for tests requiring metabolic activation. Plates were counted after 63 h (*25*) by an Artek Model 880 automatic colony counter (Artek Corp., Farmingdale, NY). The modified techniques of Alfheim et al. (*26*) were employed with 60 × 15 mm Petri dishes for samples having masses less than 5 mg (e.g., HPLC fractions).

The positive controls used were 2-nitrofluorene (Aldrich Chemical Co., Milwaukee, WI), 2-aminoanthracene (Aldrich), and 1-nitro- and 1,6-dinitropyrenes (from Dr. Dennis Schuetzle, Ford Motor Co.). Controls were run on each test date and included solvent (dimethyl sulfoxide, Me_2SO) controls for spontaneous revertant levels, genotypic checks, reagent and medium sterility tests, and checks for sample toxicity to the tester strains.

Data Analysis. Ames assay dose–response data were used to calculate revertants per microgram values with a computer program that first determined the linear portion of the dose–response curve. A power function model formula (*4*) was then used to determine activity as revertants per microgram of sample. Revertants per microgram values were then multiplied by volumetric values (milligrams per cubic meter) for SOF or VOC to produce raw exhaust estimates of mutagenicity as revertants per cubic meter. All raw exhaust values (reported on a cubic meter basis) were calculated at standard conditions for

Table II. Caterpillar 3208 Engine Emissions with and without Traps

		engine emissions[b,c]								
mode[a]	n	NO_x,[d] ppm	NO,[e] ppm	NO_2,[f] ppm	HC,[g] ppm	HC,[g] mg/m^3	TPM,[h] mg/m^3	SOF,[h] mg/m^3	VOC,[i] mg/m^3	SO_4^{2-},[j] mg/m^3
4B	20	709 (12.8)	513 (5.1)	65.7 (13.5)	147 (7.5)	85.2 (4.4)	56.8 (7.5)	41.2 (8.2)	30.3 (7.4)	3.0 (0.4)
4T	35	693 (21.5)	526 (14.2)	32.6 (6.4)	145 (6.7)	83.9 (3.9)	16.8 (3.2)	12.1 (2.8)	33.2 (9.7)	1.5 (0.15)
5B	4	956 (1.0)	910 (0.9)	44.1 (<0.1)	90.6 (7.8)	52.5 (4.5)	42.7 (0.9)	7.6 (1.3)	15.4 (1.2)	3.5 (0.1)
5T	4	929 (9.3)	894 (5.4)	34.1 (4.5)	49.7 (1.7)	28.8 (1.0)	5.8 (0.6)	2.8 (0.4)	7.7 (1.6)	1.5 (0.3)

[a] Speed for all modes = 1680 rpm; load for mode 4 = 320 N·m; load for mode 5 = 480 N·m; B = base line (no trap); T = trap. [b] Reported as mean value (standard deviation). [c] All mg/m^3 values reported at standard conditions: T_{STD} = 294.2 K; P_{STD} = 101 kPa. [d] Measured by Beckman Instruments 955 NO/NO_x analyzer after reduction of NO_2 to NO. [e] Measured directly by Beckman 955. [f] Obtained by difference of NO_x and NO. [g] Measured by Beckman Instruments 402 heated flame ionization detector. [h] From 47-mm filters, gravimetrically. [i] From XAD-2 resin, gravimetrically. [j] From 47-mm filters by ion chromatography.

temperature and pressure, which, for this study, were 294.2 K and 101 kPa, respectively.

Engine emissions data were compared by the Kruskal–Wallis single-factor ranks test (27) as several samples had to be pooled from separate engine test dates in order to provide sufficient SOF and VOC masses for biological and chemical characterizations. The null hypothesis was that there was no significant difference between the compared groups at an α level of 0.05.

Results and Discussion

Emission and Activity of SOF and VOC. The effects of the ceramic traps on measured emissions can be seen from the typical values reported in Table II. Use of the ceramic traps significantly reduced emissions of TPM, SOL, SOF, and SO_4^{2-} for both modes 4 and 5; for mode 5, a significant decrease in HC was seen with the traps. There were no significant differences in the measured emission rates for NO or NO_x for base line vs. trap at mode 4. The mode 5 trap NO, NO_x, and NO_2 emission levels were significantly reduced compared to base line. The VOC levels showed the same trends as NO/NO_x emissions; i.e., the trap had little effect at mode 4, while mode 5 trap levels were significantly lower.

As can be seen in Figure 4, the use of the ceramic traps coincided with reduced raw exhaust emission levels of mutagenicity for mode 4 and 5 SOF and VOC. On the basis of revertants per cubic meter of raw exhaust, this trend was observed for both direct (TA98 – S9) and indirect (TA98 + S9) activities; the activity of mode 4 VOC with S9 was the single exception. Sample toxicity to tester strain TA98 – S9 was observed with all the VOC samples as well as both of the mode 5 SOF samples. Ames assays on organic material extracted from unexposed XAD-2 resin and polyurethane foam showed no toxicity. The observed activity of this extracted material accounted for 5% (or less) of the activity of the VOC extracts.

The reduced activity observed with the mode 4 base-line and trap SOF samples when tested with TA98NR and TA98DNP strains (see Figure 4) indicates the presence of nitro aromatic PAH in these samples. The mode 4 base-line and trap VOC samples were not tested with the nitroreductase-deficient strains due to the low activities associated with these VOC samples. In preliminary tests with mode 4 base-line VOC samples, there were no detectable activities with TA98NR. There was insufficient sample available to test the mode 5 SOF and VOC with either S9 or the nitroreductase-deficient strains.

It is interesting to note that the traps do not produce equal reductions in particulate levels and raw exhaust mutagenicity associated with the particulate. This same observation was made in previous studies with the Corning Ex:47 ceramic traps at Michigan Technological University over additional engine operating conditions (4).

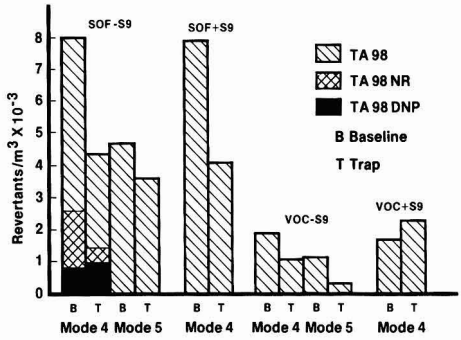

Figure 4. Raw exhaust emission mutagenicity levels of modes 4 and 5 with (T) and without (B) ceramic particulate filters. Mode 4 and 5 samples were run in duplicate on two separate dates with 100 × 15 mm Petri dishes. Responses (revertants per plate) for the solvent (Me_2SO) blank for mode 4 sample runs were 30 ± 5 for TA98 – S9, 42 ± 4 for TA98 + S9, 20 ± 1 for TA98NR, and 12 ± 2 for TA98DNP; the solvent blank value for mode 5 was 26 ± 2 revertants per plate. Positive control responses (revertants per plate) for the mode 4 samples with 2-nitrofluorene (3.2 μg/plate) were 732 ± 37 for TA98, 93 ± 13 for TA98NR, and 145 ± 1 for TA98DNP; the 2-nitrofluorene response for TA98 – S9 with the mode 5 samples was 679 ± 23 revertants per plate. Response with TA98 + S9 to 2-aminoanthracene (1.5 μg/plate) was 2145 ± 290 revertants per plate. The responses (revertants per plate) to 1-nitropyrene (0.33 μg/plate; – S9) were 816 ± 34 for TA98, 188 ± 15 for TA98NR, and 529 ± 40 for TA98DNP. The responses (revertants per plate) to 1,6-dinitropyrene (0.025 μg/plate; – S9) were 2789 ± 120 for TA98, 244 ± 65 for TA98NR, and 150 ± 20 for TA98DNP.

Hydrocarbon balances that were calculated for both modes (11) showed that more hydrocarbons were unaccounted for (i.e., neither adsorbed onto the filter particulate nor trapped on XAD-2 resin) when the ceramic traps were used. Considering only the hydrocarbons that could be collected during this study (i.e., those trapped by XAD-2 and particulate filters), the mode 4 VOC contributed 20–25% and 20–30% of the direct-acting mutagenicity per cubic meter of raw exhaust detected under base-line and trap conditions, respectively. There was no change in the percent contribution to mutagenicity observed with S9 metabolic activation at mode 4 under base-line conditions; however, the trap VOC contributed up to 50% of the observed mutagenicity per cubic meter when tested with S9. The VOC collected under base-line conditions from mode 5 had the same percent contribution to direct-acting mutagenicity as found at mode 4. In contrast, the VOC collected with the traps in use had half the mutagenic contribution (10–15%) as at mode 4.

The contribution of the collected gaseous-phase material to the overall exhaust mutagenicity found in this study is similar to that reported by Rannug (19) for gaseous-phase

Table III. Mutagenic Activities of Mode 4 Base-Line and Trap SOF HPLC Fractions

sample	fraction	fraction mass, % of total	mutagenic activities, revertants/μg^a			
			TA98 – S9	TA98 + S9	TA98NR	TA98DNP
4B-SOF	1	12.5	0.003	NT[b]	NT	NT
	2	8.5	2.553	NT	0.255	NC[c]
	3	7.5	2.642	NT	0.264	0.145
	4	8.0	1.211	NT	0.254	0.545
	5	10.4	0.513	NT	NC	NC
	6	7.3	0.077	0.071	NT	NT
	7	45.9	0.017	0.020	NT	NT
4T-SOF	1	40.5	0.031	NT	NT	NT
	2	9.6	1.754	NT	0.175	0.439
	3	8.9	4.221	NT	0.612	1.351
	4	8.0	3.741	NT	0.767	0.187
	5	6.7	1.061	1.931	0.477	0.265
	6	3.7	1.316	1.319	NT	NT
	7	22.7	0.163	0.135	NT	NT

[a] Samples were run in duplicate on two separate dates with 60 × 15 mm Petri dishes (*26*). Responses (revertants per plate) for the solvent (Me_2SO) blanks were 24 ± 4 for TA98 – S9, 36 ± 3 for TA98 + S9, 13 ± 2 for TA98NR, and 15 ± 2 for TA98DNP. Positive control (– S9) responses (revertants per plate) with 2-nitrofluorene (3.2 μg/plate) were 588 ± 33 for TA98, 70 ± 12 for TA98NR, and 105 ± 13 for TA98DNP. Response with TA98 + S9 to 2-aminoanthracene (1.56 μg/plate) was 1112 ± 32 revertants per plate. [b] Not tested. [c] Not calculated due to lack of dose–response.

Table IV. Mutagenic Activities of Mode 4 Base-Line and Trap VOC HPLC Fractions

sample	fraction	fraction mass, % of total	mutagenic activities, revertants/μg^a			
			TA98 – S9	TA98 + S9	TA98NR	TA98DNP
4B-VOC	1	20.2	0.087	NT[b]	NT	NT
	2	12.7	0.428	NT	NC[c]	NC
	3	9.1	1.020	NT	NT	NC
	4	10.5	0.907	NT	0.200	0.086
	5	5.5	0.079	NT	0.008	NC
	6	9.4	0.035	0.042	NT	NT
	7	32.6	0.018	0.021	NT	NT
4T-VOC	1	26.8	0.038	NT	NT	NT
	2	10.2	0.461	NT	NC	NC
	3	10.1	0.334	NT	NC	NC
	4	9.9	0.341	NT	NT	NT
	5	10.6	0.039	0.071	NC	NT
	6	7.1	0.017	0.106	NT	NT
	7	25.3	0.011	0.022	NT	NT

[a] See footnote *a* in Table III for responses of solvent blanks and positive controls. [b] Not tested. [c] Not calculated due to lack of dose–response.

material collected by a cryogradient technique (after a particulate filter) from a light-duty diesel engine without any emission control systems; that is, from 25–30% of the total raw exhaust direct-acting mutagenicity (reported as revertants per kilowatt hour) was associated with the gaseous-phase material. The gaseous-phase contribution to the total mutagenicity was 5–20% when tested with S9 metabolic activation.

Separation and Activity of SOF and VOC. Prior to the HPLC separation, the mode 4 SOF or VOC was partitioned between water-washed hexane and methanol. This initial step produced a fraction that was more concentrated in direct-acting mutagens; typically, the methanolic fraction contained only 11–16% of the original SOF or VOC mass but yet was still more active (as revertants per cubic meter) with TA98 – S9 than the hexane fraction. The use of the traps had little effect on the proportions of mass partitioning into the relatively polar (methanolic) or nonpolar (hexane) fractions for either the SOF or VOC.

The methanolic fractions of the base-line and trap SOF showed reductions in activities of 65–80% compared to TA98 – S9 when retested with TA98NR and TA98DNP (Figure 5). In contrast, only a 15–30% reduction was observed with the trap VOC methanolic fraction. (There was insufficient mass available for the base-line VOC methanolic fraction to be reassayed with these nitroreductase-deficient strains.) These results indicate, as found in previous studies with diesel (*20*, *28–35*) and gasoline (*36*) particulate extracts, that the direct mutagens are concentrated in a relatively small fractional mass of the extractable organics and that the mutagenicity is due, in part, to the presence of nitro-substituted PAH.

The methanolic fractions were further separated into seven reverse-phase HPLC fractions. The middle fractions showed the greatest activities with TA98 – S9. Typically, fractions 2–5 contained less than 40% of the methanolic SOF or VOC mass (base line or trap), yet these fractions accounted for more than 85% of the direct-acting activity (Tables III and IV). Absolute mass recovery data were not included because we were unable to accurately determine the quantities injected on the HPLC. However, the relative proportions of the collected fractions are given in Tables III and IV.

Some of the HPLC fractions were tested with S9 and/or nitroreductase-deficient tester strains, depending on the types of compounds expected to be present in each fraction from tests with standard PAH compounds (Table I). S9 was used with fractions 5–7 as these fractions might have contained compounds requiring metabolic activation and also generally had low levels of direct-acting mutagenicity. Comparison of activities with TA98 ± S9 are presented in Tables III and IV for SOF and VOC fractions, respec-

Table V. Compounds Identified in Most Active Mode 4 Methanolic HPLC Fractions

HPLC fraction	compound	base line		trap	
		SOF	VOC	SOF	VOC
2	naphthaleneacetic acid	X	NT[a]	X	NT[a]
	naphthalenedicarboxylic acid anhydride	X		X	
	2-naphthylethanol	X		X	
	C-2 aldehyde of naphthalene	X			
	fluorenone			X	
3	fluorenone	X	X		X
	methylfluorenone		X	X	X
	anthracenedione		X		X
	phenanthridine/acridine/benzoquinoline[b]	X		X	
	C-3 ketone of anthracene/phenanthrene[b]		X		
	5*H*-cyclopenta[*def*]phenanthrenone				X
	dihydroxymethylfluorene	X			
	C-2 aldehyde of naphthalene				X
	nitronaphthalene				X
	quinoline/isoquinoline[b]				X
	xanthone				X
4	fluoranthene	X	X	X	X
	phenanthridine/acridine/benzoquinoline[b]	X	X	X	X
	pyrene	X	X	X	X
	methylanthracene/methylphenanthrene[b]	X	X		X
	C-2 alkylfluorene		X		X
	anthracene/phenanthrene[b]		X		X
	dimethylnitroanthracene/dimethylnitrophenanthrene[b]	X		X	
	methyldibenzothiophene		X		X
	C-4 alkylfluorenone		X		
	C-3 alkylnaphthalene				X
	dibenzothiophene				X
	methylfluorenecarboxaldehyde			X	
	methylnitroanthracene/methylnitrophenanthrene[b]	X			
	nitropyrene/nitrofluoranthene[b]			X	
	octahydromethylnaphthalenone			X	

[a] Fraction not characterized by GC and GC/MS. [b] Isomeric structure not determined. One or more isomers of the listed compounds may be present.

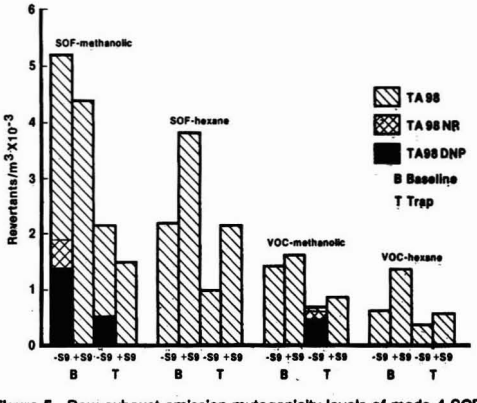

Figure 5. Raw exhaust emission mutagenicity levels of mode 4 SOF and VOC methanolic and hexane fractions with (T) and without (B) ceramic particulate traps. Samples were run in duplicate on the same test date as the mode 4 base-line and trap SOF and VOC samples. See the legend to Figure 4 for responses of solvent blanks and positive controls.

tively. (There was insufficient sample to test fraction 5 of the base-line SOF or VOC with S9). Some increases with S9 metabolic activation were found, but the resulting activities were still low compared to the direct-acting activities found with fractions 2–4.

Fractions 2–5 were tested with TA98NR and TA98DNP. As presented in Tables III and IV, the responses with these nitroreductase-deficient strains were less than that for TA98 – S9 for all fractions tested. With many of the VOC fractions, the TA98 response was very low initially, and no increase above spontaneous revertant levels at the sample concentrations tested could be found with TA98NR and TA98DNP. The responses with the trap and base-line SOF fractions 2–4 (Table III) indicate that these fractions might contain not only dinitropyrenes (fraction 3) and nitropyrenes (fraction 4) but also other types of nitro-PAH to which these tester strains have reduced responses (*34*).

Identification of PAH. The HPLC fractions having the most direct-acting mutagenicity were further separated with GC and GC/MS techniques to assess what types of PAH compounds might be present. Mode 4 base-line and trap SOF fractions 2–4 and base-line and trap VOC fractions 3 and 4 were used in these analyses.

Table V gives a summary of all tentatively identified compounds. The GC retention times, major EI fragments, and other evidence used to support the identifications of compounds are given in the supplementary table (see paragraph at end of paper regarding supplementary material).

Fluorenone appears to be the most abundant of the PAH identified in the methanolic fractions, and as seen in Table V, it is found in both SOF and VOC for the base-line and trap samples. Fluorenone has an HPLC retention time that puts it on the border between fractions 2 and 3; in one case it appeared in fraction 2 of the trap SOF, and in all other cases it was found in fraction 3. Fluorenones and alkylfluorenones are present in diesel exhaust but are theorized to be produced by combustion of the more abundant phenanthrenes via a route proposed by Yu and Hites (*29*). Alkylated fluorenes may also be produced via this scheme. These compounds, by virtue of their vapor pressures, would be expected to be found both on the particulate and in the gaseous phase. They would be expected to pass through a ceramic trap with

some reduction in concentration due to adsorption onto trapped particulate. Increased residence time of these species in the trap matrix could generate nitrated fluorenes and fluorenones. Although these compounds were not conclusively identified in this study, the presence of nitrofluorenone (in low abundance) was suspected in fraction 3 of the trap SOF.

Phenanthrene and/or anthracene and their alkylated derivatives were also present in relatively great abundance in a number of the HPLC fractions of the methanolic extract of the mode 4 base-line and trap SOF and VOC. These compounds were expected to partition into the hexane fraction; due to their great abundance and the slight solubility of hexane in methanol, however, these PAH were also found in the methanolic fraction. The same explanation can be given for the presence of pyrene and fluoranthene. The vapor pressures of anthracene, phenanthrene, pyrene, and fluoranthene are sufficiently high that they could be present either on particulate or in the gaseous phase (*20*); this was the case in this study.

Four nitro-PAH compounds were tentatively identified: nitronaphthalene, dimethylnitroanthracene/dimethylnitrophenanthrene, methylnitroanthracene/methylnitrophenanthrene, and nitropyrene/nitrofluoranthene. Nitronaphthalene was found in fraction 3 trap VOC while the other nitro-PAH were found in fraction 4 SOF. Nitropyrene was found only in fraction 4 of the trap SOF. This correlates with the expected elution of these compounds from the HPLC. Nitronaphthalene and nitropyrene are known to be direct-acting mutagens (*37*), as are nitrofluorenone and nitroanthracene (*38*). However, all of the mutagenic nitro-PAH seemed to be present at low or trace levels and probably would not account for all of the observed mutagenicity of the fractions that comprise them.

None of the hydroxynitro- or polynitro-PAH isomers were detected in any of the most active fractions. A variety of these compounds, especially the derivatives of pyrene, fluorene, and fluorenone, have been reported as components of diesel exhaust (*35*, *39–41*). The polar nature, thermal instability, and low concentrations of these compounds make their quantitative detection by gas chromatography somewhat difficult. Sample discrimination is a previously identified problem, and cold on-column injection techniques have been prescribed (*40*) for improved recoveries. Schuetzle and co-workers (*35*) reported that hydroxynitropyrene, some isomers of which have been identified as mutagens (*20*), decomposed to pyrenequinone. However, neither hydroxynitropyrene nor pyrenequinone have been conclusively identified in any fraction in this study.

Most of the detected heterocyclic compounds, i.e., dibenzothiophene, xanthone, and acridine/phenanthridine, are present in relatively large abundance in fractions 3 and 4. Quinoline/isoquinoline was tentatively identified as a low abundance component of fraction 3 of the trap VOC. Jensen and Hites (*38*) found the major heterocyclic compounds in diesel particulate to be dibenzothiophene, xanthone, and thioxanthone. Of the heterocyclics tested for mutagenicity, however, only quinoline has been reported to be mutagenic (*42*).

Anthracenedione, a weak mutagen (*43*), was found in only the VOC (base-line and trap) fraction 3. Schuetzle has proposed that quinones may be VOC sampling artifacts produced by the reaction of XAD-2 resin with exhaust gas (*20*).

The ceramic trap surface probably provides active (as well as adsorptive) sites for PAH. The expected reactions at the trap operating temperatures and in the presence of oxygen, unburned fuel, nitric and sulfuric acids, and NO_2 include oxidations, nitrations, alkylations, and the formation of sulfonates. In the Ames-active HPLC fractions that were chemically characterized, an increase in type and concentration of nitro-, polynitro-, and oxynitro-PAH was therefore expected.

Although more types of compounds were identified in the trap SOF and VOC samples than for base line, this may be due to differences in the sample background levels and the analyte concentrations for the various HPLC fractions. The compounds that were unique to the trap samples included heterocyclics (dibenzothiophene, xanthone, and quinoline/isoquinoline), ketones and aldehydes (cyclopenta[*def*]phenanthrenone, C-2 aldehyde of naphthalene, methylfluorenecarboxaldehyde, and octahydromethylnaphthalenone), and nitro compounds (nitrofluoranthene/nitropyrene and nitronaphthalene). On the basis of these qualitative screens, it did appear that there were indeed more oxidative processes occurring that altered the composition of the particulate-associated SOF and the VOC collected with the ceramic trap than without the trap. Compounds unique to trap SOF extracts included methylfluorenecarboxaldehyde, nitropyrene/nitrofluoranthene, and octahydromethylnaphthalenone; the latter compound was not previously reported for diesel exhaust. Dihydroxymethylfluorene and methylnitroanthracene/phenanthrene were unique to the base-line SOF, although dimethylnitroanthracene/phenanthrene was identified in both base-line and trap SOF. Dihydroxymethylfluorene was previously reported in one study by Schuetzle and co-workers (*35*), which focused on polar PAH of the particulate phase. It is reasonable to assume that such a compound would predominate in the particulate phase due to its decreased volatility.

Of the 12 compounds identified that were unique to VOC, only 2 (C-3 ketone of anthracene/phenanthrene and C-4 alkylfluorenone) were found in the base-line VOC and not in the trap VOC. Previously reported diesel exhaust components that were found only in the trap VOC in this study included xanthone (*20*), nitronaphthalene (*33*), dibenzothiophene (*29*), C-3 alkylnaphthalene (*44*), and cyclopenta[*def*]phenanthrenone (29). Methyldibenzothiophene (*45*), C-2 alkylfluorene (*29*), anthracene/phenanthrene (*29*), and anthracenedione (*29*) occurred in both base-line and trap VOC extracts.

These observations correlate well with the principles associated with the operation of the trap, i.e., decreases in particulate and SOF, provision of surfaces and increased residence time for oxidations, and increases in the proportion of VOC to SOF. Quantitative concentration data for specific PAH compounds would be needed to support these qualitative observations.

All samples had common components that were classified as contaminants. Several phthalate esters (from laboratory plastics) and a homologous series of polysiloxanes (from many potential sources including the GC injection port liner, its O-ring seal, and the analytical column itself) gave intense and characteristic fragment ions, the most common of which were m/e 279, 167, and 149 for phthalates and m/e 429, 355, 281, 207, and 133 for the siloxanes.

Conclusions and Recommendations

Sampling and analysis protocols were developed to determine some of the PAH components of the most mutagenic subfractions of particulate-associated and gaseous-phase diesel hydrocarbon extracts in order to assess the effects of particulate traps. The use of the traps caused

reduced raw exhaust mutagenicity and emissions of TPM, SOF, SOL, and SO_4^{2-} at modes 4 and 5. At mode 5, the traps also reduced HC, VOC, NO, NO_x, and NO_2 emissions.

The moderately polar HPLC subfractions of mode 4 methanolic SOF and VOC exhibited the highest mutagenicity. A significant portion of the activity of these fractions was shown to be due to the presence of nitro compounds. The use of S9 metabolic activation had little effect on the mutagenicity of the mode 4 trap or base-line SOF; mutagenicity of the mode 4 VOC with S9 activation more than doubled (in terms of raw exhaust emissions) when the traps were used.

Twenty-eight PAH were identified, but these qualitative differences did not account for the observed difference in mutagenicities of base-line and trap samples. However, three compounds (anthracenedione, nitronaphthalene, and quinoline/isoquinoline) tentatively identified as unique components of the VOC are reported mutagens (*42*, *43*).

More oxygenated PAH compounds were identified as components of the trap SOF and VOC extracts than for base line, which is consistent with the proposed mechanism of the trap's function (i.e., retention of particulate and oxidation of retained exhaust products). Although the separation scheme employed was an effective means of concentrating mutagens, it should be coupled with quantitative analyses of PAH known to be mutagenic in future studies.

The observed levels of mutagenicity and the similarities in the composition of the SOF and VOC underscore the importance of collecting and analyzing both the particulate-associated and gaseous-phase hydrocarbons when attempting to quantitate the biological activity or environmental impact of diesel exhaust emissions and control devices. As recommended by Williams and co-workers (*46*), quantitative PAH measurements that are the sum of particulate and gaseous-phase levels are less dependent upon the sampling system than are the levels in each phase separately.

The effects of the exhaust and sampling systems also need to be quantitated in order to make meaningful interlaboratory comparisons or extrapolate laboratory data to the environment. The muffler, dilution tunnel, gas-transfer lines, filters, and other collection media all provide considerable surface area for the sorption, condensation, agglomeration, and revolatilization of exhaust products.

Acknowledgments

We thank Jiangang Lu, Paul Wiczynski, and Peter Woon, who were responsible for the operation, maintenance, and improvement of the engine–dynamometer test facility, dilution tunnel, and sampling systems. We also thank Marilyn McKay and Lisa Bain for their assistance with the Ames assays.

Supplementary Material Available

A table detailing the evidence summary for structures identified from HPLC fractionation of mode 4 SOF and VOC methanol extraction (4 pages) will appear following these pages in the microfilm edition of this volume of the journal. Photocopies of the supplementary material from this paper or microfiche (105 × 148 mm, 24× reduction, negatives) may be obtained from Microforms Office, American Chemical Society, 1155 16th St., N.W., Washington, DC 20036. Full bibliographic citation (journal, title of article, authors' names, inclusive pagination, volume number, and issue number) and prepayment, check or money order for $11.50 for photocopy ($13.50 foreign) or $10.00 for microfiche ($11.00 foreign), are required.

Registry No. Naphthaleneacetic acid, 26445-01-2; naphthalenedicarboxylic acid anhydride, 34314-32-4; 2-naphthylethanol, 108121-75-1; 2-naphthaldehyde, 66-99-9; fluorene, 86-73-7; methyl fluorenone, 79147-47-0; anthracenedione, 108121-76-2; phenanthridine, 229-87-8; acridine, 260-94-6; benzoquinoline, 39327-16-7; 3-anthracenone, 108121-79-5; 5*H*-cyclopenta[*d*,*e*,*f*]-phenanthrenone, 108121-80-8; dihydroxymethylfluorene, 108121-77-3; nitronaphthalene, 27254-36-0; quinoline, 91-22-5; isoquinoline, 119-65-3; xanthone, 90-47-1; fluoranthene, 206-44-0; pyrene, 129-00-0; methylanthracene, 26914-18-1; methylphenanthrene, 31711-53-2; anthracene, 120-12-7; phenanthrene, 85-01-8; dimethylnitroanthracene, 80191-45-3; dimethylnitrophenanthrene, 80182-27-0; methyldibenzothiophene, 30995-64-3; dibenzothiophene, 132-65-0; methylfluorene carboxaldehyde, 108121-78-4; methylnitroanthracene, 80191-43-1; methylnitrophenanthrene, 80191-44-2; nitropyrene, 63021-86-3; nitrofluoranthene, 55345-04-5; octahydromethylnaphthalenone, 108148-17-0; nitrogen oxide, 11104-93-1; nitrogen oxide (1:1), 10102-43-9; nitrogen dioxide, 10102-44-0.

Literature Cited

(1) Environmental Protection Agency *Fed. Regist.* **1985**, *50*(*51*), 10606.
(2) Howitt, J. S.; Montierth, M. R. *SAE Trans.* **1981**, *90*, 493–501.
(3) Ludecke, O. A.; Dimick, D. L. *SAE Trans.* **1983**, *92*, 288–308.
(4) Miller, P. R.; Scholl, J.; Bagley, S.; Leddy, D.; Johnson, J. H. *SAE Trans.* **1983**, *92*, 287–315.
(5) Ludecke, O. A.; Bly, K. B. *SAE Tech. Pap. Ser.* **1984**, *No. 840077.*
(6) Sachdev, R.; Wong, V. W.; Shahed, S. M. *SAE Tech. Pap. Ser.* **1984**, *No. 840076.*
(7) Wiedemann, B.; Doerges, U.; Engeler, W.; Poettner, B. *SAE Tech. Pap. Ser.* **1984**, *No. 840078.*
(8) Danis, A. M.; Partridge, P. A.; Cernasky, N. P. *SAE Tech. Pap. Ser.* **1985**, *No. 850011.*
(9) Lepperhoff, G.; Kroon, G. *SAE Tech. Pap. Ser.* **1985**, *No. 850013.*
(10) Simon, G. M.; Stark, T. L. *SAE Tech. Pap. Ser.* **1985**, *No. 850016.*
(11) Bagley, S. T.; Dorie, L. D.; Leddy, D. G.; Johnson, J. H. *An Investigation into the Effect of a Ceramic Particle Trap on the Chemical Mutagens in Diesel Exhaust*; Research Report No. 5; Health Effects Institute: Cambridge, MA, 1987.
(12) Wiczynski, P. D.; Johnson, J. H. *SAE Tech. Pap. Ser.* **1986**, *No. 860620.*
(13) MacDonald, J. S. *SAE Tech. Pap. Ser.* **1983**, *No. 831711.*
(14) Pauli, E.; Lepperhoff, G.; Pischinger, F. *SAE Tech. Pap. Ser.* **1983**, *No. 830180.*
(15) Bissett, E. J. *Chem. Eng. Sci.* **1984**, *39*, 1233.
(16) Bissett, E. J.; Shadman, F. J. *AIChE J.* **1985**, *31*, 753.
(17) McCabe, R. W.; Sinkevitch, R. M. GM Research Publication GMR-5108; General Motors Research Laboratories: Warren, MI, 1985.
(18) Pattas, K. N.; Kyriakis, N. A.; Samaras, Z. C. *SAE Tech. Pap. Ser.* **1985**, *No. 850012.*
(19) Rannug, U. *EHP, Environ. Health Perspect.* **1983**, *47*, 161–169.
(20) Schuetzle, D. *EHP, Environ. Health Perspect.* **1983**, *47*, 65–80.
(21) Alfheim, I.; Lindskog, A. *Sci. Total Environ.* **1984**, *34*, 203–222.
(22) Hughes, T. Y.; Pellizzari, E.; Little, L.; Sparacino, C.; Kolber, A. *Mutat. Res.* **1980**, *76*, 51–83.
(23) Stump, F.; Bradow, R.; Ray, W.; Dropkin, D.; Zweidinger, R.; Sigsby, J.; Snow, R. *SAE Tech. Pap. Ser.* **1982**, *No. 820076.*
(24) Maron, D. M.; Ames, B. N. *Mutat. Res.* **1983**, *113*, 173–215.
(25) Belser, W. L., Jr.; Shaffer, S. D.; Bliss, R. D.; Hynds, P. M.; Yamamoto, L.; Pitts, J. W.; Winer, J. A.; *Environ. Mutagen.* **1981**, *3*, 123–139.
(26) Alfheim, I.; Becher, G.; Hongslo, J. K.; Ramdahl, T. *Environ. Mutagen.* **1984**, *6*, 91–102.
(27) Zar, J. H. *Biostatistical Analysis*, 2nd ed.; Prentice-Hall: Englewood Cliffs, NY, 1984.
(28) Campbell, J.; Scholl, J.; Hibbler, F.; Bagley, S.; Leddy, D.; Abata, D.; Johnson, J. *SAE Trans.* **1981**, *90*, 3074–3111.

(29) Yu, M.; Hites, R. A. *Anal. Chem.* **1981**, *53*, 951–954.
(30) Newton, D. L.; Erickson, M. D.; Tomer, K. B.; Pellizzari, E. D.; Gentry, P.; Zweidinger, R. B. *Environ. Sci. Technol.* **1982**, *16*, 206–213.
(31) Gorse, R. A., Jr.; Riley, T. L.; Ferris, F. C.; Pero, A. M.; Skewes, L. M. *Environ. Sci. Technol.* **1983**, *17*, 198–202.
(32) Henderson, T. R.; Sun, J. D.; Royer, R. E.; Clark, C. R.; Li, A. P.; Harvey, T. M.; Hunt, D. H.; Fulford, J. E.; Lovette, A. M.; Davidson, W. R. *Environ. Sci. Technol.* **1983**, *17*, 443–449.
(33) Paputa-Peck, M. C.; Marano, R. S.; Schuetzle, D.; et al. *Anal. Chem.* **1983**, *55*, 1946–1954.
(34) Salmeen, I. T.; Pero, A. M.; Zator, R.; Schuetzle, D.; Riley, T. L. *Environ. Sci. Technol.* **1984**, *18*, 375–382.
(35) Schuetzle, D.; Jensen, T. E.; Ball, J. C. *Environ. Int.* **1985**, *11*, 169–181.
(36) Alsberg, T.; Stenberg, U.; Westerholm, R.; et al. *Environ. Sci. Technol.* **1985**, *19*, 43–50.
(37) McCann, J.; Choi, E.; Yamasaki, E.; Ames, B. N. *Proc. Natl. Acad. Sci. U.S.A.* **1975**, *72*, 5135–5139.
(38) Jensen, T. E.; Hites, R. A. *Anal. Chem.* **1983**, *55*, 594–599.
(39) Schuetzle, D.; Perez, J. M. *J. Air. Pollut. Control Assoc.* **1983**, *33*, 751–755.
(40) Ramdahl, T.; Urdal, K. *Anal. Chem.* **1982**, *54*, 2256–2260.
(41) Liberti, A.; Ciccioli, P.; Cecinato, A.; Brancaleoni, E.; DiPalo, C. *HRC CC, J. High Resolut. Chromatogr. Chromatogr. Commun.* **1984**, *7*, 389–397.
(42) Rinkus, S. J.; Legator, M. S. *Cancer Res.* **1979**, *39*, 3289–3318.
(43) Liberman, D. F.; Fink, R. C.; Shaeffer, F. L. *Appl. Environ. Microbiol.* **1982**, *43*, 1354–1359.
(44) Behymer, T. D.; Hites, R. A. *Environ. Sci. Technol.* **1984**, *18*, 203–206.
(45) Tong, H. Y.; Karasek, F. W. *Anal. Chem.* **1984**, *56*, 2129–2134.
(46) Williams, R. L.; Perez, J. M.; Griffing, M. E. *SAE Tech. Pap. Ser.* **1985**, *No. 852081*.

Received for review September 11, 1986. Accepted March 25, 1987. Research described in this paper was conducted under contract to the Health Effects Institute (HEI), an organization jointly funded by the U.S. Environmental Protection Agency (EPA) (Assistance Agreement V-812059) and automotive manufacturers. The contents of this paper do not necessarily reflect the views of the HEI, nor do they necessarily reflect the policies of the EPA or automotive manufacturers.

Toxic Chemicals, Including Aromatic and Chlorinated Hydrocarbons and Their Derivatives, and Liver Lesions in White Croaker (*Genyonemus lineatus*) from the Vicinity of Los Angeles

Donald C. Malins,* Bruce B. McCain, Donald W. Brown, Mark S. Myers, Margaret M. Krahn, and Sin-Lam Chan

Environmental Conservation Division, Northwest and Alaska Fisheries Center, National Marine Fisheries Service, National Oceanic and Atmospheric Administration, U.S. Department of Commerce, Seattle, Washington 98112

■ High concentrations of toxic chemicals in sediment and white croaker (*Genyonemus lineatus*), as well as liver diseases (e.g., carcinomas) in this species, were found in the Los Angeles area. The highest concentrations of aromatic hydrocarbons (AHs) in the sediment were in San Pedro Bay, and the highest concentrations of 1,1,1-trichloro-2,2-bis(*p*-chlorophenyl)ethane (DDT) derivatives were in sediment from near the White Point sewer outfall. Concentrations of AHs, polychlorobiphenyls (PCBs), and DDT derivatives were generally higher in food organisms (benthic invertebrates) from the croaker's stomach than in sediment. Moreover, croaker from San Pedro Bay and White Point were substantially contaminated with DDT derivatives and metabolites of aromatic compounds (in bile), compared to croaker from the Hyperion outfall and Dana Point (reference area). The evidence suggests that the observed pathological conditions of the liver were associated with exposure of the croaker to toxic chemicals, which occurred, at least in part, through the ingestion of contaminated food organisms.

Introduction

Bottom-feeding fish in urban coastal waters are exposed to myriad toxic chemicals (*1*, *2*), and several studies indicate that many of the chemicals accumulate in these fish (*3*, *4*) and thus create a potential for altering their health (*5–8*). For example, accumulations of metabolites of toxic chemicals in the bile (*9*, *10*), of English sole, *Parophrys vetulus*, from Puget Sound were recently shown to be associated with liver diseases, including liver cancers. In another study (*5*), similar associations were observed between toxic chemicals [e.g., aromatic hydrocarbons (AHs)] in sediments and various diseases in English sole.

Marine waters adjacent to Los Angeles are known to receive considerable amounts of industrial and municipal wastes (*11–13*). This environment thus affords an opportunity to expand limited knowledge available on the bioaccumulation, disposition, and food chain transfer of toxic chemicals. White croaker *Genyonemus lineatus*, were of particular interest because of their wide distribution along the California coast and because they are an important component of the skiff sports fishery. This bottom-feeding fish also forms the basis for a growing gill net fishery and is a mainstay of pier catches in Southern and Central California (*14*). Love et al. (*14*) reported that adult white croaker spawn in shallow waters (8–12 m) and younger fish tend to reside in shallow waters, migrating to deeper waters (22–36 m) as they become mature adults. Accordingly, chemical analyses were performed on sediments and on stomach contents (food organisms), liver, and bile from white croaker collected in the Los Angeles area (San Pedro Bay and near the 5-mi Hyperion and White Point sewer outfalls) and a nonurban reference area (Dana Point) (Figure 1). Observations were also made on histopathologic conditions in these fish.

Methods and Materials

Sediment samples and white croaker were collected in December 1984 from San Pedro Bay (Queensway Bay, Cerritos Channel, and near Reservation Point) and from the vicinity of the White Point and 5-mi Hyperion sewer outfalls (Figure 1). Comparable samples were obtained from Dana Point in September 1984. Surface sediments (top 2 cm) were collected with a modified Van Veen grab (0.1 m^2), and three grab samples taken at each site were composited. Between 23 and 27 white croaker, collected

*Address correspondence to this author at his present address: Pacific Northwest Research Foundation, Seattle, WA 98104.

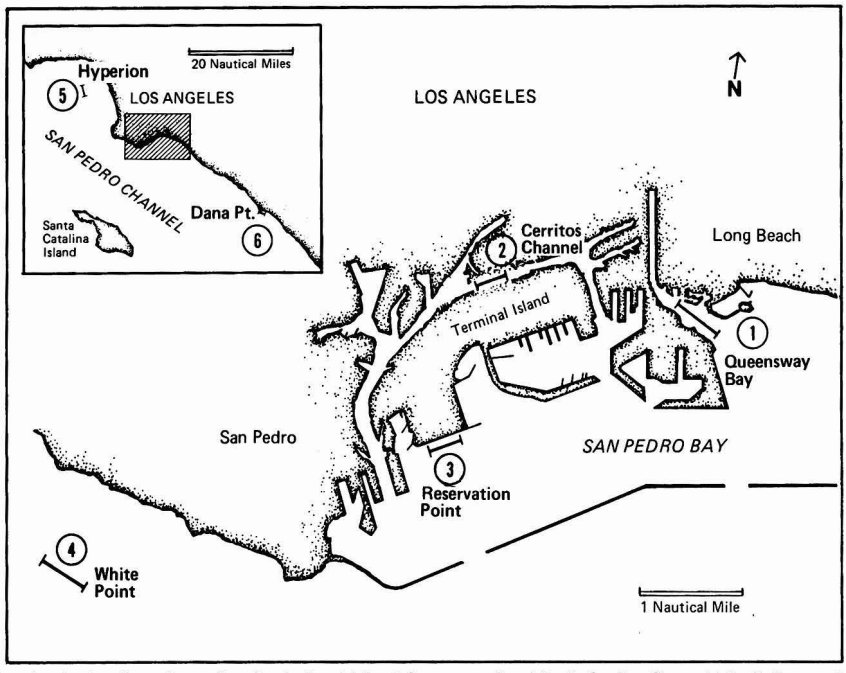

Figure 1. Map showing locations of sampling sites in the vicinity of Queensway Bay (site 1), Cerritos Channel (site 2), Reservation Point (site 3), White Point sewer outfalls (site 4), (inset) near the 5-mi Hyperion outfall (site 5) and Dana Point (site 6). The coordinates for the sampling sites were as follows: Queensway Bay, 33° 45′ 20″ N × 118° 11′ 20″ W; Cerritos Channel, 33° 43′ 49″ N × 118° 14′ 48″ W; White Point, 33° 42′ 24″ N × 118° 21′ 06″ W; Hyperion, 33° 54′ 29″ N × 118° 31′ 57″ W; Dana Point, 33° 26′ 54″ N × 117° 42′ 24″ W.

at each site by otter trawl, were measured (mm), weighed (g), and necropsied. At each site, the following samples were collected for chemical analyses: bile, from 10 individual fish; stomach contents (food organisms), a composite from 10 fish; liver, a composite from 5 fish. The mean lengths (mm) of fish from each site used for chemical analyses were as follows: Queensway Bay, 221 ± 41; Cerritos Channel, 153 ± 13; Reservation Point, 200 ± 36; White Point, 201 ± 7; Hyperion, 255 ± 7; Dana Point, 191 ± 21. All samples were kept at −20 °C until analyzed. Sediments and stomach contents were analyzed for a broad spectrum of AHs and chlorinated hydrocarbons (CHs) by using capillary column gas chromatography with mass spectrometry, flame ionization, and electron capture detectors (*15*). A high-pressure liquid chromatographic/fluorescence detection technique (*9, 10*) was employed to measure metabolites of aromatic compounds in bile. This technique was used because analyses of AHs (e.g., components of fossil fuels and their combustion products) in tissues are of limited value due to the extensive metabolism of these compounds, especially in the liver (*16–18*). Samples of liver tissues were analyzed (*15*) for the more metabolically resistant CHs (*2*). Stomach contents from a composite of five fish were also collected at each site and preserved in 10% neutral, buffered formalin for taxonomic characterization. Also, as part of the fish necropsy procedure, liver tissue was routinely collected for histopathological examination and preserved and processed by previously reported methods (*5*). Lesion classification followed previously described diagnostic criteria (*19–23*).

Results

Chemicals in Sediments and Stomach Contents. Sediment-associated AHs, including benzo[*a*]pyrene (BaP), were found at the San Pedro Bay sites at summed concentrations of 890–2800 ng/g dry weight. ("Summed concentrations" refers to total concentrations of compounds in Table I; all concentrations for sediments, stomach contents, and liver are on a dry-weight basis.) Concentrations of AHs in sediment from Dana Point were generally close to, or below, the limits of detection (Table I). The highest concentrations of 1,1,1-trichloro-2,2-bis-(*p*-chlorophenyl)ethane- (DDT-) related compounds and PCBs were found in sediments from the vicinity of the White Point sewer outfalls (summed concentrations, 1300 and 520 ng/g, respectively). The concentrations of DDT and related compounds were 15 and 100 times lower than those previously reported for sediments collected in the vicinity of this site by Brown et al. (*24*) in 1982 and by Young et al. (*25*) in 1976, respectively. These differences do not necessarily imply reductions in sediment concentrations over time; they could be due to an uneven distribution of chemical contaminants in surface sediments at the White Point site.

Stomach contents (food organisms) of white croaker captured inside San Pedro Bay contained substantially higher summed concentrations of AHs than did samples from the Hyperion and White Point sites (Table I). For example, the stomach contents from Cerritos Channel had 20 times the summed concentrations of AHs (30 000 ng/g) than did the sample from the Hyperion site. Concentrations of AHs in the stomach organisms from Dana Point were all close to or below the limits of analytical detection (Table I).

Highest concentrations of CHs in the stomach contents were found in fish from near White Point; the summed concentrations of DDT-related compounds and PCBs were 13 000 and 1000 ng/g, respectively (Table I). DDT and

Table I. Aromatic and Chlorinated Compounds (ng/g, Dry Weight) in Sediment (S), Stomach Contents (SC), and Livers (L) of White Croaker from the Los Angeles Area and a Reference Area (Dana Point)[a]

	Queensway Bay (1)			Cerritos Channel (2)			Reservation Point (3)			White Point (4)			Hyperion (5)			Dana Point (6)		
compounds[b]	S	SC	D[c]	S	SC	L	S	SC	L	S	SC	L	S	SC	L	S	SC	L
aromatic hydrocarbons																		
methylnaphthalenes	80	410		14	91		<4[d]	94		17	<27		120	180		<4	<17	
phenanthrene	220	1100		65	2100		10	330		<2	310		19	150		10	<12	
1-methylphenanthrene	14	1100		4	300		<3	<7		<2	<20		<10	<4		<3	<11	
anthracene	20	520		6	1100		11	<7		<2	<20		<1	<4		<3	<11	
fluoranthene	430	1200		180	7100		29	370		67	310		26	280		22	<13	
pyrene	560	1100		180	4900		670	1200		290	1100		47	500		13	<12	
benz[*a*]anthracene	240	98		53	3100		51	160		4	52		51	58		<2	<15	
chrysene	530	1000		160	4200		160	560		9	160		52	76		<3	<15	
benzo[*e*]pyrene	250	570		93	2700		160	350		26	<22		21	64		9	<14	
benzo[*a*]pyrene	210	330		73	2900		180	310		19	<26		16	27		<2	<17	
perylene	140	380		39	680		400	590		110	680		21	190		<2	<24	
dibenz[*a,h*]anthracene	63	230		26	480		14	64		22	<33		<2	<6		<3	<41	
aromatic hydrocarbons	2800	8000		890	30000		1700	4000		560	2600		370	1500		54	NA[e]	
chlorinated hydrocarbons																		
α-chlordane	22	160	1000	7	<1	460	<	5	63	7	10	140	2	20	86	1	75	19
trans-nonachlor	18	130	1300	6	<1	620	1	5	99	4	10	170	1	18	110	<1	4	42
o,p'-DDE	<1	110	3200	<1	110	1400	7	39	1900	190	1100	6000	9	35	220	<1	<4	37
p,p'-DDE	51	370	33000	15	920	14000	39	420	18000	890	11000	89000	100	1100	6000	1	<2	1400
p,p'-DDD	43	170	4300	12	730	8700	5	36	2200	200	1200	7100	7	72	320	1	<5	79
p,p'-DDT	9	16	67	4	71	380	<1	3	18	<4	18	63	<1	10	18	<1	<3	26
DDT and related compds	100	670	41000	31	1800	24000	51	500	22000	1300	13000	100000	120	1200	6600	2	NA	1500
trichlorobiphenyls	40	81	330	15	81	160	2	31	51	35	83	330	21	32	71	<1	36	48
tetrachlorobiphenyls	140	290	3700	53	540	3700	24	110	840	160	260	2000	80	250	750	<1	56	150
pentachlorobiphenyls	150	340	4300	54	380	8800	64	160	2100	220	380	2800	110	350	1600	3	290	240
hexachlorobiphenyls	82	200	2400	30	230	7900	47	110	1700	71	210	1600	74	210	1200	3	77	290
heptachlorobiphenyls	38	77	1600	15	120	2300	10	27	420	21	59	540	27	54	310	<1	14	120
octachlorobiphenyls	8	29	220	5	24	440	1	6	110	9	20	150	7	22	100	<1	3	34
nonachlorobiphenyls	3	11	77	3	9	130	1	1	36	4	4	60	2	5	29	<1	<4	15
polychlorobiphenyls	460	1000	13000	170	1400	23000	150	450	5300	520	1000	7500	320	920	4100	6	480	900

[a] Only major components in each category of compounds are presented. [b] concentrations were calculated with internal standards (*16*). [c] Aromatic hydrocarbons were not measured in liver. [d] The less than symbol (<) indicates that the chemical was not detected; the value given is the detection limit. [e] Not applicable.

Table II. Concentrations of Metabolites of Aromatic Compounds, Measured at Benzo[*a*]pyrene (BaP) and Naphthalene (NPH) Wavelengths, in Bile of White Croaker

site	equivalents, mean ± SD, ng/g (wet weight)	
	BaP (*n*)	NPH (*n*)
Queensway Bay (1)	330 ± 160 (11)[a]	140 000 ± 52 000 (11)[a]
Cerritos Channel (2)	5500 ± 1200 (8)	330 000 ± 100 000 (6)
Reservation Point (3)[b]	3700 ± 3100 (7)	410 000 ± 230 000 (7)
White Point (4)	960 ± 1600 (12)	170 000 ± 61 000 (12)
Hyperion (5)	78 ± 25 (5)	64 000 ± 47 000 (5)
Dana Point (6)	79 ± 75 (8)	39 000 ± 13 000 (8)

[a] It was not possible to obtain sufficient bile from fish sampled at this site in December 1984; accordingly, values obtained from a subsequent sampling (August 1985) are given. [b] Individual compounds in the bile were determined in our laboratories by gas chromatographic/mass spectroscopic analysis. The results (wet weight) from the analysis of bile from one white croaker from Reservation Point, for example, were as follows: BaP, 160 ng/g; dibenzofuranol, 1500 ng/g (two isomers); 9-fluorenol, 520 ng/g; fluoranthanol, 6400 ng/g (two isomers); pyrenol, 21 000 ng/g (three isomers); 3-hydroxybenzo[*a*]pyrene, 44 ng/g.

related compounds were not detected in the stomach contents from the Dana Point fish; however, 480 ng/g PCBs were found. Relatively high concentrations of both DDT and related compounds and PCBs were found in the stomach contents of fish from the Cerritos Channel, Queensway Bay, and Hyperion sites.

The taxonomic analyses of stomach contents revealed that the white croaker had fed primarily on benthic invertebrates. Analyses were performed on stomach contents of fish from the Queensway Bay, Cerritos Channel, Reservation Point, and Hyperion sites. (Sufficient sample was not available from the White Point fish for taxonomic analysis.) The mean percentages, by weight, of the identifiable food organisms for the four sites were as follows: 53 ± 13% polychaetes, 27 ± 10% crustaceans, 4 ± 2% bivalves, 7 ± 2% small fish, and 7 ± 4% nemertean worms. (Only trace amounts of nonbiological material, mostly fine sand particles, were found in the stomach contents.) The composition of food organisms in fish from Dana Point was quite similar to that of fish from the other sampling sites (41% polychaetes, 12% crustaceans, 9% bivalves, 5% small fish, and 6% nemertean worms), except that brachipods (27%) were also found.

Chemicals in Liver and Bile of White Croaker. CHs were present in the livers of white croaker from all six sites; however, substantial differences in concentrations were found between samples from Dana Point and those from the Los Angeles area. For example, summed concentrations of DDT and related compounds in the livers of the White Point fish (100 000 ng/g; Table I) were about 70 times higher than those in the livers of the Dana Point fish. Relatively high concentrations of these compounds were also found in the livers of fish from the Queensway Bay, Cerritos Channel, and Reservation Point sites. In San Pedro Bay, the summed concentrations of PCBs in livers were 6 and 25 times higher for Reservation Point and Cerritos Channel fish, respectively, compared to livers from the Dana Point fish (Table I).

In addition, the analyses of bile (Table II) revealed large differences in concentrations of metabolites of aromatic compounds in fish from the Los Angeles area (except those from the Hyperion site) compared to fish from Dana Point, regardless of whether the values were obtained at BaP or naphthalene (NPH) wavelengths. The values obtained at BaP and NPH wavelengths primarily represent metabolites of polynuclear AHs, characteristic of fossil fuel combustion products, and metabolites of diaromatic hydrocarbons present in the kerosene/gasoline fraction of petroleum, respectively. White croaker from Cerritos Channel had concentrations of bile metabolites fluorescing at BaP wavelengths that were approximately 75 times higher than those obtained from the Dana Point and the Hyperion outfall fish. The pattern of values obtained at NPH wavelengths was similar to that for BaP; the highest concentrations measured at NPH wavelengths were for bile of white croaker from certain sites in San Pedro Bay (e.g., Cerritos Channel and Reservation Point), whereas the lowest values were from the Dana Point and Hyperion fish. The bile metabolite values obtained at BaP wavelengths from the Dana Point and Hyperion fish were comparable to those obtained with English sole from nonurban reference areas in Puget Sound (*6*, *7*, *9*, *10*); however, the NPH values in white croaker were 5–7 times higher.

Liver Lesions in White Croaker. The white croaker subjected to chemical analysis were also examined for histopathological conditions. Of the liver lesions detected, only the most apparently serious conditions are reported here. A more detailed description of the histopathological characterstics of these lesions will be presented elsewhere (*26*). The liver lesions included neoplasms, putatively preneoplastic lesions (i.e., basophilic foci of hepatocellular alteration), megalocytic hepatosis, and hepatocellular nuclear pleomorphism (*5–7*, *19*, *21–23*, *27*, *28*). The types of fish liver neoplasms and the sites from which they were captured are as follows: a cholangiocellular carcinoma in one fish (25 fish examined) from Queensway Bay; a hepatocellular carcinoma in one fish (25 fish examined) from near Reservation Point; a cholangioma in one fish (25 fish examined) from near the Hyperion outfall (Figure 2). A basophilic focus was detected in the liver of another fish from Queensway Bay. Megalocytic hepatosis was detected only in white croaker from Cerritos Channel, at a prevalence of 13% (3 of 23 fish). It is noteworthy that none of the above-mentioned liver lesions were detected in fish from Dana Point (27 fish examined). The prevalence of nuclear pleomorphism in white croaker from Cerritos Channel (26.1%) was significantly higher ($P \leq 0.05$) than that in fish from Dana Point (3.7%) and near Reservation Point (4.0%) as determined by the G test for heterogenecity (*29*).

In other fish (*20*, *30*) and mammalian species (*31*), the probability of developing detectable liver neoplasms, as well as certain other liver lesions, increases with age. Because the presence of white croaker with liver neoplasms at the Los Angeles sites could partially be due to the capture and sampling of older fish rather than the results of exposure to environmental carcinogens, it is important that the age composition of white croakers from reference areas be comparable to that of croaker from urban areas. The approximate mean age of white croaker with liver neoplasms and preneoplasms, estimated from a published growth curve (*14*), was between 5 and 7 years (mean length = 255 ± 30 mm). Only two white croaker with lengths corresponding to this 5–7-year age group were captured at Dana Point (the reference site); however, 32 white croaker in this age group (mean length = 249 ± 18 mm), collected during the same time period in 1984 along the central coast of California (Bodega Bay and San Francisco Bay) as part of NOAA's National Status and Trends Program, did not have detectable liver neoplasms or preneoplastic lesions (*32*).

Discussion

The chemical analyses revealed that sediments from the Los Angeles area contained substantially higher concen-

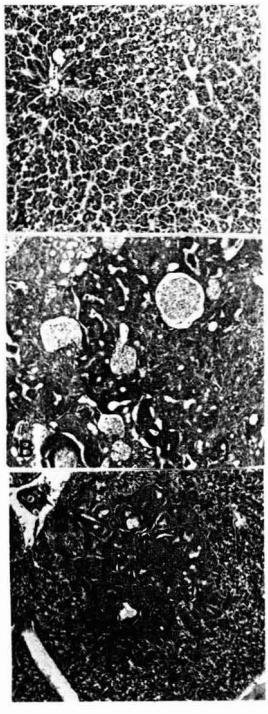

Figure 2. Photomicrographs of livers of white croaker showing representative histopathological conditions. (A) Liver with normal architecture, including hepatocytes arranged in regular cords of a thickness of 1 to 2 cells, with the cords separated by sinusoids. Arrows indicate melanomacrophage centers: 132×, hematoxylin and eosin (H and E). (B) Cholangiocellular carcinoma in the liver of a male white croaker from San Pedro Bay. The biliary cells composing the neoplasm were anaplastic and had a disorganized architecture. The borders of the nodule were irregular, and neoplastic components had clearly invaded the surrounding normal parenchyma: 80×, H and E. (C) Cholangioma in the liver of a female white croaker from the site near the Hyperion 5-mi outfall. The ductular structures in the nodule were composed of moderately well-differentiated biliary epithelium, and the noninvasive margin (arrows) of the nodule was surrounded by normal parenchyma: 80×, H and E.

trations of AHs and CHs compared to sediments from Dana Point. Most striking, however, were the differences in concentrations of AHs and CHs in the biological samples with respect to the Los Angeles area and Dana Point. Differences, for example, in the concentrations of bile metabolites measured at BaP wavelengths for fish from Cerritos Channel and Reservation Point were, as indicated, many times greater than those for Dana Point. These findings provide clear evidence of the high degree to which the white croaker form the Los Angeles area had been exposed to toxic chemicals. Interestingly, the concentrations of aromatic compounds in the bile of fish from Cerritos Channel and Reservation Point were higher than those obtained with English sole from Eagle Harbor in Puget Sound where the sediments were heavily impregnated with creosote AHs (*7*). In Eagle Harbor, the English sole had bile values, determined at BaP wavelengths, of 21 ± 1500 ng/g (*7*).

The observed high degree of uptake of aromatic compounds, such as fossil fuel hydrocarbons, by white croaker from the Los Angeles area and the contamination of food organisms with AHs and CHs have not been reported previously. In this regard it is important to point out that the application of the relatively new technique for bile analysis (*9*, *10*) made it possible to firmly establish the uptake and metabolism of aromatic compounds by white croaker.

Chlorinated hydrocarbons have previously been identified in white croaker from the Los Angeles area. Brown et al. (*4*) reported concentrations of DDT and related compounds similar to our values for livers of white croaker from White Point and Dana Point (178000 and 2800 ng/g, respectively, converted to dry weight by using a multiplier of 5; n = 10 per site). Gossett et al. (*12*) reported the concentrations of DDT and related compounds in muscle of white croaker from White Point and Dana Point to be 38000 and 700 ng/g, respectively. Although studies reported by Young et al. (*33*) and Bascum (*34*) demonstrated that body burdens of DDTs and PCBs increased with trophic level, no prior evidence relating to the important question of contamination of food organisms consumed by white croaker, or the route(s) of uptake of chemicals by this species, was provided.

The liver neoplasms, preneoplasms, and other liver lesions (e.g., megalocytic hepatosis) in white croaker, demonstrated here for the first time, resemble those found in bottom-feeding fish from other polluted coastal areas (*5–7*, *19*, *20*, *27*). Furthermore, the megalocytic hepatosis, as well as the neoplastic and preneoplastic liver lesions in the white croaker, compares morphologically to those identified in laboratory animals exposed to toxic and/or carcinogenic chemicals (*21*, *28*). Overall, the chemical and biological findings suggest a possible relationship between toxic environmental chemicals and the observed liver lesions; however, on the basis of previous data from Puget Sound (*2*, *5–7*, *10*), it was surprising to find relatively low prevalences of neoplastic and preneoplastic liver lesions in the white croaker from the Los Angeles area. Clearly, more work is needed to determine if these differences are species-related and/or are attributable to other factors. In this regard, we do not feel that seasonal variability was a significant factor in the differences observed. For example, there is no reason to believe on the basis of present evidence that tissue concentrations of xenobiotics would vary significantly over a 3-month period. Moreover, for the five sites sampled in a single month (December), substantial differences were found in concentrations of chemical contaminants in sediments and fish, as well as in prevalences of fish diseases.

The benthic invertebrates eaten by the Los Angeles fish had apparently bioconcentrated AHs and CHs present in polluted sediments. That is, the concentrations of chemicals in the food organisms were generally higher than those in the sediment. For example, food organisms of the fish from Cerritos Channel had concentrations of summed AHs, PCB, and DDT-related compounds that were 34, 8 and 58 times those in the sediment, respectively.

The observed contamination of the fish through the consumption of benthic food organisms revealed an important route of exposure to toxic chemicals; however, other routes are possible—both AHs and CHs are known to be bioconcentrated by fish from the sediment (*35*, *36*) and water column (*16*, *37*, *38*). Undoubtedly, the relative impact on the croaker of the various routes of exposure will have to await further studies in the field and laboratory.

Clearly, the complementary use of chemical analytical data on stomach contents, bile, and liver of the white croaker, in conjunction with histopathologic examination of the liver, has provided an important new dimension on the pollution problems of the Los Angeles area that would

not be generally attainable from sediment analyses alone. Moreover, in the broad sense, the findings reported here heighten interest in the extent of contamination of food chain organisms in urban coastal environments and the consequences to higher forms of marine life and to humans.

Acknowledgments

We thank W. D. Gronlund, L. D. Rhodes, L. L. Johnson, O. P. Olson, E. Hawk, D. R. Bunnel, A. J. Friedman, L. K. Moore, D. G. Burrows, R. G. Bogar, J. A. Werner, J. C. Drury, K. L. Tilbury, O. Maynes, D. L. Del Beccaro, C. A. Wigren, and R. W. Pearce for sample collection, processing, and analysis. Appreciation is also given for sample collection to the personnel of the vessels *Nautilus*, *McArthur*, *Marine Surveyor*, and *Sea-S-Dee*; to G. A. Blackledge, N. Morrow, and L. A. Wirick for typing; to J. Peacock and B. S. Kuhne for figures; and to U. Varanasi, M. H. Schiewe, W. MacLeod, Jr., W. T. Roubal, C. A. Krone, and P. A. Robisch for manuscript review.

Registry No. DDT, 50-29-3; *o,p'*-DDE, 3424-82-6; *p,p'*-DDE, 72-55-9; *p,p'*-DDD, 72-54-8; methylnaphthalene, 1321-94-4; phenanthrene, 85-01-8; 1-methylphenanthrene, 832-69-9; anthracene, 120-12-7; fluoranthrene, 206-44-0; pyrene, 129-00-0; benz[*a*]anthracene, 56-55-3; chrysene, 218-01-9; benzo[*e*]pyrene, 192-97-2; benzo[*a*]pyrene, 50-32-8; perylene, 198-55-0; dibenz-[*a,h*]anthracene, 53-70-3; α-chlordane, 5103-71-9; *trans*-nonachlor, 39765-80-5; trichlorobiphenyl, 25323-68-6; tetrachlorobiphenyl, 26914-33-0; pentachlorobiphenyl, 25429-29-2; hexachlorobiphenyl, 26601-64-9; heptachlorobiphenyl, 28655-71-2; octachlorobiphenyl, 55722-26-4; nonachlorobiphenyl, 53742-07-7.

Literature Cited

(1) Kraybill, H. F. *Ann. N.Y. Acad. Sci.* **1977**, *298*, 80–89.
(2) Malins, D. C. *Environ. Sci. Technol.* **1980**, *14*, 32–37.
(3) O'Connor, J. M.; Klotz, J. B.; Kneip, T. J. In *Ecological Stress and the New York Bight: Science and Management*; Mayer, G. F., Ed.; Estuarine Research Foundation: Columbia, SC, 1982; pp 631–653.
(4) Brown, D. A.; Gossett, R. W.; Jenkins, K. D. In *Physiological* Mechanisms *of Marine Pollution Toxicity*; Vernberg, W. B.; Calabrese, A.; Thurberg, F. P.; Vernberg, F. J. Eds.; Academic: New York, 1982; pp 197–213.
(5) Malins, D. C.; McCain, B. B.; Brown, D. W.; Chan, S.-L.; Myers, M. S.; Landahl, J. T.; Prohaska, P. G.; Friedman, A. J.; Rhodes, L. D.; Burrows, D. G.; Gronlund, W. D.; Hodgins, H. O. *Environ. Sci. Technol.* **1984**, *18*, 705–713.
(6) Malins, D. C.; Krahn, M. M.; Brown, D. W.; Rhodes, L. D.; Myers, M. S.; McCain, B. B.; Chan, S.-L. *JNCI, J. Natl., Cancer Inst.* **1985**, *74*, 487–494.
(7) Malins, D. C.; Krahn, M. M.; Rhodes, L. D.; Brown, D. W.; Krone, C. A.; McCain, B. B.; Chan, S.-L. *Carcinogenesis (London)* **1985**, *6*, 1463–1469.
(8) Sherwood, M. J. In *Ecological Stress and the New York Bight: Science and Management*; Mayer, G. F., Ed.; Estuarine Research Federation: Columbia, SC, 1982; pp 359–377.
(9) Krahn, M. M.; Myers, M.S.; Burrows, D. G.; Malins, D. C. *Xenobiotica* **1984**, *14*, 633–646.
(10) Krahn, M. M.; Rhodes, L. D.; Myers, M. S.; Moore, L. K.; MacLeod, W. D., Jr.; Malins, D. C. *Arch. Environ. Contam. Toxicol.* **1986**, *15*, 61–67.
(11) Schafer, H. In *Biennial Report for 1983–1984*; Bascom, W., Ed.; Southern California Coastal Water Research Project: Long Beach, CA, 1984; pp 11–19.
(12) Gosset, R. W.; Puffer, H. W.; Arthur, R. H.; Alfafar, J. F.; Young, D. R. *Mar. Pollut. Bull.* **1983**, *14*, 60–65.
(13) Eganhouse, R.; Kaplan, I. *Environ. Sci. Technol.* **1982**, *16*, 180–186.
(14) Love, M. S.; McGowen, G. E.; Westphal, W.; Lavenberg, R. J.; Martin, L. *Fish. Bull.* **1984**, *82*, 179–198.
(15) MacLeod, W. D., Jr.; Brown, D. W.; Friedman, A. J.; Burrows, D. G.; Maynes, O.; Pearce, R.; Wigren, C. A.; Bogar, R. G. NOAA Technical Memo; U.S. Department of Commerce: Washington, DC, 1985; NMFS F/NWC-92.
(16) Roubal, W. T.; Collier, T. K.; Malins, D. C. *Arch. Environ. Contam. Toxicol.* **1977**, *5*, 513–529.
(17) Varanasi, U.; Gmur, D. J. *Aquatic Toxicol.* **1981**, *1*, 49–67.
(18) Gmur, D. J.; Varanasi, U. *Carcinogenesis (London)* **1982**, *3*, 1397–1403.
(19) Myers, M. S.; Rhodes, L. D.; McCain, B. B. *JNCI, J. Natl. Cancer Inst.* **1987**, *78*, 333–351.
(20) Malins, D. C.; McCain, B. B.; Brown, D. W.; Sparks, A. K.; Hodgins, H. O.; Chan, S.-L. NOAA Technical Memo; U.S. Department of Commerce: Washington, DC, 1982; OMPA-19.
(21) Jones, G.; Butler, W. In *Mouse Hepatic Neoplasia*; Butler, W. H.; Newberne, P. M., Eds.; Elsevier: Amsterdam, 1975; pp 21–60.
(22) Stewart, H. L.; Williams, G.; Keysser, C. H.; Lombard, L. S.; Montoli, R. J. *JNCI, J. Natl. Cancer Inst.* **1980**, *64*, 179–206.
(23) Frith, C. H.; Ward, J. M. *J. Environ. Pathol. Toxicol.* **1980**, *3*, 329–351.
(24) Brown, D. A.; Gossett, R. W.; Hershelman, G. P.; Ward, C. F.; Westcott, A. M.; Cross, J. N. *Mar. Environ. Res.* **1986**, *18*, 291–310.
(25) Young, D. R.; McDermott-Ehrlich, D. J.; Heesen, T. C. *J.—Water Pollut. Control Fed.* **1976**, *48*, 1919–1928.
(26) Myers, M. S.; Johnson, L. L.; Rhodes, L. D.; Olson, O. P.; McCain, B. B., unpublished data.
(27) Murchelano, R. A.; Wolke, R. E. *Science (Washington, D.C.)* **1985**, *228*, 587–589.
(28) Hendricks, J. D.; Meyers, T. R.; Shelton, D. W.; Casteel, J. L.; Bailey, G. S. *JNCI, J. Natl. Cancer Inst.* **1985**, *74*, 839–851.
(29) Zar, J. H. *Biostatistical Analysis*; Prentice-Hall: Englewood Cliffs, NJ, 1974; p 620.
(30) Rhodes, L. D.; Myers, M. S.; Gronlund, W. D.; McCain, B. B. *J. Fish. Biol.*, in press.
(31) Robbins, S. L.; Cotran, R. S.; Kumor, V. *Pathologic Basis of Disease*, 3rd ed.; W. B. Saunders: Philadelphia, PA, 1984; p 1467.
(32) Malins, D. C.; Chan, S.-L.; MacLeod, W. D., Jr.; McCain, B. B.; Clark, R. C., Jr. *Oceans* '86, conference record; The Institute of Electrical and Electronics Engineers: Piscataway, NJ, 1986; pp 566–571.
(33) Young, D. R.; Mearns, A. J.; Jan, T.-K.; Hessen, T. C.; Moore, M. D.; Eganhouse, R. P.; Hershelman, G. P.; Gossett, R. W. *Calif. Coop. Oceanic Fish. Invest.* **1980**, *21*, 197–206.
(34) Bascom, W. *Environ. Sci. Technol.* **1982**, *16*, 226A–236A.
(35) Stein, J. E.; Hom, T.; Varanasi, U. *Mar. Environ. Res.* **1984**, *13*, 97–117.
(36) Varanasi, U.; Reichert, W. L.; Stein, J. E.; Brown, D. W.; Sanborn, H. R. *Environ. Sci. Technol.* **1985**, *19*, 836–841.
(37) Jarvinen, A. W.; Hoffman, M. J.; Thorslund, T. W. *J. Fish. Res. Board Can.* **1977**, *34*, 2089–2103.
(38) Malins, D. C.; McCain, B. B.; Krahn, M. M.; Myers, M. S.; Stein, J. E.; Roubal, W. T.; Brown, D. W.; Varanasi, U.; Hodgins, H. O.; Chan, S.-L. In *Water Chlorination: Chemistry, Environmental Impact and Health Effects*; Jolley, R. L.; Bull, R.; Davis, W.; Katz, S.; Roberts, M., Jr.; Jacobs, V., Eds.; Louis: Chelsea, MI, 1985; pp 399–414.

Received for review June 16, 1986. Revised manuscript received December 8, 1986. Accepted March 20, 1987. Portions of this study were sponsored by the California Water Resources Control Board. Support for the collection and analysis of fish and sediment samples from Dana Point was also provided by the Ocean Assessments Division, National Ocean Services, National Oceanic and Atmospheric Administration (NOAA), as part of the NOAA National Status and Trends Program.

Environ. Sci. Technol. 1987, 21, 771–777

Movement and Neutralization of Alkaline Leachate at Coal Ash Disposal Sites

Masahiro Sakata

Central Research Institute of Electric Power Industry (CRIEPI), 1-6-1 Otemachi, Chiyoda-ku, Tokyo 100, Japan

■ Chemical analyses have been carried out on core samples of coal ash and soil taken from two coal ash disposal sites in Japan. The results showed that alkaline leachate containing relatively high amounts of Ca^{2+} and SO_4^{2-} moves downward through the coal ash and the underlying soil layers and that calcium carbonate with low solubility is secondarily formed in the coal ash layer. The pH of the underlying soil layer ranged from 5.7 to 8.1. It was observed that the coal ash leachate is neutralized mostly near the coal ash–soil interface, primarily due to ion exchange of H^+ and Al^{3+} with Ca^{2+} in the leachate.

Introduction

The high ash content of coal is one of the inherent disadvantages in coal-fired power generation. Approximately 3.8×10^6 tons of coal ash was produced by electric utilities in Japan in 1984, and 42% of the coal ash was beneficially used for cement and concrete products, road construction, etc. (*1*). The balance (58%) was disposed of by landfill in coastal or inland areas. The establishment of ash disposal facilities is important for new coal-fired power plants.

Fly ash from coal-fired power plants occasionally produces highly alkaline leachate containing relatively high levels of trace elements such as chromium, arsenic, boron, and molybdenum (*2–6*). Thus, the expanding use of coal for petroleum in power generation may lead to the increase in environmental problems related to coal ash disposal. To clarify potential surface water and groundwater pollution caused by coal ash disposal, it is necessary to study the interaction of the coal ash leachate with soils.

In general, it is expected that the alkaline leachate from coal ash will be neutralized through interaction with the acidic soils that are common in Japan. In order to obtain data on movement and neutralization of alkaline leachate at actual coal ash disposal sites, core samples of coal ash and soil were taken from two sites in Japan. Chemical analyses were performed on these samples.

Experimental Section

Site Description. Schematic illustrations of coal ash disposal sites studied are shown in Figure 1. The disposal sites are located in inland areas of Japan. The disposal periods were 1964–1973 at site A and 1978 at site B. The areas of disposal sites A and B are 12.6 and about 2 ha, respectively. Both power plants A and B utilize low-sulfur (about 0.5%), high-ash (about 35%) domestic coal, and there are no significant differences in coal firing methods between the two power plants. More than 80% of the coal ash produced is collected by electrostatic precipitators and cyclone collectors of power plant A and by electrostatic precipitators of power plant B.

Sampling. Cores containing coal ash and soil (core diameter, 86 mm) were taken by boring at one station in each disposal site during July 1984. The thickness of the coal ash layer and the unsaturated soil layer at the sampling station of disposal site A was 11.6 and 2.1 m, respectively. At the sampling station of disposal site B, the thickness was 3.5 and >3.6 m, respectively (the groundwater level was not reached at this site). Each core was immediately cut into 10- or 20-cm sections. Fly ash samples were obtained from one of the hoppers of the electrostatic precipitator of each power plant.

Analytical Procedures. Coal ash and soil samples were air-dried at room temperature. Particle size distribution of soil sieved to a <2-mm fraction was determined by the hydrometric method (*7*). Chemical analyses of coal ash and soil were carried out upon the fraction that passed through a 0.4-mm sieve to remove coarse particles. The levels of chemical constituents, except for pH, were normalized to dry-sample weight. The analytical procedures are described below. The bulk mineralogy of the selected coal ash and soil samples was also examined by X-ray powder diffraction measurement, with a Rigaku Denki diffractometer (Model RV-200) with copper Kα radiation at 50 kV and 200 mA.

Major Elements in Coal Ash. Coal ash samples were dissolved by fusion with Na_2CO_3 for the determination of Si, Al, Fe, Ca, and Mg and with $CaCO_3$ for the determination of K and Na. Then, the solution obtained after decomposition was analyzed for Si by gravimetry and for Al, Fe, Ca, Mg, K, and Na by atomic absorption spectrometry. Total carbon contents were measured with a CHN analyzer (Yanagimoto Model MT-2).

pH of Coal Ash and Soil. Coal ash or soil sample was mixed with distilled water at 1:2.5 weight ratio for 24 h at room temperature. Then, the pH in the supernatant was determined with a glass electrode pH meter.

Water-Soluble Constituents in Coal Ash and Soil. A total of 10 g of coal ash or soil sample was extracted with 25 mL of distilled water for 2 h at room temperature. The procedure was repeated 3 times. Then, the combined solution was analyzed for Ca, Mg, K, and Na by atomic absorption spectrometry and for SO_4 S by ion chromatography. Prolonging the extraction time may decrease the amounts of Ca, Mg, and SO_4 extracted from coal ash, due to precipitation and/or adsorption on ash particles (*6*). No significant amounts of the water-soluble Ca, Mg, K, Na, and SO_4 were released from coal ash or soil after the third 2-h extraction. Therefore, three successive 2-h extractions were selected somewhat arbitrarily to leach chemical constituents in the water-soluble fraction of coal ash and soil. The water-soluble constituents in coal ash may be representative of those leached from coal ash with infiltration of rainwater and snowmelt water.

Carbonate Carbon in Coal Ash and Soil. Carbonate carbon in coal ash or soil was determined by digesting the sample with 1 M CH_3COOH solution while bubbling N_2 gas, passing the evolved CO_2 into a 0.02 M $Ba(OH)_2$ solution, and then titrating the remaining $Ba(OH)_2$ with standard 0.1 M HCl solution (*8*).

Cation-Exchange Capacity and Exchangeable Cations in Soil. A total of 2–5 g of soil sample was treated with 100 mL of neutral 1 M CH_3COONH_4 solution (*9*) for 24 h at room temperature. Then, Ca, Mg, K, and Na in the solution were determined by atomic absorption spectrometry. The exchangeable Ca^{2+}, Mg^{2+}, K^+, and Na^+ contents of the soil were calculated by subtracting the water-soluble fraction from the amounts leached by this treatment. The exchangeable H^+ and Al^{3+} contents (exchange acidity) of the soil were calculated from the difference between the sum of the exchangeable Ca^{2+}, Mg^{2+},

0013-936X/87/0921-0771$01.50/0

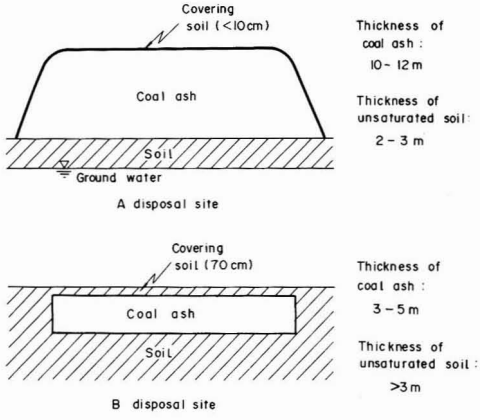

Figure 1. Schematic presentation of coal ash disposal sites.

Table I. Bulk Composition Data for Weathered Coal Ashes from Disposal Sites and for Fresh Fly Ashes (as mg/g)

element	disposal site A		disposal site B		fresh ash	
	mean	range	mean	range	power plant A	power plant B
Si	271	262–276	268	259–279	275	273
Al	121	108–129	131	120–139	114	130
Fe	33.0	29.8–39.0	27.2	22.7–34.2	39.9	28.4
Ca	16.7	14.0–18.0	22.4	20.2–23.9	22.3	19.2
Mg	11.0	9.7–13.3	9.6	8.5–10.3	12.1	10.2
K	22.2	20.4–24.6	20.8	19.2–23.5	16.9	19.2
Na	7.7	7.1–8.5	5.6	4.7–6.5	8.1	6.8
C	21.9	8.9–31.1	14.0	9.6–19.2	20.7	10.9

K^+, and Na^+ contents and the cation-exchange capacity (CEC) determined by the method of Peech et al. (*9*), because the contents of other exchangeable bases such as NH_4^+ and Ba^{2+} were negligibly small (<0.1 mequiv/100 g). In most acidic soils, exchangeable H^+ and Al^{3+} contribute to soil acidity (*10*), although their contents in the soils studied were not determined directly.

Organic Carbon in Soil. Organic carbon in soil was determined with a CHN analyzer (Yanagimoto Model MT-2) after the residue had been treated with 0.5 M HCl solution to remove carbonates.

Dithionite-Extractable Iron in Soil. A total of 0.5 g of soil sample was extracted with 25 mL of solution containing 0.5 g of sodium dithionite and 5 g of sodium citrate (*11*) for 24 h at room temperature, and iron in this solution was measured by atomic absorption spectrometry. The dithionite-extractable iron is regarded as being derived chiefly from iron oxide and hydroxide in soil.

Results and Discussion

Chemical Constituents of Coal Ash. Table I summarizes the bulk composition data (Si, Al, Fe, Ca, Mg, K, Na, and C) for weathered coal ashes from the disposal sites and also for fresh fly ashes. There was no significant difference at the 95% confidence level in the average contents of major elements except for Ca and Na in the weathered ashes between the two disposal sites. The contents of major elements, other than C, were almost constant with depth in the coal ash layers at disposal sites A and B. The bulk composition of the fresh ashes from power plants A and B is similar to that of the weathered ashes from disposal sites A and B, respectively.

Figure 2 shows the vertical distribution of pH and water-soluble Ca, Mg, K, Na, and SO_4 S amounts in the

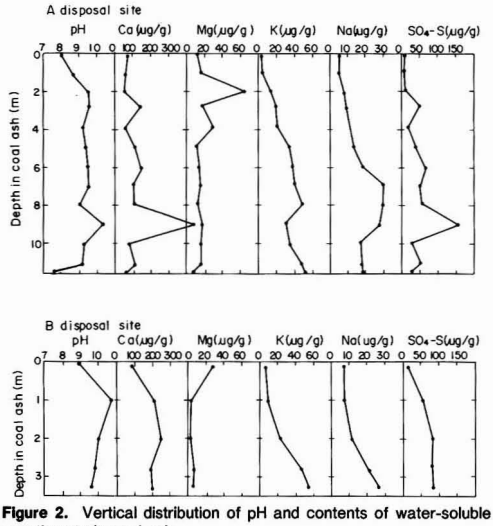

Figure 2. Vertical distribution of pH and contents of water-soluble constituents in coal ash.

Table II. pH and Contents of Water-Soluble Constituents in Fresh Fly Ashes

constituent	power plant A	power plant B
pH	12.5	12.4
Ca, μg/g	1990	2000
Mg, μg/g	0.94	0.77
K, μg/g	37	62
Na, μg/g	79	73
SO_4 S, μg/g	187	452

coal ash. The pH of coal ash was 7.7–10.3 at disposal site A and 8.9–10.7 at disposal site B. Thus, coal ashes from disposal sites A and B produce alkaline extracts. The pH of coal ash is relatively low close to the surface and then in deeper layers reaches a nearly constant value. Relatively high concentrations of Ca and SO_4 S are observed in the water-soluble fraction of coal ash. The amounts of water-soluble Ca, K, Na, and SO_4 S of coal ash increase gradually with increasing depth in the core. This result shows that Ca, K, Na, and SO_4 are leached from the water-soluble fraction and then migrate to the deeper layer through infiltration of water. Vertical distribution of water-soluble Mg in the coal ash layer is quite different from that of other constituents, and its content is low in coal ash with pH >9.5. It is likely that the water-soluble Mg content of coal ash is controlled by carbonate and hydroxide solid phases, as described by Talbot et al. (*12*).

There is a high positive correlation between water-soluble Ca and SO_4 S contents, which is represented by a straight line passing close to the origin with a slope of 2.4 (Figure 3). Thus, the Ca/SO_4 S weight ratios in the water-soluble fraction of coal ash samples exceed the value of 1.25 corresponding to gypsum or anhydrite, which is the dominant sulfate species in most coal ashes (*13*, *14*) (Figure 3). It was seen from the anion concentrations in the water extract of coal ash under CO_2-free conditions (*15*) that the percentages of HCO_3^- and CO_3^{2-} equivalents in the total anion (OH^-, SO_4^{2-}, HCO_3^-, CO_3^{2-}, and Cl^-) equivalents are 57–81% for disposal site A and 39–75% for disposal site B. This suggests that the significant part of water-soluble Ca in coal ashes taken from disposal sites A and B was dissolved as carbonate.

Table II gives the pH and water-soluble Ca, Mg, K, Na,

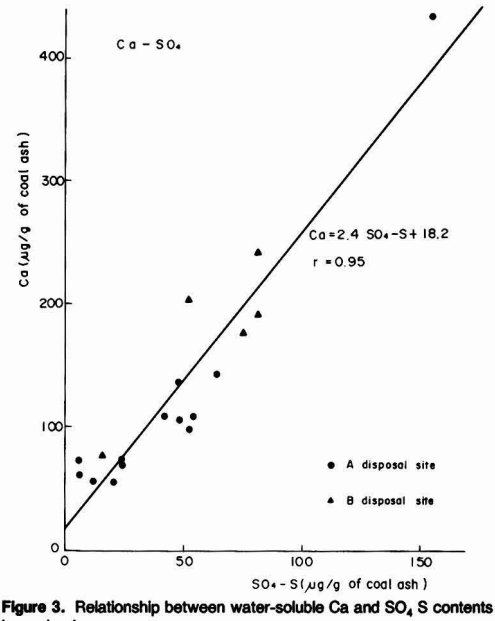

Figure 3. Relationship between water-soluble Ca and SO_4 S contents in coal ash.

Table III. Extractability (%) of Ca, Mg, K, and Na from Weathered Coal Ashes in Disposal Sites and from Fresh Fly Ashes

element	weathered ash		fresh ash	
	mean	range	power plant A	power plant B
Ca	0.63	0.30–1.20	8.9	10.4
Mg	0.15	0.009–0.48	0.008	0.008
K	0.11	0.01–0.25	0.22	0.32
Na	0.21	0.07–0.40	0.98	1.07

and SO_4 S amounts in the fresh fly ashes from power plants A and B. Both fresh fly ashes produce extremely alkaline extracts containing a large amount of Ca relative to other constituents. That is similar to the extracts of many fly ashes from coal-fired power plants in Japan. The high alkalinity of extracts from fresh fly ashes is largely attributable to the hydrolysis of calcium oxide. The significantly low amount of water-soluble Mg is probably due to the precipitation of brucite under high alkaline conditions (*12*).

Chemical Reactions of Coal Ash. Table III indicates the extractability of Ca, Mg, K, and Na from weathered coal ashes in disposal sites A and B and from fresh fly ashes (the percentages of the contents of water-soluble constituents for the total contents of ash). The extremely low extractability of Mg from fresh fly ashes is probably caused by the precipitation of brucite under highly alkaline conditions, as described previously. The extractability of Ca from weathered coal ashes after landfilling in disposal sites A and B is 0.3–1.2%, which is significantly lower than that (~10%) from fresh fly ashes before landfilling. Compared to the extractability of Ca, there is a small difference in the extractability of K and Na between weathered coal ashes and fresh ashes. This may be due to the following: (1) a large amount of Ca was leached from coal ash after landfilling and then migrated to the underlying soil layer with infiltrating water; (2) Ca-bearing water-soluble solids in coal ash were transformed to less soluble compounds after landfilling.

It is generally assumed that Ca^{2+} in coal ash leachate migrates vertically and is adsorbed on the underlying soil through ion-exchange reactions, as will be described in the next section. Thus, the amount of Ca migrating to the underlying soil layer is estimated from the vertical distribution of exchangeable Ca^{2+} content in the soil layer, according to Figure 4, although the background level of exchangeable Ca^{2+} was not always constant because of the heterogeneity of soil (Figure 6). The amounts in 40–50- and 10–20-cm layers were used as background levels of exchangeable Ca^{2+} in the soil layers at disposal sites A and B, respectively (Figure 6). The results indicate that the amounts of Ca migrating to the underlying soil layers are 560 g/m^2 in disposal site A and 190 g/m^2 in disposal site B, which are only 0.37% and 0.28% of the total amounts of Ca (A, 150 kg/m^2; B, 68 kg/m^2) in the coal ash layers at disposal sites A and B, respectively. Therefore, the relatively low extractability of Ca from the coal ashes of disposal sites A and B is primarily due to the transformation of Ca-bearing water-soluble solids to less soluble compounds after landfilling.

The coal ashes at sites A and B contained carbonates. The carbonate C content of coal ash ranges from 0.44 to 1.66 mg/g. On the other hand, the carbonate C content of fresh ashes from power plants A and B is less than 0.03 mg/g. The extremely high pH of extracts from fresh ashes is largely attributable to hydrolysis of calcium oxide, as assumed earlier. A portion of the calcium oxide upon contact with water is later converted to less soluble calcium carbonate by carbon dioxide from ambient air and/or soil environment. Thus, calcium carbonate is secondarily formed in coal ash after landfilling. In fact, calcitic calcium carbonate was identified in the ash samples by X-ray diffraction. Assuming that all of the carbonates in the coal ashes from disposal sites A and B are in the form of calcium carbonate ($CaCO_3$), the Ca content of carbonate is estimated to be 1.5–5.5 mg/g, which corresponds to 10–25% of the total Ca content in the coal ashes. The formation of calcium carbonate in coal ash after landfilling is likely to account for the difference in the extractability of Ca between weathered and fresh ashes (Table III).

Movement and Neutralization of Coal Ash Leachate in Soil. Soil texture at disposal site A, based on particle size measurements, varied with increasing depth in soil from clay loam or silty clay loam to loamy sand. On the other hand, soil texture at disposal site B was predominantly clay loam or clay, independent of depth in soil. The organic C content of the underlying soil layer was 3.1–10.3 mg/g in disposal site A and 0.3–13.7 mg/g in disposal site B. The soil layer below about 1.2 m depth at disposal site B contained little organic matter (0.3–1.1 mg/g as organic C). Carbonate C content in the underlying soil layers at both disposal sites was less than the detection limit (0.03 mg/g as carbonate C). The bulk mineralogy of the soils was similar in both disposal sites and was dominated by quartz and feldspars. The mineralogy of the clay fraction (<2 μm) was not determined by X-ray diffraction analysis.

Figure 5 shows the vertical distribution of pH and the contents of water-soluble constituents (Ca, Mg, K, Na, and SO_4 S) in the underlying soil layer. Figure 6 shows the vertical distribution of cation-exchange capacity (CEC) and exchangeable cations (Ca^{2+}, Mg^{2+}, K^+, Na^+, and H^+ and Al^{3+}) in the soil layer. The percentages of exchangeable cation contents in CEC are also included in Figure 6.

The water-soluble SO_4 S content in the underlying soil in disposal site B decreased with depth (Figure 5), clearly

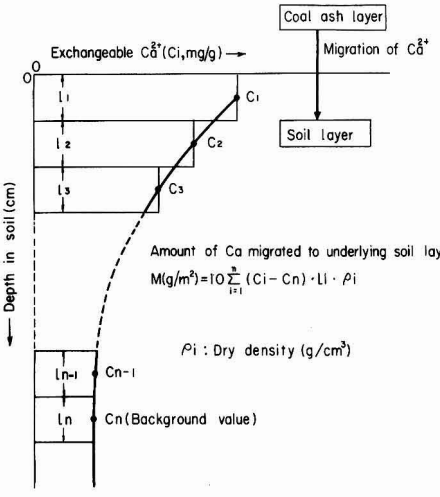

Figure 4. Schematic presentation of vertical distribution of exchangeable Ca^{2+} content in soil.

showing that coal ash leachate containing high concentrations of SO_4^{2-} has moved vertically through the soil layer. It is generally assumed that new water infiltrating from the coal ash layer simply pushes old water downward in the unsaturated soil layer without mixing and dispersion (*16, 17*). Therefore, the average velocity at which SO_4^{2-} moves through soil can be estimated from the depth (130 cm) to which SO_4^{2-} from the coal ash leachate has reached (Figure 5) in the time (6 yr) since the start of landfilling. The estimated velocity at disposal site B was 20 cm/yr. The soils from disposal site B contain 3.1–16.4 mg/g of dithionite-extractable Fe, which is regarded as being derived chiefly from iron oxide and hydroxide (*11*). The soils may have adsorbed SO_4^{2-} to some extent during the infiltration of coal ash leachate, because iron oxide and hydroxide are considered to be active SO_4^{2-} adsorbents (*18, 19*). This suggests that the average infiltration velocity of coal ash leachate through soil at disposal site B was somewhat more than 20 cm/yr.

The vertical distribution of water-soluble SO_4 S at disposal site A was quite different from that at disposal site B. Slightly higher levels were observed in the deeper soil layer (Figure 5). This vertical distribution probably re-

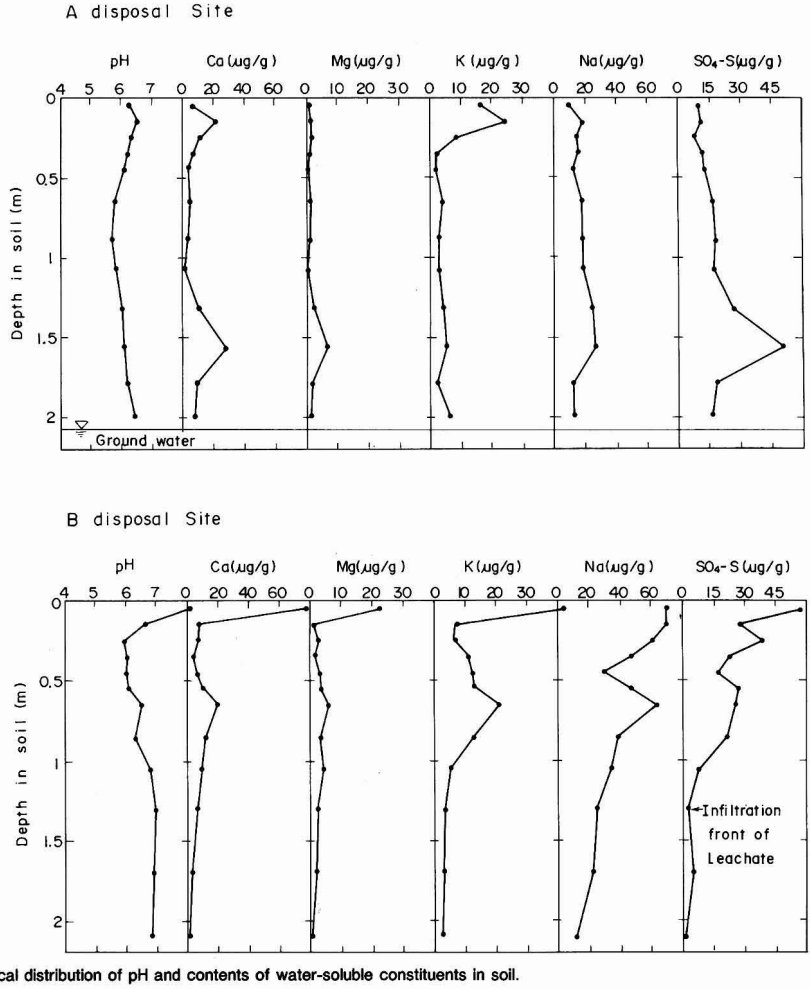

Figure 5. Vertical distribution of pH and contents of water-soluble constituents in soil.

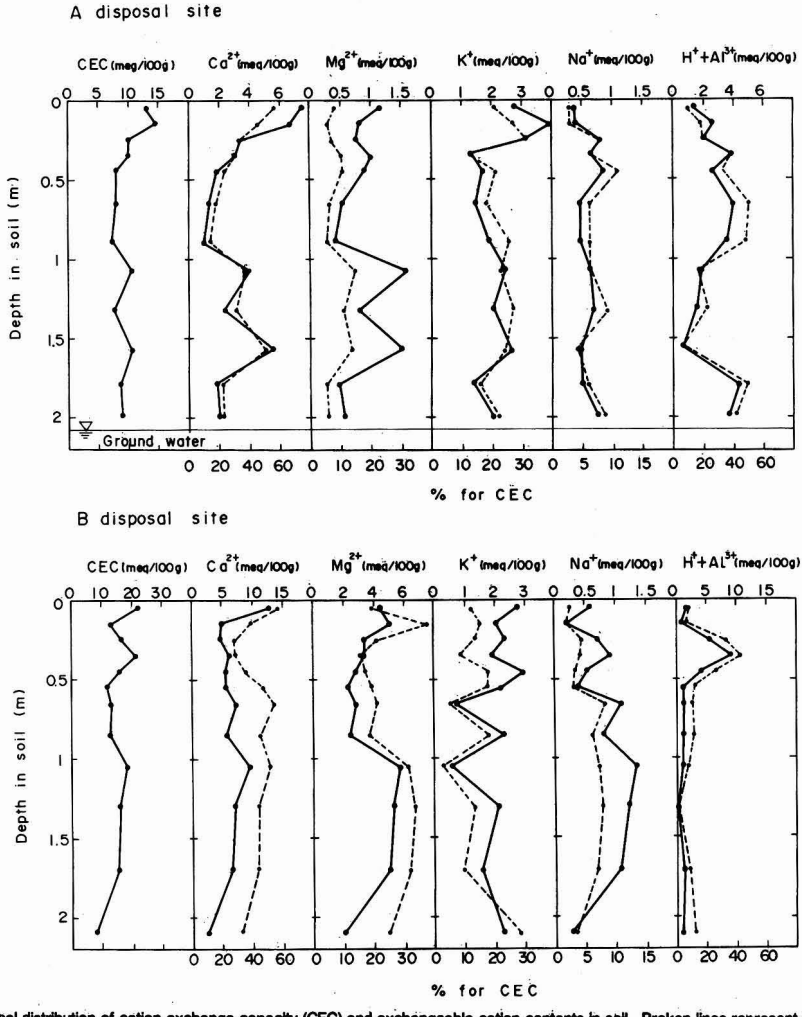

Figure 6. Vertical distribution of cation-exchange capacity (CEC) and exchangeable cation contents in soil. Broken lines represent the percentages of exchangeable cation contents for CEC.

flects the rapid dissolution of sulfates in coal ash during early stages of leaching, as described by Dudas (*20*). The infiltration front of coal ash leachate may have already descended to the groundwater level because of the lapse of 20 yr since landfilling.

The water-soluble Ca content in the soil layer at disposal site B rapidly decreased with depth to a background level. The vertical distribution of water-soluble Ca is quite different from that of water-soluble SO_4 S (Figure 5). The relationship between water-soluble Ca and SO_4 S contents of coal ash samples is represented by a straight line passing close to the origin with a slope of 2.4 (Figure 3). However, as shown in Figure 7, the Ca/SO_4 S weight ratios in the water-soluble fraction of soil samples were mostly less than unity. These results show that Ca^{2+} in the coal ash leachate was adsorbed on the underlying soil layer through ion exchange. The exchangeable Ca^{2+} content and also its percentage for CEC in the soil layer are higher near the coal ash–soil interface and decreased with depth in the upper soil layer (Figure 6). This vertical distribution of exchangeable Ca^{2+} is attributed to the adsorption of Ca^{2+} in the coal ash leachate on the underlying soil layer. In contrast to the exchangeable Ca^{2+} content, the exchangeable H^+ and Al^{3+} contents (exchange acidity) and also their percentages for CEC of the soil layer in the coal ash disposal sites studied were relatively low near the coal ash–soil interface and increased with depth in the upper soil layer, although the background values are not always certain due to the heterogeneity of the soil (Figure 6). This shows that H^+ and Al^{3+} were desorbed from the soil layer through ion exchange during the infiltration of the coal ash leachate. Therefore, the vertical distribution of exchangeable Ca^{2+}, H^+, and Al^{3+} in the soil layer indicates that the neutralization of alkaline coal ash leachate is primarily due to the exchange of H^+ and Al^{3+} for Ca^{2+} in coal ash leachate, i.e.

$$2H^+\text{–soil} + Ca^{2+} + 2OH^- \rightleftharpoons Ca^{2+}\text{–soil} + 2H_2O$$

$$^2/_3Al^{3+}\text{–soil} + Ca^{2+} + 2OH^- \rightleftharpoons Ca^{2+}\text{–soil} + {}^2/_3Al(OH)_3$$

The pH of the underlying soil layer ranges from 5.7 to 8.1, and the pH in the upper layer (0–20 cm) at disposal site B rapidly decreased with depth from 8.1 to 6.6 (Figure 5).

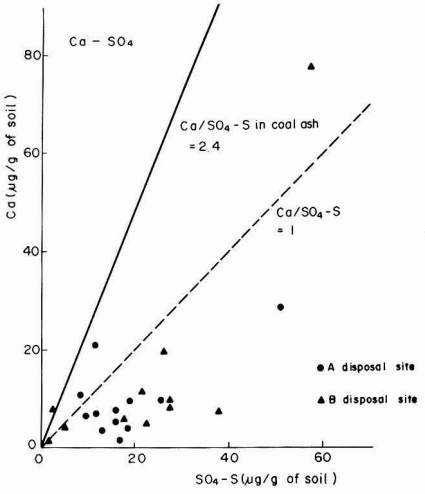

Figure 7. Relationship between water-soluble Ca and SO_4 S contents in soil.

These results show that the neutralization of coal ash leachate occurs mainly near the coal ash–soil interface. Thus, no effect of coal ash leachate on pH of groundwater was observed at disposal sites A and B.

The exchangeable Mg^{2+}, K^+, and Na^+ contents of the soil layer show unsystematic vertical profiles, which were probably due to the heterogeneity of the soil (Figure 6). It is likely, however, that Mg^{2+} and K^+ in the coal ash leachate were adsorbed on the underlying soil layer through ion exchange, because the water-soluble Mg and K contents in the soil layer at disposal site B rapidly decreased with depth to a background value (Figure 5). On the other hand, the water-soluble Na content in the coal ash layer is smaller than the water-soluble Ca, K, and SO_4 S contents (Figure 2), although the water-soluble fraction of the underlying soil layer contains relatively high levels of Na (Figure 5). In addition, the vertical profile of water-soluble Na in the soil layer was similar to that of water-soluble SO_4 S (Figure 5). These results suggest that there was little adsorption of Na^+ in the underlying soil layer through ion exchange during the infiltration of coal ash leachate.

Conclusions

In order to clarify movement and neutralization of alkaline leachate at coal ash disposal sites, core samples of coal ash and soil were taken from two sites (disposal sites A and B). Chemical analyses have been performed on these samples. The major results from this study are as follows:

(1) The vertical distribution of pH and the contents of water-soluble constituents (Ca, Mg, K, Na, and SO_4 S) showed that the coal ashes from disposal sites A and B produce alkaline leachates containing relatively high amounts of Ca^{2+} and SO_4^{2-}, which move downward with infiltrating water.

(2) The extractability of Ca from weathered coal ashes after landfilling in the disposal sites (the percentage of the water-soluble Ca content for the total Ca content of ash) was 0.3–1.2%, which was significantly less than that ($\sim$ 10%) from fresh fly ashes before landfilling. This difference is primarily due to the transformation of water-soluble calcium oxide to less soluble calcium carbonate by carbon dioxide from the ambient air and/or the soil environment.

(3) It was clearly observed that coal ash leachate moves downward through the soil layer. The average infiltration velocity of coal ash leachate through soil at disposal site B was estimated to be somewhat more than 20 cm/yr on the basis of the vertical distribution of water-soluble SO_4 S.

(4) The pH of the underlying soil layer ranged from 5.7 to 8.1. The vertical distribution of pH and exchangeable Ca^{2+}, H^+, and Al^{3+} in the soil layer showed that the neutralization of alkaline coal ash leachate is primarily due to the exchange of H^+ and Al^{3+} for Ca^{2+} in coal ash leachate and that the neutralization occurs mainly near the coal ash–soil interface.

Acknowledgments

I thank Y. Kitano of Sugiyama Jogakuen University and Y. Ishihara and R. K. Kawaratani of CRIEPI for critically reading the manuscript and for various suggestions. I am indebted to the late T. Yatabe and T. Seki, T. Yokoyama, and K. Sato of CRIEPI for their assistance and advice in this study.

Registry No. Si, 7440-21-3; Al, 7429-90-5; Fe, 7439-89-6; Ca, 7440-70-2; Mg, 7439-95-4; K, 7440-09-7; Na, 7440-23-5; C, 7440-44-0.

Literature Cited

(1) Igarashi, K. *J. Jpn. Electr. Assoc.* **1986**, *No. 751*, 25–31 (in Japanese).
(2) Chu, T.-Y. J.; Ruane, R. J.; Krenkel, P. A. *J.—Water Pollut. Control Fed.* **1978**, *50*, 2494–2508.
(3) Chu, T.-Y. J.; Kim, B. R.; Ruane, R. J. *Behavior of Coal Ash Particles in Water: Trace Metal Leaching and Ash Settling*; U.S. Environmental Protection Agency: Washington, DC, 1980; EPA-600/7-80-067.
(4) Turner, R. R.; Lowry, P.; Levin, M.; Lindberg, S. E.; Tamura, T. *Leachability and Aqueous Speciation of Selected Trace Constituents of Coal Fly Ash*; Electric Power Research Institute: Palo Alto, CA, 1982; EA-2588.
(5) Watanabe, I.; Tanabe, K.; Furuya, K.; Matsushita, H. *Bunseki Kagaku* **1985**, *34*, T45–T50 (in Japanese).
(6) Sato, K. *Leaching Characteristics of Various Elements from Coal Fly Ash*; Central Research Institute of Electric Power Industry: Tokyo, Japan, 1986; No. ET86001.
(7) *Method of Grain-Size Analysis of Soils*; Japan Standard Association: Tokyo, Japan, 1978; JIS A 1204 (in Japanese).
(8) Koyama, T.; Handa, N.; Sugimura, Y. *Analyses of Lake and Sea Waters*; Kodan-sha: Tokyo, Japan, 1972 (in Japanese).
(9) Peech, M.; Cowan, R. L.; Baker, J. H. *Soil Sci. Soc. Am. Proc.* **1962**, *26*, 37–40.
(10) Bolt, G. H.; Bruggenwer, M. G. M. *Soil Chemistry A. Basic Elements*; Elsevier: Amsterdam, 1978.
(11) Holmgren, G. G. S. *Soil Sci. Soc. Am. Proc.* **1967**, *31*, 210–211.
(12) Talbot, R. W.; Anderson, M. A.; Andren, A. W. *Environ. Sci. Technol.* **1978**, *12*, 1056–1062.
(13) Henry, W. M.; Knapp, K. T. *Environ. Sci. Technol.* **1980**, *14*, 450–456.
(14) Kaufherr, N.; Shenasa, M.; Lichtman, D. *Environ. Sci. Technol.* **1985**, *19*, 609–614.
(15) Sakata, M. *Neutralization of Coal Ash Leachate by Soil: Analytical Results for Boring Core Samples from Coal Ash Disposal Sites*; Central Research Institute of Electric Power Industry: Tokyo, Japan, 1985; No. 285906 (in Japanese).

(16) Zimmermann, U.; Munnich, K. O.; Roether, W.; Kreutz, W.; Schubach, K.; Siegel, O. *Science (Washington, D.C.)* **1966**, *152*, 346–347.
(17) Schmalz, B. L.; Polzer, W. L. *Soil Sci.* **1969**, *108*, 43–47.
(18) Harward, H. E.; Reisenauer, H. M. *Soil Sci.* **1966**, *101*, 326–335.
(19) Aylmore, L. A. G.; Karim, M.; Quirk, J. P. *Soil Sci.* **1967**, *103*, 10–15.
(20) Dudas, M. J. *Environ. Sci. Technol.* **1981**, *15*, 840–843.

Received for review February 20, 1986. Revised manuscript received September 8, 1986. Accepted April 7, 1987.

Aqueous Ozonolysis Products of Methyl- and Dimethylnaphthalenes

Michael D. Gaul,* Gregor A. Junk, and Harry J. Svec

Ames Laboratory, Iowa State University, Ames, Iowa 50011

■ The ozonolyses of 1- and 2-methylnaphthalene and 1,2-, 1,3-, 1,4-, and 2,3-dimethylnaphthalene were performed in dilute aqueous solution, and the resulting nonperoxidic products were extracted, concentrated, and identified. Identification of the ozonolysis products was confirmed by comparison of retention indexes and mass and infrared spectroscopy data with those from authentic samples when possible. The compound identifications were facilitated by comparisons with products from parallel ozonolysis reactions performed in *n*-hexane and methanol at higher concentrations. The aqueous ozonolysis of 1-methylnaphthalene yielded four major products: 2-acetylbenzaldehyde due to the cleavage of two double bonds and (*E*)- and (*Z*)-3-(2-acetylphenyl)-2-butenal and (*Z*)-3-(2-acetylphenyl)propenal due to the cleavage of a single double bond. The products resulting from the ozonolysis of 2-methylnaphthalene and the isomeric dimethylnaphthalenes were analogous to those formed for 1-methylnaphthalene.

Introduction

Current methods of water treatment using chlorination are known to produce chlorinated hydrocarbons from dissolved humic and fulvic acids and other trace organic compounds (*1–3*). Virtually all of these chlorinated hydrocarbons tend to persist in the environment and bioaccumulate, and many have been shown to be toxic or oncogenic. The production of chlorinated hydrocarbons is one of many problems caused by chlorination that has increased the popularity of ozonation as an alternative for water treatment.

The question of ozonation byproducts is only just beginning to be addressed. There have been a few reports involving the ozonation of natural and waste water (*4–8*) where elevated concentrations of hydroxy aromatic compounds, alkyl phthalates, aliphatic aldehydes and acids, alkanes, and aromatic hydrocarbons were found in waste water. One problem with these reports is that the precursors to many of the compounds produced were unknown. A simpler approach than studying the complex mixtures in ozone-treated natural or waste water is to characterize incomplete ozonation products from model compounds such as aliphatic alcohols, ketones, acids (*9, 10*), amino acids, sugars (*11*), and, perhaps most importantly, benzene derivatives (*12–17*) and polynuclear aromatic hydrocarbons (*18–26*).

Increased interest in the benzene derivatives is due to the fact that many, such as phenols, are toxic and known to be present in industrial wastes or to be produced under certain conditions with ozone. Interest in the polynuclear aromatic hydrocarbons (PAHs) has been generated because of the toxicity and carcinogenicity of these compounds and the possibility that ozone might promote the formation of epoxides. Epoxides of the PAHs, in general, show a tendency to be toxic and carcinogenic (*27*). The reaction of the simplest PAH naphthalene with ozone in water has been reported (*22–26*), but only three of these reports had any specific information about the mechanism or products produced. There have been no studies involving the aqueous ozonation of the methyl- and dimethylnaphthalenes despite the fact that these compounds are known contaminants of potable water supplies at trace levels (*28*) and they are principal constituents of crude oils and oil products (*29*) that regularly contaminate our water systems. Naphthalene and its methyl derivatives are also generally more soluble in water than the higher molecular weight fused-ring aromatic compounds, and consequently, their partial ozonation products are of greater concern.

The mechanism shown in Figure 1 is general for the ozonolyses of naphthalene derivatives in "participating" or nucleophilic solvents, although it is written specifically for the reaction in methanol, the solvent most frequently chosen for mechanistic studies. Ozone has electrophilic character and, therefore, normally adds to the most electron-rich ring of a substituted naphthalene, i.e., the methylated ring for the methyl- and dimethylnaphthalenes. Ozone adds to the double bond via a 1,3 dipolar cycloaddition to form the unstable 1,2,3-trioxalane ring system, which rearranges to form an aldehyde or ketone and the carbonyl oxide. The zwitterionic carbonyl oxide is very reactive, and therefore, in participating solvents, such as methanol or water, the zwitterion reacts with the solvent to form a methoxy or hydroxy intermediate. The reaction sequence is then repeated for the second double bond, which generally reacts with ozone much more easily due to the lesser degree of resonance stabilization of this bond. The breaking of the second double bond yields two intermediates, an aromatic methoxy or hydroxy hydroperoxide and a two-carbon aliphatic hydroperoxide. In aqueous solution, the aromatic hydroxy hydroperoxide either decomposes to phthalaldehyde and hydrogen peroxide or cyclizes. The cyclic peroxide is isolatable (*24*) but easily decomposed in the presence of acid and a reducing agent to phthalaldehyde.

This general mechanism appears to be operable for the ozonolysis of the isomeric methyl- and dimethylnaphthalenes in dilute aqueous solution as described in this paper. Efforts were made to simulate the ozonation conditions of natural or waste water treatment, and an emphasis was placed on the qualitative characterizations of the secondary, nonperoxidic reaction products since these would be the compounds most likely to persist after water treatment. The particular isomeric dimethyl-

* Address correspondence to this author at his present address: Dow Corning Corp., Midland, MI 48640.

0013-936X/87/0921-0777$01.50/0

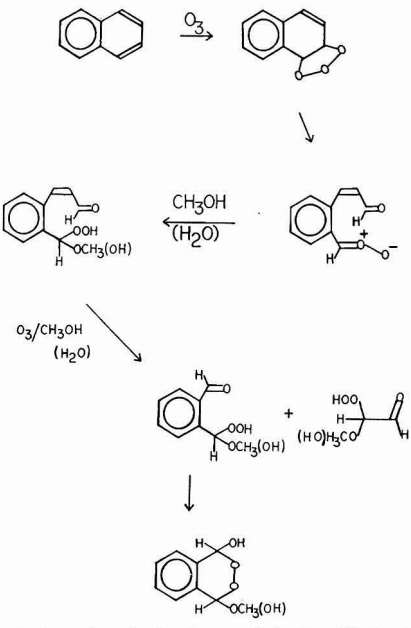

Figure 1. General mechanism for ozonolysis of naphthalene in participating solvents such as methanol and water (*30*).

naphthalenes were chosen for two reasons. The first reason was that the alkyl substitution can have a strong effect on the orientation of the reaction and the products produced when ozone attacks an unsaturated system (*30*, *31*). The second reason was that the methyl groups can act as a structural tag, much as an isotopic label, and this should aid in the mass spectral identification of unusual products.

Background knowledge for the products of the aqueous ozonolyses was obtained by reacting these compounds with ozone in *n*-hexane and methanol at higher concentrations. Capillary gas chromatography (GC) and capillary gas chromatography/mass spectrometry (GC–MS) were used as the primary methods of product characterization.

Experimental Section

Solution Preparation. The methyl- and dimethylnaphthalenes used for the ozonolysis experiments were obtained from commercial sources. 1-Methylnaphthalene, 2-methylnaphthalene, 1,2-dimethylnaphthalene, and 1,3-dimethylnaphthalene were obtained from Aldrich Chemical Co., Milwaukee, WI. 1,4-Dimethylnaphthalene and 2,3-dimethylnaphthalene were supplied by Pfaltz and Bauer, Inc., Stanford, CT. Four of the six compounds were used without further purification; however, 2-methylnaphthalene and 1,4-dimethylnaphthalene were purified by passage through a short column of Florisil before use. Aqueous solutions of 1-methyl- and 2-methylnaphthalene were prepared in 1-L Erlenmeyer flasks by dissolving approximately 18 mg of each in HPLC-grade water, supplied by J. T. Baker Chemical Co., Phillipsburg, NJ. The solutions were stirred for 48 h at 30 °C to dissolve the methylnaphthalenes and then equilibrated at 25 °C before actual concentrations of the methylnaphthalenes were measured.

One-liter aqueous solutions of the dimethylnaphthalenes were prepared in the same manner as the methylnaphthalenes, except only 1.5–2.0 mg of each dimethylnaphthalene was added to solution. The crystalline 2,3-dimethylnaphthalene was an exception. The aqueous solution containing 2,3-dimethylnaphthalene was heated to 95 °C for 2 h with stirring and then held at 50–60 °C overnight in an effort to dissolve the sample. The excess 2,3-dimethylnaphthalene was removed by filtering with a 5 μm porosity sintered glass funnel.

Reaction Conditions. The purity of the oxygen feed gas was 96.6% or greater, and a 4-Å molecular sieve drying tube was used to remove any residual moisture. The ozonater was a Model O3V9-O ozone generator made by Ozone Research and Equipment Corp., Phoenix, AZ. A standard 500-mL gas wash bottle with a 12 mm coarse porosity gas dispersion tube was used as an ozonation vessel. The outlet of gas wash bottle was connected to an all-glass cold trap in early experiments when purging of the starting materials or products was a concern, but in latter experiments this cold trap was omitted. The output of the ozone generator was determined by iodometric titrations as described by Boelter et al. (*32*).

The aqueous ozonations of the methylnaphthalenes were performed with 200 mL of the 1-L stock solutions. The oxygen feed gas flow was 70 mL/min, and the discharge tube pressure and current were 4 psi and 0.4 A, respectively. All reactions were performed at room temperature. The reaction times were adjusted depending on the methylnaphthalene concentration and desired completeness of reaction; generally, the reactions were stopped after reaction of 95% of the starting material. Each reaction solution was flushed for about 10 s with a high flow of nitrogen to remove any residual ozone.

The aqueous ozonations of the dimethylnaphthalenes were performed in the same manner as those of the methylnaphthalenes; only 300 mL of the stock solutions was used for each ozonation.

The ozonations of *n*-hexane and methanol were performed with the same apparatus as the aqueous reactions only at higher concentrations. Approximately 2.6–2.9 mmol of the methyl- and dimethylnaphthalenes was dissolved in 150 mL of either *n*-hexane or methanol, and the solutions were treated with ozone by using 0.8–1.0 L/min oxygen flow, discharge tube pressure of 4 psi, and discharge tube current of 0.7 A. Reactions were performed at room temperature, and reaction time criteria were the same as for the aqueous reactions. The reacted solutions were purged for 1 min with nitrogen to remove residual ozone and then covered and allowed to stand 48–72 h.

Product Isolation. The aqueous ozonation solutions of 1- and 2-methylnaphthalene were acidified with 2.0 mL of 1 M hydrochloric acid and then extracted with methylene chloride. The extracts were then dried over sodium sulfate and concentrated with Kuderna–Danish evaporative concentrators as modified by Junk et al. (*33*). The extracts were then transferred to 5.0-mL volumetric flasks and diluted with methylene chloride and a small amount of diazomethane reagent.

The ozonation solutions of the dimethylnaphthalenes were treated in a similar manner as the solutions from 1- and 2-methylnaphthalene, except that extraction volumes were 75 mL and final solution volumes were adjusted to 1.0 mL.

The ozonation solutions in *n*-hexane and methanol were simply concentrated before analysis. In the case of *n*-hexane, the concentrated solution was derivatized with diazomethane.

The methylene chloride, along with all other organic solvents used in this investigation, was supplied by Burdick and Jackson Laboratories, Inc., Muskegon, MI, and was redistilled before use.

Table I. Products from Ozonolysis of 1-Methylnaphthalene in Water, Methanol, and *n*-Hexane

product	retention index	% M yields in H_2O	% M yields in CH_3OH	% M yields in C_6H_{14}	identification data
phthalic anhydride	1310	–[a]	1	–	GC, GC–MS, GC–FTIR
2-acetylbenzaldehyde	1334	17	6	8	GC–MS, GC–FTIR
methyl 2-formylbenzoate	1354	–	1	–	GC, GC–MS, GC–FTIR
3-methoxyphthalide	1402	–	3	–	GC, GC–MS, GC–FTIR
methyl 2-acetylbenzoate	1414	–	3	46	GC, GC–MS, GC–FTIR
methyl 2-formyl-6-methylbenzoate (or isomer)	1420	–	2	5	GC–MS
methyl 2-formyl-3-methylbenzoate (or isomer)	1466	–	3	11	GC–MS, GC–FTIR
unidentified	1470	–	4[b]	–	GC–MS
unidentified	1479	–	7[b]	–	GC–MS
3-methoxy-4-methylphthalide	1497	–	4	–	GC–MS, GC–FTIR
dimethyl 3-methylphthalate	1542	–	2	–	GC–MS, GC–FTIR
(*Z*)-3-(2-formylphenyl)-2-butenal	1545	16	2	9	GC–MS
methyl (*Z*)-3-(2-formylphenyl)-2-butenoate	1566	–	5	–	GC–MS, GC–FTIR
(*E*)-3-(2-formylphenyl)-2-butenal	1583	5	–	–	GC–MS
methyl (*E*)-3-(2-formylphenyl)-2-butenoate	1616	–	3	–	GC–MS, GC–FTIR
methyl (*Z*)-3-[2-[(methyloxy)carbonyl]phenyl]-2-butenoate	1619	–	3	–	GC–MS, GC–FTIR
(*Z*)-3-(2-acetylphenyl)propenal	1622	11	–	–	GC–MS

[a] Dashes indicate a yield of less than 1% for the listed product. [b] The yield of unidentified products was estimated by assuming that the response factor for this product was equal to that of dimethyl phthalate.

Product Identification. All GC analysis for the ozonolysis products of the methyl- and dimethylnaphthalenes was performed with a Carlo Erba Fractovap 4160 gas chromatograph obtained from Erba Instruments, Inc., Peabody, MD. The capillary separations were made with a fused silica SE-54 capillary, 30 m × 0.25 mm, made by J & W Scientific, Inc., Rancho Cordova, CA. Hydrogen carrier gas, a splitless injection mode, and oven programming of 40–220 °C at 6 deg/min with a 1-min initial hold were used. The chromatographic output for most samples was recorded with a HP3388 integrator obtained from Hewlett-Packard, Avondale, PA. Kovats retention indexes were recorded for all sample components by comparison to a C_8–C_{22} normal hydrocarbon standard (*34*). The quantification of sample components was done with external standards, making corrections for the extraction efficiencies for the water reactions. The extraction efficiencies and response factors were estimated for products for which there were no authentic samples.

Packed-column gas chromatographic analyses were performed with a Perkin-Elmer 3920B gas chromatograph from Perkin-Elmer, Norwalk, CT, by using either a 3% SE-30, a 5% FFAP, or a Tenax column (1 m × 3 mm). These columns were used solely for quantitative analysis of starting materials with naphthalene as an internal standard.

All GC–MS analyses were performed with a Finnigan 4000 equipped with a Model 8600 GC and the Incos 2300 data system, Finnigan Corp., Sunnyvale, CA. The scanning of the mass spectrometer and data collection was controlled by a Data General Model Nova 3 computer with the Incos 2300 software. Electron ionization at 70 eV was used for all samples, and data were collected over the mass range of 45–400 atomic mass units with scan cycle times of 1 s. Chemical ionization spectra were recorded for some samples with isobutane or methane as the reagent gas. Data were collected over a 75–300 mass range, again with a 1-s scan cycle time. The gas chromatographic column used was a fused silica DB-5, with the same temperature programming described earlier and helium carrier gas. The GC and GC–MS retention data were correlated with an easily characterized major component as a reference compound.

Capillary gas chromatography–Fourier transform infrared spectrometry (GC–FTIR) analyses were also performed on selected product mixtures with a Bruker–IBM Model 98 Fourier transform infrared spectrometer obtained from IBM Instruments, Inc., Danbury, CT. The instrument was linked to a Hewlett-Packard 5800 gas chromatograph equipped with a thick film (1.0 μm) fused silica DB-5 capillary column, 30 m × 0.25 mm. The gas chromatographic conditions were the same as those described previously. The scan rate of the instrument was approximately 3.4 scans per second with 8-cm^{-1} resolution. Data were collected over the range of 4000–800 cm^{-1}.

Synthesis of Authentic Standards. An authentic standard of 3-methoxy-3-methylphthalide was synthesized from 2-acetylbenzoic acid by refluxing in HCl-acidified methanol. Some of the properties of 3-methoxy-3-methylphthalide have been reported in the literature (*35*). A mixture of *cis*- and *trans*-1,3-dimethoxyphthalan was made from phthalaldehyde and 3-methoxyphthalide was made from 2-formylbenzoic acid by the same procedure as that described for 3-methoxy-3-methylphthalide.

Results and Discussion

Product Characterization. Tables I–IV list the name, retention index, molar yields, and identification data of the ozonolysis products for each of the methyl- and dimethylnaphthalenes in water, methanol, and *n*-hexane.

All the products characterized from the six aqueous ozonolysis reactions were aldehydes and ketones. No acids were characterized. Determination of the extraction efficiencies of aromatic acid products, such as 2-acetylbenzoic acid and 2-formylbenzoic acid, at 1 ppm concentrations indicated that these products would have been isolated if present. Previous studies (*24–26*) involving the aqueous ozonolyses of naphthalene had shown increased yields of phthalaldehyde in comparison with reactions in organic solvents, but not to the total exclusion of the aromatic acid products. Acidic products would be expected from the oxidation of corresponding aldehydes by peroxides present, particularly hydrogen peroxide formed by elimination from the hydroxy hydroperoxide precursor as shown in Figure 1. Ozone should play a minor role in the formation of acids because it is relatively unreactive toward aldehydes (*30*). Apparently little or no oxidation of the aldehydes occurred, probably because the solutions were 2.5–40 times more dilute than in previous work (*26*) and product residence times in the water were short.

The products resulting from the cleavage of two double bonds in the naphthalene ring system were expected on

Table II. Products from Ozonolysis of 2-Methylnaphthalene in Water, Methanol, and *n*-Hexane

product	retention index	% M yields in H_2O	% M yields in CH_3OH	% M yields in C_6H_{14}	identification data
phthalaldehyde	1238	20	10	12	GC, GC-MS, GC-FTIR
phthalic anhydride	1310	–[a]	–	6	GC, GC-MS, GC-FTIR
(*E*)- and (*Z*)-1,3-dimethoxyphthalan	1318	–	9	–	GC, GC-MS, GC-FTIR
	1321				
methyl 2-formylbenzoate	1354	–	16	14	GC, GC-MS, GC-FTIR
2-formyl-4-methylbenzaldehyde	1360	4	–	–	GC-MS, GC-FTIR
3-methoxyphthalide	1402	–	14	–	GC, GC-MS, GC-FTIR
dimethyl phthalate	1455	–	3	3	GC, GC-MS, GC-FTIR
methyl 2-formyl-5-methylbenzoate (or isomer)	1474	–	5	4	GC-MS, GC-FTIR
methyl 2-formyl-4-methylbenzoate (or isomer)	1479	–	5	4	GC-MS, GC-FTIR
(*Z*)-2-(3-oxo-1-butenyl)benzaldehyde	1517	9	–	–	GC-MS
3-methoxy-6-methylphthalide (or isomer)	1520	–	5	–	GC-MS, GC-FTIR
3-methoxy-5-methylphthalide (or isomer)	1530	–	5	–	GC-MS, GC-FTIR
(*Z*)-3-(2-formylphenyl)-2-methylpropenal	1554	2	–	–	GC-MS
(*E*)-3-(2-formylphenyl)-2-methylpropenal	1569	2	–	–	GC-MS
dimethyl 4-methylphthalate	1574	–	1	–	GC-MS, GC-FTIR
(*Z*)-3-(2-formyl-5-methylphenyl)propenal (or isomer)	1601	2	–	–	GC-MS
(*Z*)-3-(2-formyl-4-methylphenyl)propenal (or isomer)	1612	2	–	–	GC-MS
(*E*)-2-(3-oxo-1-butenyl)benzaldehyde	1621	2	–	–	GC-MS
(*E*)-3-(2-formyl-5-methylphenyl)propenal (or isomer)	1658	2	–	–	GC-MS
(*E*)-3-(2-formyl-4-methylphenyl)propenal (or isomer)	1664	2	–	–	GC-MS

[a] Dashes mean a yield of less than 1% for listed product.

Table III. Products from Ozonolysis of 1,2-Dimethylnaphthalene in Water, Methanol, and *n*-Hexane

product	retention index	% M yields in H_2O	% M yields in CH_3OH	% M yields in C_6H_{14}	identification data
(*E*)- or (*Z*)-1-methyl-1,3-dimethoxyphthalan	1296	–[a]	2	–	GC-MS, GC-FTIR
phthalic anhydride	1310	–	2	2	GC, GC-MS, GC-FTIR
2-acetylbenzaldehyde	1334	65	11	8	GC-MS, GC-FTIR
3-methoxy-3-methylphthalide	1381	–	12	–	GC, GC-MS, GC-FTIR
3-methoxyphthalide	1402	–	7	–	GC, GC-MS, GC-FTIR
methyl 2-acetylbenzoate	1414	–	6	27	GC, GC-MS, GC-FTIR
unidentified	1479	–	9[b]	–	GC-MS
methyl (*Z*)-3-(2-formylphenyl)-2-methyl-2-butenoate	1611	–	2	–	GC-MS
methyl 2-formyl-3,4-dimethylbenzoate (or isomer)	1617	–	–	3	GC-MS
(*Z*)-3-(2-formylphenyl)-2-methyl-2-butenal	1618	32	–	4	GC-MS
3-methoxy-6,7-dimethylphthalide (or isomer)	1647	–	3	–	GC-MS
methyl (*E*)-3-(2-formylphenyl)-2-methyl-2-butenoate	1685	–	6	–	GC-MS
(*Z*)-1-(2-acetylphenyl)-1-buten-3-one	1686	–	–	2	GC-MS

[a] Dashes mean a yield of less than 1% for the listed product. [b] The yield of unidentified products was estimated by assuming that the response factor for this product was equal to that of dimethyl phthalate.

Table IV. Products from Ozonolysis of 1,3-Dimethylnaphthalene in Water, Methanol, and *n*-Hexane

product	retention index	% M yields in H_2O	% M yields in CH_3OH	% M yields in C_6H_{14}	identification data
(*E*)- and (*Z*)-1-methyl-1,3-dimethoxyphthalan	1279	–[a]	8	–	GC-MS, GC-FTIR
	1296	–	11	–	
2-acetylbenzaldehyde	1334	27	12	14	GC-MS, GC-FTIR
3-methoxy-3-methylphthalide	1381	–	4	–	GC, GC-MS, GC-FTIR
3-methoxyphthalide	1402	–	8	–	GC, GC-MS, GC-FTIR
methyl 2-acetylbenzoate	1414	–	7	26	GC, GC-MS, GC-FTIR
(*Z*)-2-(1-methyl-3-oxo-1-butenyl)benzaldehyde	1547	21	3	4	GC-MS
methyl 2-formyl-4,6-dimethylbenzoate (or isomer)	1578	–	–	3	GC-MS
3-methoxy-4,6-dimethylphthalide (or isomer)	1606	–	1	–	GC-MS
dimethyl 3,5-dimethylphthalate	1611	–	1	–	GC-MS
methyl (*Z*)-2-(1-methyl-3-oxo-1-butenyl)benzoate	1616	–	2	–	GC-MS
(*Z*)-3-(2-acetylphenyl)-2-methylpropenal	1637	11	–	–	GC-MS

[a] Dashes mean a yield of less than 1% for the listed product.

the basis of previous literature results. The aromatic products 2-acetylbenzaldehyde and phthalaldehyde from 1- and 2-methylnaphthalene were strong evidence that the normal ozonolysis mechanism described in Figure 1 had occurred. These two aldehydes would have been expected from the decomposition of their respective hydroxy hydroperoxides. As predicted from the mechanism, the normal ozonolysis products for the dimethylnaphthalenes were observed to be 2-acetylbenzaldehyde, phthaldehyde, 2-formyl-4-methylbenzaldehyde, and 1,2-diacetylbenzene, as shown in Tables III–VI.

The predominate products for the aqueous ozonolyses were from the cleavage of only one double bond in the naphthalene ring system. Previous literature (*30*, *36*, *37*)

Table V. Products from Ozonolysis of 1,4-Dimethylnaphthalene in Water, Methanol, and *n*-Hexane

product	retention index	% M yields in H_2O	% M yields in CH_3OH	% M yields in C_6H_{14}	identification data
(*E*)- and (*Z*)-1,3-dimethyl-1,3-dimethoxyphthalan	1328	–[a]	3	–	GC–MS
	1339	–	5	–	
3-methoxy-3-methylphthalide	1381	–	11	–	GC, GC–MS, GC–FTIR
1,2-diacetylbenzene	1399	20	21	25	GC, GC–MS, GC–FTIR
methyl 2-acetylbenzoate	1414	–	4	7	GC, GC–MS, GC–FTIR
methyl 2-formyl-3,6-dimethylbenzoate	1538	–	–	3	GC–MS, GC–FTIR
methyl (*Z*)-3-(2-acetylphenyl)-2-butenoate	1585	–	3	4	GC–MS, GC–FTIR
(*Z*)-3-(2-acetylphenyl)-2-butenal	1598	17	–	6	GC–MS, GC–FTIR
(*E*)-3-(2-acetylphenyl)-2-butenal	1639	2	–	–	GC–MS

[a] Dashes mean a yield of less than 1% for the listed product.

Table VI. Products from Ozonolysis of 2,3-Dimethylnaphthalene in Water, Methanol, and *n*-Hexane

product	retention index	% M yields in H_2O	% M yields in CH_3OH	% M yields in C_6H_{14}	identification data
phthalaldehyde	1238	4	7	27	GC, GC–MS, GC–FTIR
phthalic anhydride	1310	–[a]	–	15	GC, GC–MS, GC–FTIR
(*E*)- and (*Z*)-1,3-dimethoxyphthalan	1318	–	14	–	GC–MS, GC–FTIR
	1321				
methyl 2-formylbenzoate	1354	–	17	27	GC, GC–MS, GC–FTIR
3-methoxyphthalide	1402	–	18	–	GC, GC–MS, GC–FTIR
dimethyl phthalate and methyl 2-formylbenzoate dimethyl acetal	1455	–	20[b]	5[c]	GC, GC–MS, GC–FTIR
(*Z*)-2-(2-methyl-3-oxo-1-butenyl)benzaldehyde	1549	8	–	–	GC–MS
2-formyl-4,5-dimethylbenzaldehyde	1557	–	–	12	GC–MS
methyl 2-formyl-4,5-dimethylbenzoate	1627	–	5	6	GC–MS
(*E*)-2-(2-methyl-3-oxo-1-butenyl)benzaldehyde	1638	1	–	–	GC–MS
3-methoxy-5,6-dimethylphthalide	1680	–	5	–	GC–MS, GC–FTIR
dimethyl 4,5-dimethylphthalate	1720	–	3	–	GC–MS

[a] Dashes mean a yield of less than 1% for the listed product. [b] Total yield of both compounds. [c] Total yield of dimethyl phthalate only.

indicated that these products were usually not isolated after the ozonolyses of naphthalene derivatives in organic solvents because the second double bond, which is olefinic, was expected to be more reactive than the first double bond, which is aromatic. The only exception to this generalization was the reaction of 1- and 2-naphthol (*38*, *39*), where the hydroxy group increased the rate of ozonolysis of the first double bond relative to the second to the extent that reaction rates were competitive. The only other report of monoozonolysis products being characterized was by Kruithof and Heertjes (*25*) for the aqueous ozonolysis of naphthalene, although only very small amounts of the monoozonolysis product were characterized early in the reaction sequence before most of the naphthalene had been consumed.

Some of the specific compounds characterized in this investigation have not been reported in the literature. The structure elucidation of these compounds is based predominantly on interpretation of the EI and CI mass spectra. Supplementary information was obtained from carbonyl infrared absorption frequencies for products formed in *n*-hexane and methanol.

The ozonolysis of 2-methylnaphthalene in water produced all four possible monoozonolysis products resulting from a double-bond cleavage in either the methylated or unmethylated ring. The major product resulted from bond cleavage in the methylated ring, and Figure 2 shows the two structural possibilities with their expected base peak m/z values. The base peak of this product at m/z 131 in the EI spectrum and the pseudo molecular ion in the CI spectrum at m/z 175 clearly indicate that an acetyl radical is lost to form the base peak, and therefore, the upper structure in Figure 2 is the only possible structure. The EI and CI mass spectra for the remaining three products were very similar, and therefore, structural assignments

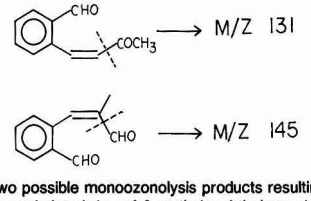

Figure 2. Two possible monoozonolysis products resulting from oxidation of the methylated ring of 2-methylnaphthalene along with the base peak m/z values from each compound's EI mass spectrum.

were made on the basis of minor differences in the GC retention indexes.

The ozonolysis of 1-methylnaphthalene in water could also produce two possible monoozonolysis products resulting from bond cleavage in the methylated ring. Unfortunately, neither the base peak fragmentation nor the CI mass spectra could distinguish between the two possible products; however, evidence gathered from the reaction of 1-methylnaphthalene in methanol indicated that the major product in water was (*Z*)-3-(2-formylphenyl)-2-butenal.

The monoozonolysis product from the aqueous ozonolysis of 1,2-dimethylnaphthalene eluted at a retention index of 1618. The base peak at m/z 159 in the EI mass spectrum indicated that this product resulted from the cleavage of the bond between carbons 3 and 4. This cleavage is consistent with the predominate product found for 1-methylnaphthalene; however, in the case of 1,2-dimethylnaphthalene the alternate product resulting from bond cleavage between carbons 1 and 2 was not found.

The product mixture resulting from the aqueous ozonolysis of 1,3-dimethylnaphthalene contained both possible monoozonolysis products resulting from the oxidation of

the methylated ring. Once again, the base peak distinguished between the two products.

Finally, the aqueous ozonolysis of the symmetrical 1,4- and 2,3-dimethylnaphthalene yielded only one monoozonolysis product for each as indicated in Tables V and VI, respectively.

The geometrical isomers of many of the monoozonolysis products were sometimes found in the product mixtures, as indicated in Table I. The expected configuration around the double bond of the monoozonolysis products is *Z*; i.e., the phenyl substituent and carbonyl-containing substituent are cis to one another. Unfortunately, the acidification of the water solutions prior to extraction would be expected to promote partial isomerizations of these double bonds by protonation of the oxygen in the carbonyl substituent. There was no direct spectral evidence to differentiate the *Z* and *E* isomers of a particular product. However, the assumptions were made that the *E* isomer was lower in concentration, had a similar mass spectrum, and a later GC retention time than the *Z* isomer. When the *E* isomers appeared, there was usually little difficulty in making structural assignments.

It is interesting that the monoozonolysis products were predominant for the aqueous reactions. Apparently, the second double bond to be broken during ozonolysis of the naphthalene ring system is very unreactive toward ozone when the ozonolysis is performed in water. This unreactivity toward ozone may be due to steric interactions promoted by the strong hydration of the polar functionality formed during the course of the reaction. When the first double bond is broken, the remaining double bond and its polar substituents can assume any one of several configurations with respect to the benzene ring. The configuration depends on both intramolecular steric interactions and intermolecular interactions, such as hydration of the polar functionality. The configuration of this double bond and the degree of hydration of its polar substituents will have a large effect on the bond's reactivity toward ozone, since the ozone molecule normally requires an orthogonal access to the double bond. The second double bond would be expected to have greater configurational freedom in organic solvents, including methanol, where solvation occurs to a smaller degree. The product characterizations in *n*-hexane and methanol were consistent with this idea since the monoozonolysis products were isolated in these solvents as only minor components of the product mixtures.

The product yields for the six ozonolysis reactions are given in Tables I–VI. For many of the products, particularly the monoozonolysis products, these yields are not exact because there were no authentic samples from which to determine accurately the response factors and extraction efficiencies. The response factors for monoozonolysis products were estimated to be the same as that found for cinnamaldehyde, or 1.5 relative to dimethyl phthalate. The relative response factors for products resulting from the cleavage of two double bonds, such as methyl 2-formylbenzoate (0.94), phthalaldehyde (1.05), and 2-acetylbenzoate (1.13), were predictably lower than those found for the monoozonolysis products due to the lower carbon–hydrogen content.

Another factor that could have affected product yields was the purging of either starting material or product from solution during the reactions. Experiments using 100 mL/min flow rates of just oxygen without ozone generation indicated that less than 5% of the starting materials were purged from water solution during the time of ozonolysis reactions. The most volatile product phthaldehyde had no tendency to be purged from solution.

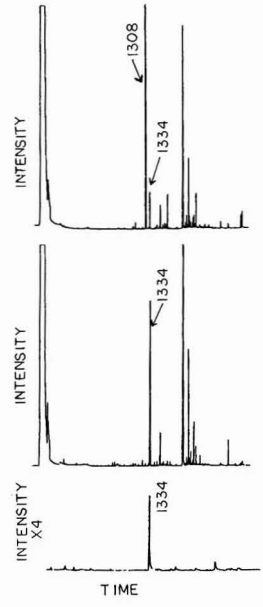

Figure 3. Chromatograms from the gas chromatographic analysis of product mixtures resulting from the ozonolyses of 1-methylnaphthalene in water with 4 (top), 12 (middle), and 48 (bottom) molar equiv of ozone.

One final note conerning the effect of large excesses of ozone on reaction yields is as follows. Ozone is a powerful oxidant, and it will continue to react with the primary products, the ortho-substituted benzenes, after the methyl- or dimethylnaphthalene has been consumed. The primary products are presumably degraded to short-chain, difunctional aldehydes, ketones, and acids and eventually to carbon dioxide and water. Indirect evidence that this occurred under the experimental conditions used in this investigation is demonstrated with the GC product profiles shown in Figure 3. The top profile in Figure 3 results from aqueous ozonolysis of 1-methylnaphthalene with only 4 molar equiv of ozone, an insufficient amount for complete reaction. The middle and bottom GC profiles represent product mixtures resulting from the addition of 12 and 48 molar equiv of ozone, respectively, to 1-methylnaphthalene. With use of product 1334 to compare the profiles, it becomes obvious that the concentrations of all products decrease dramatically with increasing amounts of ozone beyond that necessary for complete reaction of the starting material. Although the ortho-substituted benzene products would normally be thought of as quite resistant to further oxidation, the addition of ozone had to be closely controlled to prevent the degradation of these products and the resulting reduction of reaction yields based on these products.

In general, the isolated product yields were reasonably good. Total product yields were greater than 50%, not including some minor unidentified products isolated for some of the product mixtures, notably that obtained from the reaction of 2,3-dimethylnaphthalene. The expected mechanism of ozonolysis suggests that the unaccounted molar yield of 20–50% for the six reactions is probably due to hydroxy peroxides, which are stable to acid but not volatile or stable enough to be gas chromatographed. Support for this suggestion comes from the results of qualitative tests for peroxides, which indicated their

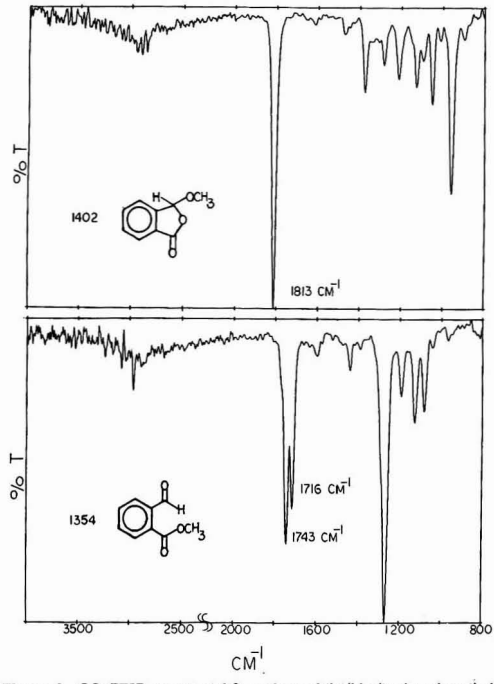

Figure 4. GC–FTIR spectra of 3-methoxyphthalide (top) and methyl 2-formylbenzoate (bottom).

presence, and previous literature (*24–26*), which indicated that the aqueous ozonolysis of naphthalene yields approximately 45% of the stable cyclic hydroxy peroxide and 55% phthalaldehyde.

Ozonolysis in *n*-Hexane and Methanol. The following paragraphs provide some general discussion concerning the products of the ozonolysis reaction performed in *n*-hexane and methanol.

The product mixtures resulting from the reactions in *n*-hexane were quite different than those mixtures obtained for the ozonolyses performed in water. The biggest difference was the presence of the carboxylic acids in the product mixtures from *n*-hexane. The acids were in all cases the more highly oxidized form of the aldehydic products observed in the aqueous ozonolyses. For example, the reaction of 1-methylnaphthalene yielded 2-acetylbenzaldehyde and methyl 2-acetylbenzoate (after derivatization) as major products. Small amounts of the expected ring-methylated products 2-formyl-2-methylbenzaldehyde and methyl 2-formyl-3-methylbenzoate were also characterized. The expected monoozonolysis product (*Z*)-3-(2-formylphenyl)-2-butenal was characterized, but its more highly oxidized analogue was not.

The presence of the acidic products was probably due to the slightly different mechanism that exists in *n*-hexane for the ozonolysis. The peroxide intermediates that are produced during the ozonolysis in *n*-hexane are believed to be predominantly polymeric (*30*) and insoluble in the nonpolar solvent. The evidence for this was the observation of a white flocculant solid that precipitated during the course of the reaction. These polymeric peroxides then decompose in a manner different from the intermediates obtained in participating solvents, such as water and methanol, and this decomposition can yield carboxylic acid substituted products directly. Experimental evidence for the oxidation of the *n*-hexane solvent also suggests that high concentrations of aliphatic peroxides might be responsible for the oxidation of aldehydic functionality associated with the aromatic products. Due to this peroxidic environment, the product mixtures in *n*-hexane were found to be unstable with time.

Another basic difference between the product mixtures in organic solvents and water was the fact that the monoozonolysis products were only minor products for the reactions in *n*-hexane and methanol and were completely absent in the product mixtures resulting from the reaction of 2-methylnaphthalene and 2,3-dimethylnaphthalene in the two organic solvents. In all cases, the molar yield of the monoozonolysis products was less than 10%, and the relative amounts of the monoozonolysis products, compared to those of products resulting from the cleavage of both double bonds, were dramatically different from that found for the aqueous reactions. For the reactions in organic solvents, the products resulting from the cleavage of both double bonds greatly predominated.

The ozonolysis product mixtures in methanol were much more complex than the product mixtures obtained in water or in *n*-hexane. The products obtained in methanol were those expected from the previous literature (*30*); however, the mixtures were complicated by the solvent's ability to promote the formation of stable cyclization products, such as acetals, ketals, and phthalides. One of the best examples of this was the product mixture resulting from the reaction of 2-methylnaphthalene in methanol. Not only were the expected products phthalaldehyde and methyl 2-formylbenzoate and the isomeric methyl 2-formyl-4(or 5)-methylbenzoates characterized, but their cyclized analogues (*E*)- and (*Z*)-1,3-dimethoxyphthalan and 3-methoxyphthalide and the isomeric 3-methoxy-5(or 6)-methylphthalides were also found.

GC–FTIR was instrumental in confirming the structure of many of the products formed in methanol. Isomeric products such as methyl 2-formylbenzoate and 3-methoxyphthalide were difficult to discriminate on the basis of their mass spectra, mainly because the molecular ions and many of their fragment ions were the same, varying only in intensity. Positive structure identification, however, can easily be made by comparing their infrared spectra as shown in Figure 4. The substituted benzoate had two carbonyl adsorptions at 1743 and 1716 cm^{-1} and the phthalide had a single adsorption at 1813 cm^{-1}.

Many compounds characterized in this study were ideal candidates for GC–FTIR analysis. Few organic functional groups are as strongly absorbing in the infrared region as the carbonyl; thus, sensitivity was excellent for carbonyl or carbon–oxygen single-bond adsorptions. In most cases, the number of and the wavelength for the carbonyl adsorptions were all that were required to confirm a structure already partially elucidated by GC–MS. A library of GC–FTIR spectra (along with the mass spectra) for each of the products and discussions of many interesting steric and electronic effects on the carbonyl adsorption frequencies is published elsewhere (*40*).

Acknowledgments

We thank W. S. Trahanovsky for his interest in the project and Mike Avery, John Richard, and Steve Veysey for instrumental assistance and general advice.

Registry No. 1-Methylnaphthalene, 90-12-0; 2-acetylbenzaldehyde, 24257-93-0; methyl 2-formyl-6-methylbenzoate, 63112-99-2; methyl 2-formyl-3-methylbenzoate, 108293-41-0; (*Z*)-3-(2-formylphenyl)-2-butenal, 108293-42-1; methyl (*Z*)-3-(2-formylphenyl)-2-butenoate, 108293-43-2; (*E*)-3-(2-formylphenyl)-2-butenal, 108293-44-3; (*Z*)-3-(2-acetylphenyl)propenal,

108293-45-4; 2-methylnaphthalene, 91-57-6; phthalaldehyde, 643-79-8; phthalic anhydride, 85-44-9; (*E*)-1,3-dimethoxyphthalan, 22882-31-1; (*Z*)-1,3-dimethoxyphthalan, 22882-30-0; methyl 2-formylbenzoate, 4122-56-9; methyl 2-formyl-5-methylbenzoate, 108293-46-5; methyl 2-formyl-4-methylbenzoate, 63112-98-1; (*Z*)-2-(3-oxo-1-butenyl)benzaldehyde, 108293-47-6; 3-methoxy-6-methylphthalide, 108293-48-7; 3-methoxy-5-methylphthalide, 63113-02-0; 1,2-dimethylnaphthalene, 573-98-8; 3-methoxy-3-methylphthalide, 1077-59-4; 3-methoxyphthalide, 4122-57-0; methyl 2-acetylbenzoate, 1077-79-8; (*Z*)-3-(2-formylphenyl)-2-methyl-2-butenal, 108293-49-8; methyl (*E*)-3-(2-formylphenyl)-2-methyl-2-butenoate, 108293-50-1; 1,3-dimethylnaphthalene, 575-41-7; (*E*)-1-methyl-1,3-dimethoxyphthalan, 60026-77-9; (*Z*)-1-methyl-1,3-dimethoxyphthalan, 60026-76-8; (*Z*)-2-(1-methyl-3-oxo-1-butenyl)benzaldehyde, 108293-51-2; (*Z*)-3-(2-acetylphenyl)-2-methylpropenal, 108293-52-3; 1,4-dimethylnaphthalene, 571-58-4; (*Z*)-1,3-dimethyl-1,3-dimethoxyphthalan, 108293-53-4; 1,2-diacetylbenzene, 704-00-7; (*Z*)-3-(2-acetylphenyl)-2-butenal, 108293-54-5; 2,3-dimethylnaphthalene, 581-40-8; dimethyl phthalate, 131-11-3; methyl 2-formylbenzoate dimethyl acetal, 87656-31-3; (*Z*)-2-(2-methyl-3-oxo-1-butenyl)-benzaldehyde, 108293-55-6; 2-formyl-4,5-dimethylbenzaldehyde, 25445-42-5; methyl 2-formyl-4,5-dimethylbenzoate, 108293-56-7; 3-methoxy-5,6-dimethylphthalide, 108293-57-8.

Literature Cited

(1) *Proceedings of the Conference on the Environmental Impact of Water Chlorination*; Jolley, R. L., Ed.; NTIS, USDC: Springfield, VA, 1976; CONG-751096, all papers therein.

(2) *Proceedings of the Second Conference on the Environmental Impact of Water Chlorination*; Jolley, R. L.; Gorchev, H.; Hamilton, D. H., Jr., Eds.; Ann Arbor Science: Ann Arbor, MI, 1978; all papers therein.

(3) *Proceedings of the Third Conference on Water Chlorination: Environmental Impact and Health Effects*: Jolley, R. L.; Brungs, W. A.; Cumming, R. B.; Jacobs, V. A., Eds.; Ann Arbor Science: Ann Arbor, MI, 1980; all papers therein.

(4) Sievers, R. E.; Barkley, R. M.; Eiceman, G. A.; Shapiro, R. H.; Walton, H. F.; Dolonko, K. J.; Field, L. R. *J. Chromatogr.* **1977**, *142*, 745–754.

(5) Chappell, W. R.; Sievers, R. E.; Shapiro, R. H. *Project Summary: The Effect of Ozonation of Organics in Wastewater*; Health Effects Research Laboratory, Office of Research and Development, U.S. Environmental Protection Agency: Cincinnati, OH, Feb. 1981; EPA-600/S1-81-005.

(6) Lawrence, J.; Tosine, H.; Onuska, F. I.; Comba, M. E. *Ozone: Sci. Eng.* **1980**, *2*, 55–64.

(7) J. Mallevialle, In *Proceedings of the 2nd International Symposium on Ozone Technology*, Montreal, 1975; Rice, R. G.; Pichet, P.; Vincent, M.; Eds.; Ozone Press Internationale: Jamesville, NY, 1975; pp 133–141.

(8) Shapiro, R. H.; Kolonko, K. J.; Binder, R. T.; Barkley, R. M.; Eiceman, G. A.; Haack, L. P.; Sievers, R. E. In *Proceedings of the Joint Conference on Sensing Environmental Pollutants, 4th*, New Orleans, LA, 1977; American Chemical Society: Washington, DC, 1978; pp 507–510.

(9) Niki, E.; Yamamoto, Y.; Saito, T.; Nagano, K.; Yokoi, S.; Kamiya, Y. *Bull. Chem. Soc. Jpn.* **1983**, *56*, 223–228.

(10) Sturesund, H. J.; Bernatek, E. *Acta Chem. Scand.* **1970**, *24*, 3237–3242.

(11) Yamada, H.; Somiya, I. *Ozone: Sci. Eng.* **1980**, *2*, 251–260.

(12) Legube, B.; Langlais, B.; Dore, M. *Prog. Water Technol.* **1980**, *12*, 553–570.

(13) Gilbert, E. *Water Sci. Technol.* **1982**, *14*, 849–861.

(14) Pringle, W. NTIS Report PB-81-115651; NTIS: Middletown, CT, Sept. 1980.

(15) Dore, M.; Langlais, B.; Legube, B. *Water Res.* **1978**, *12*, 413–425.

(16) Legube, B.; Langlais, B.; Sohm, B.; Dore, M. *Ozone Sci. Eng.* **1981**, *3*, 33–48.

(17) Leitis, E. NTIS Report PB80-174394; NTIS: Springfield, VA, Feb. 1980.

(18) Helleur, R.; Malaiyandi, M.; Benoit, F. M.; Benedek, A. *Ozone: Sci. Eng.* **1979**, *1*, 249–261.

(19) Sturrock, M. G.; Cline, E. L.; Robinson, K. R. *J. Org. Chem.* **1963**, *28*, 2340–2343.

(20) Chen, P. N.; Junk, G. A.; Svec, H. J. *Environ. Sci. Technol.* **1979**, *13*, 451–454.

(21) Meineke, I.; Klamberg, H. *Fresenius' Z. Anal. Chem.* **1978**, *293*, 201–204.

(22) Meineke, I.; Klamberg, H. *Fresenius' Z. Anal. Chem.* **1978**, *293*, 205–207.

(23) Neely, W. C. NTIS Report PB82-254970; NTIS: Springfield, VA, Jan. 1981.

(24) Sturrock, M. G.; Cravy, B. J.; Wing, V. A. *Can. J. Chem.* **1971**, *49*, 3047–3051.

(25) Kruithof, J. C.; Heertjes, P. M. In *Chemistry in Water Reuse*; Cooper, W. J.; Ed.; Ann Arbor Science: Ann Arbor, MI, 1981; Chapter 19.

(26) Legube, B.; Guyon, S.; Sugimitsu, H.; Dore, M. *Water Res.* **1986**, *20*, 197–208.

(27) Weil, C. S.; Condra, N.; Haun, C.; Striegel, J. A. *Am. Ind. Hyg. Assoc. J.* **1963**, *24*, 305–325.

(28) Junk, G. A.; Stanley, S. E. Ames Laboratory Report IS-3671; Ames Laboratory: Ames, IA, July 1975.

(29) Neff, J. M. *Polycyclic Aromatic Hydrocarbons in the Aquatic Environment. Sources, Fates, and Biological Effects*; Applied Science: London, 1979.

(30) Bailey, P. S. *Ozonation in Organic Chemistry*; Academic: New York, 1982; Vol. II.

(31) Bailey, P. S. *Ozonation in Organic Chemistry*; Academic: New York, 1978; Vol. I.

(32) Boelter, E. D.; Putnam, G. L.; Lash, E. I. *Anal. Chem.* **1950**, *22*, 1533–1535.

(33) Junk, G. A.; Richard, J. J.; Gieser, M. D.; Witiak, D.; Witiak, J. L.; Arguello, M. D.; Vick, R.; Svec, H. J.; Fritz, J. S.; Calder, G. V. *J. Chromatogr.* **1974**, *99*, 745–762.

(34) Stoodley, K. D. C.; Lewis, T.; Stainton, C. L. S. *Applied Statistical Techniques*; Ellis Horwood: West Sussex, England, 1980; Chapter 2.

(35) Erley, D. S.; Potts, W. J.; Jones, P. R.; Desio, P. *J. Chem. Ind. (Moscow)* **1964**, 1915–1916.

(36) Wibaut, J. P.; Van Dijk, J. *Recl. Trav. Chim. Pays-Bas* **1946**, *65*, 413–426.

(37) Callighan, R. H.; Wilt, M. H. *J. Org. Chem.* **1961**, *26*, 5212–5214.

(38) Bernatek, E.; Frengen, C. *Acta Chem. Scand.* **1962**, *16*, 2421–2428.

(39) Bailey, P. S.; Johnson, C. D. *J. Org. Chem.* **1964**, *29*, 703–707.

(40) Gaul, M. D. Ph.D. Dissertation, Iowa State University, Ames, IA, 1984.

Received for review October 6, 1986. Accepted April 6, 1987. This work was supported by National Science Foundation Grant CHE 7906108. The facilities of the Ames Laboratory, U.S. Department of Energy, were used with support by the Pollutant Characterization and Safety Research Division, Office of Health and Environmental Research, Office of Energy Research.

Environ. Sci. Technol. 1987, 21, 785–790

Biouptake of Chlorinated Hydrocarbons from Laboratory-Spiked and Field Sediments by Oligochaete Worms

Barry G. Oliver*

Environmental Contaminants Division, National Water Research Institute, Canada Centre for Inland Waters, Burlington, Ontario, Canada L7R 4A6

■ The uptake and depuration of 37 chemicals from spiked Lake Ontario sediments by oligochaete worms has been studied at 8 and 20 °C in laboratory aquaria. The worms were found to rapidly accumulate the chemicals and reach peak concentrations within 2 weeks. The concentration of chemicals in the sediment pore water appeared to be the major factor controlling the bioconcentration of chemicals by the worms. The worm bioconcentration factors increased with increasing octanol–water partition coefficient of the chemicals. The worm-mediated fluxes of the chemicals from the sediments have also been estimated. Depuration studies showed the half-lives of the chemicals in the worms ranged from less than 5 days to several months. Field worms and associated sediments from Lake Ontario near the Niagara River were analyzed. The agreement between the field and laboratory results was good for the more persistent chemicals but poor for the less persistent contaminants because of time differences for sorting the two sample types.

Introduction

Contaminated sediments are a major problem in the Great Lakes region and in many other industrialized countries throughout the world. Many chlorinated hydrocarbons exhibit a strong tendency for adsorption to suspended and/or bottom sediments when they are discharged to the aquatic environment (*1*). Polychlorinated biphenyls (PCB's) (*2*), chlorobenzenes (*3*), mirex (*4*), and chlorostyrenes (*5*) are some of the chemicals that have been found at high concentrations in Great Lakes sediments. Knowledge of the bioavailability of these sediment-associated chemicals is a critical requirement for assessing their potential hazards in sediments.

Benthic organisms can influence the availability of chemicals in two ways: they can enhance the rate of diffusion of chemicals out of bottom sediments into the water column by the process of bioturbation (*6*, *7*), or they can incorporate the chemicals into their tissue by absorption from ingested sediments and/or pore water (*8*, *9*). The chemicals are then available to higher organisms such as fish in the first case through bioconcentration from water processes (*10*) and in the second case through the food chain process (*11*). In a field study, Fox et al. (*12*) demonstrated a strong correlation between sediment hexachlorobenzene (HCB) concentration and oligochaete HCB concentration for several Lake Ontario sediments. Polychaete worms in marine systems have been shown to accumulate PCB's from contaminated sediments (*13*, *14*). The degree of accumulation by the worms seemed to be inversely correlated with worm size (*13*) and likely with organic matter content of the sediment (*15*).

In an earlier laboratory study it was demonstrated that oligochaete worms could become contaminated by feeding on and living in anthropogenically contaminated sediment from Lake Ontario (*8*). In that study only a limited number of chemicals could be studied because of detection limit problems at the environmentally encountered concentrations. In this study, spiked sediments were used to obtain a broader compound coverage, and a flow-through (instead of static) system was employed. Two different temperatures, 8 and 20 °C, were used to assess the effect of this variable. Oligochaetes and associated sediments were collected from several contaminated Lake Ontario field sites to find out whether the laboratory-derived data could be applied in the field.

Experimental Section

A large sediment sample (4.6% organic carbon) was collected from the central basin of Lake Ontario for the experiment. A sediment slurry (≈20% solids) was prepared to which the chemicals in acetone were added slowly dropwise over a period of several days with constant stirring. The spiked sediment slurry was then stirred periodically and "aged" for 6 weeks prior to use. Karichkoff (*16*) has previously shown that, depending on the chemical, days to several weeks may be required for diffusion processes within the sediments to achieve equilibrium. Three kilograms of the sediment was then placed in each of four (30 cm × 60 cm × 30 cm deep) aquaria and allowed to settle for 3 days (sediment depth 5–6 cm). The water supplied to the tanks was carbon filtered tap water from Lake Ontario. The water was circulated through coils submersed in 8 or 20 °C thermostats prior to entering the aquaria, and cooling coils at the appropriate temperature were placed in each aquaria to maintain the temperature at 8 ± 1 and 20 ± 1 °C. The two tanks used at each temperature were connected in series, and the water flow rates were 110 ± 10 mL/min for the 8 °C tanks and 150 ± 15 mL/min for the 20 °C tanks.

Approximately 13 g wet weight of worms (≈7000 worms/m^2) from Toronto Harbour (Lake Ontario) was added to each tank to begin the exposure period. The worms were analyzed before the start of the experiment and found to contain insignificant concentrations of the study chemicals. The worms, which were mainly *Tubifex tubifex* and *Limnodrilus hoffmeisteri*, had an average dry weight of 13% and a lipid content of 1%. In order to make a correction for contaminant present in the gut on ingested sediments, the dry worms were heated to 500 °C in a muffle furnace to measure the amount of sediment they contained. This sediment accounted for 15% of the worm dry weight. Since concentration measurements showed fecal pellets had virtually the same chemical concentrations as sediments, the most cases, the gut sediments comprise a negligible amount of contaminant in the worm. Worms and sediments were recovered from the tanks after 4, 11, 39, and 79 days of exposure. At 79 days the remaining worms from the two cold tanks were combined and placed in an 8 °C tank containing clean Lake Superior sediments. Similarly, worms from the two warm tanks were combined and added to a 20 °C tank containing Lake Superior sediments to begin the depuration phase of the study. Samples were collected after 5, 12, 21, 36, and 84 days of depuration.

* Address correspondence to the author at his present address: ELI Eco Laboratories Inc., Rockwood, Ontario, Canada N0B 2K0.

Published 1987 by the American Chemical Society

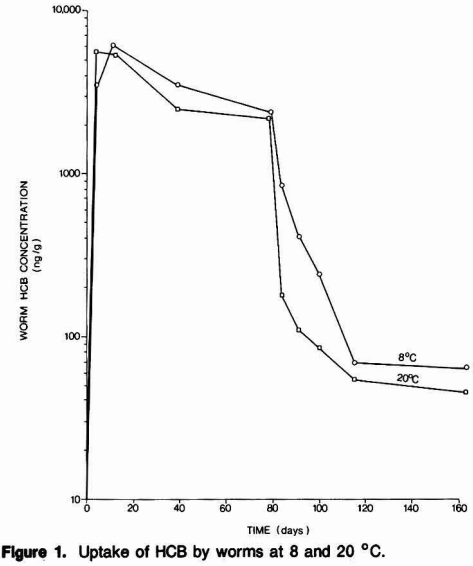

Figure 1. Uptake of HCB by worms at 8 and 20 °C.

Soxhlet extraction with acetone/hexane was used to extract the chemicals from the sediments and worms are previously described (*17*). Water samples were pressure filtered through a glass fiber filter (1 μm) prior to extraction with hexane. Pore water samples, collected by submersing a pipet in the sediment and slowly sucking up the water with a rubber bulb, were centrifuged and pressure filtered prior to liquid–liquid extraction with hexane. All procedures were thoroughly tested prior to use, and recoveries were excellent, >80% [see also Oliver and Nicol (*17*)]. Quantification was carried out by a dual-column capillary gas chromatographic method with 30-m DB5 and DB17 columns and electron capture detectors. Reproducibility of the analysis on replicate samples was ±10%.

Field samples of worms and sediments were collected with a box corer (0.25 m^2). The sediment was screened on site with a 500-μm plankton net, and the benthic organisms and debris were transferred to wide-mouth jars on site. The jars were kept cool until return to the laboratory where the organisms were sorted. The sorting was completed within 3 days of collection, and the worm samples and sediments were then frozen until analysis.

Results and Discussion

The 37 chemicals used in the study are listed with their abbreviations and octanol–water partition coefficients, K_{ow}, in Table I. The chemicals were chosen to span a wide range of physical/chemical properties. With 37 chemicals, four aquaria, and nine sampling times for worms, sediments, water, and pore water, a large quantity of data has been generated. Only a small fraction of the data will be presented here for brevity.

Samplings of the replicate tanks at each temperature showed excellent agreement; measured concentrations were within ±10% of the mean of the two replicates for all compartments. There were some differences in the uptake and elimination rates for the two temperatures, which will be discussed later. But only averaged data for worms and sediments in the 8 °C aquaria are shown in Table II. With the exception of αBHC and lindane, only minor changes in the sediment concentrations occurred during the 79-day exposure period. αBHC and lindane seemed to be only weakly bound to the sediments, and most of these chemicals were lost from the sediments over the course of the study. This observation agrees with field measurements, which show these chemicals to be present at fairly high concentrations in water but at very low concentration in sediments (*27*). The uptake of the chemicals by the worms is shown for HCB and OCS in Figures 1 and 2. The worms at 20 °C seem to achieve their peak concentrations faster than the worms at 8 °C, probably because of higher metabolic activity, but both worm sets reach about the same maximum concentration.

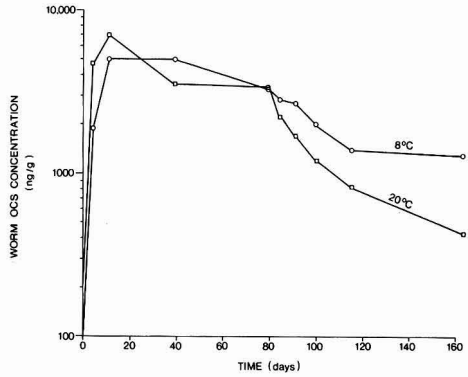

Figure 2. Uptake of OCS by worms at 8 and 20 °C.

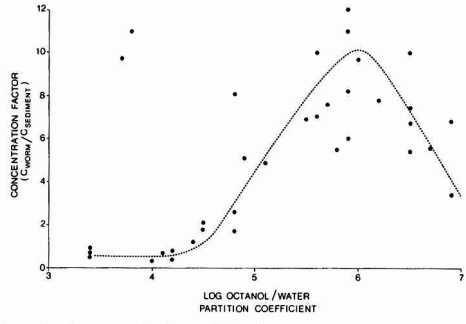

Figure 3. Concentration factor [chemical concentration in worm (ng/g dry weight)/chemical concentration in sediment (ng/g dry weight)] vs. log octanol–water partition coefficient, K_{ow}.

A plot of maximum concentration factor (CF) vs. log octanol/water partition coefficient (Figure 3) has a shape similar to that found previously by Oliver (*8*). The CF increases until log K_{ow} reaches about 6; then, the CF levels off and shows a decline for the larger molecules with very high K_{ow}'s. The chemicals αBHC and lindane plot well above the curve, probably because of their low sediment affinity.

For all chemicals at both temperatures the chemicals reached a maximum concentration; then the concentrations declined with continuing exposure. These observations can be readily explained by examination of the changes in chemical concentrations in the water and pore water in the aquaria. These concentrations were steady for the first 2 weeks of the study and the declined gradually over time. Thus, the worms are exposed to lower water and pore water concentrations as the experiment progressed, and reduced residue levels were observed. Decreasing pore water concentrations would be expected in this flow-through system as the more readily desorbable portion of the sediment-associated contaminant is depleted (*28*).

Table I. Study Chemicals, Abbreviations, and log Octanol/Water Coefficients (log K_{ow}) with Literature Source in Parentheses

chemical	abbreviation	log K_{ow}
1,3-dichlorobenzene	1,3-DCB	3.4 (*18*)
1,4-dichlorobenzene	1,4-DCB	3.4 (*18*)
1,2-dichlorobenzene	1,2-DCB	3.4 (*18*)
1,3,5-trichlorobenzene	1,3,5-TCB	4.2 (*19*)
1,2,4-trichlorobenzene	1,2,4-TCB	4.0 (*20*)
1,2,3-trichlorobenzene	1,2,3-TCB	4.1 (*19*)
1,2,4,5-tetrachlorobenzene	1,2,4,5-TeCB	4.5 (*19*)
1,2,3,4-tetrachlorobenzene	1,2,3,4-TeCB	4.5 (*19*)
pentachlorobenzene	QCB	4.9 (*18*)
hexachlorobenzene	HCB	5.5 (*20*)
2,4,5-trichlorotoluene	2,4,5-TCT	4.8 (*21*)[a]
2,3,6-trichlorotoluene	2,3,6-TCT	4.8 (*21*)[a]
2,3,4,5,6-pentachlorotoluene	PCT	6.2 (*21*)[a]
3,4-dichlorobenzotrifluoride	3,4-DCBTF	4.4 (*21*)[a]
2,4-dichlorobenzotrifluoride	2,4-DCBTF	4.4 (*21*)[a]
hexachlorobutadiene	HCBD	4.8 (*18*)
2,3,4-trichloranisole	2,3,4-TCA	4.2 (*21*)[a]
1,2,3,4-tetrachloronaphthalene	1,2,3,4-TeCN	5.5 (*22*)[b]
octachlorostyrene	OCS	6.2 (*23*)
α-hexachlorocyclohexane	αBHC	3.8 (*24*)
γ-hexachlorocyclohexane	lindane	3.7 (*24*)
γ-chlordan	γ-CHLOR	6.0 (*23*)
1,1-dichloro-2,2-bis(4-chlorophenyl)ethylene	pp-DDE	5.7 (*25*)
1,1,1-trichloro-2,2-bis(4-chlorophenyl)ethane	pp-DDT	5.8 (*25*)
mirex	mirex	6.9 (*23*)
2,5,2′-trichlorobiphenyl	PCB18[c]	5.6 (*22*)[b]
2,5,4′-trichlorobiphenyl	PCB31	5.6 (*22*)[b]
2,5,2′,6′-tetrachlorobiphenyl	PCB53	5.9 (*22*)[b]
2,5,2′,5′-tetrachlorobiphenyl	PCB52	5.9 (*22*)[b]
2,3,2′,3′-tetrachlorobiphenyl	PCB40	5.9 (*22*)[b]
2,4,3′,4′-tetrachlorobiphenyl	PCB66	5.9 (*22*)[b]
2,4,6,2′,4′,6′-hexachlorobiphenyl	PCB155	6.5 (*22*)[b]
2,4,5,2′,4′,5′-hexachlorobiphenyl	PCB153	6.5 (*22*)[b]
2,3,4,2′,3′,4′-hexachlorobiphenyl	PCB128	6.5 (*22*)[b]
2,3,4,5,3′,4′-hexachlorobiphenyl	PCB156	6.5 (*22*)[b]
2,3,4,6,2′,3′,4′-heptachlorobiphenyl	PCB171	6.7 (*22*)[b]
2,3,4,5,2′,3′,4′,5′-octachlorobiphenyl	PCB194	6.9 (*22*)[b]

[a] Calculated by the II method of Hansch and Leo (*21*). [b] Calculated by the method of Kaiser (*22*). [c] PCB numbering system of Ballschmiter and Zell (*26*).

Although it was not possible to detect all the study chemicals in the pore water, because of the small volume sampled, measurable concentrations were obtained for 17 chemicals. Table III lists the average pore water concentrations at 8 °C for the first two samplings and the bioconcentration factors, BCF's, for the worms expressed as chemical concentration in worms dry weight (ng/kg)/pore water concentration (ng/L). Also shown in the table are BCF values obtained from our earlier studies for rainbow trout. Although the worms have a lipid content of only 1% on a wet weight basis, their lipid content on a dry weight basis is about 8%, very close to that of the rainbow trout. For many of the chemicals, the worm BCF's are in good agreement with the fish BCF's. For some of the larger chemicals, the fish BCF's are lower than the worm BCF's because equilibrium concentrations were not attained for these chemicals during the time course of the fish experiment. This general agreement between the worm and fish BCF's for chemicals at equilibrium indicates that the worms' body burden of chemicals comes mainly from the pore water rather than from ingestion of contaminated sediment particles. This hypothesis is further supported by the observation that fecal pellets contained the same chemical concentration (within experimental error) as the sediments and that gut sediment contents made an insignificant contribution to body burden for most chemicals.

Thus, the measurement of pore water chemical concentrations will likely be an important requirement for prediction of chemical concentrations of worms at contaminated field sites. But such measurements are extremely difficult to perform for organic chemicals. Therefore, conversely, it may be possible to estimate pore water concentrations at various sites by using the analysis of oligochaetes (if present) and applying either laboratory-derived worm BCF's or BCF measurements on fish with similar lipid contents or fish BCF's expressed on a lipid basis.

The presence of oligochaete worms has been shown to enhance the flux of contaminants out of the sediments by the process of bioturbation (*7*). Table IV shows the average chemical concentration in the aquaria water over the first 2 weeks of the study together with the estimated chemical flux. Since the chemicals were present at different concentrations in the sediments, the flux was normalized to 1000 ppb by multiplying it by 1000/chemical concentration in the sediment, so the fluxes of the chemicals could be compared. This normalization is applied for convenience and does not necessarily imply that the fluxes are linearly related to sediment concentrations. On average, the flux out of the sediments was 4 times higher at 20 °C than at 8 °C. Lindane and αBHC are seen to have by far the highest flux at both temperatures. The flux out of the sediments for the various chemicals was consistent with the chemicals' properties—the flux decreased as the chemical K_{ow} increased or as its water solubility decreased. The exceptions to this rule are lindane and αBHC, which have an order of magnitude higher K_{ow} and lower water

Table II. Mean Concentration (ng/g Dry Weight) in Sediment and Worms from 8 °C Aquaria and Estimated Half-Lives

	sediment		worms' uptake phase (CF)[a]				worms' depuration phase					half-life, days (r^2)[b]	growth corrected half-life, days (r^2)[b]
	4 d	79 d	4 d	11 d	39 d	79 d	5 d	12 d	21 d	36 d	84 d		
1,3-DCB	830	590	610 (0.7)	500 (0.6)	350 (0.5)	330 (0.6)	ND[c]	ND	ND	ND	ND	<5	<5
1,4-DCB	530	370	200 (0.4)	270 (0.5)	70 (0.2)	60 (0.2)	ND	ND	ND	ND	ND	<5	<5
1,2-DCB	280	230	260 (0.9)	220 (0.8)	140 (0.6)	40 (0.2)	ND	ND	ND	ND	ND	<5	<5
1,3,5-TCB	180	160	150 (0.8)	130 (0.7)	110 (0.6)	90 (0.6)	14	5	ND	ND	ND	<5	<5
1,2,4-TCB	630	550	180 (0.3)	190 (0.3)	90 (0.2)	100 (0.2)	ND	ND	ND	ND	ND	<5	<5
1,2,3-TCB	290	230	130 (0.4)	190 (0.7)	150 (0.6)	100 (0.4)	ND	ND	ND	ND	ND	<5	<5
1,2,4,5-TeCB	250	210	320 (1.3)	430 (1.8)	210 (0.9)	150 (0.7)	ND	ND	ND	ND	ND	<5	<5
1,2,3,4-TeCB	270	230	400 (1.5)	540 (2.1)	300 (1.2)	150 (0.7)	ND	ND	ND	ND	ND	<5	<5
QCB	460	420	1600 (3.5)	2300 (5.1)	1100 (2.5)	800 (1.9)	67	31	36	9	19	<5	<5
HCB	900	770	3500 (3.9)	6100 (6.9)	3500 (4.2)	2400 (3.1)	840	410	240	69	66	24 (0.69)	27 (0.70)
2,4,5-TCT	340	300	420 (1.2)	570 (1.7)	320 (1.0)	210 (0.7)	48	25	ND	ND	ND	<5	<5
2,3,6-TCT	250	210	480 (1.9)	630 (2.6)	350 (1.5)	290 (1.4)	ND	ND	ND	ND	ND	<5	<5
PCT	690	640	3000 (4.3)	5300 (7.8)	3000 (4.5)	2000 (3.1)	680	670	220	63	57	22 (0.72)	26 (0.73)
3,4-DCBTF	220	180	270 (1.2)	250 (1.2)	120 (0.6)	130 (0.7)	ND	ND	ND	ND	ND	<5	<5
2,4-DCBTF	140	110	130 (0.9)	170 (1.2)	90 (0.7)	70 (0.6)	ND	ND	ND	ND	ND	<5	<5
HCBD	120	88	510 (4.3)	930 (8.1)	400 (3.8)	230 (2.6)	26	16	14	9.2	5.3	<5	<5
2,3,4-TCA	710	610	150 (0.2)	160 (0.2)	290 (0.4)	200 (0.3)	38	29	120	57	79	?	?
1,2,3,4-TeCN	1300	1200	3200 (2.5)	6400 (4.9)	4000 (3.2)	2800 (2.3)	1100	730	370	110	63	20 (0.83)	30 (0.50)
OCS	560	520	1900 (3.4)	5000 (9.1)	5000 (9.3)	3300 (6.3)	2800	2700	2000	1400	1300	71 (0.75)	100 (0.84)
αBHC	310	60	2400 (7.7)	3400 (11)	1000 (5.0)	610 (10)	68	76	57	37	27	<5	<5
lindane	740	120	4800 (6.5)	6600 (9.7)	1600 (3.6)	900 (7.5)	61	55	32	20	16	<5	<5
γ-CHLOR	390	360	1800 (4.6)	3800 (9.7)	2700 (7.2)	1700 (4.7)	1000	790	680	290	310	46 (0.67)	63 (0.66)
pp-DDE	290	280	860 (3.0)	2200 (7.6)	2000 (7.0)	1200 (4.3)	960	890	830	460	500	80 (0.63)	130 (0.50)
pp-DDT	100	92	170 (1.7)	540 (5.5)	190 (2.0)	50 (0.5)	47	21	33	9.2	14	53 (0.39)	74 (0.27)
mirex	600	570	720 (1.2)	2300 (3.8)	4000 (6.8)	2900 (5.1)	3200	3100	2600	2400	2400	200 (0.60)	∞ (ref)
PCB18	620	600	3800 (6.1)	6500 (10)	3400 (5.6)	2200 (3.7)	670	450	320	75	66	24 (0.75)	26 (0.75)
PCB31	770	740	2800 (3.6)	5400 (7.0)	3200 (4.2)	2100 (2.8)	1000	680	470	180	120	26 (0.83)	30 (0.85)
PCB53	770	760	4500 (5.8)	9000 (12)	5600 (7.3)	3400 (4.5)	1900	1300	830	320	210	26 (0.83)	30 (0.86)
PCB52	780	740	3800 (4.9)	8400 (11)	5500 (7.2)	3300 (4.5)	2100	1600	1000	440	440	36 (0.69)	43 (0.70)
PCB40	720	710	3300 (4.6)	5900 (8.2)	3800 (5.3)	2500 (3.5)	1300	840	610	230	140	26 (0.86)	29 (0.88)
PCB66	850	840	2000 (2.4)	5100 (6.0)	3800 (4.5)	2400 (2.9)	1600	1400	920	360	240	28 (0.85)	33 (0.87)
PCB155	1000	990	3100 (3.1)	8500 (8.5)	10000 (10)	6400 (6.5)	6300	5800	3700	2800	3800	120 (0.29)	310 (0.11)
PCB153	820	800	2100 (2.6)	5200 (6.3)	6000 (7.4)	3700 (4.6)	3300	3000	2700	2100	1800	92 (0.88)	170 (0.91)
PCB128	920	910	1800 (2.0)	5000 (5.4)	4700 (5.1)	2900 (3.2)	2400	2300	1900	1300	820	50 (0.96)	63 (0.97)
PCB156	430	410	900 (2.1)	2100 (4.9)	2800 (6.7)	1600 (3.9)	1300	1300	790	510	500	58 (0.67)	80 (0.70)
PCB171	410	370	680 (1.7)	1400 (3.5)	2200 (5.6)	1500 (4.1)	1100	1200	740	560	690	110 (0.37)	260 (0.22)
PCB194	960	940	750 (0.8)	2100 (2.2)	3200 (3.4)	2400 (2.6)	2300	2300	2200	1900	1400	100 (0.99)	220 (0.54)

[a] CF = concentration factor (concentration in worm dry weight/concentration in sediment). [b] r^2 = square of correlation coefficient for equation. [c] ND = not detected.

Table III. Pore Water Concentrations and Bioconcentration Factors (BCF's) for Worms and Fish

compd	pore water, ng/L	worm BCF[a]	fish BCF	compd	pore water, ng/L	worm BCF[a]	fish BCF
QCB	120	19000	20000[b]	pp-DDE	76	29000	14000[c]
HCB	250	24000	20000[b]	mirex	180	22000	740[c]
PCT	190	28000	6800[c]	PCB40	250	24000	17000[c]
HCBD	32	29000	17000[b]	PCB66	180	28000	
1,2,3,4-TeCN	310	21000	5100[c]	PCB155	290	34000	4800[c]
OCS	160	31000	8100[c]	PCB153	240	25000	
αBHC	1400	2400	2400[c]	PCB128	260	19000	
lindane	3500	1900	2000[c]	PCB194	220	15000	
γ-CHLOR	150	25000	22000[c]				

[a] Worm BCF = chemical concentration (ng/kg) in worm dry weight/pore water concentration (ng/L). [b] From reference 10. [c] From reference 29.

solubility than the dichlorobenzenes and yet are desorbed more than 10 times faster. Most of the chemicals in Table IV are aromatic, whereas αBHC and lindane are cyclic aliphatic compounds. Unfortunately, because no measurements were made over sediments that did not contain worms, the influence of the worms on the chemical flux cannot be quantified.

Although there are very few chemical flux measurements from sediments in the literature, it is interesting to compare these results to those of Karickhoff and Morris (7). Their fluxes for QCB and HCB from sediments containing 1000 ppb of the chemicals and with about the same worm populations at 20 °C were about 220 and 120 μg/(m²·day) in contrast to 9 and 5 μg/(m²·day) in this study. In Karickhoff and Morris' experiment, the water was continually purged to remove the chemicals so that diffusion from the sediments was occurring into relatively "clean" water. Also, the organic carbon content of their sediment (0.8%) was much lower than that in this study (4.6%). The availability of organics in sediments is considered to be much lower for sediments with higher organic carbon content (1).

After the exposure period, the remaining worms were recovered and placed in 8 and 20 °C aquaria containing "clean" Lake Superior sediments. The worms were first sampled from the new aquaria after 5 days and showed

Table IV. Average Water Concentrations in Aquaria at 8 and 20 °C for the First Two Study Weeks and Normalized Desorption Fluxes

	8 °C		20 °C			8 °C		20 °C	
compd	water concn, ng/L	normalized flux,[a] μg/(m²·day)	water concn, ng/L	normalized flux, μg/(m²·day)	compd	water concn, ng/L	normalized flux,[a] μg/(m²·day)	water concn, ng/L	normalized flux, μg/(m²·day)
1,3-DCB	6.0	6	9.3	13	αBHC	24	70	75	290
1,4-DCB	2.8	5	5.8	13	lindane	61	70	180	290
1,2-DCB	2.4	8	4.0	17	γ-CHLOR	0.6	1	1.6	5
1,3,5-TCB	1.1	5	1.6	11	pp-DDE	0.05	0.2	0.2	0.8
1,2,4-TCB	1.8	3	2.5	5	pp-DDT	ND	ND	0.1	1
1,2,3-TCB	1.8	5	2.1	9	mirex	0.1	0.1	0.5	1
1,2,4,5-TeCB	1.2	4	2.1	10	PCB18	0.8	1	3.6	7
1,2,3,4-TeCB	1.5	5	2.9	13	PCB31	0.8	0.9	1.9	3
QCB	1.6	3	3.6	9	PCB53	1.6	2	5.0	8
HCB	1.3	1	3.6	5	PCB52	1.4	2	3.8	6
2,4,5-TCT	1.2	3	1.8	6	PCB40	0.6	0.7	2.5	4
2,3,6-TCT	1.3	5	1.7	8	PCB66	0.2	0.2	1.0	1
PCT	0.9	1	2.5	4	PCB155	0.4	0.4	1.2	1
3,4-DCBTF	1.1	4	1.7	9	PCB153	0.3	0.3	1.0	1
2,4-DCBTF	0.7	4	1.5	13	PCB128	0.2	0.2	0.7	0.9
HCBD	0.1	0.7	0.2	2	PCB156	0.1	0.2	0.5	1
2,3,4-TCA	2.3	3	9.5	16	PCB171	0.1	0.2	0.4	1
1,2,3,4-TeCN	0.9	0.6	7.0	6	PCB194	0.1	0.1	0.6	0.7
OCS	0.1	0.2	0.4	0.9					

[a] Normalized flux = flux × (1000/chemical concentration in sediment).

Table V. Chemical Concentrations (ng/g Dry Weight) in Worms and Sediments in Lake Ontario near the Niagara River

	worm/sediment					
chemical	site 1	site 2	site 3	site 4	site 5	site 6
QCB	3.4/12	20/22	7.1/15	3.9/11	3.1/11	3.1/15
HCB	18/43	46/60	24/39	17/36	14/56	13/40
HCBD	2.4/9.2	8.6/11	6.4/8.4	3.6/11	2.2/11	2.0/7.3
OCS	8.7/2.8	31/3.8	14/3.5	13/2.5	21/3.9	7.5/4.1
pp-DDE	33/16	69/15	34/7.2	29/8.4	32/11	54/38
mirex	47/13	79/19	31/9.3	29/6.2	35/7.9	56/15
total PCB's	380/220	4300/310	1600/270	1300/190	1200/300	460/420
TOC, %	4.2	3.7	2.9	3.2	2.9	5.6

a marked decline in contaminant levels during this period (Table II). This is probably due to the considerable energy and stress expended establishing and building new burrows. After this initial adjustment period, the decline in contaminant levels followed normal first-order kinetics. For half-life ($T_{1/2}$) calculations, the 5-day sample was considered the zero point of the depuration phase. Many of the chemicals were not detected in the worms at the first samplings in the new aquaria, so their half-lives must be less than 5 days. For the other chemicals, the $T_{1/2}$ ranged from a few weeks to several months. The $T_{1/2}$'s of the chemicals systematically increased with increasing chlorine content and with increasing K_{ow}.

Niimi and Cho (*30*) have shown that half-lives of chemicals in fish should be corrected for "growth dilution" to obtain accurate values. Since we did not label the worms, such a direct correction was not possible in this experiment. But, if it is assumed that the most recalcitrant substance, mirex, is completely retained by the worms, we can estimate the impact of this growth correction on the data (Table II, column 14). As expected, this correction increases the $T_{1/2}$ and is particularly significant for compounds with longer half-lives.

The $T_{1/2}$ values of the chemicals at 20 °C were similar to the 8 °C data. The $T_{1/2}$ for PCB's measured in this study is in reasonable agreement with the value of 27 days reported for marine worms by Elder et al. (*14*).

A limited field sampling of sediments and worms from Lake Ontario sites at 5-km intervals about 10 km off the mouth of the Niagara River was conducted in June 1985 for comparison with the laboratory tests. The data for a few of the study chemicals are shown in Table V. The sediment samples had a similar organic carbon content to the sediment used in the laboratory study. A range of concentration factors was found in the various samples. The lowest concentration factors were observed in the sediments having the highest organic content, indicating a lower bioavailability of contaminants in these sediments. The mean concentration factors (CF) for the field data are as follows: QCB, 0.34; HCB, 0.48; HCBD, 0.43; OCS, 4.6; pp-DDE, 3.2; mirex, 4.0; PCB's, 5.6. The field CF's for QCB, HCB, and HCBD are more than an order of magnitude lower than the laboratory CF's, whereas, for OCS, pp-DDE, mirex, and PCB's, the field CF's are about half the laboratory values. Thus, the field and laboratory data are in reasonable agreement for the more persistent compounds. The reason for the large discrepancy for the other chemicals is likely due to differences in sampling methodology. For the field samples, the period between sample collection and sorting/freezing is of the order of 3 days, whereas for the laboratory experiment this procedure took less than 3 h. It can be seen from Table II that when the worms are removed from their normal environment (sieved and transferred to different sediment), a large decrease of about 1 order of magnitude in the concentration of QCB, HCB, and HCBD was observed. A much smaller change in concentration was found for the more persistent chemicals. Thus, the data for worms in Table V are probably not a true reflection of residue levels for the less persistent chemicals. Sampling, sorting, and freezing must be ac-

complished within a few hours to obtain accurate data for these compounds.

In summary, oligochaete worms can play an important role in the mobilization of contaminants from bottom sediments by bioconcentration and bioturbation. The pore water concentration of the chemicals was the major driving force for contaminant uptake by the worms. The half-lives of the chemicals ranged from less than 5 days to several months depending on chemical structure. The laboratory-derived uptake data provided useful information for developing appropriate field sampling protocols and for predicting bioconcentration factors for worms in the environment.

Acknowledgments

I thank Karen Nicol and Lee Durham for their technical assistance and the Technical Operations Division for their help in sampling the worms and sediments.

Registry No. 1,3-DCB, 541-73-1; 1,4-DCB, 106-46-7; 1,2-DCB, 95-50-1; 1,3,5-TCB, 108-70-3; 1,2,4-TCB, 120-82-1; 1,2,3-TCB, 87-61-6; 1,2,4,5-TeCB, 95-94-3; 1,2,3,4-TeCB, 634-66-2; QCB, 608-93-5; HCB, 118-74-1; 2,4,5-TCT, 6639-30-1; 2,3,6-TCT, 2077-46-5; PCT, 877-11-2; 3,4-DCBTF, 328-84-7; 2,4-DCBTF, 320-60-5; HCBD, 87-68-3; 2,3,4-TCA, 54135-80-7; 1,2,3,4-TeCN, 20020-02-4; OCS, 29082-74-4; αBHC, 319-84-6; lindane, 58-89-9; γ-CHLOR, 5566-34-7; pp-DDE, 72-55-9; pp-DDT, 50-29-3; mirex, 2385-85-5; PCB18, 37680-65-2; PCB31, 16606-02-3; PCB53, 41464-41-9; PCB52, 35693-99-3; PCB40, 38444-93-8; PCB66, 32598-10-0; PCB155, 33979-03-2; PCB153, 35065-27-1; PCB128, 38380-07-3; PCB156, 38380-08-4; PCB171, 52663-71-5; PCB194, 35694-08-7.

Literature Cited

(1) Karickhoff, S. W. *Chemosphere* **1981**, *10*, 833.
(2) Frank, R.; Thomas, R. L.; Holdrinet, M.; Kemp, A. L. W.; Braun, H. E. *J. Great Lakes Res.* **1979**, *5*, 18.
(3) Oliver, B. G.; Nicol, K. D. *Environ. Sci. Technol.* **1982**, *16*, 532.
(4) Van Hove Holdrinet, M.; Frank, R.; Thomas, R. L.; Hetling, L. J. *J. Great Lakes Res.* **1978**, *4*, 69.
(5) Kaminsky, R.; Hites, R. A. *Environ. Sci. Technol.* **1984**, *18*, 275.
(6) Fisher, J. B.; Lock, W. J.; McCall, P. L.; Robbins, J. A. *J. Geophys. Res.* **1980**, *85*, 3997.
(7) Karickhoff, S. W.; Morris, K. R. *Environ. Sci. Technol.* **1985**, *19*, 51.
(8) Oliver, B. G. *Can. J. Fish. Aquat. Sci.* **1984**, *41*, 878.
(9) Eadie, B. J.; Faust, W.; Gardner, W. S.; Nalepa, T. *Chemosphere* **1982**, *11*, 185.
(10) Oliver, B. G.; Niimi, A. J. *Environ. Sci. Technol.* **1983**, *17*, 287.
(11) Borgmann, U.; Whittle, D. M. *Can. J. Fish. Aquat. Sci.* **1983**, *40*, 328.
(12) Fox, M. E.; Carey, J. H.; Oliver, B. G. *J. Great Lakes Res.* **1983**, *9*, 287.
(13) McLeese, D. W.; Metcalfe, C. D.; Pezzack, D. S. *Arch. Environ. Contam. Toxicol.* **1980**, *9*, 507.
(14) Elder, D. L.; Fowler, S. W.; Polikarpov, G. G. *Bull. Environ. Contam. Toxicol.* **1979**, *21*, 448.
(15) Lynch, T. R.; Johnson, H. E. In *Aquatic Toxicology and Hazard Assessment: Fifth Conference*; Pearson, J. G.; Foster, R. B.; Bishop, W. E., Eds.; American Society for Testing and Materials: Philadelphia, PA, 1982; ASTM STP766, pp 273–287.
(16) Karickhoff, S. W. In *Contaminants and Sediments*; Baker, R. A., Ed.; Ann Arbor Science: Ann Arbor, MI, 1980; Vol. II, pp 193–205.
(17) Oliver, B. G.; Nicol, K. D. *Chromatographia* **1982**, *16*, 336.
(18) Banerjee, S.; Yalkowsky, S. H.; Valvani, S. C. *Environ. Sci. Technol.* **1980**, *14*, 1227.
(19) Köneman, H.; Zelle, R.; Busser, F.; Hammers, W. E. *J. Chromatogr.* **1979**, *178*, 559.
(20) Chiou, C. T.; Schmedding, D. W. *Environ. Sci. Technol.* **1982**, *16*, 4.
(21) Hansch, C.; Leo, A. *Substituent Constants for Correlation Analysis in Chemistry and Biology*; Wiley: New York, 1979.
(22) Kaiser, K. L. E. *Chemosphere* **1983**, *12*, 1159.
(23) Veith, G. D.; DeFoe, D. L.; Bergstedt, B. U. *J. Fish. Res. Board Can.* **1979**, *36*, 1040.
(24) Kurihara, N.; Uchida, M.; Fujita, T.; Nakajima, M. *Pestic. Biochem. Physiol.* **1973**, *2*, 383.
(25) O'Brien, R. D. In *Environmental Dynamics of Pesticides*; Hague, R.; Freed, V. H., Eds.; Plenum: New York, 1974; pp 331–342.
(26) Ballschmiter, K.; Zell, M. *Fresenius' Z. Anal. Chem.* **1980**, *302*, 20.
(27) Oliver, B. G.; Bourbonniere, R. A. *J. Great Lakes Res.* **1985**, *11*, 366.
(28) Oliver, B. G. *Chemosphere* **1985**, *14*, 1087.
(29) Oliver, B. G.; Niimi, A. J. *Environ. Sci. Technol.* **1985**, *19*, 842.
(30) Niimi, A. J.; Cho, C. Y. *Can. J. Fish. Aquat. Sci.* **1981**, *38*, 1350.

Received for review August 29, 1986. Accepted March 31, 1987.

Environ. Sci. Technol. 1987, 21, 791–798

Structural Characterization of Aquatic Humic Material. 2. Phenolic Content and Its Relationship to Chlorination Mechanism in an Isolated Aquatic Fulvic Acid

Daniel L. Norwood* and Russell F. Christman

Department of Environmental Sciences and Engineering, School of Public Health, University of North Carolina, Chapel Hill, North Carolina 27514

Patrick G. Hatcher

United States Geological Survey, Reston, Virginia 22092

■ The complementary techniques of solid-state ^{13}C nuclear magnetic resonance spectroscopy and chemical degradation were utilized to examine the lignin/phenolic substructure of an isolated aquatic fulvic acid capable of producing upon aqueous chlorination a number of organohalides typically found in municipal drinking water. Results indicate that while phenolic moieties are present in the fulvic acid, they account for only a minor fraction of the total carbon. A sequential chemical degradation experiment utilizing aqueous chlorine and CuO demonstrated that the lignin/phenolic substructure was attacked by the chlorine. It is concluded that while phenolic ring rupture mechanisms appear to be important in organohalide generation, other aqueous chlorination mechanisms involving aliphatic and other types of aromatic structures should also be considered.

Introduction

It is well documented that disinfection of natural waters with aqueous chlorine results in drinking waters that contain organically bound halogen (referred to as total organic halide or TOX). A portion of this TOX is composed of volatile, relatively hydrophobic organohalides such as the trihalomethanes, principally chloroform (*1*). Another portion is composed of hydrophilic organohalides, principally di- and trichloroacetic acids (*2–4*). It is attractive to hypothesize that rupture of phenolic rings contained in natural aquatic humic material by aqueous chlorine is the principal formation pathway for TOX. Indeed, such mechanisms have been invoked to rationalize the formation of certain organohalides produced from the aqueous chlorination of humic substances (*5–7*).

Isolated aquatic humic substances, however, produce a significant number and variety of chlorinated organic compounds when subjected to aqueous chlorination (*8–11*). For certain of these organohalides, phenolic ring rupture is not the most likely formation pathway.

Humic substances are complex, macromolecular organic structures formed during the diagenesis of plant material. They are ubiquitous throughout the environment and constitute the bulk of organic material in soil and approximately half of the dissolved organic carbon in terrestrial streams (*12, 13*). Lignin, a phenolic polymer and a major component of woody tissue, is thought to be an important precursor for humic substances. The lignin/phenol content of humic substances has been extensively investigated via oxidative chemical degradation (*14*). Alkaline solutions of cupric oxide (CuO) (*15, 16*) as well as other oxidizing agents (*14*) have been used to degrade lignin and humic substances with the resulting production of phenolic aldehydes and acids.

Solid-state carbon-13 nuclear magnetic resonance spectroscopy (^{13}C NMR) employing cross-polarization (CP), magic-angle spinning (MAS), and high-power proton decoupling is a relatively new technique that is being widely utilized to assess qualitative and quantitative carbon distributions in humic substances (*17*) and other macromolecular materials (*18, 19*). The technique is capable of assessing oxygen-substituted aromatic carbon contents in lignins (*19*) and humic substances (*20*), providing a powerful complement to chemical degradation.

This paper describes the application of NMR techniques [including CP/MAS ^{13}C NMR, relaxation experiments, and proton (^1H NMR)] and chemical degradation procedures to an isolated aquatic fulvic acid. Inferences are drawn from the combination of NMR and chemical degradation results regarding the overall macromolecular structure and mechanisms of chlorination of the aquatic fulvic acid.

Experimental Methods

Fulvic Acid Isolation. Aquatic fulvic acid was isolated from Singletary Lake according to the adsorption chromatography procedure of Thurman and Malcolm (*21*). Singletary Lake is a highly colored natural lake located on the North Carolina coastal plain near Black Lake. The latter was utilized as a source of humic substances in several prevous studies (*3, 4, 8–11*), including the first in this series (*22*). Lignin utilized in this study was extracted from Douglas fir according to Hatcher (*23*). Soil- and peat-derived humic substances were obtained according to procedures described by Hatcher et al. (*20*).

Elemental Analysis. Elemental analysis of solid fulvic acid samples was accomplished by Huffman Laboratories, Inc., Wheat Ridge, CO, utilizing standard gravimetric procedures (*24*).

^1H NMR. ^1H NMR spectra were acquired at 250 MHz with a Bruker WM-250 Fourier transform spectrometer (Bruker Instruments, Inc., Manning Park, Billerica, MA). Two hundred scans were averaged with a total cycle time of 2 s to produce an acceptable spectrum.

^{13}C NMR. ^{13}C NMR spectra of aquatic humic substances in the solid state were obtained by the cross-polarization, magic-angle spinning (CP/MAS) technique with high-power proton decoupling. A Chemagnetics CMC100 spectrometer (Chemagnetics, Fort Collins, CO) equipped with a 2.35-T superconducting magnet (25.2 MHz for carbon) was utilized for these experiments. Each pulse experiment involved the basic sequence of events described by Hatcher et al. (*25*), with a 1-ms cross-polarization contact time according to the Hartman–Hahn condition (*26*) and 500-ms–1-s pulse delay. The solid fulvic acid was held in a 300-μL KEL-F rotor and spun at a rate of 3.2 kHz

*Address correspondence to Research Triangle Institute, Analytical and Chemical Sciences, Research Triangle Park, NC 27709.

0013-936X/87/0921-0791$01.50/0

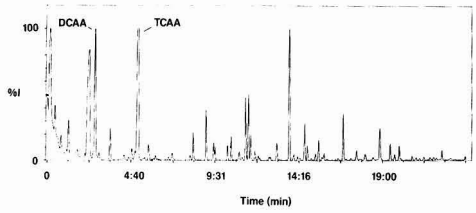

Figure 1. EI total ion chromatogram of the ether-extractable aqueous chlorination products of Singletary Lake fulvic acid: 15 m × 0.2 mm DB-1 fused silica capillary column (J&W Scientific, Rancho Cordova, CA); injector temperature 270 °C; initial column temperature 60 °C (2-min initial hold); 6 deg/min program; final column temperature 250 °C; 10:1 split injection.

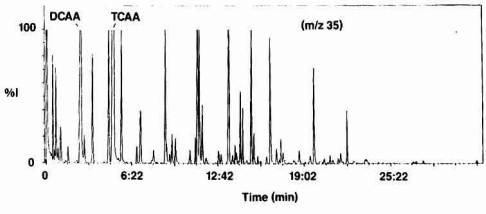

Figure 2. NCI selected mass chromatogram (m/z 35) of the ether-extractable aqueous chlorination products of Singletary Lake fulvic acid.

at the magic angle (54.7° to the applied field) over the course of the experiment. CP/MAS ^{13}C NMR relaxation studies involved alternate pulse sequences, which are described later. Relative amounts of various types of protons and carbons were determined by area measurement of the appropriate spectral regions. It has been determined in this laboratory that errors in such area measurements are approximately ±5%.

Aqueous Chlorination. Procedures for the chlorination and analysis of the resulting organohalide products from Singletary Lake fulvic acid were similar to those described previously for Black Lake fulvic acid (*9, 11*). To summarize, 300 mg of fulvic acid was reacted in 450 mL of pH 11.2 NaOH solution at an initial chlorine-to-carbon (HOCl/C) molar ratio of 2:1 under headspace-free conditions. No buffers were employed, and the pH was allowed to drop to 9.6 over the 26-h reaction time period. A quenched, acidified 300-mL aliquot was removed for ether extraction, concentration, derivatization (diazomethylation), and qualitative analysis by combined gas chromatography/mass spectrometry (GC/MS). A system blank including all components except the fulvic acid was chlorinated and subjected to an identical analytical procedure.

The GC/MS system and analytical conditions employed were the same as those utilized in previous studies (VG 7070F GC/MS system) (*3, 4, 8–11*). Chromatography conditions are indicated in Figure 1. The operation of the VG 7070F instrument in the low-resolution electron ionization (EI) mode has been described (*11*). Isobutane positive chemical ionization (PCI), negative chemical ionization (NCI, isobutane buffer gas), and low-resolution accurate mass measured EI spectra (tetraiodoethylene internal reference) were collected as a complement, utilizing the manufacturer's recommended conditions.

CuO Oxidation. CuO oxidation of Singletary Lake fulvic acid and the extraction and analysis of the resulting oxidation products were carried out by the procedures described by Hedges and Ertel (*16*) with only minor modification. Quantification of individual ether-extractable phenols was achieved by gas chromatographic analysis (Perkin-Elmer Sigma 2; Perkin-Elmer, Norwalk, CT) with flame ionization detection (FID) of the corresponding trimethylsilyl derivatives in pyridine under appropriate GC conditions (*16*). Mass spectral analyses were carried out on the VG 7070F system.

Sequential Chemical Degradation. The first degradation in the sequence was aqueous chlorination. Singletary Lake fulvic acid (301 mg) was reacted in 450 mL of deionized/distilled water at an initial chlorine-to-carbon molar ratio of 0.3:1 and neutral pH for 5 h and 40 min in the dark. The final reaction mixture pH (before sodium arsenite quenching) was 5.

Partially reacted fulvic acid was isolated from the reaction mixture by absorption onto a 200-mL bed volume column to solvent-extracted (acetone/hexane) XAD-8 resin (Rohm and Haas, Philadelphia, PA). The acidified (pH 1) reaction mixture was then eluted through the column at a flow rate of 5 mL/min. The column was then eluted with one column volume of distilled/deionized water to remove chloride, followed by one column volume of 0.1 N NaOH to desorb the fulvic acid. A brightly colored solution of 350-mL volume was collected and was immediately passed through a 130-mL bed volume column of methanol-extracted AG-MP-50 (Rohm and Haas) cation-exchange resin at a moderate flow rate for desalting. The resulting solution was lyophilized (Labconco Model 18, Fisher) to produce 150 mg of solid hydrogen exchanged fulvic acid.

CuO oxidation was used as the second degradation in the sequence. Chromatographic analyses of oxidation products were performed on the Perkin-Elmer system and on a Carlo-Erba 5160 HRGC (Carlo-Erba, Milan, Italy) utilizing the previously indicated conditions.

Results and Discussion

Elemental Analysis. The elemental composition of Singletary Lake fulvic acid (average of eight different batch determinations) was determined to be C 53.06% (S_x = 1.21), H 4.57% (S_x = 0.36), and N 1.22% (S_x = 0.32) on an ash-free basis. The resulting H/C ratio of 1.03 is in the range reported for aquatic humic substances by Thurman (*27*) and indicates a relatively high degree of unsaturation and/or heteroatom substitution. The C/N ratio of 50.7 is also typical of aquatic humic substances (*27*).

Aqueous Chlorination. A reconstructed total ion chromatogram (EI) of the methylated product ether extract is shown in Figure 1. The identification of individual chlorination products utilized the EI fragmentation pattern, an element map provided by the accurate mass measured EI spectrum, and the protonated molecular ion from the PCI spectrum (when available). Where authentic standards were available these were analyzed and their EI spectra and retention indices (relative to methyl *p*-chlorobenzoate internal reference) compared with the appropriate unknown data set. The complexity of the organohalide product mixture is indicated in Figure 2, which shows an NCI mass chromatogram of m/z 35 (Cl^-). Each chromatographic peak represents an individual organohalide.

Figure 1 also indicates two of the most prominent organohalides formed, dichloroacetic acid (DCAA) and trichloroacetic acid (TCAA). These and several other of the 20 major organohalide products are listed in Table I. Table I includes examples of possible phenolic ring rupture products (chloroform, dichloromaleic acid) as well as products that are not so easily rationalized by such mechanisms (dichlorosuccinic acid). The overall distribution of organohalides and other chlorination products

Table I. Major Organohalide Chlorination Products

$CHCl_3$	chloroform	*a*
$HCCl_2CO_2H$	dichloroethanoic acid (dichloroacetic acid, DCAA)	
CCl_3CO_2H	trichloroethanoic acid (trichloroacetic acid, TCAA)	*a*
$HO_2CCCl_2CO_2H$	dichloropropanedioic acid (dichloromalonic acid)	*b*
$HO_2CCCl_2CH_2CO_2H$	2,2-dichlorobutanedioic acid (dichlorosuccinic acid)	*b*
$HO_2CCCl{=}CClCO_2H$	*cis*-dichlorobutenedioic acid (dichloromaleic acid)	*a*

[a] Confirmed. EI spectrum and GC retention index match those of an authentic standard; other spectral data agree. [b] Confident. Sufficient data are available to preclude all but the most closely related structures.

Table II. ^{13}C (A) and ^{1}H (B) Chemical Shift Regions

region	carbon type	% contribution
I (0–50 ppm)	methyl, methylene, methine (etc.)	29
II (50–110 ppm)	alcohol, amine, carbohydrate, ether, methoxyl, acetal (etc.)	22
III (110–160 ppm)	olefinic, aromatic, phenolic	21
IV (160–220 ppm)	carboxyl, ester, amide, aldehyde, ketone	24

region	proton type	% contribution
I (0.4 – 1.7 ppm)	methyl, methylene, methine (etc.)	38
II (1.7–3.3 ppm)	methyl, methylene (α to aromatic rings or carboxyl groups), α and β groups of indanes and tetralins	36
III (3.3–4.6 ppm)	protons on carbons, α to oxygen	16
IV (6.5–8.1 ppm)	aromatic	9

is qualitatively and semiquantitatively identical with those observed in previous studies (*8–11*) from other aquatic humic substances.

^{13}C and ^{1}H NMR Spectral Interpretations. CP/MAS ^{13}C and ^{1}H NMR spectra of Singletary Lake fulvic acid are shown in Figure 3. The CP/MAS spectrum (Figure 3A) resulted from the collection and averaging of 95 000 individual free-induction decays and is striking similar to spectra reported for other aquatic fulvic acids (*27*). Our treatment of these data is patterned after the work of Hatcher et al. (*20*) and divides the spectrum into four regions as outlined in part A of Table II. These include region I, paraffinic carbons; region II, aliphatic carbons substituted with oxygen; region III, aromatic/olefinic carbons; and region IV, carbonyl carbons.

The most interesting piece of information contained in this spectrum is the relative importance of aliphatic structures in this aquatic fulvic acid (regions I and II). The anisotropic peak in region I with resonance maxima at 23.5 and 40.8 ppm is probably due to highly cross-linked methylene and methine carbon chains. Region II shows an intense resonance centered at 76 ppm, which is usually assigned to a polyhdyroxy aliphatic carbon such as carbohydrate carbon. The presence of carbohydrates cannot, however, be confirmed since a distinct peak for the anomeric carbon of polysaccharides (105 ppm) is not present. The aliphatic carbon in these two spectral regions accounts for 51% of the total carbon.

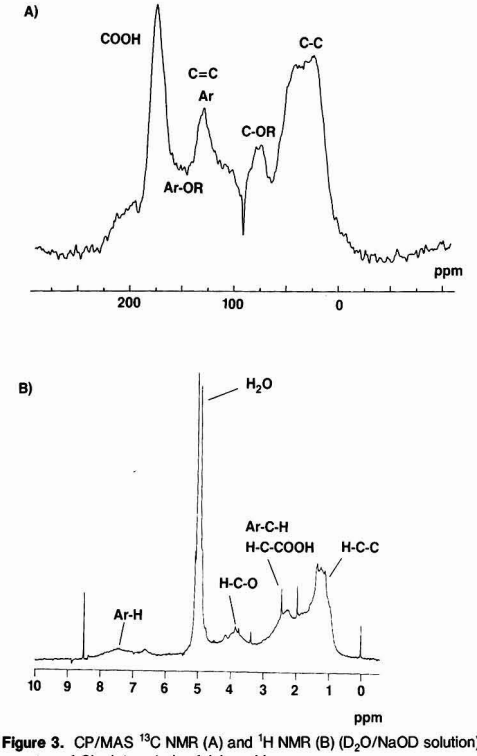

Figure 3. CP/MAS ^{13}C NMR (A) and ^{1}H NMR (B) (D_2O/NaOD solution) spectra of Singletary Lake fulvic acid.

The aromatic/olefinic region (III) has a maximum centered at 129 ppm, most likely due to aromatic carbons not substituted with heteroatoms. Oxygen-substituted aromatic carbons of phenols and aryl ethers should exhibit signals at approximately 150 ppm. Note that a reasonably intense shoulder but no distinct peak is apparent at 150 ppm in this spectrum. The aromatic region accounts for 21% of the total fulvic acid carbon, which translates to three aromatic rings per 100 carbon atoms in the macromolecule. These results are surprising with regard to the traditional view of humic chlorination chemistry that emphasizes the reactivity of aromatic organohalide precursors. The carbonyl region (IV) has a maximum at 173 ppm (carbonyl of carboxy groups) and a more diffuse resonance centered at approximately 205 ppm (carbonyl of aldehydes and ketones).

A typical proton spectrum of Singletary Lake fulvic acid appears in Figure 3B. Our interpretations have been influenced by Wilson's (*17*) summary of chemical shift assignments for humic substances and are summarized in part B of Table II. Like the CP/MAS spectrum, the proton spectrum can be divided into four regions. These include region I, protons on aliphatic carbons at least two carbons removed from aromatic rings or other polar functional groups; region II, protons on carbons α to aromatic rings or carboxyl groups; region III, protons on carbons attached to oxygen functions; and region IV, protons bound to aromatic rings. Note the excellent correlation between this proton spectrum and the CP/MAS spectrum. An interesting observation is that the aromatic protons account for only 9.2% of the total nonexchangeable proton whereas 21% of the carbon is present in aromatic rings. This result implies that aromatic rings

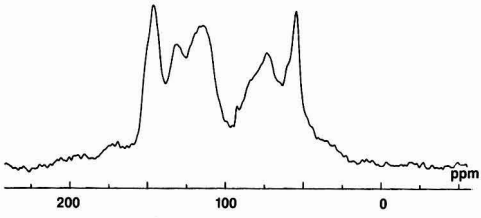

Figure 4. CP/MAS ^{13}C NMR spectrum of a lignin extracted from Douglas fir.

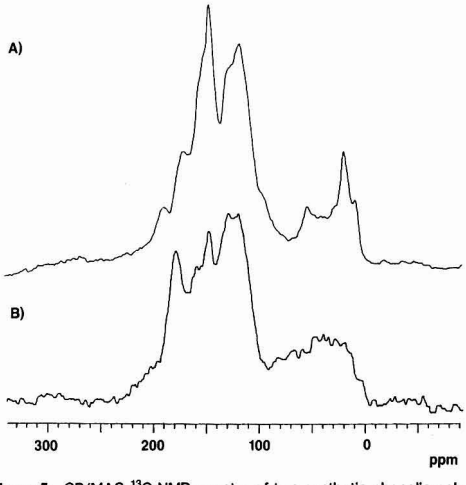

Figure 5. CP/MAS ^{13}C NMR spectra of two synthetic phenolic polymers formed from (A) hydroxytoluenes and phenols and (B) hydroxybenzoic acids.

present in the fulvic acid macromolecular structure are heavily substituted. Olefinic protons should be observed in the 5.0–6.5 ppm region, and although the water peak prevents the results from being conclusive, few if any appear to be present.

CP/MAS Spectra of Phenolic Polymers. Lignin is a natural polymer (composed of oxygen-substituted phenylpropane units) that is a primary constituent of woody tissue and is thought to be an important precursor for humic substances. The CP/MAS spectrum of a softwood lignin is presented in Figure 4. This spectrum shows five principal resonances. Two maxima in the aliphatic region centered at 55 and 75 ppm are due to methoxyl carbon and other oxygen-substituted aliphatic carbons, respectively. Three other resonances are in the aromatic/olefinic region at approximately 110, 130, and 150 ppm. The peak at 150 ppm represents oxygen-substituted aromatic carbons of the phenols and methoxyl-substituted aromatic rings. The other two resonances are due to non-heteroatom-substituted aromatic carbons.

If Singletary Lake fulvic acid contains intact or slightly modified lignin as a major constituent, one would expect to find resonance maxima at these five points. An examination of Figure 3A shows maxima at 75 and 130 ppm but only shoulders at 55, 120, and 150 ppm.

Other phenolic polymers are also available. Figure 5 shows the CP/MAS spectra of two phenolic polymers synthesized as "model humic acids" by Martin and coworkers (*28*, *29*). One polymer was made from a series of hydroxytoluenes and phenols and the other from a series of hydroxybenzoic acids. Resonances characteristic of

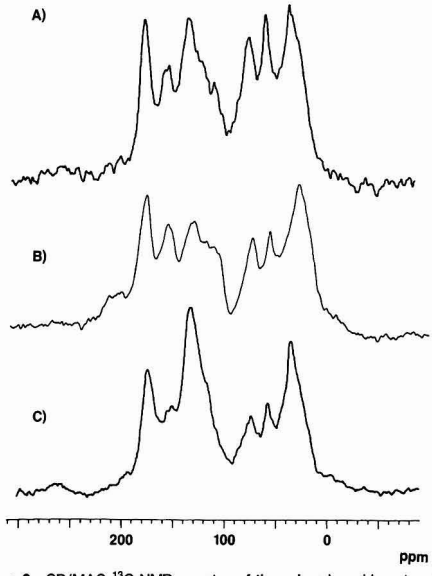

Figure 6. CP/MAS ^{13}C NMR spectra of three humic acids extracted from (A) Everglades peat, (B) histosol soil, and (C) mollisol soil.

oxygen-substituted aromatic structures are apparent in both spectra (120 and 150 ppm). The polymer derived from hydroxytoluenes and phenols also shows a peak at 15 ppm characteristic of terminal methyl groups on the toluenes, and the polymer derived from hydroxybenzoic acids shows a peak at 180 ppm characteristic of carbonyl carbon of carboxyl groups. Significant quantities of these phenols incorporated into Singletary Lake fulvic acid should produce characteristic resonances present in these synthetic polymers.

The above discussion begs the question: Can any humic material be found that exhibits resonances indicative of lignin/phenol content? Figure 6 shows CP/MAS spectra from three soil- and peat-derived humic substances that clearly show such signals in varying amounts. This is further evidence that Singletary Lake fulvic acid is not predominantly composed of such structures.

CP/MAS Relaxation Studies. Spin–lattice relaxation in pulse NMR is defined as the overall process by which the Boltzmann energy distribution of nuclear spins is reestablished after an rf pulse. The exponential relaxation process is defined by a spin–lattice relaxation time (T_1). For a comprehensive treatment of relaxation theory and measurement the reader is referred to Levy et al. (*30*) and Fukushima and Roeder (*31*). In CP/MAS experiments, the spin–lattice relaxation time of protons observed through carbons [T_1(H)] determines the rate at which pulsing can be repeated in order to achieve quantitative results. An "inversion–recovery" experiment (*30*) for T_1(H) measurement in Singletary Lake fulvic acid is shown in Figure 7. These spectra were generated with the alternate pulse sequence described by Levy et al. (*30*) and Wilson et al. (*32*). The τ value resulting in the nulled spectrum defines the average T_1(H). At this point T_1(H) may be estimated as follows: $T_1(H) = \tau/\ln 2 \simeq 14.4$ ms. The 500-ms–1-s pulse delays were, therefore, adequate for spin reequilibration, and saturation should not be a problem with these experiments.

Cross-polarization contact time must also be optimized in order to achieve sensitive and quantitative results.

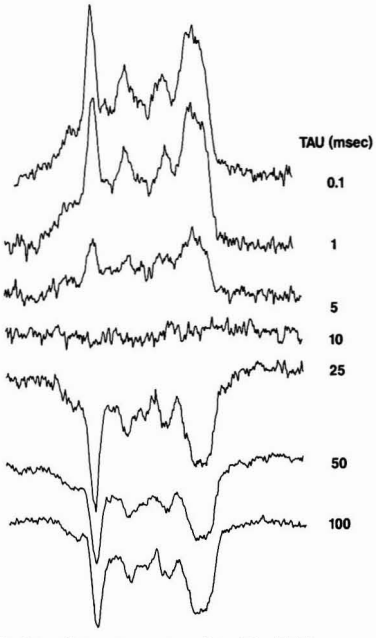

Figure 7. Inversion–recovery experiment for T_1(H) measurement in Singletary Lake fulvic acid.

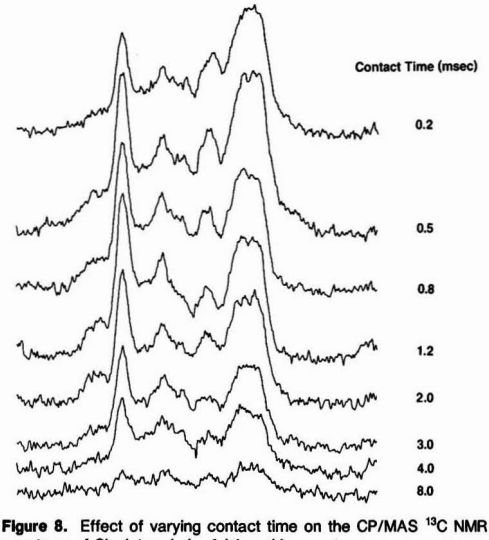

Figure 8. Effect of varying contact time on the CP/MAS ^{13}C NMR spectrum of Singletary Lake fulvic acid.

Figure 8 shows the influence of varying contact time on the CP/MAS spectrum of Singeltary Lake fulvic acid. The decay of signal is termed proton relaxation under the influence of the spin locking field (*30–32*) as observed through carbon and is defined by a relaxation time $T_{1\rho}$(H). From this experiment, $T_{1\rho}$(H) for Singletary Lake fulvic acid was determined to be 3.95 ms; therefore, a contact time of 1 ms was deemed optimum.

Differences in relaxation and signal dephasing rates for carbon atoms under a variety of $^1H/^{13}C$ dipolar interactions can be utilized to produce CP/MAS spectra free from certain carbon atom types. The "dipolar dephasing" pulse

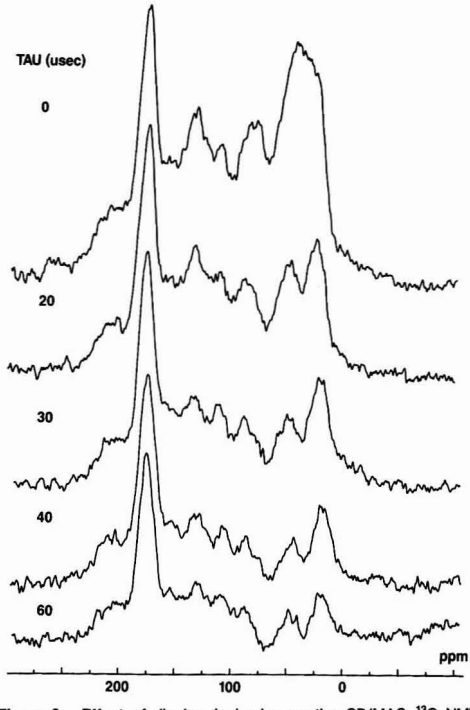

Figure 9. Effect of dipolar dephasing on the CP/MAS ^{13}C NMR spectrum of Singletary Lake fulvic acid.

sequence, first applied to humic substances by Wilson et at. (*32*), can produce spectra free from signals produced by CH and CH_2 carbons. In this experiment the normal CP/MAS pulse program is modified to include a time period (τ) after cross-polarization contact in which the decoupler is gated off. After τ the decoupler is turned back on and the signal collected. During τ, $^1H/^{13}C$ dipolar interactions take place with a resulting dephasing of signals from CH and CH_2 carbons.

The dipolar dephasing experiment for Singletary Lake fulvic acid is shown in Figure 9. In spectral region I (Table IIA) there is a rapid loss of signal as τ increases, indicating that much of this aliphatic carbon is protonated. The main resonance also splits into two peaks centered at approximately 20 and 50 ppm in the $\tau = 40$ μs spectrum. The 20 ppm signal is probably due to terminal methyl groups [which behave as if they were nonprotonated because rapid molecular motion effectively reduces ^{13}C–^1H dipolar interactions (*32*)] while the 50 ppm signal may be due to methoxyl or quaternary carbon. Other nonprotonated aliphatic carbon may also contribute to these signals.

The most interesting results appear in region III where a loss of aromatic/olefinic signal is apparent, implying significant aromatic protonation. It is difficult to reconcile this observation with the proton spectrum. The loss of aromatic signal is, however, useful in that it reduces peak overlap and reveals a definite signal from oxygen-substituted aromatic carbon in the $\tau = 40$ μs spectrum centered at approximately 150 ppm. This is the first clear indication from CP/MAS spectra that phenolic structures are present in Singletary Lake fulvic acid.

Evidence that the dipolar dephasing results are being correctly interpreted is given in Figure 10, which shows the result of a 40-μs dephasing experiment on the hy-

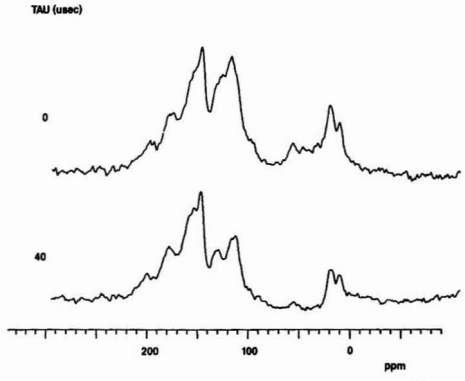

Figure 10. Effect of dipolar dephasing on the CP/MAS ^{13}C NMR spectrum of the synthetic phenolic polymer formed from hydroxytoluenes and phenols.

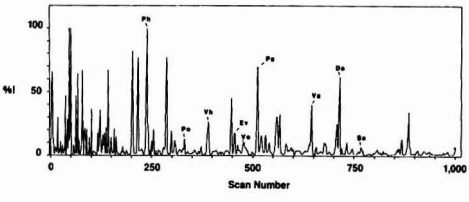

Figure 11. EI total ion chromatogram of the ether-extractable CuO oxidation products of Singletary Lake Fulvic acid.

droxytoluene/phenol synthetic polymer. There is no loss of signal from oxygen-substituted aromatic carbon (150 ppm), carbonyl carbon (170–220 ppm), or terminal methyl groups on the toluenes (10–20 ppm). It is further comforting to note that in region IV of the Singletary Lake spectra there is little loss of carbonyl signal from the carboxyl group peak.

CuO Oxidation. Qualitative and quantitative analysis of ether-extractable oxidation products first employed a target compound approach. Individual target compounds can be divided into five categories: *p*-hydroxyl (P), vanillyl (V), syringyl (S), cinnamyl (C), and *m*-dihydroxy (D). The V, S, and C phenols are considered to be lignin derived (*16*). The *p*-hydroxylphenols have been found as CuO oxidation products of nonvascular plants and are not considered to be unambiguously lignin derived. *m*-Dihydroxy structures are not components of lignin but may be found in flavonoids and other similar compounds (*33*).

A reconstructed total ion chromatogram of the ether-extractable oxidation products from Singletary Lake fulvic acid is shown in Figure 11. Column A in Table III lists the identified oxidation products together with their average yields for the duplicate oxidation reactions. The identification of most of the target compounds indicates that Singletary Lake fulvic acid does indeed possess a phenolic structure partly composed of intact lignin subunits. Many of these phenols were previously shown to be reactive with aqueous halogen (*6*, *7*). Of particular interest is 3,5-dihydroxybenzoic acid, which aside from *p*-hydroxybenzaldehyde (whose quantification may be overestimated due to interferences), was the most abundant phenol produced. This structure undergoes aqueous halogenation by a ring rupture mechanism to produce chloroform and other aliphatic chlorinated acids (*7*).

The discovery of 3,5-dihydroxybenzoic acid brings up the pervasive issue of artifact formation in the CuO reaction. We define artifact in this instance as an oxidation product whose formation pathway is incorrectly interpreted. Cheshire et al. (*34*) have detected this structure from the KOH fusion at elevated temperature of synthetic polymers derived from *o*- and *p*-benzoquinones and furfural as well as from a peat-derived humic acid. They postulated that 3,5-dihydroxybenzoic acid was a secondary substance "resulting from the breakdown of the complex products into relatively simple units which recombine under the fusion condition". This conclusion can be criticized since the synthetic "polymers" were not characterized and secondary reactions may have taken place during the "polymerization" to produce *m*-dihydroxy structures. However, these criticisms are as much without verification as Cheshire's conclusions. It may be impossible to demonstrate the absence of artifact formation from oxidation of a complex natural product like aquatic fulvic acid; however, in our opinion it is asking a great deal of an artifact-generating reaction to produce phenols known to constitute lignin and related plant components as major products.

Table III. CuO Oxidation Products from Singletary Lake Fulvic Acid

target compound	yield, mg/g of C	
	A[a]	B[b]
p-hydroxybenzaldehyde (Ph)	1.93[c,d]	ND[e]
p-hydroxyacetophenone (Po)	0.351[c]	trace
p-hydroxybenzoic acid (Pa)	0.902[c]	0.640[c,d]
vanillin (Vh)	0.654[c]	0.550[c,d]
acetovanillone (Vo)	0.146[c,d]	0.329[c,d]
vanillic acid (Va)	0.738[c]	0.933[c,d]
syringaldehyde (Sh)	0.170[c,d]	ND
acetosyringone (So)	0.211[c,d]	ND
syringic acid (Sa)	0.202[c,d]	ND
trans-*p*-coumaric acid (Ca)	0.138[c,d]	trace
3,5-dihydroxybenzoic acid (Da)	1.08[c]	0.672[c,d]
trans-cinnamic acid (Cn)	trace[c]	ND
ethylvanillin (Ev)	IS[f]	IS[f]

[a] Unreacted Singletary Lake fulvic acid; average of two CuO degradations. [b] Partially chlorinated Singletary Lake Fulvic acid; average of two CuO degradations. [c] Component identification confirmed by comparison of electron ionization mass spectrum and gas chromatographic retention index relative to ethylvanillin with those of an authentic standard. [d] The presence of coeluting components may have caused an overestimation of yield. [e] Not detected. [f] Internal standard.

Sequential Chemical Degradation. The partially reacted fulvic acid isolated from the aqueous chlorination solution was subjected to duplicate to CuO oxidation and product analysis. As a first approach to observing possible effects of aqueous chlorination it is instructive to compare the general chromatographic appearance of the CuO product mixtures from raw and partially reacted Singletary Lake fulvic acid. Figure 12 illustrates this comparison with FID chromatograms (Carlo-Erba GC). The two product mixtures were derived from approximately the same amount of starting material, and the dilutions and internal standard (Ev) amounts were exactly the same.

The first obvious conclusion is that the CuO product distributions from the two materials are different. Further, the difference appears to be selective and quantitative in nature. Certain products that dominate the raw fulvic acid product mixture, such as 3,5-dihydroxybenzoic acid (Da), appear to be much less important from the chlorinated residue. The corresponding mass spectra data reveal that all of the target phenols are reduced in the chlorinated mixture relative to other components. Notice especially the relative size of the four large peaks between 10 and 13 min compared to Da and Ev for the two product mixtures.

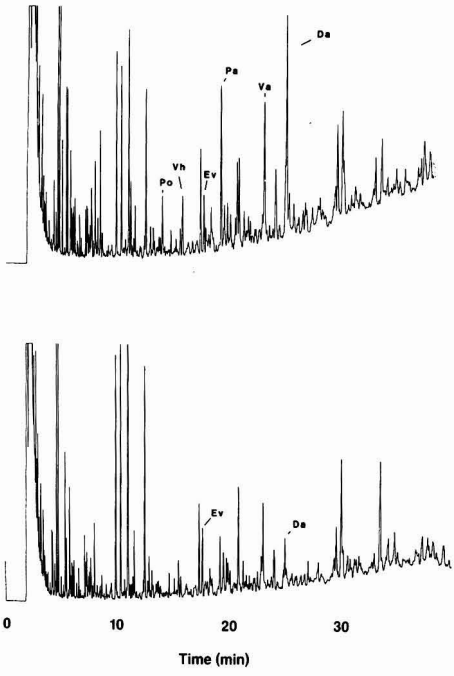

Figure 12. FID chromatograms of the ether-extractable CuO oxidation products of (A) Singletary Lake fulvic acid and (B) partially chlorinated Singletary Lake fulvic acid (Carlo-Erba GC).

Yields of the target phenols normalized to the amount of starting carbon are given in Table III, column B. Note that the presence of only five of the phenols (Pa, Vh, Vo, Va, and Da) could be confirmed by mass spectrometry compared with eleven from the raw fulvic acid. Six other phenols (Ph, Po, Sh, So, Sa, and Ca) detected from the raw fulvic acid were either not detected or were present at only trace levels. The vanillyl phenols appear to have been least affected by the aqueous chlorination process with measured yields changing only slightly. The 3,5-dihydroxybenzoic acid yield was apparently reduced by aqueous chlorination by 40%.

It is attractive to assume that the observed differences in CuO product distribution from these two samples are due to the effects of mild aqueous chlorination. In our opinion, however, these sequential chemical degradation results should be considered tentative until they can be confirmed by analysis of a humic substance with greater phenolic content.

Conclusions

The major conclusions derived from this work may be summarized as follows:

(1) Singletary Lake fulvic acid produces aqueous chlorination products identical with those produced from other isolated aquatic fulvic acids (*11*). Many of these products are indicative of phenolic ring rupture mechanisms.

(2) Singletary Lake fulvic acid contains a measureable phenolic substructure, some of which is lignin derived.

(3) Mild aqueous chlorination appears to alter this phenolic substructure selectively and quantitatively.

Reactive phenolic structures within the aquatic humic macromolecular system are further implicated as precursors for the formation of organohalides in drinking water. It remains to be determined whether sufficient phenolic content is present to account for the majority of TOX or if other potential precursor structures should be investigated.

NMR data in this study indicate that aliphatic and non-heteroatom-substituted aromatic carbon types constitute the majority of carbon in this fulvic acid. The formation of certain organohalides may be better rationalized by invoking such structures as precursors. A similar dominance of these carbon types was noted for an extracted aquatic sedimentary fulvic acid by Saleh et al. (*35*). They speculated that this result was artifactual, caused by the masking of phenols and other heteroatom-substituted carbons by stable free radicals present in the solid fulvic acid. Although this cannot be ruled out in the case of Singletary Lake fulvic acid, it should be pointed out that all natural and synthetic phenolic polymers examined in this study as well as a number of soil- and peat-derived humic substances showed appropriate signals for these latter types of carbon.

Acknowledgments

We express our appreciation to Robert Haddad, Chris Martens, J. Donald Johnson, D. S. Millington, and J. Ronald Hass for their invaluable assistance. The samples of synthetic phenolic polymers were provided by J. P. Martin.

Literature Cited

(1) Rook, J. J. *Water Treat. Exam.* **1974**, *23*, 234–243.
(2) Uden, P. C.; Miller, J. W. *J.—Am. Water Works Assoc.* **1983**, *75*, 524–527.
(3) Norwood, D. L.; Thompson, G. P.; Johnson, J. D.; Christman, R. F. In *Water Chlorination: Chemistry, Environmental Impact and Health Effects*; Jolley, R. L., Bull, R. J., Davis, W. P., Katz, S., Roberts, M. H., Jacobs, V. A., Eds.; Lewis: Chelsea, MI, 1985; Vol. 5, Chapter 89.
(4) Norwood, D. L.; Christman, R. F.; Johnson, J. D.; Hass, J. R. *J.—Am. Water Works Assoc.* **1986**, *78*, 175–180.
(5) Rook, J. J. *J.—Am. Water Works Assoc.* **1976**, *68*, 168–172.
(6) Norwood, D. L.; Johnson, J. D.; Christman, R. F.; Hass, J. R.; Bobenrieth, M. J. *Environ. Sci. Technol.* **1980**, *14*, 187–190.
(7) Boyce, S. D.; Hornig, J. F. *Environ. Sci. Technol.* **1983**, *17*, 202–211.
(8) Christman, R. F.; Johnson, J. D.; Pfaender, F. K.; Norwood, D. L.; Webb, M. R.; Hass, J. R.; Bobenrieth, M. J. In *Water Chlorination: Environmental Impact and Health Effects*; Jolley, R. L., Brungs, W. A., Cumming, R. B., Jacobs, V. A., Eds.; Ann Arbor Science: Ann Arbor, MI, 1980; Vol. 3, Chapter 7.
(9) Norwood, D. L.; Johnson, J. D.; Christman, R. F.; Millington, D. S. In *Water Chlorination: Environmental Impact and Health Effects*; Jolley, R. L., Brungs, W. A., Cotruvo, J. A., Cumming, R. B., Mattice, J. S., Jacobs, V. A., Eds.; Ann Arbor Science: Ann Arbor, MI, 1983; Vol. 4, Chapter 13.
(10) Johnson, J. D.; Christman, R. F.; Norwood, D. L.; Millington, D. S. *EHP, Environ. Health Perspect.* **1982**, *46*, 63–71.
(11) Christman, R. F.; Norwood, D. L.; Millington, D. S.; Johnson, J. D.; Stevens, A. A. *Environ. Sci. Technol.* **1983**, *17*, 625–628.
(12) Leenheer, J. A. *Environ. Sci. Technol.* **1981**, *15*, 578–587.
(13) Malcolm, R. L. In *Humic Substances: I. Geochemistry, Isolation and Characterization*; Wiley: New York, 1984.
(14) Hayes, M. H. B.; Swift, R. S. In *The Chemistry of Soil Constituents*; Greenland, D. J., Hayes, M. H. B., Eds.; Wiley-Interscience: New York, 1978; pp 179–320.
(15) Christman, R. F.; Ghassemi, M. *J.—Am. Water Works Assoc.* **1966**, *58*, 23–41.
(16) Hedges, J. I.; Ertel, J. R. *Anal. Chem.* **1982**, *54*, 174–178.

(17) Wilson, M. A. *J. Soil Sci.* **1981**, *32*, 167–186.
(18) Mikais, F. P.; Sullivan, M.; Bartuska, V. J.; Maciel, G. E. *Org. Geochem.* **1981**, *3*, 19–28.
(19) Maciel, G. E.; O'Donnell, J. D.; Ackerman, J. J. H.; Hawkins, B. H.; Bartuska, V. J. *Makromol. Chem.* **1981**, *182*, 2297–2304.
(20) Hatcher, P. G.; Breger, I. A.; Dennis, L. W.; Maciel, G. E. In *Aquatic and Terrestrial Humic Materials*; Christman, R. F.; Gjessing, E. T., Eds.; Ann Arbor Science: Ann Arbor, MI, 1983; pp 37–81.
(21) Thurman, E. M.; Malcolm, R. L. *Environ. Sci. Technol.* **1981**, *15*, 463–466.
(22) Liao, W. T.; Christman, R. F.; Johnson, J. D.; Millington, D. S. *Environ. Sci. Technol.* **1982**, *16*, 403–410.
(23) Hatcher, P. G. *Org. Geochem.*, in press.
(24) Huffman, E. W. D.; Stuber, H. A. In *Humic Substances in Soil, Sediment and Water*; Aiken, G. R., McKnight, D. M., Wershaw, R. L., MacCarthy, P., Eds.; Wiley-Interscience: New York, 1985; pp 433–455.
(25) Hatcher, P. G.; Schnitzer, M.; Dennis, L. W.; Maciel, G. E. *Soil. Sci. Soc. Am. Proc.* **1981**, *45*, 1089–1094.
(26) Hartmann, S. R.; Hahn, E. L. *Phys. Rev.* **1962**, *128*, 2042–2053.
(27) Thurman, E. M. *Organic Geochemistry of Natural Waters*; Martinus Nlihoff/Dr. W. Junk: Dordrecht, The Netherlands, 1985.
(28) Martin, J. P.; Haider, K. *Soil. Sci. Soc. Am. J.* **1980**, *44*, 983–988.
(29) Hatcher, P. G.; Martin, J. P., unpublished data.
(30) Levy, G. C.; Lichter, R. L.; Nelson, G. L. In *Carbon-13 Nuclear Magnetic Resonance Spectroscopy*; Wiley-Interscience: New York, 1980.
(31) Fukushima, E.; Roeder, S. B. W. In *Experimental Pulse NMR. A Nuts and Bolts Approach*; Addison-Wesley: Reading, MA, 1981.
(32) Wilson, M. A.; Pugmire, R. J.; Grant, D. M. *Org. Geochem.* **1983**, *5*, 121–129.
(33) *Biochemistry of Phenolic Compounds*; Harborne, J. B., Ed.; Academic: London, 1964.
(34) Cheshire, M. V.; Cranwell, P. A.; Haworth, R. D. *Tetrahedron* **1968**, *24*, 5155–5167.
(35) Saleh, F. Y.; Chang, D. Y.; Frye, J. S. *Anal. Chem.* **1983**, *55*, 862–866.

Received for review August 18, 1986. Revised manuscript received March 23, 1987. Accepted April 30, 1987. This work was supported by National Science Foundation Grant CEE83-12997.

Field Comparison of Polyurethane Foam and XAD-2 Resin for Air Sampling for Polynuclear Aromatic Hydrocarbons

Jane C. Chuang,*,† Steve W. Hannan,† and Nancy K. Wilson‡

Battelle Columbus Division, Columbus, Ohio 43201, and Environmental Monitoring Systems Laboratory, U.S. Environmental Protection Agency, Research Triangle Park, North Carolina 27711

■ A study of the sampling efficiency for polynuclear aromatic hydrocarbons (PAH) in air of two adsorbents, XAD-2 resin and polyurethane foam (PUF), was performed under summer and winter ambient conditions. Two aspects were investigated: (1) collection efficiency for ambient PAH vapor and (2) retention efficiency for native and perdeuteriated PAH spiked onto the adsorbents before sampling. The XAD-2 resin had a higher collection efficiency for naphthalene than did PUF. Some spiked PAH that were volatile or reactive were also recovered more efficiently with XAD-2 resin than with PUF. Lower sampling temperatures improved the recoveries of volatile PAH with PUF, but the recoveries of reactive PAH, such as cyclopenta[*cd*]pyrene, were not improved at lower temperatures for either adsorbent. The stability of PAH collected on quartz-fiber prefilters and XAD-2 or PUF backup traps as a function of the storage time was also investigated. Storage at room temperature in the dark for 30 days did not have an adverse effect on ambient PAH collected with XAD-2 resin or on perdeuteriated PAH spiked onto the adsorbent prior to sampling. However, a decreasing concentration trend with storage time for naphthalene, anthracene, and [$^2H_{12}$]benzo[*a*]pyrene collected or spiked on PUF was found. Most of the particle-bound PAH collected on quartz-fiber filters were not affected significantly during storage, except that cyclopenta[*cd*]pyrene decreased to approximately half the original level after 30 days of storage.

Introduction

Polynuclear aromatic hydrocarbons (PAH) have been studied extensively and have received increased attention in studies of air pollution in recent years because some of these compounds are potent carcinogens, mutagens, or both (*1–5*). To understand the extent of human exposure to PAH, reliable sampling and analytical methodology must be established for monitoring the concentrations of PAH in air. In general, the analytical methodology is well developed; however, the ambiguities introduced by sampling procedures can often reduce the validity of conclusions based on the analytical results. Several studies (*6–9*) have shown that PAH having two to four rings are present in air primarily in the vapor phase and are not retained by filters because of their volatility.

With regard to health effects, the collection of gas-phase PAH in air may be as important as the collection of particle-bound PAH. Thus, a wide variety of adsorbents such as XAD-2 resin, Tenax GC, and polyurethane foam (PUF) has been used to collect PAH vapors (*10–14*). All these adsorbents have been demonstrated to have a high collection efficiency for certain PAH. Typically, Tenax GC is used for sampling volatile analytes for subsequent thermal desorption rather than for semivolatile analytes for subsequent solvent elution, for which PUF and XAD-2 are used. Therefore, Tenax GC was excluded from this study. Polyurethane foam has relatively better flow characteristics than XAD-2 resin and is easy to handle in the field. However, PUF was found to give rise to unknown components that interfered with the PAH analyses, even after extensive cleanup by Soxhlet extraction (*14*). A new cleanup procedure was developed (*12*) that was found to eliminate the interferences. This new procedure was employed in this study. The overall comparative effectiveness of these adsorbents and the degree to which quantification of PAH is affected by sampling, handling, and storage have not been fully investigated. This uncertainty precludes an accurate assessment at this time of

†Battelle Columbus Division.
‡U.S. Environmental Protection Agency.

 0013-936X/87/0921-0798$01.50/0

the relative overall merit of each adsorbent.

The investigation reported here had two goals: (1) comparison of two adsorbents, PUF and XAD-2 resin, for their effectiveness in air sampling of PAH vapors and (2) comparison of the stability of PAH vapors collected on PUF and XAD-2 resin and of particle-bound PAH collected on quartz-fiber filters, as a function of the storage time between collection and extraction.

Experimental Section

Adsorbent Preparation. The PUF cartridges were purchased from Southwest Research Institute. The modified and improved cleanup procedure included sequential (50 times) compression/decompression of the PUF plug in 800 mL each of toluene, acetone, and 10% ether/hexane. The PUF plug was then Soxhlet extracted with acetone for 16 h and dried in a vacuum oven for 6 h at room temperature. The PUF plug was placed in a clean glass cartridge (2.3-in. i.d., 5-in. length), wrapped with hexane-rinsed aluminum foil, and stored in a clean screw-capped jar. All PUF plugs were cleaned by this procedure 24 h before air sampling.

The XAD-2 resin, which is a styrene–divinylbenzene polymer, was purchased as a precleaned resin from Supelco and was further cleaned by Soxhlet extraction with methylene chloride for 16 h and dried with a nitrogen gas stream. The clean XAD-2 resin was placed in the same type of glass cartridge described above. A nickel wire screen was placed in the bottom of the glass cartridge to retain the resin. The nickel wire screen was purchased from UNIQUE Wire Weaving Co. (mesh size 200/200, wire size 0.0021–0.0022 in.). The XAD-2 resin bed depth was 2 in., which allowed a maximum sampling flow rate of approximately 7 cfm.

Sampling Apparatus and Location. Modified medium-volume samplers (modified General Metals PS-1 samplers with General Metals bypass motors) were employed in the ambient air sampling. The samplers, which are described elsewhere (*15*), were equipped with a shelter that shields the filter and the PUF or XAD-2 backup trap from sunlight during sampling. Samplers were placed on the ground in an open space outside Battelle's laboratories in Columbus, OH. This location can be classified as a medium size, midwestern city with relatively clean air quality for an urban environment. The sampling was performed on weekends or holidays to reduce the contribution of local vehicle exhaust emissions to the sample. A 5-ft exhaust hose leading away from the sample module was attached to each sampler. Each sampler was calibrated with a dry gas meter (Rockwell Model 415) to obtain a flow rate of 6.7 cfm. Flow measurements from the sampler Magnehelic gauge were then recorded. The sample module was then placed on the sampler, and adjustment was made by the orifice calibrator to obtain the same calibrated reading on the Magnehelic gauge. Air was sampled for 24 h at 6.7 cfm. The flow was checked approximately every 6 h and maintained at 6.7 cfm throughout the sampling period. The same flow was used for both PUF and XAD-2. To ensure that only vapor-phase PAH were collected on the PUF and XAD-2, quartz-fiber filters (104-mm QAST, Pallflex) were located upstream of the PUF or XAD-2 in all sampling experiments (both the sampling efficiency comparision and the storage stability studies).

Sampling Procedure. (A) PUF and XAD-2 Sampling Efficiency Comparison. In the PUF and XAD-2 sampling efficiency comparison, two sets of three samplers were located in parallel, approximately 2 ft apart. The three samplers of each set were separated from each other by approximately 1 ft. In one set of three samplers PUF cartridges were used, and in the other set XAD-2 cartridges were used. Just prior to sampling, two each of the three PUF and XAD-2 cartridges were spiked with 100 μL of a methylene chloride solution containing 2.0 μg of each of the target PAH. The target PAH were [$^2H_8$]naphthalene, [$^2H_{10}$]phenanthrene, [$^2H_{10}$]pyrene, [$^2H_{12}$]chrysene, [$^2H_{12}$]benzo[*a*]pyrene, phenanthrene, anthracene, fluoranthene, pyrene, cyclopenta[*cd*]pyrene, benz[*a*]anthracene, benzo[*e*]pyrene, and benzo[*a*]pyrene. The spiking was performed by injecting the solution into the center of the PUF plug or XAD-2 resin bed at about 1-in. depth, followed by 5 min of air-drying. These experiments were performed twice under the same conditions except that during the first experiments the ambient temperature ranged from 66 to 86 °F and during the second experiments it ranged from 17 to 27 °F.

(B) Sampling Module Storage Stability Study. In the storage stability study, eight samplers in two sets of four were used. Sampler location was similar to the comparison study described above. In the first experiment, PUF cartridges were used for all eight samplers, and in the second experiment, XAD-2 cartridges were used for all samplers. All PUF and XAD-2 cartridges were spiked before sampling as described above but with only the perdeuteriated PAH. After the sampling, the PUF and XAD-2 cartridges were stored in the dark at room temperature for 0-, 10-, 20-, and 30-day intervals before extraction and were analyzed as replicate pairs. The eight quartz-fiber filters obtained from the XAD-2 sampling were similarly stored and extracted after the same time intervals. The filters from the PUF sampling were not used in this study.

Analytical Method. Quartz-fiber filters, PUF, and XAD-2 samples were Soxhlet-extracted for 16 h with 10% ether/hexane (PUF) or methylene chloride (filters and XAD-2). The extracts were concentrated to 1 mL with Kuderna–Danish (K–D) evaporation and analyzed by 70-eV electron impact (EI) gas chromatography/mass spectrometry (GC/MS). A Finnigan 4500 quadrupole GC/MS system and an INCOS 2300 data system were used. The evaporator cavity GC injector at 300 °C was used in the splitless mode (55 s) for a 2.0-μL injection. The GC column was an Ultra No. 2 fused silica capillary column (50-m length, 0.31-mm i.d., 0.17 μm film thickness, Hewlett-Packard Co.), and the column outlet was located in the MS ion source. Following injection, the GC was held at 45 °C for 1.5 min and temperature programmed to 100 °C over 5 min and then to 320 °C at 6 deg/min. The molecular ion of each compound of interest was monitored in the multiple ion detection mode (*16*). Identifications of PAH were based on the GC retention times of the individual monitored molecular ion signals relative to that of the internal standard 9-phenylanthracene. Quantifications of PAH were based on comparisons of the respective integrated ion current responses for the monitored molecular ions to that of the internal standard, with calibration response curves generated from four different concentrations (0.1 ng/μL, 2.0 ng/L, and 5.0 ng/L) of each target PAH.

Results and Discussion

PUF and XAD-2 Sampling Efficiency Comparison. PAH recoveries from the PUF and XAD-2 resin were determined by subtracting the levels of PAH in a nonspiked background sample from those in the corresponding spiked samples and dividing by the spiked levels (2.0 μg). The PAH recovery data are summarized in Figures 1 and

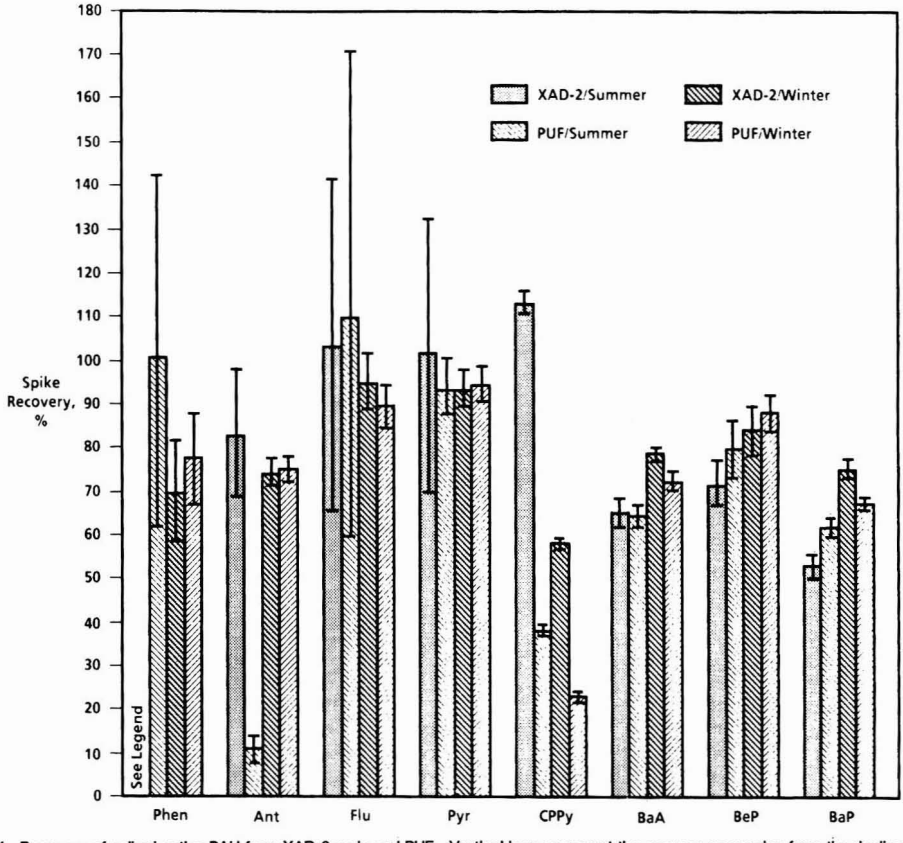

Figure 1. Recovery of spiked native PAH from XAD-2 resin and PUF. Vertical bars represent the average recoveries from the duplicate pairs, shown as the range of deviation from the average. Phe, phenanthrene; Ant, anthracene; Flu, fluoranthene; Pyr, pyrene; CPPy, cyclopenta[*cd*]pyrene; BaA, benz[*a*]anthracene; BeP, benzo[*e*]pyrene; BaP, benzo[*a*]pyrene. Phenanthrene recovery data in the summer experiment cannot accurately be calculated because of high background levels.

Table I. Background Concentrations of PAH in Air Collected on PUF and XAD-2 Resin[a]

	summer experiment			winter experiment		
	concn, ng/m^3		ratio,	concn, ng/m^3		ratio,
compound	XAD-2	PUF	XAD-2/PUF	XAD-2	PUF	XAD-2/PUF
naphthalene	182	7.7	24	68	5.5	12
phenanthrene	152	134	1.1	17	17	1.0
anthracene	3.0	3.8	0.8	0.8	0.9	0.9
fluoranthene	37	47	0.8	2.6	3.4	0.8
pyrene	11	13	0.8	1.7	2.1	0.8
cyclopenta[*cd*]pyrene	ND[b]	ND		ND	ND	
benz[*a*]anthracene	ND	ND		ND	ND	
benzo[*e*]pyrene	ND	ND		ND	ND	
benzo[*a*]pyrene	ND	ND		ND	ND	

[a] A total of 273 m^3 of air was sampled with a given sampler in a given run in both summer and winter experiments. [b] ND = not detected.

2. The background PAH levels collected on the PUF and XAD-2 resin are given in Table I. On the basis of our previous studies with these sampling and analysis procedures, a variance of approximately 20% for identical samples is to be expected. Thus, the PUF and XAD-2 results in Table I are similar for all compounds except naphthalene, the most volatile PAH of the series. As shown in Table I, levels of ambient naphthalene adsorbed on XAD-2 resin are about 24 and 12 times higher than those on PUF in the summer and winter experiments, respectively. The summer phenanthrene levels are slightly higher for XAD-2 resin than for PUF, but identical levels were observed for both adsorbents in the winter experiment. This finding suggests that XAD-2 resin has better collection efficiency for volatile PAH than does PUF and that the collection efficiency for volatile PAH on PUF improves at lower ambient sampling temperatures. In addition, only two- to four-ring PAH are found in both adsorbents. As we expected, the nonvolatile, high molecular weight PAH were predominantly present as ad-

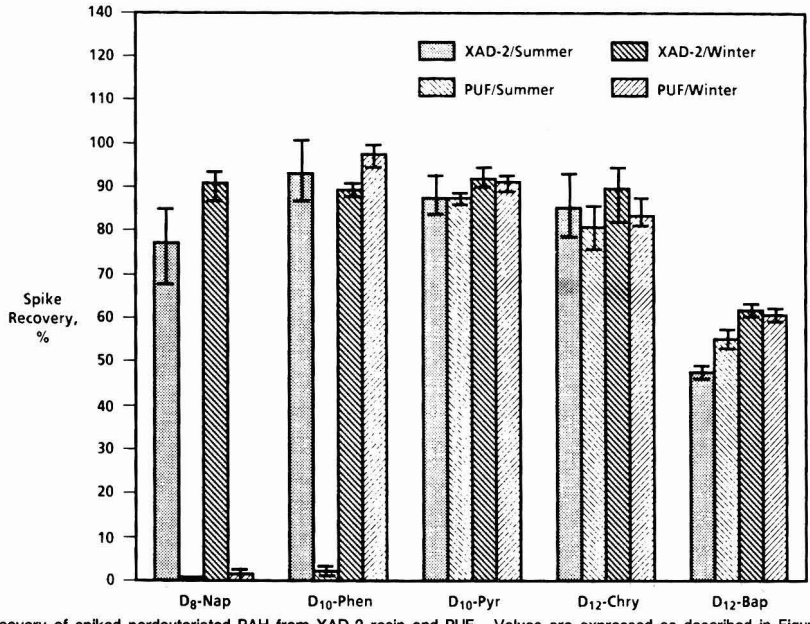

Figure 2. Recovery of spiked perdeuteriated PAH from XAD-2 resin and PUF. Values are expressed as described in Figure 1. D_8-Nap, [$^2H_8$]naphthalene; D_{10}-Pyr, [$^2H_{10}$]pyrene; D_{12}-Chry, [$^2H_{12}$]chrysene; D_{12}-BaP, D_{12} [$^2H_{12}$]benzo[*a*]pyrene.

sorbed species on particulate matter and were thus retained on the filter.

As shown in Figures 1 and 2, generally good recoveries are obtained for most spiked PAH from both adsorbents after exposure to ambient air at a flow rate of 6.7 cfm for 24 h. Comparison of the [$^2H_8$]naphthalene recoveries shows that the spiked XAD-2 resin give substantially higher recoveries than the spiked PUF, in agreement with the finding for native naphthalene noted above. Thus, XAD-2 resin appears to be significantly more effective in retaining two-ring PAH, since approximately 80% of [$^2H_8$]naphthalene was recovered after ambient air exposure even at the summer sampling temperature (66–86 °F). Similarly, lower recoveries of the spiked [$^2H_{10}$]-phenanthrene and spiked native anthracene were obtained from PUF than from XAD-2 resin in the summer experiment. As expected, these PUF recoveries improved significantly in the winter experiment, becoming comparable to those from XAD-2 resin. In an apparent contradiction to this observation with spiked deuteriated compounds, the background levels of ambient phenanthrene and anthracene (Table I) did not differ significantly between XAD-2 and PUF. The discrepancy is explainable in terms of more facile breakthrough of the spiked PAH than of ambient native PAH vapor. The spike was added as a liquid to the center of the adsorbent at approximately 1-in. depth and, therefore, had achieved 20% of its breakthrough for PUF and 50% breakthrough for XAD-2 before sampling began. In addition, the concentrated application of the spiked compounds might have created a localized adsorbent overload that could have increased the breakthrough tendency of these spike PAH. Nevertheless, the results clearly show that temperature is an important factor to be considered in ambient air sampling.

It was noted that the phenanthrene recovery data cannot be accurately addressed in the summer experiment because the ambient air background levels were about 19 times higher than the spiked levels. Thus, due to the expected variations in sampling and analytical procedures, negative recoveries were sometimes observed for spiked phenanthrene after subtraction of these high ambient background levels. For the same reason, a greater variance for fluoranthene recoveries was observed from both adsorbents in the summer experiment. In the winter experiment, the phenanthrene and fluoranthene background levels were only about 2.5 and 0.5 times the spiked levels, respectively, and good recoveries were obtained from both adsorbents. Low recoveries of cyclopenta[*cd*]pyrene were obtained with PUF in both the summer and the winter experiments, 40 and 23%, respectively. The recoveries of this compound from spiked XAD-2 resin also showed a similar trend, decreasing from 100% (summer) to 58% (winter). The loss of spiked cyclopenta[*cd*]pyrene almost certainly results not from volatilization but from decomposition, possibly oxidation; this is also indicated by the storage stability results (see below). The recoveries of the remaining PAH were good, and better retention of some PAH was observed at lower sampling temperatures for both adsorbents.

Sampling Module Storage Stability Study. The stability study was conducted to determine whether a significant loss of PAH adsorbed on PUF, XAD-2, or quartz-fiber prefilters occurs during the storage period between collection and extraction. Since the experimental design required duplicate samples for four storage times and since only eight medium-volume samplers were available, only perdeuteriated PAH were spiked onto the adsorbents prior to sampling. Thus, comparisons of the native PAH levels can be made without any background level corrections. The results are summarized in Figure 3 and 4.

For XAD-2 resin, no loss of perdeuteriated PAH was detected over the 30-day storage interval. For PUF, the [$^2H_8$]phenanthrene storage stability results are not meaningful since only 1.2% of the spiked [$^2H_8$]naphthalene was retained on the PUF at the end of the 24-h sampling. The decrease in [$^2H_{12}$]benzo[*a*]pyrene, however, does apparently indicate storage instability of this compound on PUF, since about 50% recovery of this spiked analyte was

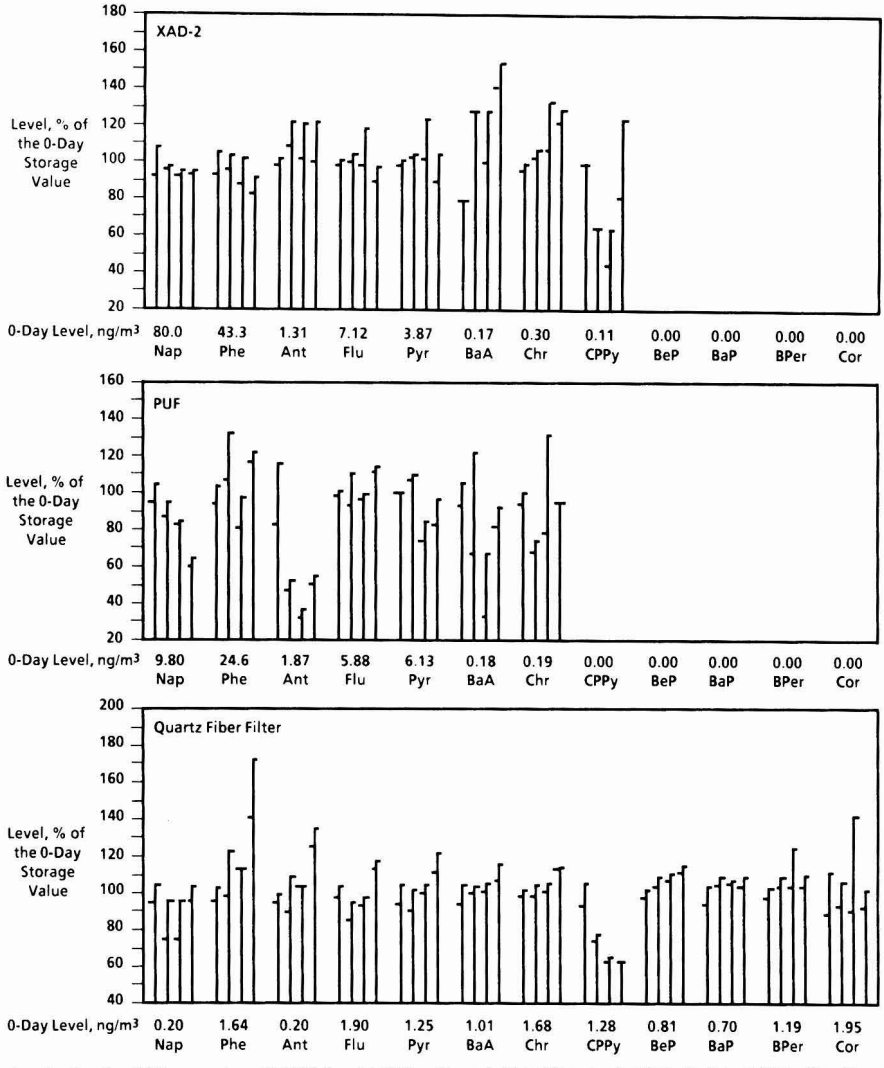

Figure 3. Levels of native PAH recoveries with XAD-2 resin, PUF, and quartz-fiber filter as a function of storage time. Chr, chrysene; BPer, benzo[*ghi*]perylene; Cor, Coronene. The remaining compound names are expressed as described in Figure 1. The four vertical bars for each PAH representing 0-, 10-, 20-, and 30-day storage intervals are shown from left to right, and values for each of two replicates, expressed as percent of the average 0-day storage values, are shown as horizontal bars.

also found for the sampling efficiency study (see Figure 2). However, this may not cause a serious problem in ambient air sampling, because benzo[*a*]pyrene is usually retained on the particulate filter and is not present in the backup adsorbent.

As shown in Figure 3, storage instability over the 30-day period is not indicated for any of the native PAH collected on XAD-2 resin. Only trace amounts of cyclopenta[*cd*]-pyrene were found on XAD-2 resin, and the variability in the data at these low levels prevents any firm stability conclusion. However, the data are consistent with a decreasing trend with storage time.

For PUF adsorbent, there appears to be a loss on storage of both native naphthalene and native anthracene. Since naphthalene evidently breaks through PUF during a 24-h sampling, it is not surprising that it could be partially lost by volatilization after storage for 30 days. Unfortunately, this hypothesis cannot be supported by the $[^2H_8]$-naphthalene PUF results because only 1.2% of the spiked material was present at the beginning of storage and the recovery levels are too low to show any trend. The greater loss from PUF of anthracene relative to its isomer phenanthrene is more consistent with the lower chemical stability of anthracene relative to phenanthrene than with a selective loss through volatilization. The nondetection of cyclopenta[*cd*]pyrene on PUF may be due to its degradation to below the detection limit (0.05 ng/m^3) since this compound was detected only at very low levels with XAD-2 resin. An overall comparison of the XAD-2 vs. PUF results of Figure 4 clearly suggests more reliable and reproducible storage performance for XAD-2 resin.

With the exception of cyclopenta[*cd*]pyrene, storage losses of particle-bound PAH collected on quartz-fiber filters were insignificant. The calculated concentration of

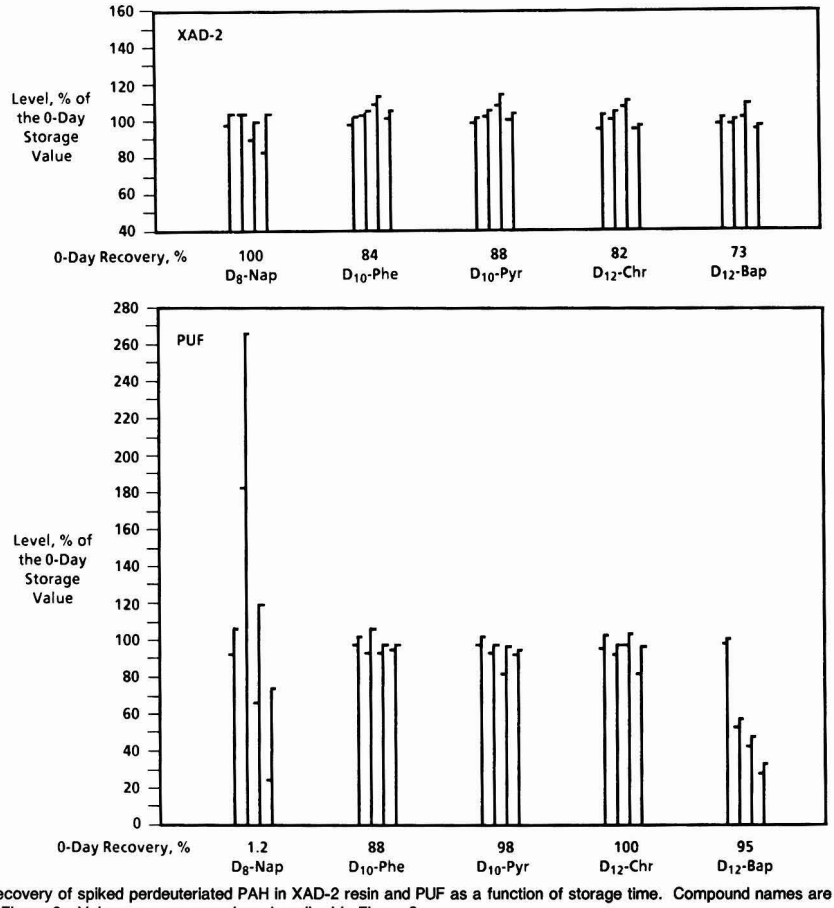

Figure 4. Recovery of spiked perdeuteriated PAH in XAD-2 resin and PUF as a function of storage time. Compound names are expressed as described in Figure 2. Values are expressed as described in Figure 3.

cyclopenta[*cd*]pyrene decreased from 1.3 ng/m^3 (34.8 ng/mg of particles) to 0.8 ng/m^3 (17.8 ng/mg of particles) after storage for 30 days. The losses of particle-bound cyclopenta[*cd*]pyrene during sample storage are probably due to its chemical instability noted above in the discussion of its low recovery in the sampling efficiency study (Figure 1). One research group (*17*) has identified a direct-acting mutagen, pyrene-1,10-dicarboxylic acid anhydride, as a possible degradation product of cyclopenta[*cd*]pyrene in diesel exhaust particles. This acid anhydride oxidation product was also found in airborne particulate material and other environmental samples by other research groups (*18–19*).

Distributions of PAH between the filter and XAD-2 resin from the stability study were as follows (Figure 3): two-ring PAH, 99% on XAD-2; three-ring PAH, 90% on XAD-2; four-ring PAH, 80% on XAD-2 for pyrene and fluoranthene and 15% on XAD-2 for benz[*a*]anthracene and chrysene; five-ring PAH, <10% on XAD-2; six- to seven-ring PAH, 100% on filter. These distributions parallel, in general, the volatilities of the individual PAH and indicate breakthrough of two- to four-ring PAH from the prefilters. Other research groups (*6–9*) have also reported that most of the volatile PAH were not retained on filters under high-volume sampling conditions. In our study, medium-volume samplers were used, and the flow rate (6.7 cfm) was lower than a typical high-volume sampling flow rate. These relative recovery results clearly demonstrate that the use of filters only to collect PAH from air is not sufficient, and correct quantitative results, even for species as large as chrysene, cannot be obtained without the use of backup adsorbents.

Conclusions

In conclusion, for air sampling for gas-phase PAH, XAD-2 resin seems to gave two performance advantages compared to PUF: (1) two- and three-ring PAH clearly break through standard PUF cartridges with a typical sampling volume of 270 m^3, and (2) PAH species that are prone to degradation during sampling or during sample storage prior to extraction exhibit greater losses from PUF than from XAD-2 resin. The retention efficiency of volatile PAH for both adsorbents, especially PUF, can be improved by lowering the sampling temperature. Certainly, the future use of quartz-fiber filter/PUF samplers should involve a minimum of sample handling and storage to reduce the losses of volatile and reactive PAH. Little is known about the degradation products of PAH due to sampling and sample handling. The critical issue of whether a significant part of the mutagenic activity in these types of air samples is from sampling artifacts or is actually present in the sampled air is still not clear, and further

investigations need to be carried out in this area.

Acknowledgments

We thank John Koetz and Warren Bresler for performing the sampling and Samuel V. Lucas and Larry E. Slivon for technical discussions and advice on manuscript revision.

Registry No. XAD-2, 9060-05-3; Chr, 218-01-9; BPer, 191-24-2; Cor, 191-07-1; naphthalene, 91-20-3; phenanthrene, 85-01-8; anthracene, 120-12-7; fluoranthene, 206-44-0; pyrene, 129-00-0; cyclopenta[*cd*]pyrene, 27208-37-3; benz[*a*]anthracene, 56-55-3; benzo[*e*]pyrene, 192-97-2; benzo[*a*]pyrene, 50-32-8.

Literature Cited

(1) National Research Council; *Polycyclic Aromatic Hydrocarbons: Evaluation of Sources and Effects*; National Academy: Washington, DC, 1983.
(2) Miller, M.; Alfheim, I. *Environ. Sci. Technol.* **1982**, *16*, 221.
(3) Dehren, W.; Pitz, N.; Tomingas, R. *Cancer Lett. (Shannon, Irel.)* **1977**, *4*, 5.
(4) Chuang, C. C.; Petersen, B. A. Report EPA-600/4-85-045; Environmental Monitoring Systems Laboratory, Office of Research and Development, U.S. EPA: Research Triangle Park, NC, 1985.
(5) Perera, F. *EHP, Environ. Health Perspect.* **1981**, *42*, 163.
(6) Galasyn, T. G.; Horning J. F.; Soderberg, R. H. *J. Air Pollut. Control Assoc.* **1984**, *34(1)*, 57.
(7) Cautreels, W.; VanCauwenberghe, K. *Atmos. Environ.* **1978**, *12*, 1133.
(8) Feng, Y.; Bidleman, T. F. *Environ. Sci. Technol.* **1984**, *18*, 330.
(9) Yamasaki, H.; Kuwata, K.; Miyamoto, H. *Environ. Sci. Technol.* **1982**, *16*, 182.
(10) Jones, P. W.; Wilkinson, J. E.; Strup, P. E. Report EPA-600/2-77-202; Environmental Monitoring Systems Laboratory, Office of Research and Development, U.S. EPA: Research Triangle Park, NC, 1977.
(11) Thrane, K. E.; Mikalsen, A. *Atmos. Environ.* **1981**, *15*, 909.
(12) Chuang, C. C.; Bresler, W. E.; Hannan S. W. Report EPA-600/4-85/055; Environmental Monitoring Systems Laboratory, Office of Research and Development, U.S. EPA: Research Triangle Park, NC, 1985.
(13) Keller, C. D.; Bidleman, T. F. *Atmos. Environ.* **1984**, *18*, 837.
(14) Chuang, C. C.; Mack, G. A.; Petersen, B. A.; Wilson, N. K.; Report EPA-600/D-85/050; Environmental Monitoring Systems Laboratory, Office of Research and Development, U.S. EPA: Research Triangle Park, NC, 1985.
(15) Lewis, R. D.; Jackson, M. D. *Anal. Chem.* **1982**, *54*, 592.
(16) Petersen, B. A.; Chuang, C. C.; Hayes, T. L.; Trayser, D. A. *Polynuclear Aromatic Hydrocarbons: Physical and Biological Chemistry*; Cooke, M.; Dennis, A. J.; Fisher, G. L., Eds.; Battelle: Columbus, OH, 1982; p 641.
(17) Rappaport, S. W.; Wang, Y. Y.; Wei, E. T.; Sawyer, R.; Watkins, B. E.; Rappaport, H. *Environ. Sci. Technol.* **1980**, *14*, 1505.
(18) Stenberg, U. R.; Alsberg, T. E. *Anal. Chem.* **1981**, *53*, 2067.
(19) Konlg, J.; Balfanz, E.; Funcke, W.; Romanowski, T. *Anal. Chem.* **1983**, *55*, 599.

Received for review October 15, 1986. Accepted April 15, 1987. Although the reseach described in this paper has been funded wholly or in part by the U.S. Environmental Protection Agency through Contract 68-02-4127, it has not been subjected to Agency review and therefore does not necessarily reflect the views of the Agency, and no official endorsement should be inferred. Mention of trade names of commercial products does not constitute endorsement or recommendation for use.

Reaction Kinetics of Hydrogen Peroxide with Copper and Iron in Seawater

James W. Moffett[†] and Rod G. Zika*

Rosenstiel School of Marine and Atmospheric Science, University of Miami, Miami, Florida 33149

■ The oxidation of Fe(II) and Cu(I) and the reduction of Fe(III) and Cu(II) by hydrogen peroxide in seawater have been studied to understand their mechanisms and probable significance in the upper marine water column. At 10^{-7} M H_2O_2, a level commonly found in surface seawater, reaction with H_2O_2 is the dominant oxidation pathway for Fe(II). Reduction of Fe(III) by peroxide was not observed in the pH range 7–8. Reduction of Cu(II) and oxidation of Cu(I) by H_2O_2 contribute to a dynamic redox cycling of that element in the upper water column. Calculations based on these data indicate that Cu(I) oxidation and Fe(II) oxidation by H_2O_2 are at least as important as nitrite photolysis as a source of OH radicals in the ocean.

Introduction

Hydrogen peroxide has been measured in a variety of natural surface waters (*1–5*) at concentrations exceeding 10^{-7} M. There is considerable evidence that it is formed photochemically through the photooxidation of dissolved organic matter. These observations have led to a considerable interest in its influence on aquatic redox processes involving minor elements such as transition metals. At the present time, however, there is little kinetic data in the literature for its reactions with transition metals in aqueous alkaline media such as seawater. Most of the earlier work has been carried out in low-pH media or in the presence of high concentrations of organic compounds such as acetonitrile and pyridine, and extrapolation of these results to natural water conditions is difficult.

In this work, the reactions of hydrogen peroxide with copper and iron in seawater have been studied. Copper and iron have been studied extensively in natural waters because both are essential elements in biological systems and Cu is toxic. Evidence suggests that bioavailability may be related to their redox properties, particularly for iron (*6*). Peroxide is important in Fe(III)/Fe(II) and Cu(I)/Cu(II) interconversion in chemical and biological systems, suggesting that it may also be important in natural waters. In addition, catalysis of a variety of reactions in the presence of Fe or Cu and H_2O_2 is well documented. Such processes may also be important in natural waters.

Hydrogen peroxide is an intermediate in the reduction of oxygen to water and can act as an oxidant or a reductant in its reactions with Fe and Cu. A generalized mechanism for Cu(I) and Fe(II) oxidation has been proposed by earlier workers (*7–8*):

$$M^{n+} + H_2O_2 \rightarrow M^{(n+1)+} + OH + OH^- \quad \text{slow} \quad (1)$$

$$M^{n+} + OH \rightarrow M^{(n+1)+} + OH^- \quad \text{fast} \quad (2)$$

[†]Present address: Chemistry Department, Woods Hole Oceanographic Institution, Woods Hole, MA 02543.

0013-936X/87/0921-0804$01.50/0

For Cu(II) and Fe(III) reduction, the following mechanism has been proposed (*8–9*):

$$H_2O_2 \rightleftharpoons H^+ + HO_2^- \quad \text{fast} \quad (3)$$

$$M^{(n+1)+} + HO_2^- \rightarrow M^{n+} + HO_2 \quad \text{slow} \quad (4)$$

$$HO_2 \rightleftharpoons H^+ + O_2^- \quad \text{fast} \quad (5)$$

$$M^{(n+1)+} + O_2^- \rightarrow M^{n+} + O_2 \quad \text{fast} \quad (6)$$

These mechanisms have been proposed for a variety of aqueous biochemical and chemical systems and are probably valid in seawater and other natural waters. At low concentrations of metals, however, OH and O_2^- formed in reactions 1 and 4 may react via other pathways than 2 and 6. Therefore in this work, bimolecular rate constants have been calculated for reactions 1 and 4, from the overall rates measured in this study. The influence of pH, chloride, temperature, and chelators has been studied to understand the mechanism and assess the importance of the reactions in natural waters.

Experimental Section

The reactions were monitored by following the decay or formation of Cu(I) and Fe(II) during the course of the reaction. Cu(I) was measured spectrophotometrically by bathocuproinedisulfonic acid with ethylenediamine to mask Cu(II) interference. The technique is described in detail elsewhere (*10*). Fe(II) was measured with ferrozine (*11*). At pH >6 there was no detectable interference from Fe(III). Both techniques had limits of detection of 1×10^{-8} M. Copper reactions were followed by withdrawing 30-mL aliquots of solution from the reaction vessel at selected times after the addition of peroxide and adding them directly to 1 mL of a 3×10^{-3} M stock solution of colorimetric reagent [plus 1.5×10^{-2} M ethylenediamine for Cu(I) determination]. For iron, 30-mL aliquots were added to 1 mL of a 10^{-2} M ferrozine solution. Full yields were obtained without prior acidification.

Reactions were carried out in a 1-L stirred glass reaction vessel immersed in a constant-temperature bath controlled to ±0.1 deg and purged continuously with N_2. All reactions were carried out at 25 °C unless noted otherwise. A plunger inserted into the top of the reaction vessel enabled the removal of 30-mL aliquots of solution during the reaction. The pH was measured throughout each experiment. For seawater solutions, pH was controlled by purging with a mixture of CO_2 and N_2. Gas flow was controlled with Matheson Dyna-Blender flow controller for precise pH control. For copper studies, carbonate-free solutions were buffered with borate (10^{-3} M) at pH >7.5 and phosphate at pH <7.5. The concentration of phosphate was varied so that the concentration of HPO_4^{2-} did not exceed 2×10^{-4} M. However, even at these levels some complexation occurs, which had to be taken into account.

All pH values were measured by an Orion Ross electrode calibrated with tris(hydroxymethyl)aminoethane (Tris) buffer prepared in seawater on the free proton scale described elsewhere (*12*). Spectrophotometric measurements were made with an HP 8450 spectrophotometer.

Stock solutions of Cu(I) were prepared fresh daily by dissolving cuprous bromide (Fluka) in a deoxygenated acidified 1 M NaCl solution heated to 50 °C. Fe(II) stock solutions (10^{-2} M) were prepared daily in distilled water at pH 3 from $FeSO_4$. A 10^{-2} M H_2O_2 stock solution was prepared from 30% H_2O_2 and stored in the refrigerator where it was stable for a number of weeks. Seawater was collected from the Florida Straits 4 mi east of Miami and filtered through a 0.2-μm filter. Chloride dependence studies were carried out in artificial seawater, substituting perchlorate for chloride.

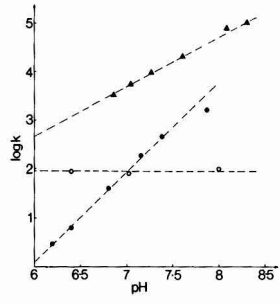

Figure 1. pH dependence of the reactions, $T = 25$ °C: k_3 for Fe(II) oxidation in seawater (▲), k_1 for Cu(I) oxidation in seawater (○), and k_4 for Cu(II) reduction in 0.7 M NaCl (●).

Results

Calculation of Second-Order Rate Constants. The reaction rates varied widely with the parameters studied. Initial concentrations were varied to enable accurate calculation of the second-order rate constants within the time and analytical constraints imposed by our procedure and so that backreactions were not significant. For very slow reactions, the rate constant was calculated directly from initial rates, usually with an excess of metal reactant so that reaction of the product with H_2O_2 would not be significant. Metal and H_2O_2 concentrations for the slow reactions were from 5×10^{-6} to 5×10^{-5} M. For faster reactions, where backreaction of the products did not affect the rate, metal reactant and H_2O_2 were added at stoichiometric ratio, i.e., $[\text{metal}]_0 \times 2[H_2O_2]_0$, and the rate constants were calculated from

$$k_{\text{oxdn}}t = (M_0/M_t - 1)/[H_2O_2]_0 \quad (7)$$

$$k_{\text{redn}}t = [(M_\infty - M_t)/M_t - 1]/[H_2O_2]_0 \quad (8)$$

These are the integrated solutions for the overall second-order reactions in eq 1–2 and 3–6, respectively. M_t in this instance is Cu(I) or Fe(II) actually measured at time t. k_{oxdn} and k_{redn} are the measured rate constants for the oxidation and reduction reactions, respectively. Metal concentrations were 2×10^{-6} M, and H_2O_2 was 1×10^{-6} M.

For the oxidation reactions studied over the range of concentrations used in these experiments, plots using eq 7 were linear down to [metal] = 10% $[\text{metal}]_0$. Therefore, two atoms of metal were oxidized per peroxide, indicating that all the OH produced in reactions 2 and 4 reacted with Fe(II) or Cu(I), either directly or through intermediates. Therefore, $k_1 = 1/2k_{\text{oxdn}}$. For Cu(II) reduction, plots derived from eq 8 were also linear, indicating $k_4 = 1/2k_{\text{redn}}$ by similar reasoning.

Results of the study are summarized in the figures and are tabulated in detail in the supplementary material (see paragraph at end of paper regarding supplementary material).

pH and Chloride Dependence of the Reactions. The results of the pH dependence studies are shown in Figure 1. The oxidation of Fe(II) by peroxide is strongly pH dependent in seawater. A plot of log k_1 vs. pH is linear with a slope of 1, indicating the reaction is proportional to $[OH^-]$. The chloride dependence was not studied. Cu(I) oxidation in seawater, by contrast, showed no pH dependence over the range 6.2–8.3. However, it was strongly dependent on chloride concentration. The chloride dependence at pH 8.0 was studied in artificial seawater,

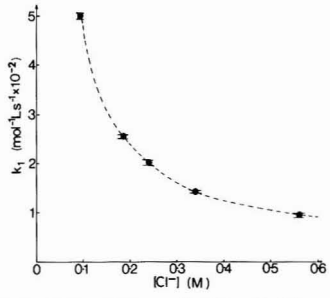

Figure 2. k_1 for Cu(I) oxidation vs. [Cl$^-$] in artificial seawater/ClO_4: T = 25 °C, pH 8.00, and I = 0.7 M.

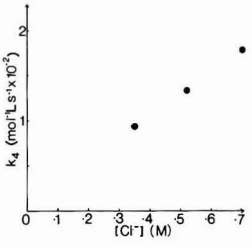

Figure 3. k_4 for Cu(II) reduction vs. [Cl$^-$]: pH 7.17, NaCl–ClO_4; I = 0.7 M; T = 25 °C.

substituting perchlorate for chloride to maintain a constant ionic strength. The results, in Figure 2, show an increase in rate with decreasing chloride concentration.

The pH dependence of Cu(II) reduction was studied in 0.7 M NaCl, to avoid carbonate chelation. A plot of log k_4 plotted against pH gives a straight line with a slope of 2, indicating the reaction is proportional to [OH$^-$]^2. The chloride dependence of the reaction was also studied, at pH 7.17. Unfortunately, the reaction could not be measured below 0.35 M [Cl$^-$], as the oxidation of the product Cu(I) was too rapid. However, the results indicate that the reaction is proportional to [Cl$^-$] in this concentration range (Figure 3).

No observable Fe(III) reduction by peroxide occurred in the pH range 7–8, possibly because of the rapid reoxidation of Fe(II) or the formation of kinetically inert ferric hydroxy colloids.

Ligand Influences. In seawater, Cu(II) speciation is dominated by carbonate and organic ligands (*13*). Addition of carbonate and model organic ligands nitrilotriacetic acid (NTA) and salicylic acid led to a decrease in rate, indicating that Cu(II) complexes with these ligands reacted slowly or not at all with H_2O_2. Cu(I) speciation is probably not influenced by ligands other than chloride (*14*), so none were examined. Ligand influences on Fe(II) oxidation were not examined though there is some evidence that they are important in freshwater systems (*15*).

Temperature Dependence. Temperature (T) dependence in seawater at pH 8.00 was determined for all three reactions over the range 5–25 °C. The reduction of Cu(II) shows the greatest variability with temperature, due in part to the variation of K_w and the K_a of H_2O_2 with temperature. The change in K_w also contributes to Fe(II) T dependence. Results are shown in Figure 4.

Rate Constants for Individual Complexes. The data can be interpreted in terms of the reactivity and abundance of individual complexes that contribute to the overall rate. Millero (*16*) has derived rate equations from which individual rate constants may be calculated for Cu(I)

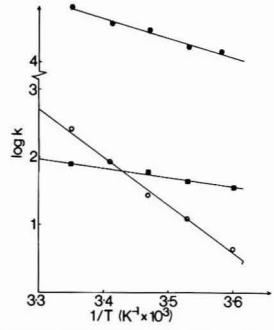

Figure 4. Temperature dependence of each reaction at pH 8.00: log k_1 for Fe(II) oxidation (●), Cu(I) oxidation (■), and log k_4 for Cu(II) reduction (○).

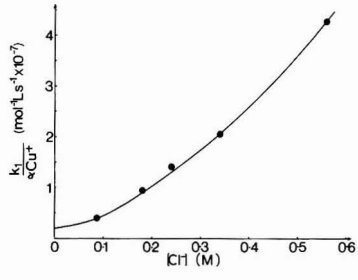

Figure 5. Data analysis for Cu(I) oxidation in artificial seawater: k_1/α_{Cu^+} vs. [Cl$^-$].

and Fe(II) oxidation by O_2, from chloride and pH dependence data. Similar equations have been developed here.

Cu(I) oxidation is independent of pH, so only chloride-dependent species contribute to the rate and pH-dependent species are ignored. However, because the rate increases with decreasing Cl$^-$, the free ion Cu^+_f must also be included in the rate equation:

$$\text{rate} = k_1[\text{Cu(I)}][H_2O_2] = (k_{Cu^+_f}[Cu^+_f] + k_{CuCl}[CuCl] + k_{CuCl_2^-}[CuCl_2^-] + k_{CuCl_3^{2-}}[CuCl_3^{2-}])[H_2O_2] \quad (9)$$

$$k_1 = k_{Cu^+_f}\alpha_{Cu^+_f} + k_{CuCl}\alpha_{CuCl} + k_{CuCl_2^-}\alpha_{CuCl_2^-} + k_{CuCl_3^{2-}}\alpha_{CuCl_3^{2-}} \quad (10)$$

$$\frac{k_1}{\alpha_{Cu^+_f}} = k_{Cu^+_f} + k_{CuCl}\beta_{CuCl}[Cl^-] + k_{CuCl_2^-}\beta_{CuCl_2^-}[Cl^-]^2 + k_{CuCl_3^{2-}}\beta_{CuCl_3^{2-}}[Cl^-]^3 \quad (11)$$

where $\alpha_{CuCl} = [CuCl]/[Cu(I)]_{total}$, $\beta_{CuCl} = [CuCl]/([Cu^+_f][Cl^-])$, etc. The left-hand side of eq 11 was plotted against [Cl$^-$] and produced a curve, to which a quadratic was fitted (Figure 5). Attempts to fit a cubic to the data with all nonnegative coefficients were unsuccessful. This indicates that $CuCl_2^-$ is reactive but $CuCl_3^{2-}$ is not. Rate constants calculated from the quadratic equation coefficients are shown in Table I. Stability constant data were taken from ref 14.

For Fe(II) oxidation, the strong pH dependence indicates that pH-dependent species dominate in the rate equation. Neglecting non pH dependent species ($FeCl^+$, $FeSO_4$, etc.), the rate equation can be written

$$\text{rate} = k_1[\text{Fe(II)}][H_2O_2] = (k_{FeX}[FeX] + k_{Fe(OH)^+}[Fe(OH)^+] + k_{Fe(OH)_2}[Fe(OH)_2])[H_2O_2] \quad (12)$$

$$k_1 = k_{FeX}\alpha_{FeX} + k_{Fe(OH)^+}\alpha_{Fe(OH)^+} + k_{Fe(OH)_2}\alpha_{Fe(OH)_2} \quad (13)$$

Table I. Second-Order Rate Constants Calculated for Reaction of Individual Cu and Fe Complexes with H_2O_2 in Seawater at 25 °C

Oxidation: $M^{n+} + H_2O_2 \rightarrow M^{(n+1)+} + OH + OH^-$

M	k, mol^{-1} L s^{-1}
$Fe(OH)^+$	$(1.9 \pm 0.1) \times 10^6$
Fe^{2+}	*a*
Cu^+	4×10^5 *b*
$CuCl^0$	$(1.6 + 0.3) \times 10^5$
$CuCl_2^-$	$(1.3 \pm 0.2) \times 10^2$
$CuCl_3^{2-}$	*a*

Reduction: $M^{n+} + HO_2^- \rightarrow M^{(n-1)+} + HO_2$

M	k, mol^{-1} L s^{-1}
$CuClOH^0$	$(3.3 \pm 0.1) \times 10^8$
Cu^{2+}	*a*

[a] No reaction or the reaction was too slow to be calculated. [b] $0 < k < 2 \times 10^{-6}$ mol^{-1} L s^{-1}, intercept value shown above.

where FeX = all non pH dependent Fe(II) species. To express k_1 as a function of $[OH^-]$, eq 10 is divided by $\alpha_{Fe^{2+}_f}$, where $\alpha_{Fe^{2+}_f} = Fe^{2+}_{free}/Fe(II)_{total}$:

$$\frac{k_1}{\alpha_{Fe^{2+}_f}} = k_{FeX}\beta_{FeX} + k_{Fe(OH)^+}\beta_{Fe(OH)^+}[OH^-] + k_{Fe(OH)_2}\beta_{Fe(OH)_2}[OH^-]^2 \quad (14)$$

Plotting the left-hand side of eq 14 against $[OH^-]$ gave a straight line with negligible intercept. Graphs of this and other linear plots in this section are included in the supplementary material. From the equation, the slope = $k_{Fe(OH)^+}\beta_{Fe(OH)^+}$, and the intercept = $k_{FeX}\beta_{FeX}$. Therefore, from the plot, the first and third terms of the equation are unimportant, indicating that only $Fe(OH)^+$ contributes significantly to the overall rate. From these values, a rate constant for $Fe(OH)^+$ was calculated (Table I) with stability constant data from ref 17. The high rate observed for $Fe(OH)^+$ accounts for the $[OH^-]$ dependence. The concentration of OH^- used in these calculations was calculated with $pK_w = 13.65$ for seawater at $T = 25$ °C (*18*). Cu(II) reduction shows an $[OH^-]^2$ dependence on pH, indicating that hydroxy complexes are reactive. However, in the generally accepted mechanism for this reaction (eq 3–6), HO_2^- is the reactive species in the rate-determining step, as indicated in systems studied by earlier workers (*19–21*). Participation of this species in the rate-determining step will contribute to the pH dependence. Therefore, rate constants based on HO_2^- and k_4 were calculated, where $k_4' = k_4[H_2O_2]/[HO_2^-]$, with a pK_a of $H_2O_2 = 12.13$ (*22*).

The pH dependence of k_4' is only a function of changes in Cu(II) speciation and can be expressed as a function of $[OH^-]$ with an equation analogous to eq 11 and 14:

$$\frac{k_4'}{\alpha_{Cu^{2+}_f}} = (k_{CuOH}\beta_{CuOH} + k_{CuClOH}\beta_{CuClOH})[OH^-] + (k_{Cu(OH)_2}\beta_{Cu(OH)_2})[OH^-]^2 \quad (15)$$

$[OH^-]$ was calculated with $pK_w = 13.71$ calculated for this medium (*23*). Plotting this equation yields a straight line with a small intercept, indicating that only $Cu(OH)^+$ and/or CuOHCl is reactive. To distinguish these two complexes, chloride dependence was studied at pH 7.17, where only the pH-dependent species are significant. The data were fitted by modifying the above equation:

$$\frac{k_4'}{\alpha_{Cu^{2+}_f}} = k_{CuOH}\beta_{CuOH} + k_{CuClOH}\beta_{CuClOH}[Cl^-] \quad (16)$$

Table II. Standard Potentials for Complexes Examined in This Work[a]

couple	E^0, V	couple	E^0, V
$Fe(OH)_2^+/Fe(OH)_2$	−0.04	Cu^{2+}/Cu^+	0.153
$Fe(OH)^{2+}/Fe(OH)^+$	0.304	$CuCl^+/CuCl^0$	0.330
Fe^{3+}/Fe^{2+}	0.771	$CuClOH^0/CuClOH^-$	0.423
$FeCl^{2+}/FeCl^+$	0.773	$CuCl_2^0/CuCl_2^-$	0.567

[a] Calculated from data in Zuehlke and Kester (*12*), Moffett and Zika (*14*), Turner et al. (*17*) and Milazzo and Caroli (*25*).

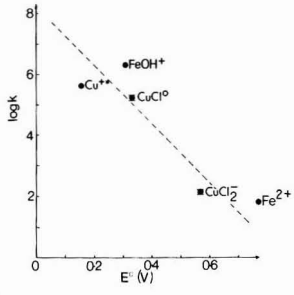

Figure 6. E^0 vs. log k for the oxidation of Cu(I) and Fe(II) complexes. Note the constant for Fe^{2+} was from ref 27. *No lower estimate for log k could be made from the data.

Thermodynamic data used to calculate the constants were taken from ref 13, except for CuOHCl, which was calculated from data for $Cu(OH)_2$ and $CuCl_2$ from ref 13, with an approximation described in ref 24, giving a value of 3.0×10^5. Complexation with phosphate was also included with data from ref 22. The intercept is close to zero, indicating negligible reactivity for $CuOH^+$. CuClOH is the most reactive species. The bimolecular rate constant is shown in Table I. Individual rate constants for the non pH dependent species could not be determined from these data because of their small contribution to the total rate.

Discussion

Mechanistic Considerations. The standard potentials for couples of the various complexes were calculated with data from ref 13, 17, and 25 and are shown in Table II. There is a general correlation between potential and reaction rate for Cu(I) and Fe(II) oxidation (Figure 6) as is to be expected from Marcus theory considerations, if the rate-determining step is a charge-transfer process (*26*). It is noteworthy that the rate constant for Fe^{2+}_{free} from ref 27 fits well on the plot. Similar trends have been observed for the oxidation of a series of copper(I)–1,10-phenanthroline complexes with H_2O_2 (*28*). A similar correlation has been observed for the autoxidation of a series of Ru amines and interpreted in terms of a charge-transfer rate-determining step (*29*). The apparent lack of reaction of $Fe(OH)_2$ is anomalous as this complex should react extremely rapidly with H_2O_2 given its low standard potential. However, steady-state concentrations of $Fe(OH)_2$ are 3 orders of magnitude lower than those of $Fe(OH)^+$ at pH 8, so the reaction would have to be almost diffusion controlled to be detectable from this data set. Other factors such as the formation rates of $Fe(OH)_2$ may act to limit its contribution.

Cu(II) reduction by peroxide deviates from this trend. $CuCl_2$ has a larger standard potential than CuClOH but shows little or no reactivity toward HO_2^-. Yet studies of the reduction of Cu(II) in chloride media by ferrocytochrome *c*, which probably occurs by an outer sphere

charge-transfer mechanism, indicate that $CuCl_2$ is very reactive (*30*). Since equilibrium concentrations of $CuCl_2$ are similar to those of CuClOH, comparable reaction rates would be detectable. Therefore, a more complex mechanism is probably involved, perhaps involving the formation of a Cu(II) complex with HO_2^- as suggested by earlier workers (*19–21*). Nevertheless, stable Cu(II) complexes such as carbonate and model ligand complexes examined here were unreactive. Work on the reduction in a series of pyridine complexes (*19*) indicates that the minor, less stable complexes are the most reactive and make the greatest contribution to the overall rate, as observed here.

Comparison with Earlier Work. Cu(I) and Fe(II) oxidation by H_2O_2 has been studied in acidic chloride media. For Cu(I), results are similar to this work (*31*). For Fe(II), the data indicate that the reaction with free Fe^{2+} is slow, in agreement with earlier work (*8*). Cu(I) and Fe(II) oxidation in seawater by oxygen has been studied (*13, 18, 32–35*). The overall rate constants are 2–3 orders of magnitude greater for H_2O_2. Furthermore, the pH, $[Cl^-]$, and temperature dependences of these reactions are different for O_2 and H_2O_2. These differences arise because of differing relative reactivities of the individual complexes. $CuCl_2^-$ is reactive with peroxide but not O_2. $Fe(OH)_2$ is the most important species for O_2 oxidation of Fe(II), but $Fe(OH)^+$ is the most important for H_2O_2 oxidation. The differences may be due to the greater reactivity and stronger oxidizing properties of H_2O_2 but may also be due to mechanistic differences, particularly if coordination of H_2O_2 or O_2 to the complex is important in the rate-determining step. Studies of Cu^{2+} reduction confirm that the free ion is relatively unreactive with H_2O_2 (*8, 36*).

Implications for Upper Marine Water Column. These reactions are likely to be important in the upper water column, where peroxide has been measured, in two general ways: (1) altering the prevailing equilibria between the two redox states of each metal; (2) acting as a source of O_2^- and OH radicals, which are far more reactive with a variety of organic and inorganic substrates than H_2O_2.

In recent years numerous processes have been proposed leading to Fe(II) and Cu(I) formation in the upper marine water column. To evaluate the influence of peroxide on these processes, rates were compared with known rates for the oxidation by O_2. In order to compare our data with the literature data for O_2 oxidation, the bimolecular rate constant for the reaction with O_2 must be determined. Consider Fe(II) oxidation by O_2 that proceeds through the following sequence first proposed by Weiss (*37*):

$$Fe(II) + O_2 \rightarrow Fe(III) + O_2^- \quad \text{slow} \quad (17)$$

$$Fe(II) + O_2^- + 2H^+ \rightarrow Fe(III) + H_2O_2 \quad \text{fast} \quad (18)$$

$$Fe(II) + H_2O_2 \rightarrow Fe(III) + OH + OH^- \quad \text{fast} \quad (19)$$

$$Fe(II) + OH \rightarrow Fe(III) + OH^- \quad \text{fast} \quad (20)$$

Relating the measured rate constant derived from $d[Fe(II)]/dt$ to k_{17} depends on the reaction pathways of OH, O_2^-, and H_2O_2. In the limiting case where all these species are scavenged by other pathways, Fe(II) oxidation occurs only through reaction 17:

$$-d[Fe(II)]/dt = -d[O_2]/dt = k_{17}[Fe(II)][O_2] \quad (21)$$

and

$$k_{measd} = k_{17} \quad (22)$$

In the other limiting case, O_2, OH, and H_2O_2 react rapidly with Fe(II) only. Steady-state levels of these three species are low under these conditions, so mass balance considerations indicate that 4 mol of Fe(II) reacts for every 1 mol of O_2. Therefore

$$-d[Fe(II)]/dt = -4d[O_2]/dt = 4k_{17}[Fe(II)][O_2] \quad (23)$$

and

$$k_{measd} = 4k_{17} \quad (24)$$

Applying a steady-state approximation for the intermediates O_2^-, H_2O_2, and OH enables a simplified rate equation to be calculated that yields eq 24, shown in the Appendix.

At the high concentrations of Fe^{2+} used by workers who have studied Fe(II) oxidation in seawater, the second limiting case is observed because of the high reactivity of O_2^- with Fe(II) shown elsewhere (*38*) and of H_2O_2 and OH (probably via Br_2^-) with Fe(II) demonstrated in this work. No other constituents present in the seawater are likely to compete. However, at natural levels in seawater (<1 nM) a variety of other minor constituents are competitive with Fe(II). Under these conditions, if there is no ambient O_2^-, H_2O_2, or OH, Fe(II) is oxidized only by reaction 17. These conditions probably exist in regions such as the deep sea sediment–water interface or hydrothermal vent regions.

The situation is different for Cu(I). During studies of Cu(I) oxidation by O_2, accumulation of H_2O_2 at stoichiometric concentrations was measured, consistent with this work, which shows that peroxide reacts much more slowly with Cu(I) than with Fe(II). Therefore, only 2 mol of Cu(I) is oxidized per mol of O_2, and the rate constant for the bimolecular reaction with O_2 is equal to half the rate constant measured in that study.

The pseudo-first-order rate constants for the reactions in seawater at pH 8.0, T = 25 °C, $[O_2] = 2.1 \times 10^{-4}$ M, and $[H_2O_2] = 1 \times 10^{-7}$ M are shown in Table III. Constants for the oxidation of Fe(II) and Cu(I) by O_2 are also shown, which were calculated from literature values with the considerations described above. Comparison indicates that oxidation by H_2O_2 is the dominant oxidation pathway for Fe(II) under these conditions. Consequently, estimates of the lifetime of Fe(II) in the upper water column should be based on this reaction. Fe(II) oxidation by O_2 is proportional to $[OH^-]^2$ and decreases more sharply with pH than Fe(II) oxidation by H_2O_2, which is proportional to $[OH^-]$. Consequently, the reaction with peroxide will be even more dominant in lower pH systems such as freshwaters. For Cu(I), oxidation by O_2 is the dominant pathway.

Cu(II) reduction is more difficult to assess because the speciation in seawater is controlled by poorly characterized

Table III. Pseudo-First-Order Rate Constants for Cu(I) and Fe(II) Oxidation by O_2 and H_2O_2 in Seawater[a]

rate constant	reference
$Fe(II) + H_2O_2 \rightarrow Fe(III) + OH + OH^-$	
$k = 5 \times 10^{-3}$ s^{-1}	this work
$Fe(II) + O_2 \rightarrow Fe(III) + O_2^-$	
$k = 2.2 \times 10^{-3}$ s^{-1}	Millero et al. (*18*)
$k = 6.7 \times 10^{-4}$ s^{-1}	Waite and Morel (*32*)
$k = 5.8 \times 10^{-4}$ s^{-1}	Murray and Gill (*34*)
$k = 7.6 \times 10^{-4}$ s^{-1}	Kester et al. (*35*)
$Cu(I) + O_2 \rightarrow Cu(II) + O_2^-$	
$k = 7.8 \times 10^{-4}$ s^{-1}	Moffett and Zika (*14*)
$Cu(I) + H_2O_2 \rightarrow Cu(II) + OH + OH^-$	
$k = 1 \times 10^{-5}$ s^{-1}	this work

[a] $[O_2] = 2.1 \times 10^{-4}$ M, $[H_2O_2] = 1 \times 10^{-7}$ M, T = 25 °C, pH 8.0.

organic chelators. Recent evidence indicates that in surface oligotrophic seawater $Cu^{2+}_{free}/Cu^{2+}_{total} \simeq 1 \times 10^{-3}$ (*39*, *40*). Using this to obtain a pseudo-first-order rate for Cu(II) reduction indicates 1–2% of total Cu present as Cu(I) at 10^{-7} M H_2O_2 (*40*). Recent measurements of Cu(I) produced by sunlight irradiation of seawater are 6–10 times higher than this, indicating other reduction processes are more important (*40*).

It is generally recognized that redox couples involving biologically mediated, multielectron transfers are not controlled by a universal p*E* in natural waters (*24*). The results of this study indicate that couples involving labile one-electron transfers are also not controlled by a unique p*E* because of differing reactivities with O_2 and oxygen intermediates such as H_2O_2.

In general, hydrogen peroxide is fairly unreactive with organic compounds, but this reactivity is enhanced in the presence of transition metals because of the formation of free radical intermediates such as O_2^- and OH. The rate of formation of OH from the $Cu(I)/H_2O_2$ reaction, with $[Cu(I)] = 10^{-10}$ M (*40*) and $[H_2O_2] = 10^{-7}$ M (*13*), is 5×10^{-12} M h^{-1}. When integrated over 1 year in the top 20 m of the water column, the production is comparable to the production from nitrite photolysis (*41*). The formation of OH by the $Fe(II)/H_2O_2$ reaction would be equally important at steady-state concentrations of Fe(II) as low as 10^{-13} M. While thermodynamic and kinetic arguments indicate even these concentrations are unlikely in bulk seawater, mechanisms have been proposed for Fe(II) production on microenvironments such as cell surfaces (*42*), so that a mean concentration of 10^{-13} M is not unreasonable. Furthermore, the formation of OH radicals in such microenvironments would have important chemical and biochemical implications.

There is considerable evidence that OH is not produced in reaction 1 for a variety of iron–organic complexes. Instead, the intermediate oxidant is the ferryl radical FeO_2^+, which is a weaker, more selective oxidant than OH (*43*). However, other work (*27*) indicates that reactions involving free Fe^{2+} do produce OH, which may also be the case for $Fe(OH)^+$. Should the ferryl ion be produced, it is still a strong oxidant with a reduction potential of 1 V or greater (cf. 2 V for OH) (*44*). Consequently, in seawater this distinction is probably not important as both species should react rapidly with Br^-, eventually forming Br_2^-, which will be the principal oxidant in subsequent reactions. For copper, OH formation in reaction 1 has also been questioned (*45*), and similar considerations probably apply.

The $Cu(I)/O_2$ and $Cu(II)/H_2O_2$ reactions were investigated as sources of O_2^-. At natural levels of copper the rates of O_2^- formation are negligible compared to measured photochemical production rates from the photooxidation of organic matter (*46*), though they are potentially significant at night in polluted waters (i.e., $[Cu] > 10^{-7}$ M), where formation rates of $(5–10) \times 10^{-9}$ M h^{-1} were calculated.

These results indicate that metal-catalyzed oxidation of organic substrates by peroxide may be important under certain conditions. Zepp and co-workers have observed that Fe enhances the light-induced oxidation of several organic compounds by peroxide (*47*), which may be interpreted in terms of a hydroxyl or ferryl radical intermediate.

Many important reactions involving transition metal redox reactions may occur in microenvironments within the water column such as the surfaces of living cells and detritus and the surface microlayer. Nevertheless, these results provide a useful starting point from which studies in more complex systems can be made.

Acknowledgments

We are indebted to F. J. Millero and R. G. Zepp for their assistance and comments.

Appendix

For the reaction sequence 17–20

$$\frac{-d[Fe(II)]}{dt} = k_{17}[Fe(II)][O_2] + k_{18}[Fe(II)][O_2^-] + k_{19}[Fe(II)][H_2O_2] + k_{20}[Fe(II)][OH] \quad (25)$$

Making the steady-state approximation for the reactive intermediates O_2^-, H_2O_2, and OH

$$\frac{d[O_2^-]}{dt} = 0 \qquad k_{17}[Fe(II)][O_2] = k_{18}[Fe(II)][O_2^-]$$

$$\frac{d[H_2O_2]}{dt} = 0 \qquad k_{18}[Fe(II)][O_2^-] = k_{19}[Fe(II)][H_2O_2]$$

$$\frac{d[OH]}{dt} = 0 \qquad k_{19}[Fe(II)][H_2O_2] = k_{20}[Fe(II)][OH]$$

Therefore, all terms in eq 25 are equivalent and

$$\frac{-d[Fe(II)]}{dt} = 4k_{17}[Fe(II)][O_2]$$

Therefore

$$k_{measd} = 4k_{17}$$

Supplementary Material Available

Three tables and two figures detailing experimental data on pH, chloride, and temperature dependences (5 pages) will appear following these pages in the microfilm edition of this volume of the journal. Photocopies of the supplementary material from this paper or microfiche (105 × 148 mm, 24× reduction, negatives) may be obtained from Microforms Office, American Chemical Society, 1155 16th St., N.W., Washington, DC 20036. Full bibliographic citation (journal, title of article, authors' names, inclusive pagination, volume number, and issue number) and prepayment, check or money order for $13.00 for photocopy ($15.00 foreign) or $10.00 for microfiche ($11.00 foreign), are required.

Registry No. Cu, 7440-50-8; Fe, 7439-89-6; H_2O_2, 7722-84-1; OH, 3352-57-6.

Literature Cited

(1) Zika, R. G.; Moffett, J. W.; Cooper, W. J.; Petasne, R. G.; Saltzman, E. S. *Geochim. Cosmochim. Acta* **1985**, *49*, 1173–84.
(2) Zika, R. G.; Saltzman, E. S.; Cooper, W. J. *Mar. Chem.* **1985**, *17*, 265–75.
(3) Cooper, W. J.; Zika, R. G. *Science (Washington, D.C.)* **1983**, *220*, 711–2.
(4) Draper, W. M.; Crosby, D. G. *Arch. Environ. Contam. Toxicol.* **1983**, *12*, 121–6.
(5) Sinelnikov, V. E.; Liberman, A. S. *Trans. Inst. Biol. Vnutr. Vod. Akach. Nank. (USSR)* **1974**, *29*, 27–40.
(6) Morel, F. M. M.; Morel-Laurens, N. M. L. In *Trace Metals in Seawater*; Wong, C. S., Ed.; Plenum: New York, 1983; pp 841–69.
(7) Haber, F.; Weiss, J. J. *Proc. R. Soc. London, A* **1934**, *147*, 332.
(8) Barb, W. G.; Baxendale, J. H.; George, P.; Hargrave, K. R. *Trans. Faraday Soc.* **1951**, *47*, 591–616.
(9) Gray, R. D. *J. Am. Chem. Soc.* **1969**, *91*, 56–62.
(10) Moffett, J. W.; Zika, R. G.; Petasne, R. G. *Anal. Chim. Acta* **1985**, *175*, 171–9.
(11) Stookey, L. L. *Anal. Chem.* **1970**, *42*, 779–81.
(12) Millero, F. J. *Limnol. Oceanogr.* **1986**, *31*, 839–47.

(13) Zuehlke, R. W.; Kester, D. R. In *Trace Metals in Seawater*; Wong, C. S., Ed.; Plenum: New York, 1983; pp 773-88.
(14) Moffett, J. W.; Zika, R. G. *Mar. Chem.* **1983**, *13*, 239-51.
(15) Miles, C. J.; Brezonik, P. L. *Environ. Sci. Technol.* **1980**, *15*, 1089-95.
(16) Millero, F. J. *Geochim. Cosmochim. Acta* **1985**, *49*, 547-53.
(17) Turner, D. R.; Whitfield, M.; Dickson, A. G. *Geochim. Cosmochim. Acta* **1981**, *45*, 855-82.
(18) Millero, F. J.; Sotolongo, S.; Izaguirre, M. *Geochim. Cosmochim. Acta* **1987**, *51*, 793-801.
(19) Otto, M.; Lerchner, J.; Pap, T.; Zuanziger, H.; Hoyer, E.; Inczedy, J.; Werner, G. *J. Inorg. Nucl. Chem.* **1981**, *43*, 1101-5.
(20) Davies, G.; Higgins, R.; Loose, D. J. *Inorg. Chem.* **1976**, *15*, 700-3.
(21) Sigel, H.; Flierl, C.; Griesser, R. *J. Am. Chem. Soc.* **1969**, *91*, 1061-4.
(22) Smith, R. M.; Martell, A. E. *Critical Stability Constants*; Plenum: New York, 1976; Vol. 4, 257 pp.
(23) Millero, F. J., personal communication, 1986.
(24) Stumm, W.; Morgan, J. S. *Aquatic Chemistry*; Wiley: New York, 1982.
(25) Milazzo, G.; Caroli, S. *Tables of Standard Electrode Potentials*; Wiley: New York, 1978; 419 pp.
(26) Basolo, F.; Pearson, R. G. *Mechanisms of Inorganic Reactions*; Wiley: New York, 1958.
(27) Walling, C. *Acc. Chem. Rs.* **1975**, *8*, 125-31.
(28) Goldstein, S.; Czapski, G. *Inorg. Chem.* **1985**, *24*, 1087-92.
(29) Stanbury, D. M.; Haas, O.; Taube, H. *Inorg. Chem.* **1980**, *19*, 518-24.
(30) Yandell, J. K. *Aust. J. Chem.* **1981**, *34*, 99-106.
(31) Nicol, M. J. *S.—Afr. Tydskr. Chem.* **1982**, *35*, 77-9.
(32) Waite, T. D.; Morel, F. M. M. *Anal. Chem.* **1984**, *56*, 787-92.
(33) Roekens, E. J.; Van Grieken, R. E. *Mar. Chem.* **1983**, *13*, 195-202.
(34) Murray, J. W.; Gill, G. *Geochim. Cosmochim. Acta* **1978**, *42*, 13-9.
(35) Kester, D. R.; Byrne, R. H.; Liang, Y.-J. In *Marine Chemistry of the Coastal Environment*; Church, T. M., Ed.; ACS Symposium Series 18; American Chemical Society: Washington, DC, 1975; pp 56-79.
(36) Berdnikov, V. M. *Russ. J. Phys. Chem. (Engl. Transl.)* **1973**, *47*, 1060-2.
(37) Weiss, J. *Naturwissenschaften* **1935**, *2o*, 64-9.
(38) Rush, J. D.; Bielski, B. H. J. *J. Phys. Chem.* **1985**, *89*, 5062-6.
(39) Sunda, W. G.; Ferguson, R. F. In *Trace Metals in Seawater*; Wong, C. S., Ed.; Plenum: New York, 1983; pp 871-91.
(40) Moffett, J. W.; Zika, R. G. In *Photochemistry of Environmental Aquatic Systems*; Zika, R. G.; Cooper, W. J., Eds.; ACS Symposium Series 327; American Chemical Society: Washington, DC, 1987; Chapter 9.
(41) Zafiriou, O. C.; True, M. B. *Mar. Chem.* **1979**, *8*, 9-32.
(42) Anderson, M. A.; Morel, F. M. M. *Limnol. Oceanogr.* **1982**, *27*, 789-813.
(43) Rush, J. D.; Koppenol, W. H. *J. Biol. Chem.* **1986**, *261*, 6730-3.
(44) Koppenol, W. H.; Liebman, J. F. *J. Phys. Chem.* **1984**, *88*, 99-101.
(45) Johnson, G. R. A.; Nazhat, N. B.; Saadalla-Nazhat, R. A. *J. Chem. Soc., Chem. Commun.* **1985**, 407-8.
(46) Petasne, R. G.; Zika, R. G. *Nature (London)* **1987**, *325*, 516-8.
(47) Skurlatov, Y. I.; Zepp, R. G.; Baughman, G. L. *J. Agric. Food Chem.* **1983**, *31*, 1065-71.

Received for review September 29, 1986. Accepted April 13, 1987. Supported by the Office of Naval Research under Contract N00014-85C-0020.

Quantitation of the Losses of Gaseous Sulfur Compounds to Enclosure Walls

William C. Kuster and Paul D. Goldan*

Aeronomy Laboratory, National Oceanic and Atmospheric Administration Environmental Research Laboratories, Boulder, Colorado 80303

■ Wall loss rates for H_2S, COS, SO_2, CS_2, CH_3SH, C_2H_5SH, CH_3SCH_3 (DMS), and CH_3SSCH_3 (DMDS) are reported in the form of enclosure throughput coefficients. Although COS and CS_2 exhibit negligible losses in all enclosures, significant wall losses were observed for all other species on some enclosure materials. These wall losses were strongly influenced by water vapor. At relative humidities between 40 and 70%, the FEP Teflon enclosure exhibited the smallest losses for all the species tested with only SO_2 and CH_3SH showing large wall losses on this material. For all species except COS and CS_2, wall losses in Pyrex, polycarbonate, and TFE Teflon enclosures are severe enough to affect significantly the interpretation of sulfur flux measurements made with enclosures of these materials.

Introduction

The use of emission flux chambers is an attractive alternative to the more difficult vertical gradient and eddy correlation techniques for the measurement of fluxes of volatile compounds into the atmosphere from natural biogenic sources. This technique involves placing an open-bottomed enclosure over an area of soil, mud, or water, including or excluding vegetation as the experimenter desires, and passing through the enclosure a sweep gas that is usually, but not necessarily, free of the species of interest. The effluent from or gas within the enclosure is then sampled and analyzed for the concentration of the species of interest. This concentration is related to the surface and biomass fluxes.

This method has been helpful in the measurement of the flux of sulfur gases to the atmosphere, not only because of its ease of use but also because of the extremely low atmospheric mixing ratios expected (less than 1 part per billion by volume, ppbv) and the predicted slow atmospheric loss processes for these species. The low concentration makes detection difficult, requiring sample concentration for even the best of the sulfur-specific detectors, the flame photometric detector, and precludes the eddy correlation approach to flux measurement because of the consequent lack of adequate time resolution. Small vertical gradients resulting from relatively slow loss processes make the accurate determination of fluxes from vertical gradient measurements equally unlikely. For these reasons, sulfur flux measurements have relied almost exclusively on the use of flux chambers made of various materials. Ingvorsen and Jorgensen (*1*) and Hansen et al. (*2*) used a Plexiglas chamber to measure H_2S flux. Delmas et al. (*3*) used an unspecified "plastic" chamber to measure H_2S flux. Adams et al. (*4*) and Carroll (*5*) used polycarbonate plastic enclosures, whereas Hill et al. (*6*) and

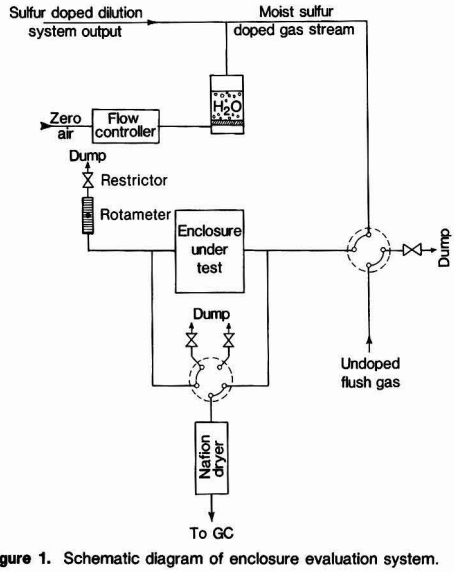

Figure 1. Schematic diagram of enclosure evaluation system.

Steudler and Peterson (*7*) used enclosures lined with some form of Teflon film.

Certainly, great care must be exercised in the use of such a technique since the very presence of the enclosure can disturb the flux of volatile sulfur compounds by altering parameters such as air mass movement, CO_2 concentration, and air temperature. Quite apart from these, however, which are beyond the scope of this study, the relationship between the concentration of a particular species in such an enclosure, the source area and/or biomass enclosed, the flush gas flow rate, and the flux of that species requires a knowledge of its loss rate on the enclosure walls. In all of the above studies, such losses have been asssumed to be negligible. Considering the reactive and labile nature of some of the species of interest, a closer look at the magnitude of wall losses is certainly desirable. Although Adams et al. (*8*) make mention of some testing of the relative merits of Teflon and polycarbonate plastic enclosures for a number of sulfur compounds, (Table 3-2 in ref 8), those tests were of a relative nature only, and no absolute wall or throughput loss rates were determined. Since we had planned to undertake a field measurement program to measure sulfur fluxes from natural biogenic sources, we felt it was essential that prospective enclosure materials be examined for possible significant wall losses for the species of interest in advance of actual field measurements. This paper presents the results of that study. These results should augment those published in the intervening time by Grosjean (*9*), who studied loss rates of many gaseous pollutants including the one sulfur compound SO_2, in FEP Teflon "smog chambers", although at much higher concentrations.

Materials Tested and Testing Procedure

The wall loss characteristics of enclosures constructed of four different materials were studied for the following sulfur compounds: H_2S, COS, SO_2, CS_2, CH_3SH, C_2H_5SH, CH_3SCH_3 (DMS), and CH_3SSCH_3 (DMDS). Of these, H_2S, COS, CS_2, DMS, and DMDS have been implicated by previous studies as being of importance in natural emissions, SO_2 has large known anthropogenic sources, and CH_3SH and C_2H_5SH have been observed in bacterial culture studies. Figure 1 shows a schematic representation of the test apparatus used. A calibration gas stream consisting of a synthetic mixture of O_2 (21%), N_2 (79%), and CO_2 (~300 ppmv) and containing one of the above compounds was generated by a dynamic dilution system described earlier (*10*). To this was added controlled amounts of water vapor to generate a synthetic "zero air" gas stream of approximately 0.25 standard liter per minute (SLPM) containing 0.5–1.5 ppbv of the species of interest, no significant levels of any other reactive species, and with relative humidity variable up to about 70%. This gas stream, or a similar flush gas stream of identical flow rate but without the trace sulfur species, was passed through the enclosure under test, which was sealed except for an inlet and outlet port. Selection between the two streams was made by a four-port Teflon valve with the unused stream being shunted to a "dump". A Teflon valve plumbed in a five-port configuration and two flow restrictors allowed samples to be taken from either upstream or downstream of the enclosure while maintaining the flow through the enclosure constant irrespective of the sample source. This provision was found to be especially important for accurate measurements in the testing of thin-film Teflon enclosures. These would change volume by "breathing" if the throughput was allowed to vary. All flows were monitored with calibrated rotameters, although only one is shown in Figure 1 for simplicity.

Enclosures tested were made of polycarbonate plastic, Pyrex glass, rigid TFE Teflon, and FEP Teflon Film. The polycarbonate enclosure was that actually used by Carroll (*5*), and its joints were sealed with a low vapor pressure silicone adhesive. The seams of the FEP Teflon enclosure were heat sealed. The Pyrex and TFE enclosures were standard commercially available vessels. Inflow into each enclosure was near one of the walls. Outflow was drawn from near the center of each enclosure, although several tests indicated that the results were independent of the placement of the outflow tube.

The analytical system, which has been described in some detail elsewhere (*11*), uses "cryogenic enrichment" of approximately 1-L samples STP A sample stream of 100 cm^3 min^{-1} is passed through Teflon lines to a Teflon capillary submerged in liquid N_2 and then into a previously evacuated vessel. Subambient pressure in the capillary ($\simeq$100 Torr) prevents the accumulation of liquid O_2. The thus acquired sample is then flash heated and injected onto a 60-m capillary column with a bonded methyl silicone stationary phase, which is temperature programmed from –50 to 200 °C at 16 deg/min. Detection takes place in an SF_6-doped flame photometric detector (FPD). The whole system, consisting of sample acquisition, gas chromatographic separation, and detection, has a detection limit of approximately 2×10^{-12} g of S per sample with negligible acquisition losses for all species tested at mixing ratios down to at least 10^{-11} (10 pptv), i.e., ~1% of the mixing ratios used for these tests.

The testing procedure for each enclosure and each sulfur species was the same. The enclosure was flushed with the undoped gas stream until the mixing ratio of all sulfur species in the effluent stream was below the detection limit. This required from 0.5 to 2 h, depending on the enclosure material and its previous use history. Prior to and during this time, the sulfur-doped source stream was allowed to equilibrate and was sampled for stability. The enclosure input stream was then switched from the undoped stream to the doped stream, and samples were drawn alternately every 20 min from the enclosure input and output streams to monitor the growth of the sulfur species concentration

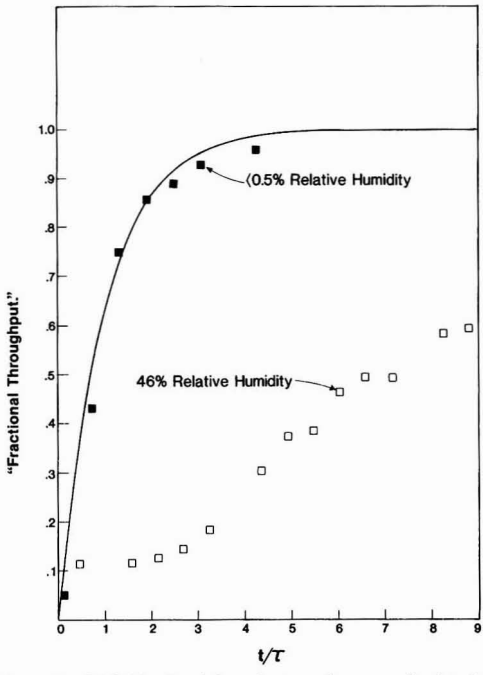

Figure 2. CH_3SH fractional throughput vs. time normalized to the residence time in a TFE Teflon enclosure for two different relative humidities.

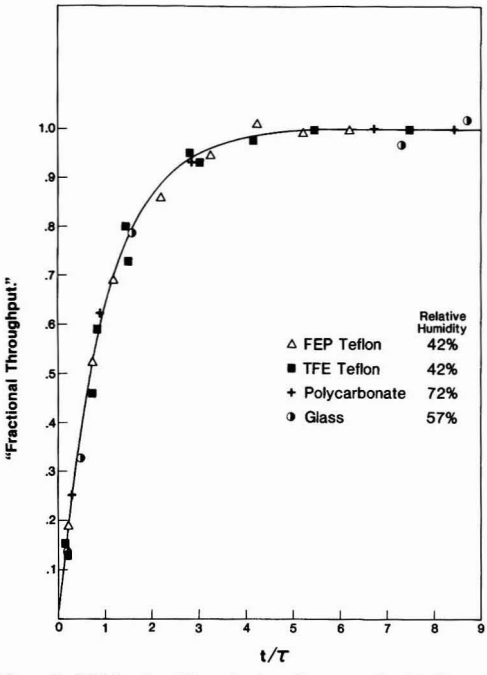

Figure 3. COS fractional throughput vs. time normalized to the residence time in four different enclosures.

issuing from the enclosure and to assure constancy of the input mixing ratio. If one assumes that the gas in the enclosure is well mixed, an assumption that the data for COS and CS_2 substantiate, the growth in mixing ratio of an input species, x, would be expected to follow

$$M_x(t) = M_{x0}(1 - e^{-tF/V}) = M_{x0}(1 - e^{-t/\tau}) \qquad (1)$$

where M_{x0} is the constant mixing ratio of x in the incoming stream, t is the time since the doped stream was introduced into the enclosure, V is the enclosure volume, F is the gas flow rate expressed as volume per unit time, and $\tau = V/F$. All the test results are compared to this ideal growth rate with the fractional throughput $M_x(t)/M_{x0}$ plotted against t/τ. Testing periods varied from 2 to 24 h depending on the enclosure volume and the actual growth rate observed. The long-period tests approaching 24 h were performed only for those species that appeared to be transmitted poorly or not at all under a given set of test conditions.

Test Results

Figure 2 shows the test results of CH_3SH in the TFE Teflon enclosure for two different relative humidities: 46% and less than 0.5% when no moisture was added. The solid line in this and all subsequent figures is the ideal growth curve derived from eq 1. The fractional transmission appears to follow the ideal growth curve with no added moisture, but a dramatic reduction in transmission occurs at a higher relative humidity. For this reason, all subsequent data were taken with relative humidities in the 40–70% range to simulate actual field sampling conditions, where considerable moisture is encountered.

Some sulfur species are relatively unreactive and have low water solubilities. Such species are expected to be well-behaved in all enclosures, even at high moisture levels. Figures 3 and 4 show that the fractional throughput vs.

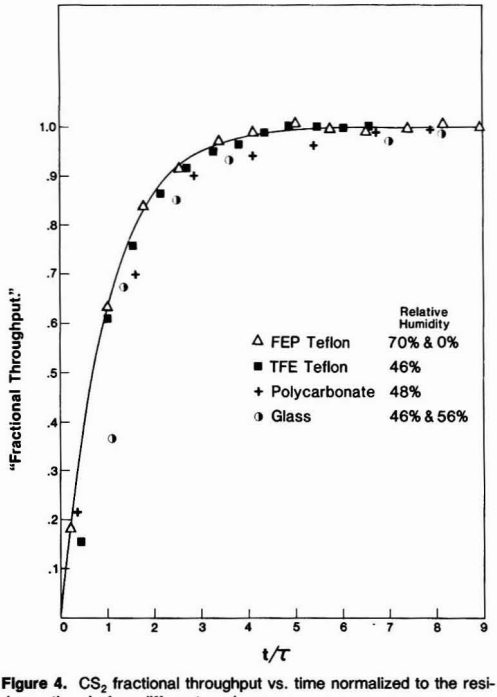

Figure 4. CS_2 fractional throughput vs. time normalized to the residence time in four different enclosures.

time for COS and CS_2 follows the ideal growth curve in all four tested enclosures. For SO_2, which has a high water solubility, high enclosure throughput losses are experienced. Figure 5 shows SO_2 throughput of only 3–10% for

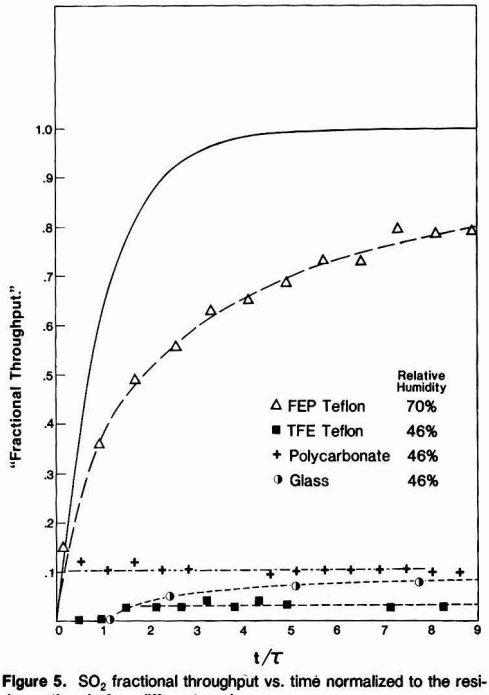

Figure 5. SO_2 fractional throughput vs. time normalized to the residence time in four different enclosures.

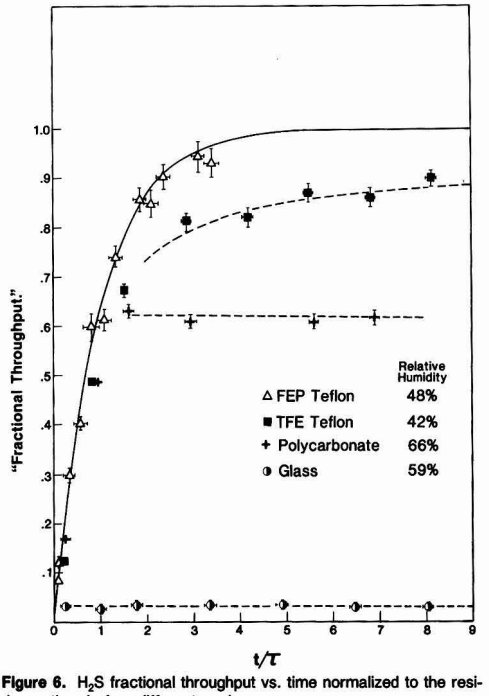

Figure 6. H_2S fractional throughput vs. time normalized to the residence time in four different enclosures.

Pyrex, polycarbonate, and TFE Teflon enclosures with realistic relative humidities. Although the FEP Teflon film appears much better, it too requires equilibration times exceeding 10 flushing times to achieve a fractional throughput exceeding 80%.

H_2S, a fairly reactive species, shows the mixed results displayed in Figure 6. Fractional throughput through the Pyrex enclosure was quite low, probably as a result of efficient chemisorption at metal ion sites in the glass. Polycarbonate and TFE Teflon showed lesser, though still significant, losses with the polycarbonate displaying an apparently constant 40% throughput loss under the test conditions used. Only FEP Teflon permitted an H_2S growth rate predicted by eq 1. The size of the error bars in Figure 6 shows the sample acquisition period by their horizontal extent and the accuracy of the gas chromatographically determined fractional throughput by their vertical extent. Although presented only in this figure, similar error bars apply to all the data shown in Figures 2–10.

Figures 7–10 show the test results for CH_3SH, C_2H_5SH, DMS, and DMDS, respectively. No CH_3SH was observed to survive transit through the Pyrex enclosure at a relative humidity of 46%, although measurements were made for 24 h or out to $t/\tau \sim 100$. Significant loss of this species was observed for all the materials tested, although the FEP Teflon and polycarbonate appeared to be approaching equilibrium for $t/\tau \sim 20$. For C_2H_5SH, only the FEP Teflon film appears to be a usable enclosure material. For both DMS and DMDS, only the polycarbonate enclosure appears to cause significant throughput losses, and these are only moderate.

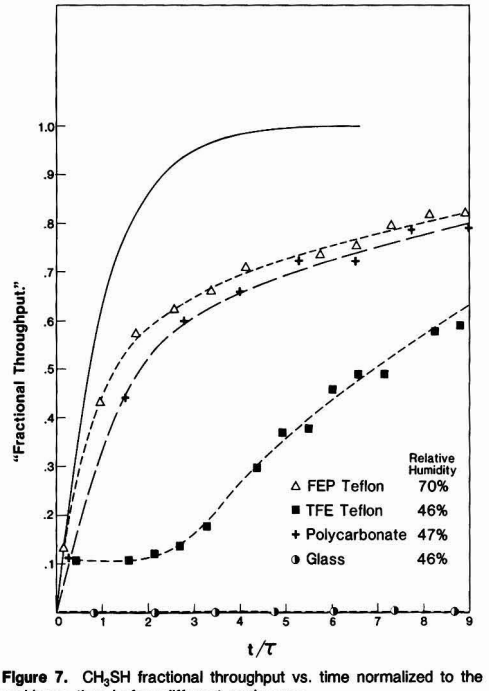

Figure 7. CH_3SH fractional throughput vs. time normalized to the residence time in four different enclosures.

Conclusions

The data presented in Figures 2–10 are not intended to be universal curves predicting the results that will be obtained with the enclosure materials tested under arbitrary field measurement conditions. Synergistic effects between trace species present, many of them probably not sulfur

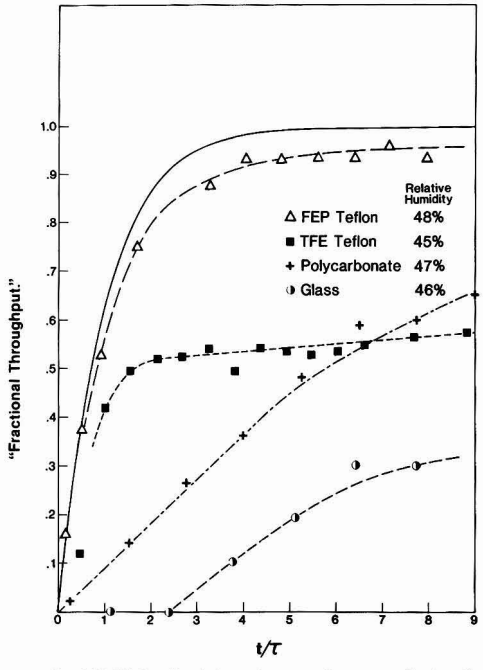

Figure 8. C_2H_5SH fractional throughput vs. time normalized to the residence time in four different enclosures.

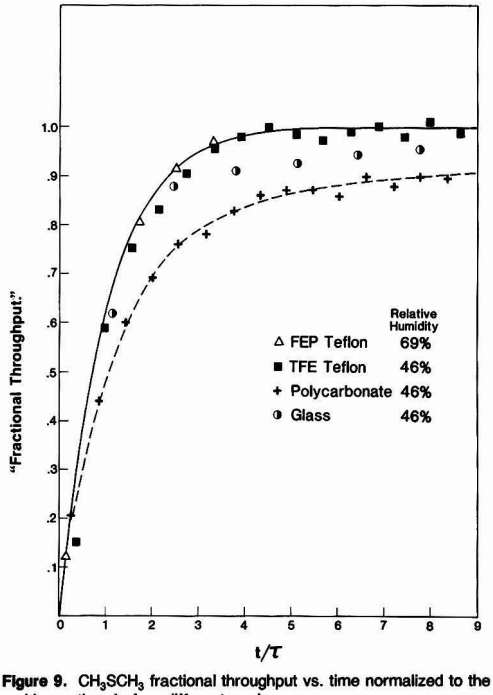

Figure 9. CH_3SCH_3 fractional throughput vs. time normalized to the residence time in four different enclosures.

bearing, and other surface contaminants are expected to play a role. The data are presented, rather, as a guide to the most appropriate materials to use for enclosures when

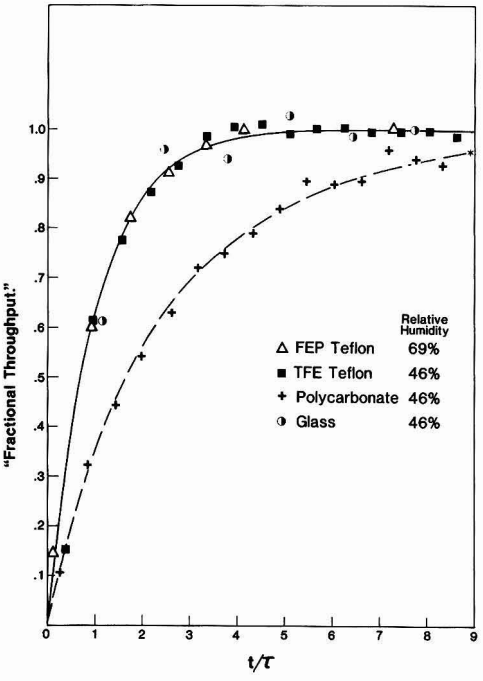

Figure 10. CH_3SSCH_3 fractional throughput vs. time normalized to the residence time in four different enclosures.

measuring sulfur fluxes and as a caution in the interpretation of data that are already in the literature. Some gases such as COS and CS_2 are easy to handle, and all the materials tested will suffice as enclosure walls. It is equally clear that the FEP Teflon film is far superior to the other materials tested for the handling of SO_2, H_2S, and C_2H_5SH and marginally superior in the handling of CH_3SH. Very significant losses of SO_2 can be experienced even in TFE Teflon tubing and fittings under moist conditions, a fact that must be taken into account even in the measurement of SO_2 mixing ratios in ambient air without the use of enclosures.

The use of enclosures for the measurement of gaseous fluxes from natural systems requires care in assuring that the enclosure itself does not influence naturally occurring source strengths, areas that have not been addressed by this study. Additionally, the enclosure material must be chosen so that the observed mixing ratios can be sensibly related to the source strengths present. FEP Teflon film appears to be the best material for the measurement of sulfur fluxes, although care must be exercised in the interpretation of SO_2 and CH_3SH flux data when this material is used for enclosure walls. Fortunately, neither of these species appears, at the present time, to be an important contributor to natural emissions.

Acknowledgments

We are indebted to M. A. Carroll (NOAA Aeronomy Laboratory, Boulder, CO) for providing the polycarbonate enclosure used in this study and to P. Zimmerman (National Center for Atmospheric Research, Boulder, CO) for providing the FEP Teflon film.

Registry No. DMS, 75-18-3; DMDS, 624-92-0; TFE, 9002-84-0; FEP, 25067-11-2; H_2S, 7783-06-4; COS, 463-58-1; SO_2, 7446-09-5; CS_2, 75-15-0; CH_3SH, 74-93-1; C_2H_5SH, 75-08-1.

Literature Cited

(1) Ingvorsen, K.; Jorgensen, B. B. *Atmos. Environ.* **1982**, *16*, 855–865.
(2) Hansen, M. H.; Ingvorsen, K.; Jorgensen, B. B. *Limnol. Oceanogr.* **1978**, *23*, 68–76.
(3) Delmas, R.; Baudet, J.; Servant, J.; Baziard, Y. *J. Geophys. Res.* **1980**, *85*, 4468–4474.
(4) Adams, D. F.; Farwell, S. O.; Pack, M. R.; Robinson, E. *J. Air Pollut. Control Assoc.* **1981**, *31*, 1083–1089.
(5) Carroll, M. A. Ph.D. Thesis, MIT, 1983.
(6) Hill, F. B.; Aneja, V. P.; Felder, R. M. *J. Environ. Sci. Health, Part A* **1978**, *A13*, 199–225.
(7) Steudler, P. A.; Peterson, B. J. *Nature (London)* **1984**, *311*, 455–457.
(8) Adams, D. F.; Farwell, S. O.; Robinson, E.; Pack, M. R. EPRI Report EA-1516, Project 856-1; Washington State University: Pullman, WA, 1980.
(9) Grosjean, D. *Environ. Sci. Technol.* **1985**, *19*, 1059–1065.
(10) Goldan, P. D.; Kuster, W. C.; Albritton, D. L. *Atmos. Environ.* **1986**, *20*, 1203–1209.
(11) Goldan, P. D.; Kuster, W. C.; Albritton, D. L.; Fehsenfeld, F. C. *J. Atmos. Chem.*, in press.

Received for review March 25, 1986. Accepted April 10, 1987. This reasearch was supported by NOAA as part of the National Acid Precipitation Assessment Program.

Mutagenic Activity Associated with Cooling Tower Waters Treated with a Biocide Containing 5-Chloro-2-methyl-4-isothiazolin-3-one†

George M. Woodall,‡ Oscar C. Pancorbo,*,§ R. Dean Blevins,∥ and Kenneth E. Ferslew⊥

Department of Environmental Health and Department of Health Sciences, School of Public and Allied Health, and Department of Pharmacology, Quillen-Dishner College of Medicine, East Tennessee State University, Johnson City, Tennessee 37614, and Environmental Health Science Program, Department of Food Science and Technology, The University of Georgia, Athens, Georgia 30602

■ With the Ames *Salmonella*–mammalian microsome test, significant mutagenic activity was detected in cooling tower water shortly (same day) after treatment with a biocide (CL2150) containing 5-chloro-2-methyl-4-isothiazolin-3-one (5-chloro-IT). Dose-related mutagenic responses with TA97 (–S9) and TA100 (–S9) were produced with the acid fraction (extracted at pH <2 with methylene chloride) of this cooling water sample (specific mutagenic activities of 281 000 and 118 000 net revertants/L equiv of water, respectively). This mutagenic activity detected in cooling water sampled in mid-summer did not persist beyond the first day of CL2150 treatment. The mutagenic activity displayed by the cooling waters with TA97 (–S9) exceeded that associated with the extractable 5-chloro-IT concentration (determined by capillary gas chromatography–mass spectrometry).

Introduction

Cooling towers are efficient, closed-cycle, evaporative systems used to dissipate heat during power generation and other processes (*1*). Although cooling towers protect our aquatic environment from thermal stress, these systems can also adversely impact surface waters through the discharge of blowdown (*2*). Blowdown is the water periodically drained from cooling towers in order to prevent excess accumulation of solids within the system. A variety of chemical agents are added to cooling waters in order to protect system components, including biocides, corrosion inhibitors, dispersants, and chelating agents (*3*). Biocides, such as chlorine, are added to cooling waters to control biological fouling (*4*) and microbial human pathogens, such as *Legionella pneumophila*, which proliferate in cooling towers and pose significant public health risks (*5*). However, chlorination of power plant cooling waters has been shown to generate organohalogens (*4*), which are produced following the reaction of chlorine with fulvic and humic acids present in natural waters (*6*). Chlorination has been found responsible for increased mutagenic activity in cooling waters from a production nuclear reactor (*7*), as well as in treated drinking waters (*8*, *9*), groundwater (*8*), surface waters (*10*, *11*), swimming pool water (*12*), and waste water effluents (*13*, *14*). It appears that aqueous chlorination of humic acids results in the formation of compounds with direct-acting (i.e., not requiring metabolic activation) mutagenic activity, such as 2-chloropropenal (*15–17*).

Because disinfection of cooling waters may generate mutagens that are discharged in the blowdown, there is a need for additional research on the mutagenic activity of these waters. Herein, we report the results of a study focusing on the mutagenic potential, as determined by the Ames *Salmonella*–mammalian microsome test, of waters from a hospital cooling tower treated with an organic biocide containing the active ingredients 5-chloro-2-methyl-4-isothiazolin-3-one (hereinafter designated 5-

Table I. Biocides and Other Compounds Added to the Hospital Cooling Tower Waters

product[a]	active compound(s)	%[b]
CL2150 (15300-24)	5-chloro-2-methyl-4-isothiazolin-3-one (biocide)	1.15
	2-methyl-4-isothiazolin-3-one (biocide)	0.35
CL216 (31910-2-15300)	sodium dimethyldithiocarbamate (biocide)	15.0
CL1406	neutralized organophosphonate (sequestrant)	–
	polyacrylate polymer (dispersant)	–
	tolyltriazole (corrosion inhibitor)	–

[a] Manufactured by Chemtreat, Inc., Ashland, VA; within parentheses are the U.S. Environmental Protection Agency's registration numbers. [b] A dash denotes that the percentage of active compound in the product was not available from the manufacturer.

† This paper was presented at the 17th Annual Meeting of the Environmental Mutagen Society, April 1986, Baltimore, MD.
‡ Department of Environmental Health.
§ Environmental Health Science Program.
∥ Department of Health Sciences.
⊥ Department of Pharmacology.

0013-936X/87/0921-0815$01.50/0

chloro-IT) and 2-methyl-4-isothiazolin-3-one (2-methyl-IT).

Experimental Section

Cooling Water Sampling Protocol. Circulating cooling water samples were obtained from a hospital cooling tower located in Johnson City, TN. This tower utilized Johnson City municipal water as makeup water following the discharge of blowdown into the city sewer system. As shown in Table I, several biocides and other active compounds were added to the cooling water in the tower. Additives CL2150 and CL216 were alternated on a regular schedule, while CL1406 was on a continuous feed. Circulating cooling water grab samples were obtained from the tower during the period of May 31–August 5, 1985, in 1-gal amber-glass bottles. All glassware was soaked in 50% HNO_3 (Fisher Scientific), triple rinsed with distilled–deionized water, and rinsed twice with acetone (Fisher Scientific). Unless otherwise specified, the organic solvents were glass distilled.

Cooling Water Extraction. All cooling water samples were stored at 4 °C for no more than 72 h before they were extracted by U.S. Environmental Protection Agency Method 625 (*18*). This method consists of the extraction of 1-L water samples with methylene chloride (Fisher Scientific) at pH >11 (for base/neutral-extractable organics) and at pH <2 (for acid-extractable organics). The acidic and basic/neutral extracts were separately concentrated to approximately 5 mL in a rotary evaporator (Haake Buchler). Each concentrated extract was then transferred to a ceramic evaporating dish with two 5-mL acetone washes of the evaporator vessel and then evaporated to dryness in a vacuum desiccator at 25 °C. The resulting residues were each dissolved in 4 mL of dimethyl sulfoxide (Me_2SO, spectrophotometric grade, Aldrich Chemical Co.) and stored at −20 °C until assayed for mutagenic activity.

Extraction of CL2150. In order to evaluate the mutagenic potency of 5-chloro-IT, a 1.15-ppm solution of this compound was prepared in ultrapure water from the CL2150 product (100 ppm of CL2150 and assuming 1.15% of 5-chloro-IT in CL2150, Table I). A 1-L sample of this 1.15-ppm 5-chloro-IT solution was then extracted in the same manner as the cooling tower water samples described in the previous paragraph. As a negative control, a 1-L sample of the ultrapure water (obtained by passage of distilled–deionized water through a Barnstead ultrapure mixed-bed cartridge) was also similarly extracted. Both of these final extracts in Me_2SO were stored at −20 °C until assayed for mutagenic activity. As an additional control, the CL2150 product was directly diluted in Me_2SO and assayed for mutagenic activity.

Mutagenicity Assay. The Ames *Salmonella*–mammalian microsome assay was used to determine the mutagenicity of the samples described above. The protocol followed was that of Maron and Ames (*19*), with the modifications recommended by Batzinger et al. (*20*). These modifications consisted of adding biotin and trace amounts of histidine to the bottom agar, rather than top agar, and replacing the NaCl in the top agar with Vogel–Bonner minimal E medium.

Three to four doses of each water extract (and also of the CL2150 product), prepared by serial dilutions in Me_2SO, were plated in triplicate at a constant volume of 100 μL. These doses represented between 0.25 and 25 mL of the original water sample per plate. Cooling water extracts were tested with the *Salmonella* strains recommended by Maron and Ames (*19*) as the standard tester set (TA97, TA98, TA100, and TA102) and with TA1535, or with only TA97, TA98, and TA100. Extracts were tested in the absence (−S9) or the presence (+S9) of the microsomal activation mix containing the Aroclor 1254 induced rat liver homogenate fraction S9 at 50 μL of S9 per plate (prepared in KCl, Litton Bionetics). The spontaneous reversion rate, both in the presence (when appropriate) and absence of S9 activation, was determined for each tester strain in triplicate with Me_2SO as the solvent control. With each assay performed, the tester strains were checked for appropriate responses to known mutagens in Me_2SO. A positive mutagenic response was defined as a dose-related response with one or more doses producing at least a 2-fold increase in revertant colonies per plate as compared to the concurrent spontaneous count per plate (*19*, *21*). The specific mutagenic activities of the water extracts were each expressed as net revertants per liter equivalent of original water and were based on the slope (determined by least-squares regression analysis) of the initial linear portion of the dose–response curve (*19*). The statistical significance (probabilities) of the resulting slope and correlation coefficient (r) for the dose–response curve of each extract was determined (*21*).

GC–MS Analysis. Gas chromatography–mass spectrometry (GC–MS) was used to determine the concentration of 5-chloro-IT in the CL2150 product and in the acidic water extracts. One milliliter each of the CL2150 product (diluted in Me_2SO), the extract (Me_2SO) of the 1.15-ppm 5-chloro-IT solution in ultrapure water, and the extract (Me_2SO) of cooling water sampled shortly after treatment with CL2150 was taken to dryness on a Sybron/Brinkman SC-248 sample concentrator and was then dissolved in 40 μL of methanol (Fisher Scientific). These samples were then analyzed on a Finnigan Model 4000 GC–MS, with a 15 m long by 0.25 mm i.d. DB-5 bonded-phase fused silica capillary column with a 1.0-μm film. A 10-μL volume, containing 9.0 μL of sample and 1.0 μL of meperidine (1.0 μg/μL) as an internal standard, was applied by splitless injection with sweep at 0.8 s. The injector and separator temperatures were maintained at 200 and 250 °C, respectively. The oven temperature was programmed to hold at 100 °C for 30 s and was then ramped at 10 deg/min to 250 °C, where it was held for 30 min. Helium was used as the carrier gas at 20 psi column pressure.

Results

Mutagenic Activity of Cooling Water Extracts. The data pertaining to the mutagenic activity of organic extracts of hospital cooling tower water samples are summarized in Table II. The first cooling water sample (31 May), taken 3 days after the treatment of the tower with the CL2150 biocide, displayed no detectable mutagenic activity in the base/neutral fraction (Table II). Moreover, the acid fraction produced a dose-related mutagenic response only with TA98 in the absence of S9 (Figure 1). When first assayed with TA98 (−S9) (14-day assay), this fraction produced a dose–response curve with a statistically significant slope ($p < 0.01$) of 2.74 revertants/mL equiv of water (specific mutagenic activity of 2740 net revertants/L equiv). This mutagenic response was reproducible after storage of the acid extract at −20 °C for 57 days. In the 57-day assay, however, there was a reduction in the revertants per plate induced by the highest water equivalent dose (Figure 1). The acid fraction also produced a statistically significant ($p < 0.01$) linear dose–response, short of 2-fold over the spontaneous rate, with TA 100 (−S9) (Figure 1). On the basis of our criteria described under Experimental Section, however, this response cannot be considered positive for mutagenesis. After the mutagenicity results of this first cooling water sample were reviewed, it was decided to employ only tester strains TA97, TA98, and TA100, in the absence of S9, for

Table II. Mutagenicity of Organic Extracts of Hospital Cooling Tower Water Samples

	water treatment[a]	fraction	net revertants per liter equivalent of water									
			TA97		TA98		TA100		TA102		TA1535	
			-S9	+S9	-S9	+S9	-S9	+S9	-S9	+S9	-S9	+S9
sample date (1985)												
31 May	CL2150	acid	T[b]	T	2740[d]	T	ND[d,e]	T	ND	ND	ND	ND
	(3 days prior)	base/neutral	ND[c]	ND	ND	ND	ND	ND	ND	ND	ND	ND
8 June	CL216	acid	ND	–	ND	–	ND	–	–	–	–	–
	(3 days prior)	base/neutral	ND	–	ND	–	ND	–	–	–	–	–
2 Aug	CL216	acid	ND	–	ND	–	ND	–	–	–	–	–
	(1 day prior)	base/neutral	ND	–	ND	–	ND	–	–	–	–	–
3 Aug	CL2150	acid	281 000[f]	–	ND	–	118 000[g]	–	–	–	–	–
	(same day)	base/neutral	ND	–	ND	–	ND	–	–	–	–	–
4 Aug	–	acid	ND[e,f]	–	ND	–	ND[e,g]	–	–	–	–	–
		base/neutral	ND	–	ND	–	ND	–	–	–	–	–
5 Aug	CL216	acid	ND	–	ND	–	ND	–	–	–	–	–
	(same day)	base/neutral	ND	–	ND	–	ND	–	–	–	–	–
controls												
1.15-ppm	–	acid	30 000[f]	–	ND	–	36 100[g]	–	–	–	–	–
5-chloro-IT		base/neutral	ND	–[h]	ND	–	ND	–	–	–	–	–
ultrapure	–	acid	ND	–	ND	–	ND	–	–	–	–	–
water		base/neutral	ND	–	ND	–	ND	–	–	–	–	–

[a] In addition to the biocides listed, the cooling water was treated continuously with CL1406 (Table I); in parentheses, the day of treatment relative to the day of sampling is indicated. [b] T = toxic responses. [c] ND = no detectable (i.e., all sample doses produced less than 2-fold increase in revertants as compared to the concurrent spontaneous plates). [d] Figure 1. [e] These samples produced a statistically significant linear dose–response short of 2-fold over spontaneous. [f] Figure 2. [g] Figure 3. [h] Dashes denote that the test was not performed.

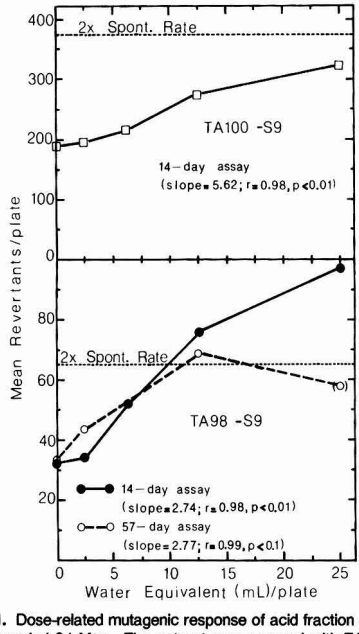

Figure 1. Dose-related mutagenic response of acid fraction of cooling water sampled 31 May. The extract was assayed with TA98 (–S9) after 14 and 57 days of storage at –20 °C and with TA100 (–S9) after 14 days of storage. Linear regression analysis data are shown [for mean revertants per plate vs. water equivalent (milliliter) per plate], which include slope, correlation coefficient (r), and probability of significance (p). The point in parentheses was not included in the regression analysis.

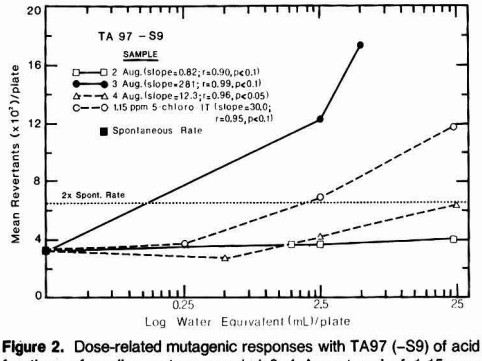

Figure 2. Dose-related mutagenic responses with TA97 (–S9) of acid fractions of cooling waters sampled 2–4 August and of 1.15-ppm 5-chloro-IT control. See Figure 1 legend for definitions of regression analysis terms.

screening all subsequent cooling water samples.

Cooling water samples were taken from the tower on 8 June, 2 August, and 5 August, which were 3, 1, and 0 days, respectively, after treatment with the CL216 biocide containing sodium dimethyldithiocarbamate. As shown in Table II, neither the acid nor base/neutral fractions of these samples were mutagenic with TA97, TA98, or TA100, in the absence of S9. Consistent with this finding, De Flora et al. (22) demonstrated sodium diethyldithiocarbamate to be negative for mutagenesis with Ames tester strains TA98, TA100, TA1535, TA1537, and TA1538. In contrast, significant mutagenic activity, with TA97 and TA100, was detected in the acid fraction of a cooling water sample (3 August) taken shortly (same day) after treatment with the CL2150 biocide (Table II). This fraction produced dose-related mutagenic responses with slopes of 281 and 118 revertants/mL equiv of water (specific mutagenic activities of 281 000 and 118 000 net revertants/L equiv, respectively) with TA97 (–S9) (Figure 2) and TA100 (–S9) (Figure 3), respectively. Although both of these dose–response curves displayed excellent correlation coefficients (r) of 0.99, the statistical significance of the slopes could only be set at $p < 0.1$ because of the low degrees of freedom (1). A cooling water sample (4 August) was subsequently taken from the tower 1 day after treatment with the CL2150 biocide (Table II). The acid fraction of this sample produced statistically significant ($p < 0.05$) linear dose–responses, short of 2-fold over the spontaneous rate, with TA97 (–S9) (Figure 2) and TA100 (–S9) (Figure 3). On the basis of our criteria described under Experimental

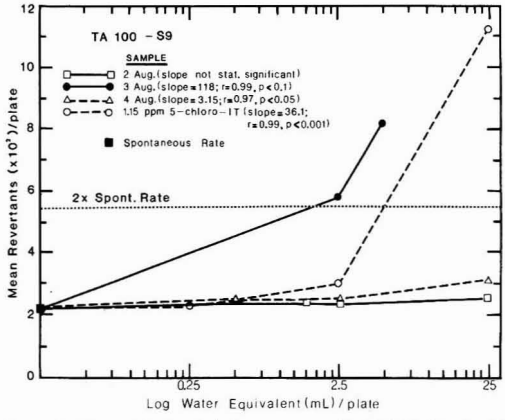

Figure 3. Dose-related mutagenic responses with TA100 (–S9) of acid fractions of cooling waters sampled 2–4 August and of 1.15-ppm 5-chloro-IT control. See Figure 1 legend for definitions of regression analysis terms.

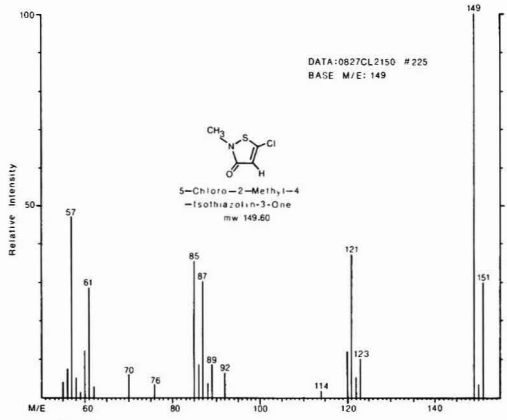

Figure 4. Mass spectrum of 5-chloro-2-methyl-4-isothiazolin-3-one.

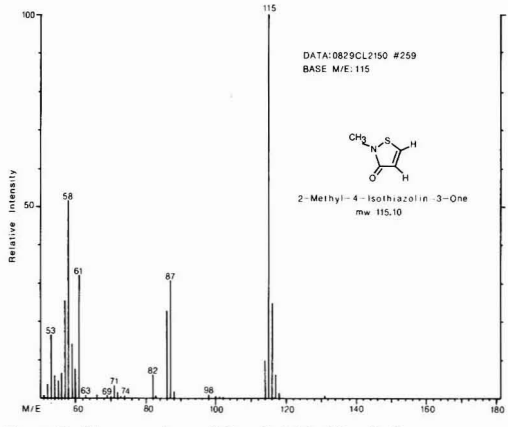

Figure 5. Mass spectrum of 2-methyl-4-isothiazolin-3-one.

Section, however, this response cannot be considered positive for mutagenesis. Moreover, both acid and base/neutral fractions of the 3 and 4 August samples were not mutagenic with TA98 and TA97, TA98, and TA100, respectively (Table II). It appears that the mutagenic activity initially detected in cooling water did not persist beyond the first day of CL2150 treatment.

Mutagenic Activity of CL2150. On the basis of the mutagenic responses, in TA97 (–S9) and TA100 (–S9), of cooling waters treated with the CL2150 biocide, it appears that this biocide contains one or more potent, direct-acting, frameshift mutagens (*19*, *23*). Unfortunately, we were unable to commercially procure pure preparations of the two active compounds in this biocide, namely, 5-chloro-IT and 2-methyl-IT. Consequently, we were unable to determine the mutagenic activity of these compounds individually. Instead, the commercial CL2150 product diluted directly in Me_2SO was assayed for mutagenic activity. While a CL2150 dose representing 1.15 μg of 5-chloro-IT (major active ingredient) per milliliter displayed notable mutagenic activity with TA97 (–S9) and TA100 (–S9) (i.e., numbers of revertants were at least 2-fold greater than the spontaneous rates), higher CL2150 doses representing 11.5–115 μg of 5-chloro-IT/mL were toxic to the tester strains (data not shown). Further testing was undertaken with a solution of CL2150 in ultrapure water containing 1.15 ppm of 5-chloro-IT (i.e., concentration of 5-chloro-IT recommended by the manufacturer for use in hospital towers). This solution of 5-chloro-IT and ultrapure water used as the diluent were extracted in the same manner as the cooling water samples and then assayed for mutagenicity. As shown in Table II, neither the acid nor the base/neutral fraction of the ultrapure water control was mutagenic with TA97, TA98, or TA100, in the absence of S9. The pattern of mutagenicity produced by the 1.15-ppm 5-chloro-IT solution was very similar to that of the 3 August cooling water sample that had been treated with CL2150 that same day (Table II). Positive mutagenicity (i.e., dose-related mutagenic response) was observed only in the acid fraction with TA97 (–S9) (Figure 2) and TA100 (–S9) (Figure 3).

GC–MS Analysis of CL2150. The total ion chromatogram (not shown) from GC–MS analysis of the CL2150 mixed residue dissolved in methanol displayed one major peak at scan 225 s. The mass spectrum of this major peak is shown in Figure 4. The NBS library of mass spectra did not include the mass spectra of the isothiazolinones. However, the mass spectrum in Figure 4 is that of 5-chloro-IT. This conclusion is based on the fact, among others, that the base ion at m/e 149 corresponds to the molecular weight of 5-chloro-IT. The mass spectrum of the other active ingredient in CL2150, namely, 2-methyl-IT, is shown in Figure 5.

Mutagenic Activity of Cooling Waters As Related to 5-Chloro-IT Concentration. The concentration of 5-chloro-IT in the acid fraction of cooling waters and control (1.15-ppm 5-chloro-IT) was determined with GC–MS by comparison of the peak height of the m/e 149 base ion in the mass spectrum of the sample to that of a standard of known 5-chloro-IT concentration (i.e., peak height is directly proportional to the concentration of 5-chloro-IT). The commercial formulation of CL2150 served as the standard solution of 5-chloro-IT with the reported 1.15% 5-chloro-IT concentration in this product (Table I). The acid-extractable, 5-chloro-IT concentration in most cooling water samples was low. As expected, the highest concentrations of 5-chloro-IT were detected in the 3 August cooling water sample, which had been treated that same day with CL2150, and in the 1.15-ppm 5-chloro-IT control. Shown in Table III are the extractable 5-chloro-IT concentrations in these two samples, expressed as micrograms per milliliter of acid extract and micrograms per liter equivalent of water. On the basis of the 1.15% content of 5-chloro-IT in the CL2150 product added to

Table III. Specific Mutagenic Activities of Acid Fractions of Cooling Water Sample and Control As Related to Extractable Concentrations of 5-Chloro-IT

sample	extractable 5-chloro-IT concentration[a]		TA97 (–S9) net revertants		TA100 (–S9) net revertants	
	acid extract, μg/mL	water equiv, μg/L	per liter equiv	per μg of 5-chloro-IT	per liter equiv	per μg of 5-chloro-IT
3 Aug, cooling water[b]	63	252	281 000	1115	118 000	468
1.15-ppm 5-chloro-IT (CL2150 in ultrapure water)	22	88[c]	30 000	341	36 100	410

[a] Extracted 1-L samples using methylene chloride at pH <2; the resulting extract (4 mL) was analyzed via GC–MS. [b] Treated on the same day with CL2150 product containing 5-chloro-IT. [c] This value represents the extraction of 7.65% of 5-chloro-IT added to the ultrapure water (i.e., based on 1.15% content of 5-chloro-IT in the CL2150 product as stated in the product label).

ultrapure water, the acid–methylene chloride extraction procedure employed was capable of extracting only 7.65% of the 5-chloro-IT in the water (Table III) (since the base/neutral extracts of cooling waters and 1.15-ppm 5-chloro-IT control were not mutagenic, no attempt was made to measure the 5-chloro-IT concentrations in these samples). Using the extractable 5-chloro-IT concentrations in these two water samples, we converted the specific mutagenic activities (i.e., with TA97 and TA100, both in the absence of S9) from net revertants per liter equivalent of water to net revertants per microgram of 5-chloro-IT. As shown in Table III, similar 5-chloro-IT-specific mutagenic activities were measured in the 3 August cooling water and 1.15-ppm 5-chloro-IT control with TA100 (–S9) (i.e., 468 and 410 net revertants per microgram of 5-chloro-IT, respectively). In contrast, there were substantially more TA97(–S9) net revertants induced per microgram of 5-chloro-IT by the 3 August cooling water as compared to the 1.15-ppm 5-chloro-IT control (i.e., 1115 vs. 341, respectively, Table III). The mutagenic responses with TA97, TA98, and TA100 (all –S9) of all cooling water samples, as a function of extractable 5-chloro-IT concentration, are shown in Figure 6. While there was no mutagenic response of 5-chloro-IT in TA98, there were dose-related mutagenic responses with statistically significant ($p < 0.001$) slopes of 1.17 and 0.44 revertants/ng of 5-chloro-IT (specific mutagenic activities of 1170 and 440 net revertants/μg of 5-chloro-IT, respectively) in TA97 and TA100, respectively (Figure 6). The 5-chloro-IT-specific mutagenic activities for the cooling waters and the 1.15-ppm 5-chloro-IT control were comparable with TA100 (i.e., 440 and 410 net revertants/μg of 5-chloro-IT, respectively) (Figure 6 and Table III). In the case of TA97(–S9), however, the 5-chloro-IT-specific mutagenic acitivity for the cooling waters was 3-fold greater than that of the 1.15-ppm 5-chloro-IT control (i.e., 1170 and 341 net revertants/μg of 5-chloro-IT, respectively).

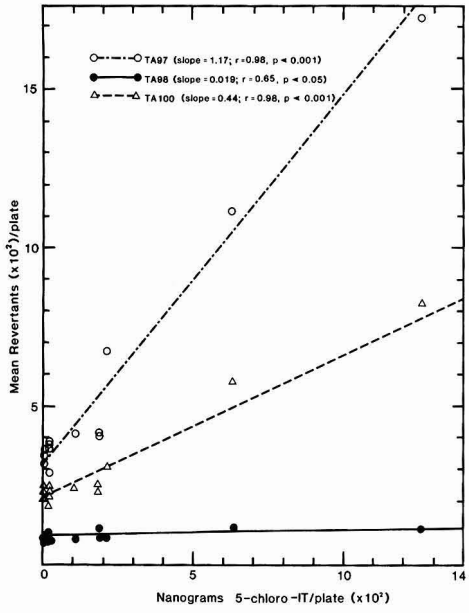

Figure 6. Mutagenic responses with TA97, TA98, and TA100 (all –S9) of cooling water extracts as a function of extractable 5-chloro-IT concentration measured via GC–MS. See Figure 1 legend for definitions of regression analysis terms.

Discussion

The specific mutagenic activities of the cooling water treated with the CL2150 biocide (281 000 and 118 000 net revertants/L equiv of water for TA97 and TA100, respectively, without S9) greatly exceeded those reported recently for chlorinated drinking waters (*8*) and chlorinated secondary waste water effluents (*14*). With the tester strain TA100 (–S9), the mutagenic activity in cooling waters appeared to be directly related to the extractable concentration of 5-chloro-IT, as evidenced by the comparable 5-chloro-IT-specific mutagenic activities of cooling waters and the 1.15-ppm 5-chloro-IT control (i.e., 440 and 410 net revertants/μg of 5-chloro-IT, respectively). Working with the biocide Kathon 886 MW, which contains 10% 5-chloro-IT and 3.4% 2-methyl-IT, Wright et al. (*24*) similarly found positive mutagenesis with TA100 (–S9). These investigators reported specific mutagenic activities, as determined by two collaborating laboratories, ranging from 1.40 to 2.69 TA100 (–S9) revertants/ng of active ingredients (i.e., the two active compounds in the biocide). The TA100 (–S9) specific mutagenic activities for CL2150 measured in this study are within 1 order of magnitude of the values reported by Wright et al. (*24*). Moreover, these investigators emphasized that significant variation in the mutagenic activity of this biocide was not uncommon between laboratories. As demonstrated in this study, Wright et al. (*24*) also found that this biocide is not mutagenic with TA98. Furthermore, they reported that the presence of S9 diminished but did not eliminate the mutagenicity of Kathon 886 MW. It should be noted that the mutagenic activity of CL2150 observed in our study cannot be attributed to the acidic water extraction procedure used. We base this conclusion on the research of Wright et al. (*24*), which demonstrated that Kathon 886 MW, containing the same active ingredients as CL2150, was mutagenic with TA100 (–S9) without requiring any type of extraction or treatment. Moreover, we also demonstrated notable mutagenic activity in CL2150 directly diluted in Me_2SO.

With TA97 (–S9), a tester strain not used by Wright et al. (*24*), we measured 5-chloro-IT-specific mutagenic ac-

tivities for the cooling waters 3-fold greater than that of the 1.15-ppm 5-chloro-IT control (i.e., 1170 and 341 net revertants/μg of 5-chloro-IT, respectively). This phenomenon may be attributed to the synergistic effect of other chemical constituents or additives (e.g., CL216 or CL1406, Table I) in the cooling water on the mutagenic activity of 5-chloro-IT (or 2-methyl-IT). Alternatively, this may indicate that there is (are) another (other) potent TA97 (–S9) mutagen(s) in the cooling waters in addition to 5-chloro-IT (or 2-methyl-IT). This (these) mutagen(s) may be breakdown products of 5-chloro-IT, breakdown products of 2-methyl-IT, or new compounds generated within the cooling tower. The latter hypothesis is supported by the positive mutagenicity with TA98 (–S9) displayed by the first cooling water sample (31 May) taken 3 days after CL2150 treatment (Figure 1). As the active compounds in CL2150 are not mutagenic with TA98, the logical conclusion is that other substances mutagenic with TA98 (–S9) were present in the cooling water. But why then were these TA98 (–S9) mutagens not detected in the cooling water sampled in August? The operation of the cooling tower during different times of the year may be responsible for the episodic nature of this mutagenic response. In May, when the demand on the cooling tower was low and the detention time of water and additives was relatively long, TA98 (–S9) mutagens were generated and accumulated to detectable levels in the cooling water. In contrast, the detention time of cooling water in the tower was very short in August. In the summer months, more makeup water must be added to the tower to compensate for that which evaporates as a result of the greater thermal load. This leads to more rapid accumulation of solids in the cooling water, which requires more frequent discharge of blowdown (*3*). Consequently, new TA98 (–S9) mutagens generated over time in the cooling water could not accumulate. Similarly, the mutagenic activity in the August cooling waters associated with CL2150 treatment did not persist beyond the first day of treatment (Table II).

The results presented here indicate that the blowdown from cooling towers treated with CL2150 could contribute significant mutagenic activity to surface waters or to municipal waste water. As this biocide is used in the manufacture of paper and in other manufacturing processes (*24*), it follows that the waste waters from these operations could also be mutagenic. Moreover, the use of this biocide in swimming pools (*24*) could pose a significant mutagenic burden to swimmers. Further research is called for aimed at determining the individual mutagenic activities of 5-chloro-IT and 2-methyl-IT and establishing the mechanism for increased TA97 (–S9) specific mutagenic activity in CL2150-treated cooling waters.

Acknowledgments

We sincerely thank Bruce N. Ames, Biochemistry Department, University of California, Berkeley, for providing us with the *Salmonella* tester strains. We also gratefully acknowledge Richard L. Tyndall and Elizabeth L. Domingue, Oak Ridge National Laboratory, Oak Ridge, TN, for their helpful suggestions and technical assistance.

Registry No. CL2150, 55965-84-9; CL216, 128-04-1; CL1406, 108674-94-8; 5-chloro-IT, 26172-55-4.

Literature Cited

(1) Miller, R. P. *Ann. Intern. Med.* **1979**, *90*, 667–670.
(2) Cooling Tower Institute *Liquid Effluent Pollution Control*; Cooling Tower Institute: Houston, TX, 1976.
(3) Cooling Tower Institute *Basic Concepts of Cooling Tower Operation*; Cooling Tower Institute: Houston, TX, 1977.
(4) Mattice, J. S. In *Water Chlorination: Chemistry, Environmental Impact, and Health Effects*; Jolley, R. L.; Bull, R. J.; Davis, W. P.; Katz, S.; Roberts, M. H., Jr.; Jacobs, V. A., Eds.; Lewis: Chelsea, MI, 1985; Vol. 5, pp 39–62.
(5) Tyndall, R. L. In *Water Chlorination: Environmental Impact and Health Effects*; Jolley, R. L.; Brungs, W. A.; Cumming, R. B.; Jacobs, V. A., Eds.; Ann Arbor Science: Ann Arbor, MI, 1980; Vol. 3, pp 29–38.
(6) Rook, J. J. *Environ. Sci. Technol.* **1977**, *11*, 478–482.
(7) Fallon, R. D.; Fliermans, C. B. *Chemosphere* **1980**, *9*, 385–391.
(8) Vartiainen, T.; Liimatainen, A. *Mutat. Res.* **1986**, *169*, 29–34.
(9) Kool, H. J.; van Kreijl, C. F.; Hrubec, J. In *Water Chlorination: Chemistry, Environmental Impact, and Health Effects*; Jolley, R. L.; Bull, R. J.; Davis, W. P.; Katz, S.; Roberts, M. H., Jr.; Jacobs, V. A., Eds.; Lewis: Chelsea, MI, 1985; Vol. 5, pp 187–205.
(10) Maruoka, S.; Yamanaka, S. *Mutat. Res.* **1980**, *79*, 381–386.
(11) Meier, J. R.; Bull, R. J. In *Water Chlorination: Chemistry, Environmental Impact, and Health Effects*; Jolley, R. L.; Bull, R. J.; Davis, W. P.; Katz, S.; Roberts, M. H., Jr.; Jacobs, V. A., Eds.; Lewis: Chelsea, MI, 1985; Vol. 5, pp 207–219.
(12) Honer, W. G.; Ashwood-Smith, M. J.; Warby, C. *Mutat. Res.* **1980**, *78*, 137–144.
(13) Reinhard, M.; Goodman, N.; Mortelmans, K. E. *Environ. Sci. Technol.* **1982**, *16*, 351–362.
(14) Meier, J. R.; Bishop, D. F. *J.—Water Pollut. Control Fed.* **1985**, *57*, 999–1005.
(15) Meier, J. R.; Lingg, R. D.; Bull, R. J. *Mutat. Res.* **1983**, *118*, 25–41.
(16) Meier, J. R.; Ringhand, H. P.; Coleman, W. E.; Munch, J. W.; Streicher, R. P.; Kaylor, W. H.; Schenck, K. M. *Mutat. Res.* **1985**, *157*, 111–122.
(17) Kringstad, K. P.; Ljungquist, P. O.; de Sousa, F.; Strömberg, L. M. *Environ. Sci. Technol.* **1983**, *17*, 553–555.
(18) *Methods for Organic Chemical Analysis of Municipal and Industrial Wastewater*; Longbottom, J. E.; Lichtenberg, J. J., Eds.; U.S. Environmental Protection Agency: Cincinnati, OH, 1982; EPA-600/4-82-057.
(19) Maron, D. M.; Ames, B. N. *Mutat. Res.* **1983**, *113*, 173–215.
(20) Batzinger, R. P.; Ou, S.-Y. L.; Bueding, E. *Cancer Res.* **1978**, *38*, 4478–4485.
(21) Chu, K. C.; Patel, K. M.; Lin, A. H.; Tarone, R. E.; Linhart, M. S.; Dunkel, V. C. *Mutat. Res.* **1981**, *85*, 119–132.
(22) De Flora, S.; Zanacchi, P.; Camoirano, A.; Bennicelli, C.; Badolati, G. S. *Mutat. Res.* **1984**, *133*, 161–198.
(23) Levin, D. E.; Yamasaki, E.; Ames, B. N. *Mutat. Res.* **1982**, *94*, 315–330.
(24) Wright, C.; Gingold, E.; Venitt, S.; Crofton-Sleigh, C. *Mutat. Res.* **1983**, *119*, 35–43.

Received for review June 9, 1986. Accepted April 9, 1987.

Environ. Sci. Technol. 1987, 21, 821–824

NOTES

Correlation of Octanol/Water Partition Coefficients and Total Molecular Surface Area for Highly Hydrophobic Aromatic Compounds

William J. Doucette* and Anders W. Andren

Water Chemistry Program, University of Wisconsin, Madison, Wisconsin 53706

■ The relationship between the calculated total molecular surface area (TSA) and the octanol/water partition coefficient (K_{ow}) is examined for a set of 32 highly hydrophobic aromatic compounds including several polychlorinated biphenyls (PCBs), polybrominated biphenyls (PBBs), polychlorinated dioxins (PCDDs), and polychlorinated furans (PCDFs). A generator column technique was used to experimentally measure log K_{ow} for each compound in order to provide an accurate, self-consistent set of values. A correlative method is presented that can be used to estimate log K_{ow} values from TSA within 14% for halogenated biphenyls, furans, and dioxins ranging from 3.89 to 8.58 in log K_{ow}.

Introduction

Mathematical models have been developed to predict the fate and transport of organic contaminants in the environment. Most of these models require as input data information about the physical and chemical properties of the compound(s) of interest. One of the most widely used properties in fate assessment modeling is the octanol/water partition coefficient (K_{ow}). As a measure of the hydrophobic character of a compound, K_{ow} has been used for predicting sorption and mobility in soils and sediments (*1–4*), bioconcentration in fish (*5*), and aquatic toxicity (*6*).

Values for K_{ow} are obtained by direct experimental measurement or are estimated by one of several techniques. Direct experimental measurement of K_{ow} with traditional shake-flask methods is extremely difficult for highly hydrophobic compounds (log $K_{ow} > 5$). Consequently, experimental values for many important classes of environmental contaminants, including polychlorinated biphenyls (PCBs), polybrominated biphenyls (PBBs), polychlorinated dibenzo-*p*-dioxins (PCDDs), and polychlorinated dibenzofurans (PCDFs), are lacking. Estimated values, calculated with group contribution techniques (*7, 8*) or from correlations with reverse-phase HPLC retention times (*9, 10*), are often used as alternatives to experimental data. However, because of the lack of reliable experimental data, the accuracy of estimation techniques has been difficult to evaluate for highly hydrophobic compounds.

In a previous study (*11*), a generator column technique was used to measure log K_{ow} values for 15 polychlorinated biphenyls (PCBs). This technique permitted the accurate experimental measurement of log K_{ow} values as large as 8.2, well beyond the range of traditional shake-flask methods. With these experimental values it was shown that group contribution techniques and a correlative technique using RP-HPLC retention times, widely used for estimating log K_{ow} values, did not accurately predict values for PCBs having log K_{ow} values greater than 5.

Since the size of a solute molecule is considered a major factor in determining its solubility and partitioning behavior (*12–15*), investigators have examined the correlation between molecular size, as described by the calculated total molecular surface area (TSA), and aqueous solubility (*16–18*) and log K_{ow} (*19*). While good correlations have been found for some types of compounds, the paucity of accurate experimental values has prevented previous correlations to be extended to compounds having log K_{ow} values greater than 5 or 6.

The main objective of this study was to examine the relationship between the calculated total molecular surface area and log K_{ow} for highly hydrophobic aromatic compounds (log K_{ow} greater than 5). A generator column technique was used to accurately measure log K_{ow} values for a set of highly hydrophobic aromatic compounds, including polychlorinated biphenyls (PCBs), polybrominated biphenyls (PBBs), polychlorinated dioxins (PCDDs), and polychlorinated furans (PCDFs). This data set was then used to develop an empirical correlation that can be used to estimate log K_{ow} from calculated TSA, for compounds ranging from 3.89 to 8.58 in log K_{ow}.

Materials and Methods

Reagents. All polychlorinated dibenzo-*p*-dioxin and dibenzofuran congeners and polybrominated biphenyls were obtained from Ultra Scientific Inc. (Hope, RI; 99.9% purity) and were used without further purification. The 1-octanol was purchased from Fisher Chemical (certified grade). Pesticide-grade isooctane was used for gas chromatography.

Equipment. The generator column used in this work has been described in detail previously (*11, 20*), and only a brief description is presented here. The 24-cm column segment was hand-packed with silanized Chromosorb W (3 g, 60/80 mesh) retained by a coarse, ground glass frit at the bottom and a plug of silanized glass wool at the top. The column was thermostated at 25 °C by pumping water from a constant-temperature bath through a jacket enclosing the column. A C_{18} Sep-Pak (Water Associates, Milford, MA) was used to extract the compound from the column effluent. A Hewlett-Packard gas chromatograph (5840A), equipped with an electron capture detector (Ni^{63}), was used for quantitation.

Procedure. Approximately 10 mg of the congener of interest was dissolved in 100 mL of 1-octanol. Fifteen milliliters of this solution was stirred with 120 mL of organic-free water for 14–18 h. After the phases were allowed to separate, an aliquot of the octanol phase was diluted with isooctane, and the concentration of the compound was

* Address correspondence to this author at his present address: Utah Water Research Laboratory, Utah State University, Logan, UT 84322.

0013-936X/87/0921-0821$01.50/0

determined by gas chromatography. The remaining octanol phase was then applied to the generator column and pulled through the dry support with gentle suction until the solid support was saturated, as evidenced by the appearance of the 1-octanol at the column base.

The aqueous phase was generated by pumping octanol-saturated water through the octanol-coated generator column. The liquid leaving the generator column was pumped through a C_{18} extraction column (Sep-Pak) and was collected in a tared weighing flask. When an amount of compound sufficient for analysis was collected on the Sep-Pak, it was removed from the generator column and eluted with 10 mL of hexane. Prior to elution, excess water was removed by purging with a gentle stream of nitrogen. The column efficiently extracted the compounds from the aqueous solution (total recovery efficiency greater than 90%). The amount of compound in the extract was then determined by gas chromatography. The K_{ow} was calculated by dividing the compound concentration in the octanol phase by that in the aqueous phase. The aqueous solute concentration exiting the generator column was found to be independent of flow rate (0.5–2.0 mL/min), of the volume of water passed through the column, and of the concentration of solute in octanol.

Calculation of TSA

Total molecular surface area values were calculated with a computer program developed by Robert Pearlman and obtained from the Quantum Chemistry Program Exchange, Chemistry Department, Indiana University, Bloomington, IN. A detailed description of the molecular surface area calculation method is provided by Pearlman (*21*).

In this program, each atom of a molecule is represented by a sphere centered at the equilibrium position of the nucleus. The radius of the sphere is equal to that of the van der Waals radius. Planes of intersection between spheres are used to estimate the contribution to surface area from individual atoms or groups. The program computes the surface area of individual atoms or groups by numerical integration, and the overlap due to intersecting spheres is excluded from the calculation. Total surface area is calculated by the summation of individual group contributions. Standard geometry, standard interatomic bond lengths and bond angles, supplemented with X-ray diffraction data, was used in constructing the molecules. The following values for interatomic distances between atoms or groups of atoms in a molecule were used: aliphatic C–C, 1.54 Å; aromatic C–H, 1.08 Å, aromatic C–Cl, 1.7 Å; aromatic C–O, 1.4 Å; aromatic C–Br, 1.8 Å. The van der Waals radii used were as foollows: aromatic C, 1.20 Å; aromatic H, 1.08 Å; aromatic Cl, 1.7 Å; aromatic Br, 1.9 Å; aromatic Br, 1.9 Å; oxygen, 1.4 Å; methyl group, 2.0 Å.

The substituted dibenzo-*p*-dioxins and dibenzofurans were assumed to have a planar conformation. For the biphenyls, a nonplanar conformation was used that gave a maximum calculated TSA. The methyl groups were approximated as a single sphere of radium 2.0 Å as suggested by Valvani et al. (*16*).

The program also allows the TSA of the solute molecule to be calculated after the addition of a suitable solvent radius. Calculation showed, however, that the addition of a solvent radius for water did not improve the correlation between TSA and log K_{ow}. Thus, TSA values reported in this study (Table I) do not include the solvent radius.

Results and Discussion

Experimental Results. The log K_{ow} values for the 15 methylbiphenyl, PBB, PCDF, and PCDD congeners measured in this study are listed in Table I. The values range from 4.31 to 8.58. At least five replicate determinations were done for each compound in the study. The confidence limits on measured log K_{ow} values are within 5% of the average values for all compounds except for 4,4′-dibromobiphenyl (10%). The log K_{ow} value of 8.58 for decabromobiphenyl is believed to be the highest measured value ever reported. A shake-flask determination of this magnitude would be impossible. The log K_{ow} values measured previously for 15 PCB congeners are also listed.

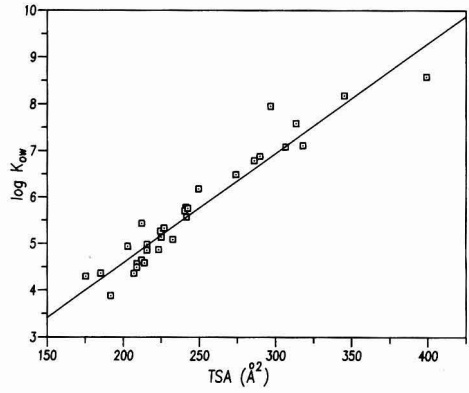

Figure 1. log K_{ow} vs. total molecular surface area (TSA) for 32 aromatic hydrocarbons.

TSA–K_{ow} Correlations. Regression analysis showed that the relationship between TSA and log K_{ow} (Figure 1) can be expressed as a linear function

$$\log K_{ow} = 0.0238(\text{TSA}) - 0.142$$

$$n = 32 \qquad R^2 = 0.924$$

or as a quadratic function

$$\log K_{ow} = -3.60 + 0.05(\text{TSA}) - (4.71 \times 10^{-5})(\text{TSA})$$

$$n = 32 \qquad R^2 = 0.939$$

The linear correlation expression appropriate at 25 °C was used to calculate the predicted log K_{ow} values presented in the last column of Table I. The absolute average error for 32 compounds was 4.6% with the errors ranging from 0 to 14%. It should be noted that the success in predicting log K_{ow} values is partially due to the fact that the compounds used in developing the correlation equations were also used in evaluating the method.

For comparison, log K_{ow} values calculated with a computerized group contribution method (*22*) are also presented. The average absolute error for 32 compounds was 11.5% with errors ranging from 1 to 47%. For the group contribution method, errors seem to increase positively with increasing log K_{ow}. For example, while the error in estimating the log K_{ow} values for biphenyl is less than 4%, the error in estimating log K_{ow} for decachlorobiphenyl is about 36%.

The calculation of TSA requires a more detailed knowledge of solute structural features, including van der Waals radii, bond lengths, and bond angles. The TSA of a specific portion of a molecule can also be calculated, which enables the effect of different functional groups to be examind (*12*). In addition, the effects of conformation and solvent radius can be investigated.

It is important to remember that all correlation methods require a set of compounds with "known" log K_{ow} values and that the accuracy of the method depends on the accuracy of these "known" values. When a correlation me-

Table I. log K_{ow} and TSA Values for PCB, PBB, PCDF, and PCDD Congeners

compound	log K_{ow}[a]	TSA[b]	estimated log K_{ow} (group contribution method)[c]	estimated log K_{ow} (TSA–log K_{ow} correlation)[d]
PBBs				
2-bromobiphenyl	4.59 ± 0.02 (12)	214.5	4.89	4.95
3-bromobiphenyl	4.85 ± 0.03 (12)	216.6	4.89	5.00
4-bromobiphenyl	4.96 ± 0.04 (10)	216.6	4.89	5.00
4,4′-dibromobiphenyl	5.72 ± 0.04 (10)	240.8	5.75	5.57
2,2′,4,5,5′-pentabromobiphenyl	7.10 ± 0.06 (5)	306.1	8.06	7.13
decabromobiphenyl	8.58 ± 0.06 (7)	399.9	12.63	9.36
dioxins				
dibenzo-*p*-dioxin	4.37 ± 0.01 (6)	185.6	4.65	4.26
2-chlorodibenzo-*p*-dioxin	4.94 ± 0.80 (10)	203.6	5.47	4.69
1,2,3,4-tetrachlorodibenzo-*p*-dioxin	6.20 ± 0.24 (9)	250.3	7.70	5.80
octachlorodibenzo-*p*-dioxin	7.59 ± 0.16 (14)	314.9	10.56	7.33
furans				
dibenzofuran	4.31 ± 0.05 (6)	176.3	4.12	4.04
2,8-dichlorodibenzofuran	5.44 ± 0.03 (12)	212.8	5.65	4.91
octachlorodibenzofuran	7.97 ± 0.08 (7)	298.0	9.96	6.94
methylbiphenyls				
4-methylbiphenyl	4.63 ± 0.08 (7)	212.9	4.68	4.91
4,4′-dimethylbiphenyl	5.09 ± 0.30 (8)	233.4	5.33	5.40
PCBs				
biphenyl	3.89 ± 0.01 (12)	192.3	4.03	4.42
2-chlorobiphenyl	4.38 ± 0.02 (9)	208.3	4.74	4.80
3-chlorobiphenyl	4.58 ± 0.03 (6)	209.9	4.74	4.84
4-chlorobiphenyl	4.49 ± 0.01 (10)	209.9	4.74	4.84
4,4′-dichlorobiphenyl	5.33 ± 0.01 (5)	227.4	5.46	5.25
3,4-dichlorobiphenyl	5.29 ± 0.01 (6)	225.4	5.46	5.22
2,2′-dichlorobiphenyl	4.90 ± 0.01 (3)	224.3	5.46	5.18
2,4′-dichlorobiphenyl	5.14 ± 0.01 (4)	225.9	5.46	5.22
2,2′,5-trichlorobiphenyl	5.60 ± 0.01 (3)	241.8	6.16	5.60
2,4,5-trichlorobiphenyl	5.81 ± 0.00 (2)	241.4	6.17	5.59
2,4′,5-trichlorobiphenyl	5.79 ± 0.00 (2)	243.4	6.17	5.63
2,4,6-trichlorobiphenyl	5.57 ± 0.09 (12)	241.8	6.17	5.60
2,2′,4,5,5′-pentachlorobiphenyl	6.50 ± 0.13 (6)	275.0	7.60	6.39
2,2′,3,3′,6,6′-hexachlorobiphenyl	6.81 ± 0.03 (6)	287.4	8.31	6.68
2,2′,4,4′,5,5′-hexachlorobiphenyl	6.90 ± 0.14 (8)	290.5	8.31	6.75
2,2′,3,3′,5,5′,6,6′-octachlorobiphenyl	7.12 ± 0.31 (9)	318.5	9.73	7.42
decachlorobiphenyl	8.20 ± 0.27 (18)	345.6	11.16	8.06

[a] Mean experimental log K_{ow} ± standard deviation (number of determinations). Generator column method used for all determinations. [b] Calculated total surface area (A^2). [c] Calculated with a program developed by Leo (*19*). [d] Calculated from regression equation: log K_{ow} = 0.0238(TSA) − 0.142.

thod is used, it is important to consider the range of log K_{ow} values employed in developing the correlation. Correlative methods are best applied to cmpounds having K_{ow} values within the range of standards used to develop the correlation.

The data set used here to develop and evaluate the correlation between TSA and log K_{ow} consisted only of compounds having experimental log K_{ow} values (measured by a generator column technique). This data set contained compounds having log K_{ow} values ranging from approximately 4 to 8.5 and is believed to be the most accurate and self-consistent set of experimental log K_{ow} values available for these aromatic compounds. The correlative method presented here can be used to predict log K_{ow} values for halogenated biphenyls, furans, and dioxins. The correlation appears to be capable of predicting log K_{ow} values within 14% for these classes of compounds. Future work will investigate the applicability of this correlation to other classes of hydrophobic compounds.

Conclusions

With a set of experimental log K_{ow} values measured by a generator column technique, the relationship between TSA and log K_{ow} was examined. A linear relationship between TSA and log K_{ow} was found for 32 highly hydrophobic aromatic compounds ranging from 3.89 to 8.58 in log K_{ow}. The resulting correlation provides an accurate method for predicting log K_{ow} values for halogenattd biphenyls, furans, and dioxins from the compound's chemical structure. This approach is also expected to be applicable to many other compound types.

Acknowledgments

We gratefully acknowledge Nick Loux for his assistance with the TSA program. Leslie Johnson provided expert typing assistance.

Registry No. Furan, 110-00-9; biphenyl, 26983-52-8; *p*-dioxin, 290-67-5; octanol, 111-87-5; 2-bromobiphenyl, 2052-07-5; 3-bromobiphenyl, 2113-57-7; 4-bromobiphenyl, 92-66-0; 4,4′-dibromobiphenyl, 92-86-4; 2,2′,4,5,5′-pentabromobiphenyl, 67888-96-4; decabromobiphenyl, 13654-09-6; dibenzo-*p*-dioxin, 262-12-4; 2-chlorodibenzo-*p*-dioxin, 39227-54-8; 1,2,3,4-tetrachlorodibenzo-*p*-dioxin, 30746-58-8; octachlorodibenzo-*p*-dioxin, 3268-87-9; dibenzofuran, 132-64-9; 2,8-dichlorodibenzofuran, 5409-83-6; octachlorodibenzofuran, 39001-02-0; 4-methylbiphenyl, 644-08-6; 4,4′-dimethylbiphenyl, 613-33-2; 2-chlorobiphenyl, 2051-60-7; 3-chlorobiphenyl, 2051-61-8; 4-chlorobiphenyl, 2051-62-9; 4,4′-dichlorobiphenyl, 2050-68-2; 3,4-dichlorobiphenyl, 2974-92-7; 2,2′-dichlorobiphenyl, 13029-08-8; 2,4-dichlorobiphenyl, 34883-43-7; 2,2′,5-trichlorobiphenyl, 37680-65-2; 2,4,5-trichlorobiphenyl, 15862-07-4; 2,4′,5-trichlorobiphenyl, 16606-02-3; 2,4,6-trichlorobiphenyl, 35693-92-6; 2,2′,4,5,5′-pentachlorobiphenyl, 37680-73-2; 2,2′,3,3′,6,6′-hexachlorobiphenyl, 38411-22-2; 2,2′,4,4′,5,5′-hexachlorobiphenyl, 35065-27-1; 2,2′,3,3′,5,5′,6,6′-octachlorobiphenyl, 2136-99-4; decachlorobiphenyl, 2051-24-3.

Literature Cited

(1) Kearney, P.; Isensee, A.; Helling, C.; Woolson, E.; Plinner, J. In *Chlorodioxins—Origin and Fate*; Advances in Chem-

istry 120; American Chemical Society: Washington, DC, 1973.
(2) Karickhoff, S. W. *Environ. Sci. Technol.* **1981**, *10*, 833.
(3) Karickhoff, S. W.; Brown, D. S.; Scott, T. A. *Water Res.* **1979**, *13*, 241.
(4) Schwarzenbach, R. P.; Westall, J. *Environ. Sci. Technol.* **1980**, *15*, 1360.
(5) Kenaga, E. E. *Environ. Sci. Technol.* **1980**, *14*, 553.
(6) Konemann, H. *Ectoxicol. Environ. Saf.* **1980**, *4*, 415.
(7) Hansch, C.; Leo, A. J. *Substituent Constants for Correlation Analysis in Chemistry and Biology*; Wiley: New York, 1979; pp 339.
(8) Nys, G. G.; Rekker, R. F. *Chem. Thermodyn.* **1973**, *8*, 521.
(9) Veith, G. D.; Austin, N. M.; Morris, R. T. *Water Res.* **1979**, *13*, 43.
(10) McDuffie, B. *Chemosphere* **1981**, *10*, 73.
(11) Woodburn, K. B.; Doucette, W. J.; Andren, A. W. *Environ. Sci. Technol.* **1984**, *18*, 457.
(12) Langmiur, I. M. *Colloid Symp. Monogr.* **1925**, *3*, 48.
(13) Herman, R. B. *J. Phys. Chem.* **1971**, *75*, 363.
(14) Herman, R. B. *J. Phys. Chem.* **1972**, *76*, 2754.
(15) Amidon, G. L.; Yalkowsky, S. H.; Valvani, S. C. *J. Phys. Chem.* **1975**, *79*, 2239.
(16) Valvani, S. C.; Yalkowsky, S. H.; Amidon, G. L. *J. Phys. Chem.* **1976**, *80*, 829.
(17) Yalkowsky, S. H.; Valvani, S. C. *J. Med. Chem.* **1975**, *19*, 727.
(18) Yalkowsky, S. H.; Valvani, S. C. *J. Chem. Eng. Data* **1979**, *24*, 127.
(19) Yalkowsky, S. H.; Valvani, S. C. *J. Pharm. Sci.* **1980**, *69*, 912.
(20) Doucette, W. J. *PhD.* Thesis, University of Wisconsin, Madison, 1985.
(21) Pearlman, R. S. In *Physical Chemical Properties of Drugs*; Dekker: New York, 1980; pp 331.
(22) Leo, A. J. *CLOGP-3.3 Computer Program, Medchem Project*; Pomona College: Clairemont, CA, 1985.

Received for review November 3, 1986. Accepted April 9, 1987. This research was funded by the University of Wisconsin Sea Grant College Program under grants from the National Sea Grant Program, National Oceanographic and Atmospheric Administration, U.S. Department of Commerce (Grant NA800-AA-D-00086, Project R/MW-21), and from the State of Wisconsin.

HP offers you more ways to do organic analysis than the EPA has methods.

we never stop asking...

"What if..."

And your analytical options keep growing.

For example, we've just added an infrared detector, an FPD, 601/602 water analyzer, and MS software specifically tailored to the newest EPA-reporting requirements. These further expand what is already one of the broadest selections of analytical instruments and automation systems available for organic analysis. They reflect, too, HP's continuing commitment to provide the application solutions you need for your organic environmental analysis methods—and the EPA's.

Our support of your environmental laboratory needs includes a full range of automated systems for data analysis, management and EPA-approved reporting. Whether you need general or application specific instrumentation, GC/MS, GC/FTIR, or LC, HP has a data system to fit.

Breadth of line also means HP can give you the bonus of one-source support. You know the value of that if you've ever had to track down and coordinate multiple vendor support teams! Contrast those complexities and frustrations with the comprehensive across-the-board response that a single phone call to HP can provide.

Plus, there's HP's time-proven quality and reliability. It's reflected in tens of thousands of HP analytical instruments that are working day-in, day-out around the world. You also see it in the 99% uptime guarantee available for our industry standard HP 5890A GC.

Quality, breadth of line and support are all a result of our "What If..." approach that sets your needs, always, as our starting point.

See for yourself. Call the HP office listed in your telephone directory white pages and ask for an analytical products representative. Or write to Hewlett-Packard Analytical Group, 1820 Embarcadero Rd., Palo Alto, CA 94303.

HEWLETT PACKARD

AG04701

Get rid of the overtime in your waste treatment facility.

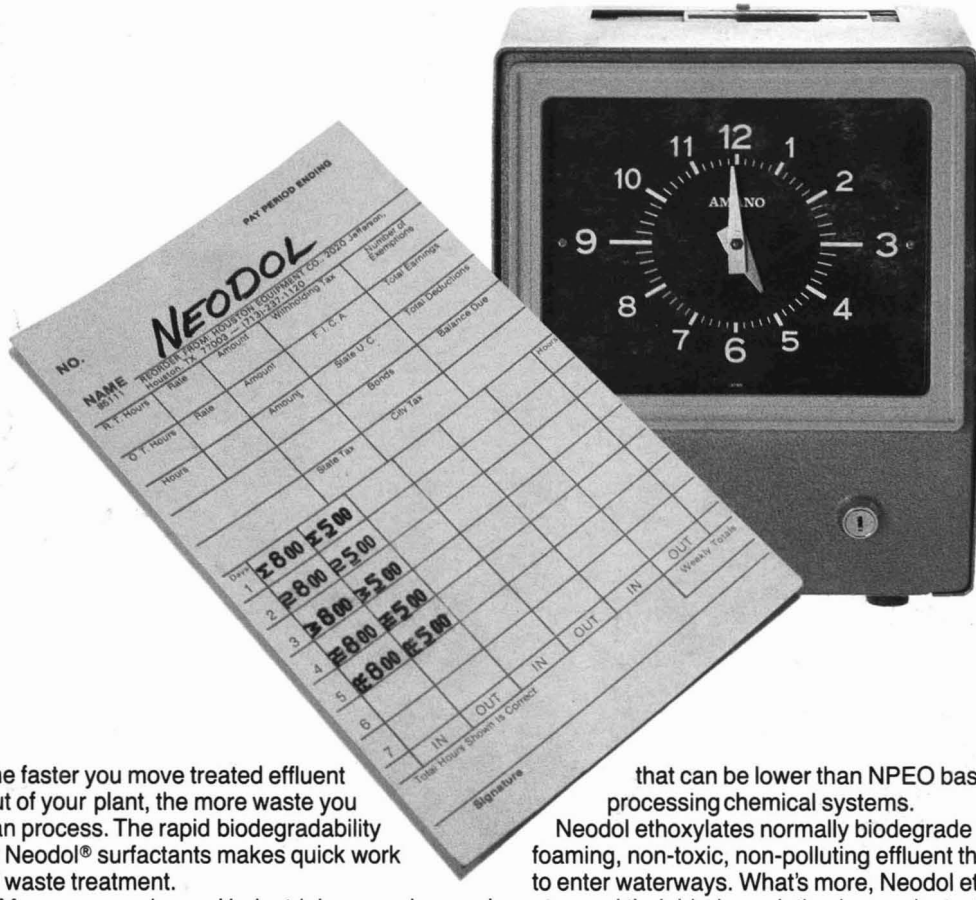

The faster you move treated effluent out of your plant, the more waste you can process. The rapid biodegradability of Neodol® surfactants makes quick work of waste treatment.

Many commonly used industrial processing products contain surfactants. Some surfactants, such as nonylphenol ethoxylates (NPEOs), biodegrade slowly. Their lengthy effluent processing time can limit a facility's treatment capacity and increase utility costs.

In contrast, processing products containing Neodol ethoxylates from Shell Chemical biodegrade much faster than those containing NPEOs, essentially increasing effluent treatment capacity without capital expenditures. And at a total processing cost that can be lower than NPEO based processing chemical systems.

Neodol ethoxylates normally biodegrade into non-foaming, non-toxic, non-polluting effluent that is safe to enter waterways. What's more, Neodol ethoxylates and their biodegradation by-products do not contain aromatic residues which react with chlorine in municipal treatment facilities to produce toxic, bioresistant compounds that can be harmful to aquatic life.

In waste treatment, time is more than money. It's also valuable treatment capacity. To find out more about time-saving, environmentally safe Neodol surfactants, write to: Shell Chemical Company, Manager Neodol Communications, P.O. Box 2463, One Shell Plaza, Houston, Texas 77252.

Shell Chemical Company